

MICROCOPY RESOLUTION TEST CHART NATIONAL BUREAU OF STANDARDS-1963-A

RADC-TR-84-183 Final Technical Report September 1984





EOS PROTECTION FOR VLSI DEVICES

Martin Marietta Denver Aerospace

David D. Wilson, William E. Echols and Mark G. Rossi

APPROVED FOR PUBLIC RELEASE; DISTRIBUTION UNLIMITED



ROME AIR DEVELOPMENT CENTER Air Force Systems Command Griffiss Air Force Base, NY 13441

This report has been reviewed by the RADC Public Affairs Office (PA) and is releasable to the National Technical Information Service (NTIS). At NTIS it will be releasable to the general public, including foreign nations.

RADC-TR-84-183 has been reviewed and is approved for publication.

APPROVED: Daniel J. Busin

DANIEL J. BURNS Project Engineer

APPROVED:

W. S. TUTHILL, Colonel, USAF Chief, Reliability & Compatibility Division

FOR THE COMMANDER:

JOHN A. RITZ Acting Chief, Plans Office

John a. Ret

If your address has changed or if you wish to be removed from the RADC mailing list, or if the addressee is no longer employed by your organization, please notify RADC (RBRP) Griffiss AFB NY 13441-5700. This will assist us in maintaining a current mailing list.

Do not return copies of this report unless contractual obligations or notices on a specific document requires that it be returned.

ECURITY CLASSIFICATION OF THIS PAGE					
REPORT DOCUMENTATION PAGE					
1a REPORT SECURITY CLASSIFICATION UNCLASSIFIED		16 RESTRICTIVE MARKINGS N/A			
28. SECURITY CLASSIFICATION AUTHORITY		3. DISTRIBUTION/A	VAILABILITY O	F REPORT	
N/A		Approved for	public rel	.ease; dist	ribution
2b. DECLASSIFICATION/DOWNGRADING SCHEE	OULE	unlimited.			
4 PERFORMING ORGANIZATION REPORT NUM	BER(S)	S. MONITORING OR	GANIZATION R	EPORT NUMBER	(S)
MCR-84-506		RADC-TR-84-18	33		
64. NAME OF PERFORMING ORGANIZATION	Sb. OFFICE SYMBOL	78. NAME OF MONITORING ORGANIZATION			
Martin Marietta Denver Aerospace	(If applicable)	Rome Air Development Center (RBRP)			
6c. ADDRESS (City, State and ZIP Code)		7b. ADDRESS (City. State and ZIP Code)			
P. O. Box 179		Griffiss AFB	NY 13441-5	700	
Denver CO 80201					
Se. NAME OF FUNDING/SPONSORING ORGANIZATION	8b. OFFICE SYMBOL (If applicable)	9. PROCUREMENT II	NSTRUMENT 10	ENTIFICATION !	NUMBER
Rome Air Development Center	(RBRP)	F30602-82-C-0	111		
8c ADDRESS (City, State and ZIP Code)		10. SOURCE OF FUN	DING NOS.		
Griffiss AFB NY 13441-5700		PROGRAM ELEMENT NO.	PROJECT NO.	TASK NO.	WORK UNIT
		62702F	2338	01	2P
11. TITLE (Include Security Classification)		 		·	
EOS PROTECTION FOR VLSI DEVICE	ES				
12 PERSONAL AUTHOR(S) David D. Wilson, William E. E	abole Mark C P	occi			
134 TYPE OF REPORT 136. TIME C		14. DATE OF REPOR	IT (Yr., Mo., Day	15. PAGE	COUNT
Final FROM _J	un 82 to Mar 84	Septembe	r 1984	274	
16. SUPPLEMENTARY NOTATION			<u>-</u>		
17 COSATI CODES	18. SUBJECT TERMS (C	ontinue on reverse if ne	cessary and ident	ify by block numb	eri
FIELD GROUP SUB. GR.	EOS	Electrostatic Discharge			
09 01	ESD	Test Methods erstress Failure Mechanisms (See Reverse)			
19. ABSTRACT (Continue on reverse if necessary an	Electrical Ove	100100	ure Mechan	1181118 (36	e keverse)
The sensitivity of eight complex integrated circuits to ESD was studied. This included both the human body ESD simulation and the charged device ESD simulation. Failure Analysis and data analysis were performed to understand the sensitivity variations and to allow recommendations to be made on input protection networks for VLSI devices.					
_	20 DISTRIBUTION/AVAILABILITY OF ABSTRACT 21 ABSTRACT SECURITY CLASSIFICATION				
UNCLASSIFIED UNCLASSIFIED					
22a. NAME OF RESPONSIBLE INDIVIDUAL		226 TELEPHONE NU		22c OFFICE SY	MBCL
Daniel J. Burns		(315) 330-		RADC (F	RBRP)
00 FORM 1473 00 A00					

SECURITY CLASSIFICATION OF THIS PAGE

18. Subject Terms (Continued)

Protection Networks Very Large Scale Integration Failure Analysis Integrated Circuits Design

17. Cosati Codes (Continued)

<u>Field</u>	Group	
14	04	
20	12	

UNCLASSIFIED

SECURITY CLASSIFICATION OF THIS PAGE

TABLE OF CONTENTS

		Page
I.	INTRODUCTION	1
II.	LITERATURE SEARCH	2
III.	TEST PROCEDURES	11
IV.	TEST EQUIPMENT	18
V.	DEVICE CHARACTERIZATION AND TESTING	25
	A. Part A Analysis	27
	B. Part B Analysis	64
	C. Part C Analysis	91
	D. Part D Analysis	111
	E. Part E Analysis	129
	F. Part F Analysis	158
	G. Part G Analysis	177
	H. Part H Analaysis	215
VI.	PROTECTION SCHEME ANALYSIS	250

Accession For			
NTIS	GRA&I	À	
DTIC :	TAB	Ϊ	
1	ounced		
Justi:	fication		
By			
	lability		
	Avail a	nd/or	
Dist	Speci	al	
	1		
1-1			
M			



EVALUATION

Many of the major semiconductor manufacturers have published the results of their own in-house design evaluations of new electrostatic discharge (ESD) protection networks. Several major users have published test and evaluation results on the ESD protection networks used on a wide cross-section of popular device types available today. The present work was undertaken to expand that data base and to compare the failure mechanisms which occur in devices subjected to both the human body and the charged device ESD simulation tests.

The conclusions of this report are similar to those other workers. Failure mechanisms induced with the human body model are primarily electrothermal junction shorting, often associated with aluminum/silicon contacts near the bonding pads (an interlevel polysilicon layer placed between the aluminum and silicon in such contacts significantly raises the failure threshold). Layout 'mistakes' such as closer spacing of protective network components to other junctions can cause significantly lowered failure thresholds for a pin. Interlayer oxide shorts were found to occur in some networks. The charged device test induced failures at much lower voltages but the failure mechanisms were similar in the best protective networks. In almost every case there were easily recognized reasons for increased sensitivity on one or more pins which could be fixed by minor layout changes.

It appears that the best approach to ESD protection is to use standard networks with identical layout placed near the bonding pad of each pin which requires ESD protection. It is also clear that the entire ESD current path through the device must be considered in addition to the local protection network.

Advances in integrated circuit technologies are resulting in basic circuit structures which are increasingly sensitive to electrostatic discharge (ESD) damage because of decreasing oxide thicknesses, shallower junction depths and smaller junction areas. A comparison of the sensitivity of present day integrated circuits to damage by ESD to that of devices designed only a few years ago must be done on a vendor-to-vendor basis and often, unfortunately, within some vendors on a department or designer basis. Even so, this work has shown that certain vendors product lines have exhibited reduced ESD sensitivity in spite of technology advances. These cases indicate that significant progress has been made in the design of effective ESD protection networks (which are integrated into virtually all of today's devices).

Further progress must be made for two reasons: 1) future devices are expected to be more sensitive to damage as scaling continues and 2) the best protective networks available today cannot withstand a healthy zap from a human (>5000v, 100 pf, 1500 ohm test) or a low level zap from themselves (2000v, charged device test).

DANIEL J. BURNS
Project Engineer
RADC/RBRP

I. INTRODUCTION

The purpose of this study is to gain further information on the sensitivity of advanced semiconductor devices to electrical overstress (EOS). The electrical overstress investigated was electrostatic discharge (ESD) using both the charged device (CD) model and the human body discharge (HBD) model.

This study included 1. Literature Search, 2. Test Procedure Development, 3. Test Equipment Fabrication, 4. ESD Sensitivity Testing, and 5. Protection Scheme Study.

II. LITERATURE SEARCH

A literature search was performed to gather published information on EOS/ESD work. This information was used in the rest of the study to establish the test procedure and test equipment in order that the best possible test could be developed.

A computer search through the Martin Marietta reference library was initiated by a subject/key word method. The subjects which were researched were electrical overstress and electrostatic discharge. The databases which were used include:

- NASA RECON Includes report literature indexed in Scientific and Technical Aerospace Reports (STAR), International Aerospace Abstracts (IAA), announcements of NASA research in progress, and reports issued by the Aerospace Safety Research and Development Institute.
- 2. Lockheed DIALOG, SDC ORBIT These database vendors offer a selection of over 125 databases covering various fields of knowledge. Four of those used are listed below:
 - a. INSPEC (Institute of Electrical Engineers) Provides on-line access to the three sections of Science Abstracts (Physics Abstracts, Electrical and Electronics Abstracts, Computer and Control Abstracts).
 - b. SPIN (American Institute of Physics) Indexes a variety of the world's physics journals.
 - COMPENDEX (Engineering Index) Provides worldwide coverage of engineering literature.
 - d. NTIS (National Technical Intormation Service) Covers government-sponsored research.
- 3. Defense RDT and E Online System (Research, Development, Test, and Evaluation) Provides access to Department of Defense current and completed research as well as projects planned for the future.

The paper abstracts and/or titles were obtained and selected articles were ordered.

Pertinent articles which were available from symposium proceedings which are kept on file in the Failure Analysis Laboratory were also obtained. The proceedings reviewed included the Physics of Failure/Reliability Physics Symposium proceedings from 1967 to present, the EOS/ESD Symposium proceedings from 1979 to present, and the ATFA/ISTFA Symposium proceedings from 1977 to present.

With the papers obtained from these sources, each was reviewed and categorized. The categories included:

- 1. Human body discharge model
- 2. Charge/discharge model (charged device)
- 3. Electrical overstress
- 4. Protection networks
- 5. Equipment
- 6. Review paper
- 7. Theoretical paper

Within each of these categories, the papers were summarized for significant information. As an example for the equipment category the type of resistors, capacitors, relays, switches, and materials were noted. Contacts were also made with several of these authors to discuss their systems.

In addition to categorizing the articles, other data was compiled. These include:

- 1. Devices tested
- 2. Failure threshold
- 3. Waveform monitoring
- 4. Voltage steps utilized
- 5. Data analysis methods

During later stages of the testing the RAC "Electrostatic Discharge (ESD) Susceptibility of Electronic Devices" publication was obtained and reviewed.

A listing of 66 articles which were reviewed follows:

Categories

- HBD Human Body Discharge Model
- CD Charged Device Model
- EOS Electrical Overstress Model
- PN Protection Networks Information
- EQ Equipment Information
- R Review Paper
- T Theoretical

ARTICLES

Category	Title
EUS, PN, K	l l. "The Application of Electrical Overstress Models to Gate Protective Networks", D. Wunsch in IRPS, 1978
EOS, T	2. "Calculation of Minimum Power Level for Device Burnout", Itsu Arimura, Boeing Document
EOS	3. "Screening of Time-Dependent Dielectric Breakdowns", E. Anolick, L. Chen in IRPS, 1982
 EOS 	4. "Electromigration Resistance of Fine-line Al for VLSI Applications", S. Vaidya, D. Fraser, A. Sinha in Elec. Comp. Conf., 1980
EUS, T	5. "Analysis of Electrical Overstress Failures", J. Smith in IRPS, 1973
EOS	6. "Electrical Overstress Failure Analysis in Microcircuits", J. Smith in IkPS, 1978
EOS	7. "Degradation of Thin-Gate MOSFETs Under High Electric Field Stress", H. Ishinchi, Y. Matsumoto. S. Sawada and O. Ozawa in IRPS, 1982
HBD, EQ, PN	8. "Keliability Intluences from Electrical Overstress on LSI Devices", A. Hart, T. Teng and A. McKenna in Elec. Comp. Conf., 1980
EOS	9. "Electromigration Failure Under Pulse Test Conditions", R. Miller in IRPS, 1978
EOS	10. "Failure of Small Thin-film Conductors due to High Current-Density Pulses", E. Kinsbron, C. Mellian-Smith, A. English and T. Chynoweth in IRPS, 1978

Category	Title
EQ	l ll. "Electrostatic Discharge Tester", T. Madzy, L. Price and M. Ruduski in IBM Bulletin, 1977
PN 	12. "Multiple I/O Protection with Single Protective Device", S. Chen, S. Park, R. Wong in IBM Bulletin, 1980
PN	13. "Voltage Programmable Protect Circuit", C. Hoffman and F. Wiedman in IBM Bulletin, 1980
 PN 	14. "Electrostatic Discharge Protective Device for Bipolar Circuits", W. Carlson, V. Klimanis and R. Seeger in IBM Bulletin, 1978
 PN 	15. "Protective Circuit for Integrated Semiconductor Devices", O. Alameddine in IBM Bulletin, 1978
R, PN	16. "Susceptibility of Semiconductors to Damage from Electrostatic Discharge", R. Funk in Int. Elec. Packaging and Prod. Conf., 1980
PN	17. "Floating Plate Protective Device", Y. Huang in in IBM Bulletin, 1977
PN, EQ	18. "The Evaluation of CMOS Static-Charge Protection Networks and Failure Mechanisms with Overstress Conditions as Related to Device Life", L. Gallace and H. Pujol, IRPS, 1977
PN	19. "CMOS/SOS Gate-Protection Networks", R. Pancholy and T. Oki in IEEE Trans. on Electron Devices, 1978
PN	20. "CMOS/SOS LSI Input/Output Protection Networks", B. Allport, J. Cricchi and D. Barth in IEEE Trans. on Electron Devices, 1978

Category	Title
 PN 	21. "H-MOS Reliability", S. Rosenberg, D. Crook and B. Euzent in IRPS, 1978
PN	22. "Voltage Breakdown Characteristics of Close Spaced Aluminum Arc Gap Structures on Oxidized Silicon", F. Hickernell and J. Crawford in IRPS, 1977
PN	23. "Gate Protection for CMOS/SOS", R. Pancholy in IRPS, 1977
EOS	24. "Electrical Overstress Failures in Silicon Devices", C. Lane in DTIC Technical Report
PN	25. "A Study of the Input Protection Networks of Some NMOS Memory Chips", D. Hinds and R. Crockett in R202 Technical Memorandum
EQ, HBD	26. "Input Protection for MOS Circuits - Supplement" Ferranti Limited in DTIC Technical Report
R, HBD, PN	27. "The Effects of Electrostatic Discharge on Micro Electronic Devices - A Review", Conf. Record of the Industry Applications Society, IEEE, 1981
HBD, CD, EQ, R	28. "Electrostatic Discharge Failures", B. Unger in Circuits Manufacturing, 1981
HBD, CD	29. "Electrostatic Discharge Failures of Semiconductor Devices", B. Unger in IRPS, 1981
HBD	30. "Electrostatic Discharge Effects on MOS Memory ICs", T. Nakamura, H. Kunita and H. Ihara in NEC Research and Development, 1980

Category	Title
 HBD, EQ -	31. "Procedure for Testing Electrostatic Discharge Susceptibility of MOS Devices", A. Goel in IRPS, 1981
EQ, HBD	32. "Surprising Patterns of CMOS Susceptibility to Electrostatic Discharge and Implications on Long Term Reliability", J. Schawank, R. Baker and M. Armendariz in EOS/ESD Proc., 1980
HBD, EQ	33. "Control of Electrostatic Discharge Damage to Semiconductors", E. Freeman, J. Beall in IRPS, 1974
Isolated Device Charge Model	34. "A New Technique for Input Protection Testing", D. Fisch in IRPS, 1981
 HBD, EQ 	35. "A Model for the Failure of Bipolar Silicon Integrated Circuits Subjected to Electrostatic Discharge", T. Speakman in IRPS, 1974
 HBD, EQ 	36. "Predicting ESD kelated Reliability Effects", A. Hart, J. Smyth and S. Gorski in IRPS, 1982
HBD, EQ	37. "Effects of Electrostatic Discharge on Linear Bipolar Integrated Circuits", R. Minear and G. Dodson in IkPS, 1978
 HBD, EQ 	38. "Electrostatic Damage Susceptibiliy of Semiconductor Devices", L. Schreier in IRPS, 1978
 R 	39. "Electrostatic Discharge in Microcircuits, Detection and Protection Techniques", A. Trigonis, JPL Report, 1975

Category	Title
HBD, EQ	40. "Failure Modes and Analysis Techniques for CMOS Microcircuits", A. Shumka, E. Miller and R. Piety, in ATFA, 1977
нво, ео	41. "741 Operational Amplifier Electrostatic Discharge Sensitivity and Subsequent Shifts in Electrical Parameters", D. Baar in Lear-Siegler Report
HBD, EQ	42. "Module Electrostatic Discharge Simulator", T. Madzy, L. Price in EOS/ESD Proc., 1979
HBD, EQ, EUS	43. "Reliability of EOS Screened Gold Doped 4002 CMOS Devices", D. McCullogh, C. Lane, A. Blore in EOS/ESD Proc., 1979
HBD, EQ, PN, EOS	44. "Electrostatic Discharge and CMOS Logic", G. Branberg in EUS/ESD Proc., 1979
EOS	45. "Effects of Electrical Overstress on Digital Bipolar Microcircuits and Analysis Techniques for Failure Site Location", D. Rutherford, J. Perkins in EOS/ESD Proc., 1979
HBD, EQ, PN	46. "Susceptibility of LSI MOS to Electrostatic Discharge at Elevated Temperature", T. Teng, A. Hart, A. McKenna in EOS/ESD Proc., 1979
HBD, EQ, PN	47. "Electrical Overstress Versus Device Geometry" C. Petrizio in EOS/ESD Proc., 1979
HBD, EQ, PN	48. "The Phanton Emitter An ESD-Resistant bipolar Transistor Design and Its Applications to Linear Integrated Circuits", R. Minear, G. Dodson in EOS/ESD Proc., 1979

Category	Title
HBD, CD	49. "ESD Damage From Triboelectrically Charged 1C Pins", P. Bossard, R. Chemelli, B. Unger in EOS/ESD Proc., 1980
PN 	50. "Transient Protection with ZnO Varistors: Technical Considerations", H. Philipp, L. Levinson in EOS/ESD Proc., 1980
PN, EQ	51. "Protection of MOS Integrated Circuits From Destruction by Electrostatic Discharge", J. Keller, in EOS/ESD Proc., 1980
HBD, PN	52. "LSI Design Considerations for ESD Protection Structures kelated to Process and Layout Variations", A. Hart, T. Teng in EOS/ESD Proc. 1980
HBD, PN	53. "Electrostatic Sensivity of Various Input Protection Networks", T. Turner, S. Morris in EOS/ESD Proc., 1980
HBD, EOS, EQ	54. "Microcircuit Electrical Overstress Tolerance Testing and Qualification", R. Antinone in EOS/ESD Proc., 1980
EQ	55. "Measurements of Fast Transients and Applications to Human ESD", H. Calvin, H. Hyatt, H. Mellberg and D. Pellinen in EOS/ESD Proc., 1980
R, HBD, EQ	56. "A Closer Look at the Human ESD Event", H. Hyatt, H. Calvin and H. Mellberg in EOS/ESD Proc., 1981
PN	57. "The Eftects of VLSI Scaling on EOS/ESD Failure Threshold", R. Pancholy in EOS/ESD Proc., 1981

Category	Title
EQ, PN	58. "On Chip Protection of High Density NMOS Devices", T. Hulett in EOS/ESD Proc., 1981
HBD, PN, EQ	59. "Input Protection Design for the 3u NMOS Process", R. Taylor in EOS/ESD Proc., 1981
EQ, HBD	60. "Susceptibility of ICs in Electrostatic Damage Step-Stress Tests", J. Enders in EOS/ESD Proc., 1981
EOS, R	61. "An Overview of Electrical Overstress Effects on Semiconductor Devices", D. Pierce, D. Durgin in EOS/ESD Proc., 1981
EOS, T	62. "Modeling of EOS in Silicon Devices", N. Kusnezov, J. Smith in EOS/ESD Proc., 1981
EUS, T	63. "Semiconductor Device Failure Criteria for Sinusoidal Stresses", R. Thomas in EOS/ESD Proc., 1981
EOS, T	64. "EOS/ESD Failure Threshold Analysis Errors, Their Source, Size and Control", E. Horgan, O. Adams, W. Rowan and L. Templar in EOS/ESD Proc., 1981
HBD, EQ	65. "Time-Related Improvements of Electrical Characteristics in Electrostatically Damaged Operational Amplifiers", G. Head in EOS/ESD Proc., 1981
HBD, CD EQ, PN	66. "Evaluation of Electrostatic Discharge (ESD) Damage to 16K EPROMS", E. Chase in EOS/ESD Proc., 1981

III. TEST PROCEDUKES

Test procedures were developed to be used as destructive step stress to failure tests to determine the voltage level at which device failure occurs. Two test procedures were written, one for the human body simulation and one for the charged device simulation.

The human body simulation test procedure was written in a manner similar to MIL-STD-883B Method 3015.1. The major difference was that each pin on the device was stressed in sequence with all of the other pins connected together as the return path. This configuration is more difficult to implement but allows the weakest path for each pin to be determined as well as testing the power pins which are normally treated differently than the other pins. It is believed that this will provide sensitivity information which closely approximates the sensitivity level of a part in a circuit.

The charged device test is a new procedure which has no similar MIL-STD Method. This method simulates handling, transportation, or non-grounded storage types of failures where a part becomes charged and then it discharges through a pin to a ground plane or to a large object at a different potential. A fixed position for the device, with the device placed upside down on an 8 mil thick teflon glass tape above a ground plane was chosen. Each pin in sequence was slowly charged to a voltage level and then discharged rapidly to ground. The two test procedures follow.

A. "Human Body" Electrostatic Discharge Step Stress to Failure

Test Procedure

1. PURPOSE

This method establishes the means for measuring the level of a simulated electrostatic discharge stress required to produce a failure on a microelectronic circuit. This method will be used for analyzing the sensitivity level of each pin on a device and for quantifying the variation in sensitivity levels between pins.

The simulated electrostatic discharge stress utilized is the waveform as illustrated in Figure 2. This is the "human body" simulation which is designed to produce a waveform comparable to that which will occur if a person charged to a potential level relative to a part comes into contact with that part and there is a current return path out of the part.

- 1.1 <u>Definition</u> The following definition for the purpose of this Test Method shall apply:
- 1.1.1 Electrostatic Discharge (ESD) An electrical current flow (induced by an electrostatic field) between two substances at different potentials.

2. APPARATUS

The apparatus required is an ESD simulation circuit similar to that shown in Figure 1 which will produce the waveform shown in Figure 2. This system should be capable of producing stress levels from -5,000 volts to +5,000 volts.

3. PROCEDUKE

The pulse waveform and parameters as specified in Figure 2 (Note 3 only) shall be verified across the DUT socket, using an oscilloscope with a 1500 ohm resistor in the test socket. A photograph of this pulse waveform shall be taken and kept for reference; one picture shall be taken for each group tested.

- a. Pretest Set high voltage supply to zero. Wire all pins to ground.

 Insert device in test socket.
- b. Set voltage level to +250 VDC. Change pin 1 from its ground connection to the output of the ESD simulation circuit. Apply stress to DUT. Reconnect pin 1 to ground and proceed to next pin. Repeat process until all pins are stressed.
- c. Measure device DC electrical parameters at 25°C. If a pin has out of specification leakage, or is non-functional, remove it from further stress by disconnecting that pin from ground and do not connect that pin to the stress circuitry. Stop test on this device when half of the pins fail this criteria.
- d. Repeat a. through c. with negative voltage at the same level.
- e. Increment voltage upward in 250 volt steps and perform a. through d.

NOTE:

- 1. Value of R_1 shall have a minimum limit of 800 kohm, and a maximum limit of 3 Gohm; and be of a high voltage type.
- 2. All components, and interconnecting wiring shall have voltage and current rating greater than the maximum specified supply value.

 (NOTE: This does not apply to resistors).
- 3. Resistors R_2 and R_3 shall be a matched pair (within 10%), and noninductive, and high voltage withstanding.
- 4. Waveform shall be measured with a 100 MHz minimum oscilloscope (see note 5).
- 5. A high voltage, high impedance (≥ 10 Mohm), low capacitance (≤ 5 pF) probe shall be used when measuring pulse waveform.

- 6. Relay RS₁ contacts shall be of bounceless type (mercury wetted or equivalent), and have a dielectric breakdown voltage and current greater than the maximum specified voltage supply value.
- 7. Effective capacitance shall be determined by charging C₁ to 2,000 Vdc +5% and with no device in test socket and test switch open, discharging C₁ into an electrometer or coulometer connected between points A and B of Figure 2 and calculating effective capacitance which shall be 100 pf + 10%. Effective insulation resistance for C₁ shall be 10¹⁰ ohms minimum.
- 8. All pins of DUT not associated with test procedure shall be connected to ground.
- 9. Resistor R_3 shall be placed in socket across terminals A and B only, when initially discharging circuit for waveform photograph (see 3). Test waveform only will be \approx 50% Vp and \approx 2t_d.

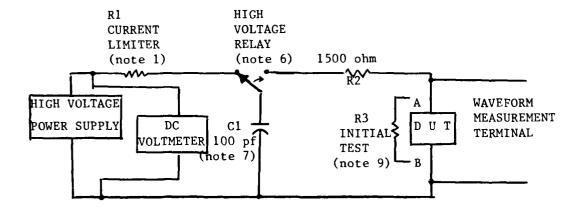


FIGURE 1 ESD Test Circuit

NOTES:

- The rise time, tr, of the pulse voltage, Vp, shall be measured from 10% to 90% of the peak amplitude, Vpeak, and shall not exceed 15 nanoseconds.
- 2. The pulse decay across R_2 to ground shall be a single exponential waveform whose decay time, t_d , when measured between Vpeak and 36.8% Vpeak, is $R_2 \times C_1 + 10\%$, or ≈ 150 ns.
- 3. For initial waveform test only the voltage waveform will have the following characteristics: $V_p = 50\% \pm 15\%$ of voltages in the pulse decay time, t_d , will be $(R_2 + R_3) \times C_1$ or ≈ 300 ns.

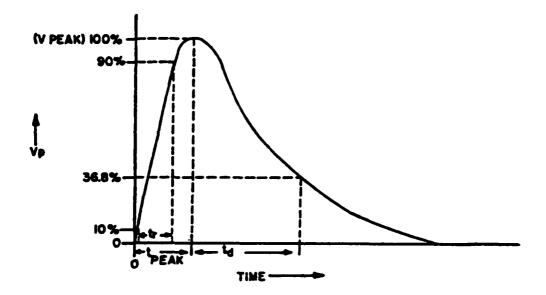


FIGURE 2 ESD Test Circuit Voltage Waveform

B. "Charged Device" Electrostatic Discharge Step Stress to Failure

Test Procedure

1. PURPOSE

This method establishes the means for measuring the level of a simulated electrostatic discharge stress required to produce a failure on a microelectronic circuit. This method will be used for analyzing the sensitivity level of each pin on a device and for quantifying the variation in sensitivity levels between pins.

The simulated electrostatic discharge stress utilized is a waveform similar to that illustrated in Figure 2 (Note 1). This is the "charged device" simulation which is designed to produce a waveform comparable to that which will occur it a part charged to a potential level comes into contact with an object at ground potential and the charge on the part is discharged into that object.

- 1.1 <u>Definition</u> The following definition for the purpose of this Test Method shall apply:
- 1.1.1 Electrostatic Discharge (ESD) An electrical current flow (induced by an electrostatic field) between two substances at different potentials.

2. APPAKATUS

The apparatus required is an ESD simulation circuit similar to that shown in Figure 1 which will produce the waveform shown in Figure 2. This system should be capable of producing stress levels from -5,000 volts to +5,000 volts.

3. PROCEDUKE

The pulse waveform and parameters as specified in Figure 2 (Note 3 only) shall be verified on the 100 pf test capacitor across a 1500 ohm resistor, using an oscilloscope. A photograph of this pulse waveform shall be taken and kept for reference; one picture shall be taken for each group tested.

- a. Pretest Set high voltage supply to zero. Place device on ground plane with leads facing upwards.
- b. Set voltage level to +250 VDC. Connect charge/discharge wire to pin 1. Actuate relays to charge and discharge device. Move charge/discharge wire to next pin. Repeat process until all pins are stressed.
- c. Measure device DC electrical parameters at 25°C. If a pin has out of specification leakage, or is non-functional, remove it from further stress. Stop test on this device when half of the pins fail this criteria.

- d. Repeat a. through c. with negative voltage at the same level.
- e. Increment voltage upward in 250 volt steps and perform a. through d.

NOTE:

- 1. Value of R₁ shall have a minimum limit of 200 Mohm, and a maximum limit of 3 Gohm; and be of a high voltage type.
- 2. All components, and interconnecting wiring shall have voltage and current rating greater than the maximum specified supply value.

 (NOTE: This does not apply to resistors).
- Waveform shall be measured with a 100 MHz minimum oscilloscope (see note 4).
- 4. A high voltage, high impedance (≥ 10 Mohm), low capacitance (≤ 5 pF) probe shall be used when measuring pulse waveform.
- 5. Relay RS₁ and RS₂ contacts shall be of bounceless type (mercury wetted or equivalent), and have a dielectric breakdown voltage and current greater than the maximum specified voltage supply value. Relay RS₂ will close before RS₁ opens and will remain closed until RS₁ opens.
- 6. All pins of DUT not associated with test procedure shall be open.
- 7. Resistor R₂ shall be placed in socket across terminals A and B instead of the shorting bar and capacitor C₁ shall be placed from C to ground when initially discharging circuit for waveform photograph.

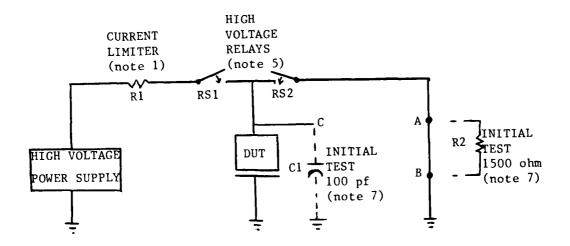


FIGURE 1 ESD Test Circuit

NOTES:

- 1. The waveform appearance during initial test is a damped sinusoid superimposed on an exponential. This is an underdamped case with LC \leq 4R²C². Actual waveform will be the overdamped case since LC > 4R²C² as R decreases.
- 2. This waveform will reach a peak higher than the input voltage level and will decay in approximately 150 nanoseconds.

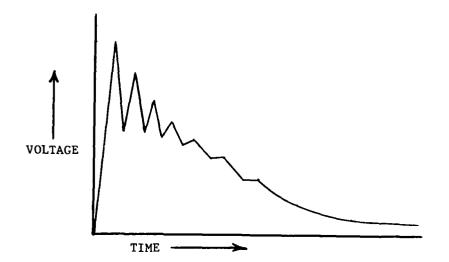


FIGURE 2 ESD Test Circuit Voltage Waveform

The objective in the design of the test equipment was to allow easy and rapid testing of devices with up to 64 pins. The original idea was to build an automatic or semi-automatic system that would stress each pin in sequence. Discussions with persons that have attempted to build an automated system and research performed for this study, determined that this was not within the scope of this effort. The system shown in Figure IV-1 was developed to accomplish the testing. Additional apparatus is shown in Figure IV-2. The boards can handle standard dual-in-line packages from 14 to 64 pins.

The test tool has a variable supply from -5,000 volts to +5,000 volts. This allows parts to be taken in a step stress manner to failure rather than establishing just a fixed susceptibility level. The polarity is controlled by a switch on the front panel and the level is controlled by two sets of potentiometers, fine and coarse. The other control on the front panel switches the model from the human body discharge simulation (HBD) to the charged device (CD) simulation. The boards have parasitic capacitance of 9.1 pf, 10.4 pf and 13.2 pf going from the 20 pin fixture up to the 64 pin fixture. The bottom sides of the zero insertion force sockets and the first termination of the wires coming from the socket are coated with silastic-E, a high breakdown voltage, silicone potting compound. This combined with silicone rubber wiring eliminates the chance for corona discharge between adjacent pins. The stress application point is connected to the appropriate device pin by a shorting pin which slips through the top jack and board, a guide hole in the middle board and into a jack connected to a copper trace on the bottom PC board. The simulation circuit is the standard 100 pf, 1500 ohm RC discharge network. The risetime of the pulse was about 5 ns with no test board in place and about 15 ns with the 64 pin fixture. It was a repeatable exponentially decaying waveform with no apparent ringing (Figure IV-3). A single pin is connected to the discharge circuit. The remaining pins are connected to a trace that goes to ground via shorting pins.

The charged device model board is as shown on the right-hand side of Figure IV-2. The part is placed upside down on a piece of teflon glass tape (8 mil) that is attached to a copper clad PC board. The copper clad board is tied directly to ground and the part is connected through a silicone wire to the stress voltage. The entire device is slowly charged to a voltage level and is then shorted to ground. The short to ground is applied before the charging voltage is removed from the device and both switches are opened at the same time. The capacitances measured between the ground pin on each device and the copper plate were:

Devi	e	Pins	Capacitance (pf)
Part	G	64	34
Part	E	40	19
Part	Α	40	18
Part	Н	40	16
Part	В	24	11
Part	С	20	8
Part	D	20	6
Part	F	18	5

To allow examination of the signal for the charged device model a plate was constructed which measured 100 pf when placed on the fixture. This had a pin which was connected to the stress circuit and a 1500 ohm resistor was used between the relay and ground. The waveform was measured across this resistor. This waveform is as shown in Figure IV-4. The ringing is due to the inductance of the discharge circuitry.

The schematic for the test tool is shown in Figure IV-5. The two time delay relays were designed into the circuit to allow control of the timing between the activation of the first mercury displacement relay and the activation of the second mercury displacement relay. Analysis with devices in the charged device circuit found that it was necessary to have the second relay discharge the device to ground prior to the first relay opening. The non-inductive 100 megohm resistor was placed between the two relays to provide additional current limiting and isolation between the device under test and the first relay.

The test tool operation is as follows:

General

- 1. Connect power cord to 120 VAC.
- 2. Set front panel rocker arm switch to ON.
- 3. Set voltage controls to zero (Counterclockwise).

Human Body Discharge

- 1. Set test switch to human body discharge.
- 2. Place test fixture on test tool (20, 40 or 64 pin).
- 3. Place part (D.U.T.) in test fixture.
- 4. Select pin to receive stress by connecting to inside (red) track.
- 5. Connect remainder of pins to ground (black).
- 6. Set polarity and voltage level, set voltage level of polarity not used to zero.
- 7. Press stress button and hold for 1 second.
- 8. Repeat steps 4 7 at next pin.

Charged Device Model

- 1. Set test switch to charged device model.
- 2. Place CDM test fixture on test tool.
- 3. Place part (D.U.T.) on test fixture with legs pointing upward.
- 4. Connect wire to pin to be stressed.

- 5. Set polarity and voltage level, set voltage level of polarity not used to zero.
- 6. Press stress button and hold for 1 second.
- 7. Repeat steps 4 6 at next pin.

The parts utilized for this test equipment are as follows:

Test Tool Parts List

Name	Number	Manufacturer
Slant Front Cabinet Mercury Displacement Relay Digital Panel Meter 72 Volt Unregulated Power Supply Positive High Voltage Power Supply Negative High Voltage Power Supply High Voltage Relay On Delay Timer 24 Volt Power Supply Potentiometer, 100 ohm, 10 turn Potentiometer, 5000 ohm, 10 turn High Voltage Silicone Wire Resistor, 100 Megohm On/Off Switch Resistor, 1500 ohm High Voltage Ceramic Disc Capacitors Interval Timer Momentary Switch	DSSF-10506 WM35A-120A RM-452TB/DC U72Y25 PMT-50A-P PMT-50A-N 24HV1A-75 SSC12AAA 524H1-C 3540S-1-101 3540S-1-502 37F2103 ROX-1 35-620 FERW DD60-XXX SSC32AAA 35-844	buckeye Magnecraft Non-Linear Systems Acopian Bertan Bertan Douglas kandall Beabout EkA Transpac Bournes Bournes Dearborn Dale Electronics GC Electronics Centralab Beabout GC Electronics
DPDT Switches Silicone Potting Connector Fuse Power Cord	35-138 E 143-012-01 1 amp 3 Prong	GC Electronics Dow Corning Amphenol

Test Board Parts List

Name	Number	Manufacturer
Copper Clad PC Boards	22-263	GC Electronics
Shorting Pins	Custom	LVC Industries
Horizontal Jacks, Red	105-0752-001	E.F. Johnson
Horizontal Jacks, Black	105-0753-001	E.F. Johnson
Zip Dip Socket, 64 Pin	264-4493-00-0602	Textool
Zip Dip Socket, 40 Pin	240-3346-00-0605	Textool
Zip Dip Socket, 20 Pin	220-3342-00-0605	Textool
Banana Jacks	Male	-
Teflon/Glass Tape	6085-06	Taconic

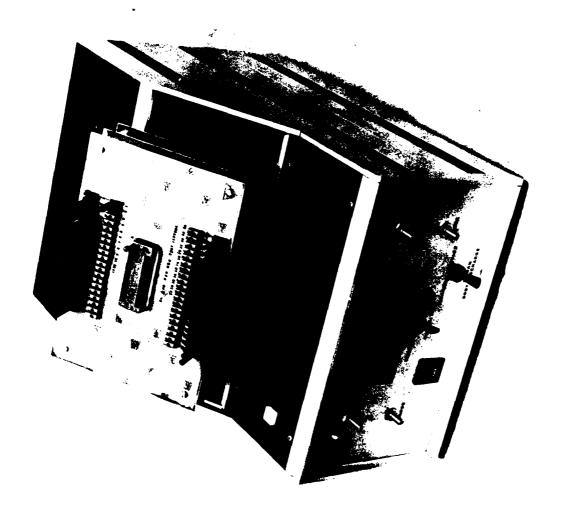


Figure IV-1 - ESB Simulation lest lool.



Figure IV-2 - ESD Test Fixtures.

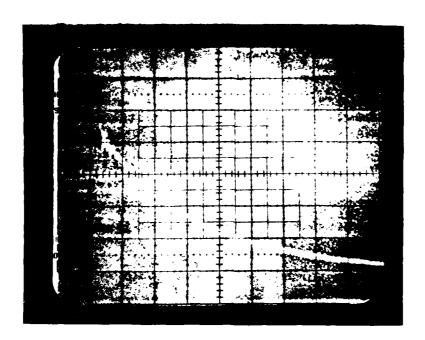


Figure IV-3 - Human Body Simulation ESD Test Waveform, 200 volts/div, 100 nanoseconds/div.

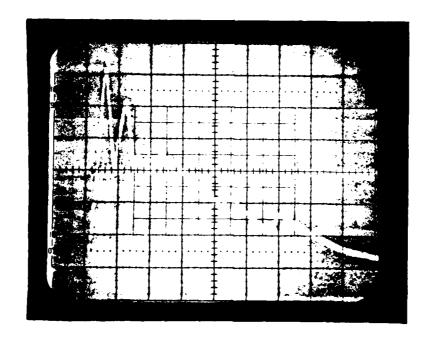


Figure IV-4 - Charged Device Simulation ESD Test Waveform, 100 volts/div, 50 nanoseconds/div.

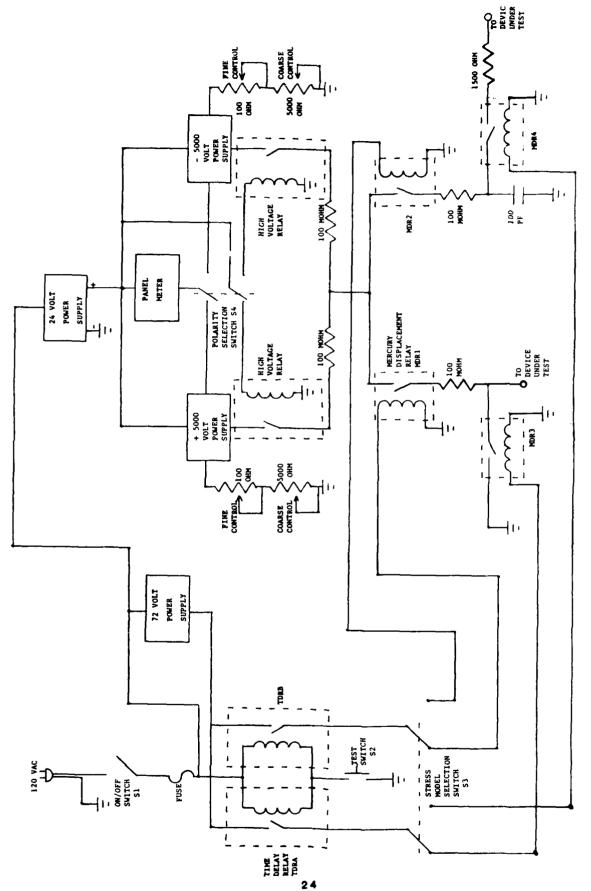


FIGURE IV-5 ESD Test Tool Schematic

Parts were selected for this study to provide a variety of technologies, functional types, and manufacturers. Within these constraints, parts with the finest linewidths were selected. The table below lists the parts chosen. Thirty-five devices of each group were ordered, providing 5 devices for physical analysis, control parts and test set up. The remaining thirty parts were divided into two groups of fifteen parts each for the two ESD simulation models.

Device	Function	Technology
Part A	lK RAM, I/O, Timer	CMOS
Part B	8K Static RAM	NMOS
Part C	Octal Latch	Schottky
Part D	Octal Latch	Schottky
Part E	2K RAM, I/O, Timer	NMOS
Part F	4K Static RAM	CMOS
Part G	Microprocessor	NMOS
Part H	Microprocessor	NMOS

The parts chosen included six MOS devices and two bipolar devices. This ratio was picked due to the greater sensitivity of MOS devices and due to the smaller dimensions generally available. NMOS was the most common technology chosen due to the number of small geometry LSI and VLSI circuits in this category. The Schottky parts were included to obtain a bipolar part in the study and due to its reported sensitivity to ESD. The difference in failure mechanisms and ESD model sensitivity was also considered. These Schottky devices were the simplest circuits functionally. The specific functional types were kept to four to allow intercomparisons between manufacturers, technologies, and function.

Characterization was performed on each of the eight devices. This characterization included schematic development of the interface circuits, electrical measurement of these components, measurement of dimensions, and microsections.

The same procedure was followed on each device. The package was opened and the die was examined on the light microscope at 50% to 600%. The general layout of the supply metallizations was traced. The layout of the circuitry for each of the other pins was examined. Variations in the layout or the appearance of the circuitry were noted at this time and specific pins were selected for schematic development. The schematics were developed for a typical input, typical output, and for a portion of the circuitry connected to the supply lines (V+, V- and ground). If variations in the electrical schematic were evident, then the schematic for each type was developed.

The glass passivation was stripped as necessary to allow examination and identification of the circuit components.

A minimum of one device of each type was microsectioned. These microsections were performed through areas that provided information related to the failure modes.

Each of the eight parts will $L_{\rm c}$ discussed individually. These are included in sections A through H which follow.

A. Part A Analysis

This device is a RAM-I/O-Timer fabricated using a P^2 CMOS silicon gate technology. This device has 1024 bits of static RAM (128 x 8), 22 programmable I/O ports, and two programmable 16-bit binary counters.

These devices have one layer of metallization and two layers of polysilicon. This was in a 40-pin dual-in-line metal lid ceramic package. An overall die photo is shown in Figure V.A.l. VCC is pin 40 at the top of Figure V.A.l and VSS is pin 20 at the bottom. VCC is also connected to the package substrate via a bond wire. VCC is distributed around the perimeter of the die by both a polysilicon stripe and an overlying metallization stripe. VSS traverses around the die on the inside edge of the bond pads.

The VCC bond pad is shown in Figure V.A.2. It is connected to the substrate, to the body connection for the N-Channel MOS transistors, and to the sources of the P-Channel MOS transistors.

The VSS bond pad is shown in Figure V.A.3. This metallization is connected to the body connection of the P-Channel MOS devices and to the sources of the N-Channel MOS devices.

An input structure is shown in Figure V.A.4 and the schematic is shown in Figure V.A.5. This structure has diodes to both VCC and VSS as shown. The junction breakdown of each of these diodes and of the drain to body junction on the N-Channel and P-Channel FETs is about 30 volts. The gate dielectric breakdown was 70 volts. The input protect resistor is polysilicon and the connections to the protect diodes comes from the point at which the resistance measurement was taken.

An input/output structure is shown in Figure V.A.6 and the schematic is shown in Figure V.A.7. The input protect diodes are incorporated into the output transistors rather than being separate components. The output is the standard CMOS configuration. The output only pins had protect diodes present. An example is shown in the photograph in Figure V.A.8 and the schematic in Figure V.A.9.

The schematics for each of the inputs and I/O combinations were identical, however the protect resistor, protect diodes and output transistor layouts varied slightly.

Microsections were performed through the input/output sections. This appeared to be the standard CMOS process with an n-type substrate. The thicknesses measured were: polysilicon = 0.35 microns, metallization = 1.2 microns, p diffusion for N-Channel body = 8 microns, n+ and p+ diffusions = 1 micron, dielectric between two polysilicon layers = 0.1 microns, dielectric between polysilicon and aluminum = 1.0 microns.

The standard CMOS processing along with a top and side view of a section through an input/output is shown in Figure V.A.10.

Electrical Test

Electrical testing was performed on the Tektronix 3260 after each stress. This testing consisted of $v_{OH},\,v_{OL},\,I_{OL}$ and $I_{IL}.$ A sample printout of the initial electrical test is provided in Figure V.A.ll. This same serial number is shown in Figure V.A.l2 following the -1500 volt stress. I_{IL} and I_{OL} provided information on the gradual degradation of the inputs and output.

This testing also provided a functional check of the following. The control logic (CE, WR, RD, IOT/M, ALE, and RESET), ports and associated data direction registers, and the address/data buffers and latches were tested for operation in their various modes. The mode definition register, the handshake logic, TO high and low order registers, and the TO prescale and command registers were partially tested. One 8 bit wide section of the 128 section RAM was accessed. The Tl high and low order registers, and the Tl prescale and command registers were not accessed.

Charged Device Data Analysis

Serial numbers 17 through 31 were subjected to the charged device model of ESD stress. Device damage occurred at low voltage levels with 5 devices being removed from stress following the +750 volt stress and the remaining parts being removed from test following the -750 volt stress.

The parameter which changed first with the stress was the $I_{\rm IL}$ reading. This parameter did not degrade through the nanoamp region as was experienced with Part B but went to high microamps or milliamps at first indication of failure. A summary of the pins that failed this parameter and the level at which this occurred is shown in Figure V.A.13. The pin 9 failures occurred at the first stress point and pin 3 failures occurred at the second stress point. As the pins failed they were removed from further stress. Pin 9 was the RD-not input which enables ADO-AD7. When pin 9 failed the $I_{\rm IL}$ test, a functional failure of $V_{\rm OH}$ and $V_{\rm OL}$ occurred on these eight pins. Other functional failures occurred related to damage at other inputs.

All of the devices were opened and analyzed. There was more damage present than had been expected from the leakage current measurements. The amount of damage explained the reason for the loss of functionality on the parts. Each device was examined and some mechanical probing and measurements were done to verify the visual indications.

The seven input pins are shown in Figures V.A.14 - V.A.20. Pins 4 and 11 have similar layout configurations, and pins 7, 8, and 10 have similar configurations. Pins 3 and 9 were different than the rest. They are shown in Figures V.A.19 and V.A.20 and have a condition which made them more susceptible to damage. Within close proximity to the input polysilicon resistor there was another polysilicon stripe.

On pin 3 the polysilicon stripe ran parallel to the input polysilicon. This parallel stripe was just a continuation of the input resistor, however, during stress a potential level would develop between these two stripes and a breakdown would occur. Electrically this created leakage down to the substrate or up to overlying metallization.

Pin 9 had a layout like pin 4 and 11 except for a polysilicon stripe that ran underneath the input resistor. This created the most easily damaged input structure.

Eight devices were categorized for failure mode appearance. These were serial numbers 17, 19, 20, 27, 28, 29, 30, and 31. The pins which had similar layouts exhibited similar damage. Pins 4 and 11 were by far the least damaged. No damage or only slight damage was seen on pin 4 on 5 of the devices. No damage or only slight damage was seen on pin 11 on 3 of the devices. The type of damage seen is shown in Figures V.A.21 - V.A.33. Pin 7, 8, and 10 were visibly damaged on all parts. This damage was generally in the bottom of the U-shaped portion of the polysilicon resistor. Several of these are shown in Figures V.A.25 - V.A.28. Two other damage conditions were seen. On serial numbers 27, 28, 30 and 31 damage occurred at the first contact point between polysilicon and metallization (Figure V.A.29). This may have been due to a resistive contact at that point. On serial number 28 pin 10, a breakdown through the thermal oxide occurred. There was likely a defect in the oxide at that point (Figure V.A.30). The failures on pin 3 appeared as shown in Figures V.A.31 and V.A.32.

The stress on pin 9 was stopped after a single application of +250 volts. Shorts were created between the two polysilicon stripes, however, there was no visible damage on 6 of the devices. Damage which was visible on the other devices is as shown in Figure V.A.33.

The charged device model stress was found to cause damage to all of the input circuits and none of the output circuits. In electrical testing pins 9 and 3 showed up first. These pins could be made less sensitive by a minor layout change. The best configuration to use if a polysilicon resistor is incorporated into the protection network is a straight run since damage occurred first at corners.

Human Body Discharge Data Analysis

Serial numbers 2 through 16 were subjected to the human body ESD simulation test method. Device damage was measurable electrically following the -250 volt stress. The first device was removed from test after the -750 volt stress and all devices were failed after the -1500 volt stress.

A summary of the cumulative leakage failures is shown in Figure V.A.34. Pin 9 was the most sensitive to stress followed by pin 3. Pins 3, 7, 8, 9, 10 and 11 are inputs and pins 19, 27 and 33 are input/outputs. Failure analysis on serial number 3 which had the failures on pins 10, 27 and 33 found that pins 27 and 33 were related to the state the output was being driven to during the measurement, rather than an actual failure in the output.

All devices were visually examined and eight of these were categorized. There was no output damage visible and the inputs were damaged as shown in Figure V.A.35. A subjective analysis of the visible surface damage was performed and the pins classified. The classification of open meant polysilicon open, short meant breakdown between two polysilicon stripes, slight damage meant minor indications of heating such as discoloration or small cracks, and damage meant significant physical damage to the polysilicon but not to the point of open.

Figure V.A.35 shows that parts that were taken through -1500 volt stress generally failed with open polysilicon. The part that was stopped at -750 volts showed only slight visible damage. These results indicate that polysilicon does degrade partially at low stress levels, however, there is no way to monitor that using external measurements. The probable change which occurs is an increase in resistance.

Photographs of the damage are shown in Figures V.A.36 - V.A.42. Figure V.A.36 shows pin 3 damage. There is a breakdown between the two adjacent polysilicon stripes and also some small cracks which ran parallel to the resistor. Figure V.A.37 shows the type of slight damage that was seen. This is pin 4 and there are small cracks in the resistor. Figure V.A.38 shows a polysilicon open on pin 4. Figure V.A.39 shows a polysilicon open on pin 7. Figure V.A.40 shows a polysilicon open on pin 10. Figures V.A.41 and V.A.42 shown opens on pin 11. All of the opens shown occur immediately before the contact window to the protect diodes. This may indicate a current crowding effect causing the heating.

The failure modes seen are different for the two stress modes. The human body discharge stress required a higher voltage however when the parts failed more severe damage was done. The location of the damage was repeatable within the two stress groups but was slightly different when comparing between the two groups. This difference is likely related to pulse duration and the polysilicon heating which occurs.

The subcatastrophic damage that occurs at low levels to the polysilicon makes it possibe for latent problems to exist. This has not been proven but is a concern. The use of polysilicon stripes in the input sections does not appear to be desirable. A latent defect study on parts which are stressed below the catastrophic level could provide this information. An ESD stress test followed by a dynamic life test would be a method to investigate this

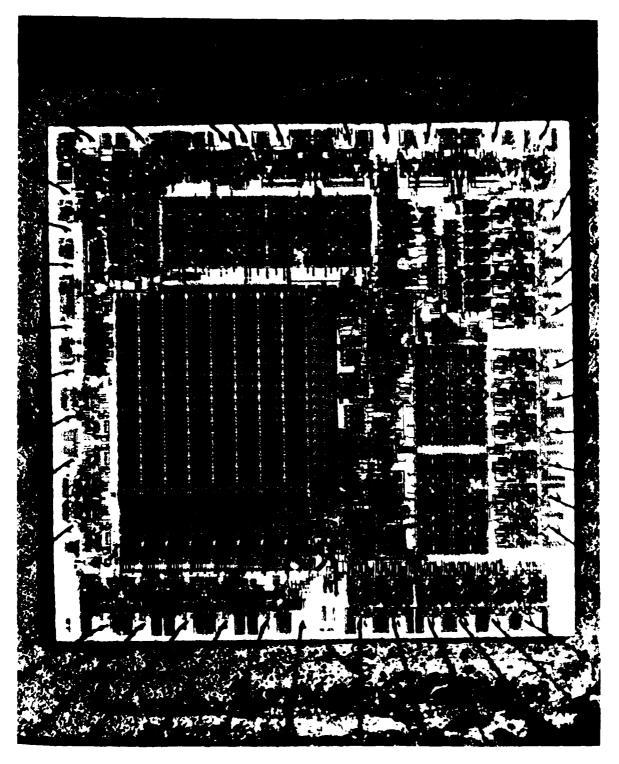


Figure V.A.1 - Overall Die Photograph

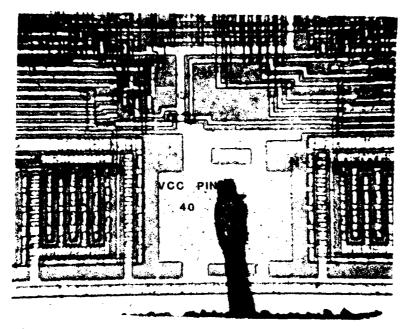


Figure V.A.2 - VCC Bond Pad and Connections

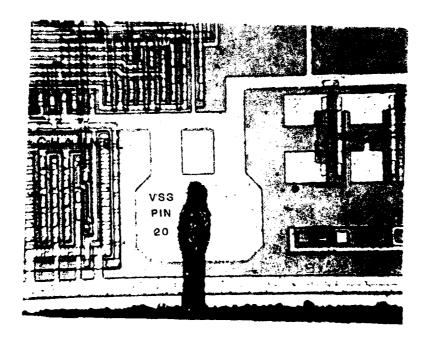


Figure V.A.3 - VSS Rond Pad and Connections

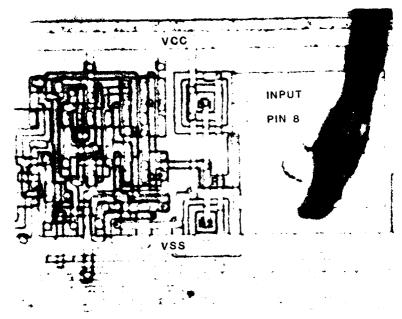


Figure V.A.4 - Pin 8 Input

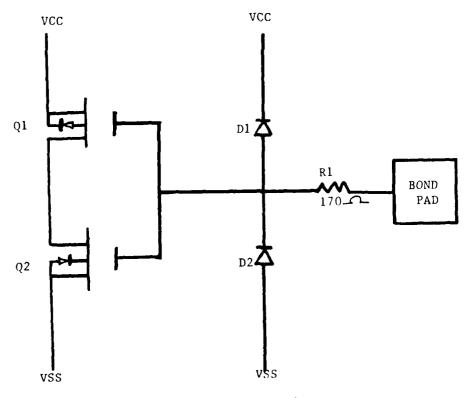


Figure V.A.5 - Input Schematic

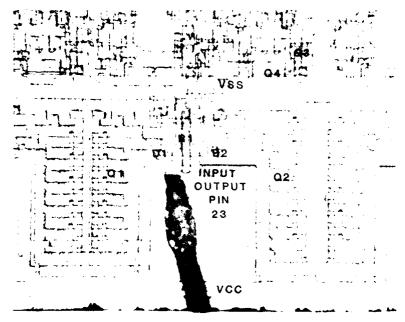


Figure V.A.6 - Pin 23 Input/Output

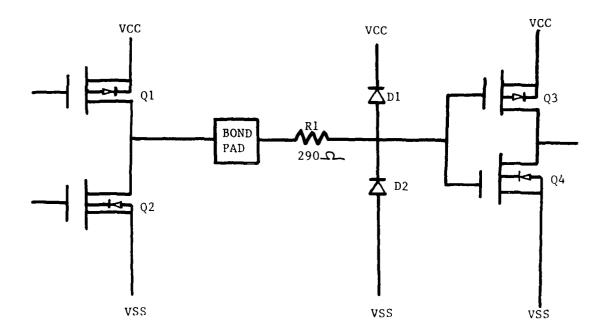


Figure V.A.7 - Input/Output Schematic

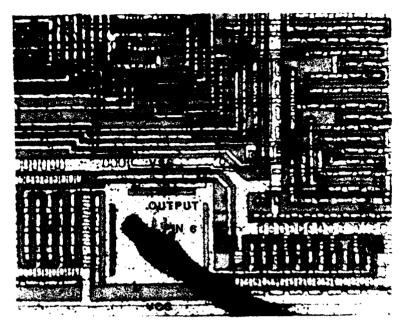


Figure V.A.8 - Pin 6 Output

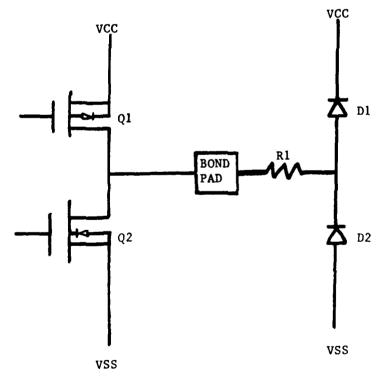


Figure V.A.9 - Output Schematic

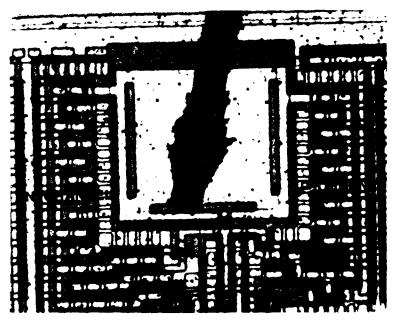


Figure V.A.10 - A. Input/Output Surface Layout

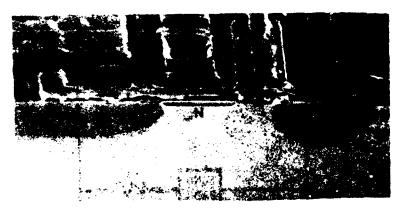


Figure V.A.10 - B. Cross-section Through Area Marked in A

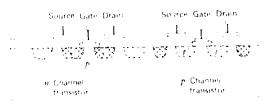


Figure V.A.10 - C. CMOS Structure

MARTIN MARIETTA AEROSPACE -- DENUER DIVISION -- PARTS EVALUATION LAB

PART NUMBER - FILE UID :149 SERIAL NUMBER - 5 TESTED AT 25 DEG. C NO. 1 ELECTRICAL ON 14 JUL 83 AT 12:55:32 WITH THE 32:60 TEST SYSTEM

ALL	TEST TYPE		MEASUREII VALUE	L I M I NUMININ	NUMINA MAXINUM	
	V0H1		4,360 U	2,400 U		
	VOH1		4,360 U	2.400 V		
	VOH1		4,360 U	2:400 V	~-	
	90H1		4,355 0	2.400 V		
	VOH1		4.350 V	2:400 V		
	('0H1		4,355 (2.400 V	~-	
	VOH1		4.350 U	2:400 V		
	VOH1		4:355 V	2:400 U		
	VOH1		4.360 0	2.400 V		
	COH1		4.360 \	2.400 0	~-	
	ยอสา		4.355 V	2:400 9	~-	
	VOH1		4.355 U	2,400.0	~-	
	110H1		4,355 V	2,400 V		
	UOH1		4.360 0	2.400 V		
	MOH1		4,365 0	2,430 U	~-	
	V0H1		4.365 V	2,400 V		
	VOH1	-	4.360 0	2:400 V		
	COHI	-	4,355 0	2,400 0		
	VOH1		4:350 V	2,400 9		
	VOH1		4.350 (2,400 V		
	QOH1		1.355 V	2.400 V		
	110H1		4,360 V	2,400 V		
	VOH1		4:365 (2-400 V		
	UOH1		4,365 V	2,400 0		
	VOH1		4.365 V	2,400 U		
	VOH1		4.355 V	2.100 V	·	
	VOH1		4.355 V	2,400 V		
	VOH1		4.355 V	2,400 V		
	VOH1		4.355 V	2,400 0		
	V0H1	-	1,355 V	2,400 V		
	VOH1		4,350 U	2,400 V		
	90H2		4,495 U	4,000		
	уона		4.495 (4,000 0		
	POHE		4,495 0	4,000 (
	V0H2	 -	4.495 !!	4,000 V		
	VOH2		4.495 0	4.000 0		
	CHON		4.495 U	4.000 0		
	V0H2	- -	4.490 U	4,000 0	- -	
	V0H2		4.495 (4,000 V		
	V0H2		4:495 (4,000 U		
	V0H2		4,495 0	4,000 (
	90H2		4,490 (1,000 V		
	VOH2		4,490 (1,000 U		
	VOH2		4,495 U	4,000 0		
	V0H2		4+495 V	4,000 V		
	VOH2		4.495 U	4.000 0		
	V0H2		4.495 U	4,000 V		
	V0H2		4:495 U	A COURT OF		

Figure V.A.11 - Initial Electrical Test

FILE UID :149 SERIAL NUMBER - S (ESTED AT 25 DEG. C. NO. 1 ELECTRICAL ON 14 JUL 83 AT 12:56:03 WITH THE 3260 TEST SYSTEM

- ATL	TEST Type		MEASURFII VALUE	L I H MINIMUM	T S MAXIBUM	
	VOH2		4,490 (4.000 U		
	U0H2		4.490 0	4,000 0		
	VOH2		4.495 U	4,000 V		
	CHON		1,495 (4,000 0		
	VOH2		4.495 0	1.000 V		
	V0H2		4,495 9	4,000 0		
	VOH2		4,495 U	1.000 0		
	UOH2		4.490 (4. <u>ტა</u> რ 🤥		
	VOH2		4:490 V	4.000 0		
	V0H2		4,495 (4.000 U		
	VOH2		4.495 V	4.000 0		
	VOHE		4,495 U	1.000		
	VOH2		4.495 U	1 000 0		
	CHOV		4 (490 - 9	1.000 9		
	VOL1		114.0nV		300 Ob	
	VOL1		106.560		*05.000	
	VOL1		105 : 0mV		100 06	
	90U1		84.50hV		ف يُ روزون	
	MOL1	-	85.50%0		Section Con	
	90 L1		85 50NY		400,000	
	**OL1		84.00hV		100. Ca	
	VOL 1		93.50mW		400.000	
	COLI		83,5000		400.364	
	VOL1		85.50NV		400.065	
	VOL1	-	86.00MV		400.006	
	1/0L1		86.50HU		100.060	
	V0L1		V400.88		400.060	
	99L1		87,50HV		400.00	
	90E1		89,0000		300.08	
	UOL1		91.00mU		400 000	
	90u t		PP.OOMU		300.09	
	VOLI		98.00mU		100.069	
	USL1		98.5060		400 004	
	W0L1		98,50hU		300,000	
	VOL1		97 (00114		400.000	
	VOL1		96.5060		460.064	
	VOL1		97.50MV		400.0ms	
	00L1		99.506U	~ +	100 2 (OH)	
	VOL 1		97.50hV		100 Ont	
	VOL1		118.069		100 000	
	VOL 1		119.0mV		300,000	
	VOL 1	~ 	125,060		100 (0m5	
	VOL1		127.0mV		400.00	
	VOL1		122.060		100.000	
	VOL1		117.080		400.0M	
	VOLO		2 (100MV		100.000	
	VOL 2		1.95080		100+0hi	
	VOLE		2,00080		100 (01)	
	VOLO	_	1.300MU		100 (61)	

Figure V.A.11 - Initial Electrical Test (Cont.)

FILE UID :149 SERIAL NUMBER - 5 TESTED AT 25 DEG. C NO. 1 ELECTRICAL ON 14 JUL 83 AT 12:56:35 WITH THE 3260 TEST SYSTEM

FAIL	TEST TYPE		NEASUREI VALUE	L I M MINIMUM	I T S MUMIXAM
	VOL2		1,000MV		100 - 0HV
	V0L2		900,000		100.060
	VOL 2		700.00V		100.0MV
	VOL2		500.000		100.0MU
	VOL 2		900.0FM		100:060
	VOL2		650.0UV		100 , 0hV
	VOL2		950.000		100.0MV
	VOL2		1,250KV		100.0NV
	VOL2		800.000		100.0hU
	VOL2		750 i OUV		100.0mV
	VOL2		500,007		100.0MU
	VOL2		750.0UV		100.000
	VOL2		1.000MU		100.000
	VOL2		1.100MV		100.089
	VOL2		750.0UV		100,0MV
	VOL2		800,000		100.0mV
	VOL2		750 ₁ 000		100,000
	VOL2		700,000		100.0340
	VOL2		790.OUV		100.0mV
	VOL2		1.000HV		100 cOhV
	ADES.		1.100MU		100.089
	VOL2		900,000		100.060
	VOL2		950.0UV		100.0NU
	VOL2		3:650MV		100.060
	VOL2	<u> </u>	3,400MV		190.040
	VOL2		3.350MV		100.080
	VOL2		3.400MV		100.00V
	IIL		2,200NA	-1.00000	1,00000
	IIL		0.000 A	-1.000UA	1.00000
	III		1 - 700FA	-1 000UA	1 00004
	IIL		200 JOPA	-1,000 <u>00</u> 0	1 99196
	IIL		1 - 85086	-1,000000	
	IIL		0.000 A	-1,00000	t . godun
	IIL		950.0PA	-1.000UA	1.000UA
	IIL		500,0PA	-1,000UA	1.00000
	III		1.600NA	-1,000UA	1,000UA
	[]]	 -	0.000 A	-1.000UA	1 : 000UA
	IIL		1,100NA	-1,000UA	1.00004
	III		400 (OF A	-1.000UA	1.00000
	IIL		1 4600NA	-1,000UA	1.000UA
	IIL		0.000 A	-1,000UA	1,000UA
	[I L		1,100NA	-1.000UA	1.000UA
	IIL		450, OF A	-1:000UA	1,00004
	IIL		300,0PA	-1.000UA	1.000UA
	ITL		0.000 A	-1,000UA	1,000UA
	I I L		300,0FA	-1.000UA	1,000UA
	IIL		400.0FA	-1,000UA	1,00000
	ſIL.		1.750NA	-1.000UA	1,0000A
	IIL		900,0PA	-1,000UA	1.000UA
	IIL		900,014	-1 i 000UA	1 - 000UA

Figure V.A.11 - Initial Electrical Test (Cont.)

FIRE HID 1149 SEPIAL MURBER - 5
HINTED AT 25 MFG. (NO 1 ELECTRICAL
ON 14 JUL 83 AT 12:57:09 WITH THE 3 AO TEST SYSTEM

F & C.	TEST TYPE	REASURED	LIG	
	11FE	 VALUE	mINIMUm 	MUNIXAM
	IIL	 1 - 15046	-1 000UA	1.สอดอันก
	IIL	 and total	-1.00000	1/05/98
	1 I T	 9 990 A	-1 : 000UA	1 , 0 and 0 $ ilde{ ext{d}}$
	IIL.	 0,000 A	-1.000UA	1.00000A
	1.14	 SOO.OPA	-1:000UA	1 000006
	III	 -190:0FA	=1 +000UA	1 000002
	111	 2.80046	-1.000UA	1,00000
	IIL	 -650.0FA	-1.000UA	1.000007
	111	 きょえいせんち	-1.0600/	$1 \times 0.0000 \mathrm{M}^{\star}$
	IIL	 -600.0PA	-1.000UA	1.000008
	111	 2:750HA	-1.000Un	1 - 500 0 UA
	IIL	 -900.0PA	- 1 / 000UA	1 (1994)
	IIL	 2.700NA	-1.000WA	1 - 000006
	IIL.	 -850.0PA	-1.000UA	1 / 900 0006
	IIL	 2:700NA	-1,000UA	1 - 000000
	IIL	 -800.0FA	-1 - 000UA	1.000006
	IIL	 2,500NA	- 1 . 000Un	1 0000UA
	IIL	 -950,0FA	-1.000UA	1.00000
	I. I. L.	 2.500MA	+1 : JUDUA	1 - 000 mga
	T [L	 -850.0FA	-1.000UA	1 . 069000
	[IL	 2 (400)46	-1.000Uñ	1 0 200
	Ill	 -1:200HA	-1,000UA	1.00006
	IIL	 2:400NA	-1.000UA	1,00000
	IIL	 -1.050NA	-1 - 00000A	1,00000
	IIL	 2 / 400NA	-1.000UA	1.00000
	IIL	 -1:100NA	-1.000UA	1,000UA
	1.11	 2:050NA	-1.000UA	1,00000
	I I L	 -1.250NA	-1.000UA	1 / 000UA
	IIL	 2 × 000M6	-1 . 00 <u>0</u> 00	1 000096
	IIL	 -1.200NA	-1+000UA	1,600006
	1.11	 2 10mm	-1 000UA	1 00000
	IIL	 ±1 450RA	-1 000UM	1.00000
	IIL	 2,000HA	-1 - 0000UA	1,0000
	IIL	 -1 (350MA	~1 : 00000h	1 - ᲛᲔᲛᲛᲡᲛ
	ILL	 2.100MA	-1 - 000006	1,000000
	111	 -1:400NA	-1.000UA	1.00000
	TIL.	 1.900NA	-1 coooun	1.000004
	IIL	 -1,500RA	-1 000Un	1 00007
	IIL IIL	 2. 100NA	-1 - 000UA	1 មិនម៉ូប៉ូត
		 -1 - 150MA	-1 : 000UA	1.00000
	IIL IIL	 1,900NA	- L - 0000UA	1. OKHADA
	IIL	 -1,750NA	-1.000UA	1.00006
	III.	 2:000NA -1:4100N	-1.000UA	1,600,00
	IIL	 -1 - 650/65	-1.000UA	1,000046
	IIL	 1,950NA	-1:000UA	1,000UA
	IIL	 -1.550MA	-1 -0 JOUA	1 00000
	ITL	 1,85086	-1.000UA	1,60000
	IIL	 -1,4LONA	-1.000UA	1.000UA
		 1,900NA	-1.000UA	1,00000
	IIL	 -1,400NA	-1 coopun	1.00000
	111	 1.950NA	-1.0000UA	1 00000

Figure V.A.11 - Initial Electrical Test (Cont.)

FILE UID :149 SERIAL NUMBER - 5 TESTED AT 25 DEG. C NO. 1 ELECTRICAL ON 14 JUL 83 AT 12:57:43 WITH THE 3260 TEST SYSTEM

	TEST		MEASURFD	LINITS		
- 6.t.L.	TYPE		VALUE	MINIMUM	AUMIXAN	
	IOF		200.0FA	-1,000UA	1 - 00906	
	IOL		2.800MA	-1,000UA	1.00000	
	IOL		-600.0PA	-1,000un	1 000UA	
	IOL		2.700NA	-1 c000UA	1.000UA	
	IOC		-700.0PA	-1.000UA	1 - 000UA	
	107		2,850NA	-1,000UA	1,000UA	
	LOL		-650.0FA	-1:000UA	1.00000	
	IOL		2:800NA	-1,000UA	1,000UA	
	101		-650.0FA	-1.000UA	1.000UA	
	IOL		2:550NA	-1.000UA	1.000UA	
	IOL		-550,0PA	-1.000UA	1 (00006	
	IOL		2.550NA	-1.000UA	1:000UA	
	IUU		-800.0PA	-1.000UA	1.000UA	
	IOL		2.500NA	-1.000UA	1.00004	
	JUL		-1.000NA	-1.000UA	1.000UA	
	IOL		2:400NA	-1.000UA	1 - 90004	
	IOL		-1,400NA	-1.000UA	1 000UA	
	rot		2.550NA	-1.000UA	1 :00006	
	10L		-1:200NA	-1 c000UA	1.000UA	
	IOU.		2:100NA	-1.000UA	1.00000	
	IDL		-500.0PA	-1.000UA	1 - 00000	
	rot		1,950%A	-1,000UA	1,000004	
	IOL		-250.0PA	-1,00000	1.00000	
	IUL		2,000NA	-1.000UA	1,00000	
	TOL		-750.0PA	-1,000UA	1,00000	
	101		2,100NA	-1,000UA	1.00004	
	[DL		-1.100NA	-1.000UA	1,00004	
	IOL		2.500NA	-1,000UA	1 / 000UA	
	ĪŪL		-1,300NA	-1.000UM	1 00000	
	TOL		2.650MA	-1.00000	1 05000	
	EUL		-1.500NA	-1.00000	1 50064	
	101		2.65000	-1 000un	1 00000	

TEST HUNTIME IS 19 SECONDS FRIN) / DISPLAY TIME IS 136 SECONDS

Figure V.A.11 - Initial Electrical Test (Cont.)

MARTIN MARIETTA AEROSPACE -- DENVER DIVISION -- PARTS EVALUATION LAB

FILE UID :149 SERIAL NUMBER - 5
TESTED AT 25 DEG. C NO.13 ELECTRICALS
ON 27 SEP 83 AT 08:06 WITH THE 3260 TEST SYSTEM

FAIL	TEST TYPE		MEASURED VALUE	MINIHUH L I H I	T S MAXIMUM
***	VOH1		-519.0MV	2.400 V	
***	190H1		-541.5MV	2.400 V	
***	VOH1		-544.0MV	2.400 V	
***	VOH1		-560.0MV	2.400 V	
***	VOH1		-573.0MV	2.400 V	
***	VOH1		-575.0MV	2.400 V	
***	VOH1		-587.0MU	2.400 V	
***	VOH1		-590.0MV	2.400 V	
***	VOH1		-585.5MV	2.400 V	
***	VOH1		-587.5MV	2.400 V	
***	VOH1		-587.5HV	2.400 V	
***	VOH1		-588.0MV	2.400 V	
***	VOH1		-589.5HV	2,400 V	
***	VOH1		-590.5MV	2.400 V	
***	VOH1		-596.0MV	2.400 V	
***	VOH1		-592.0MV	2.400 V	
***	VOH1		-590.0MV	2.400 V	
***	VOH1		-596.0MV	2.400 V	
***	VDH1		-590.5MV	2.400 V	
***	VOH1		-590.0MV	2.400 V	
***	VOH1		-589.0MV	2,400 V	
***	VOH1		-591.5HV	2.400 V	
***	VOH1		-591.5MV	2.400 V	
***	VOH1		-590.5MV	2.400 V	
***	VOH1		-591.5MV	2.400 V	
***	VBH1		-602.5MV	2.400 V	
***	VOH1		-602.5HV	2.400 V	
***	V0H1		-469.0MV	2.400 V	
***	VOH1		-469.0MV	2.400 V	
***	VOH1		-466.5MV	2.400 V	
	VOH1		4.345 V	2.400 V	
***	V0H2		-325.0MV	4.000 V	
***	VOH2		-340.5MV	4.000 V	
***	VOH2		-339.5MV	4.000 V	
***	VOH2		-347.5MV	4.000 V	
***	VOH2		-355.0MV	4.000 V	
***	VOH2		-362.0MV	4.000 V	
***	VOH2		-369.5MV	4.000 V	
***	VOH2		-377.0MV	4.000 V	
***	VOH2		-367.5MV	4.000 V	
***	VOH2		-369.5MV	4.000 V	
***	VOH2		-370.0MV	4.000 V	
***	VOH2		-372.0MV	4.000 V	
***	V0H2		-372.5MV	4.000 V	
***	VOH2		-374.0MV	4.000 V	
***	VOH2		-370.0MV	4.000 V	
***	VOH2		-374.0MU	4.000 V	
***	VOH2		-374.0HV	4.000 V	

Figure V.A.12 - Post -1500 Volt Electrical Test

FILE UID :149 SERIAL NUMBER - 5
TESTED AT 25 DEG. C NO.13 ELECTRICALS
ON 27 SEP 83 AT 08:06 WITH THE 3260 TEST SYSTEM

**** **** ****	V0H2 V0H2 V0H2 V0H2 V0H2 V0H2 V0H2 V0H2	-373.5MV -374.0MV -371.0MV -371.0MV -373.5MV -373.5MV -373.5MV -377.0MV -378.0MV -273.0MV -273.0MV -273.0MV -273.0MV -274.0	4.000 V 4.000 V	400.0MV 400.0MV 400.0MV 400.0MV 400.0MV 400.0MV 400.0MV 400.0MV 400.0MV
京本市市市市市市市市市市市市市市市市市市市市市市市市市市市市市市市市市市市市	VOH2 VOH2 VOH2 VOH2 VOH2 VOH2 VOH2 VOH2	-374.0HV -371.0HV -372.0MV -373.5HV -373.5HV -373.5HV -377.0HV -378.0HV -273.0HV -273.0HV -273.0HV -243.5HV 4.940 V 4.940 V	4.000 V 4.000 U	400.0MU 400.0MU 400.0MU 400.0MU 400.0MU 400.0MU 400.0MU 400.0MU 400.0MU 400.0MU 400.0MU
	VOH2 VOH2 VOH2 VOH2 VOH2 VOH2 VOH2 VOH2 VOH2 VOH2 VOL1	-371.0HV -372.0HV -373.5HV -373.5HV -373.5HV -373.0HV -378.0HV -273.0HV -273.0HV -243.5HV 4.490 V 4.940 V	4.000 V 4.000 V	400.0MU 400.0MU 400.0MU 400.0MU 400.0MU 400.0MU 400.0MU 400.0MU 400.0MU 400.0MU
	V0H2 V0H2 V0H2 V0H2 V0H2 V0H2 V0H2 V0H2	-374.0HV -373.5HV -373.5HV -373.5HV -377.0HV -378.0HV -273.0HV -273.0HV -243.5HV 4.490 V 4.940 V	4.000 V 4.000 V 4.000 V 4.000 V 4.000 V 4.000 V 4.000 V 4.000 V 4.000 V	400.0MV 400.0MV 400.0MV 400.0MV 400.0MV 400.0MV 400.0MV 400.0MV 400.0MV 400.0MV
	VOH2 VOH2 VOH2 VOH2 VOH2 VOH2 VOH2 VOH2	-373.5MV -372.0MV -373.5MV -377.0MV -378.0MV -273.0MV -273.0MV -243.5MV 4.490 V 4.940 V	4.000 V 4.000 V 4.000 V 4.000 V 4.000 V 4.000 V 4.000 V 4.000 U	400.0MV 400.0MV 400.0MV 400.0MV 400.0MV 400.0MV 400.0MV 400.0MV 400.0MV
· · · · · · · · · · · · · · · · · · ·	VOH2 VOH2 VOH2 VOH2 VOH2 VOH2 VOH2 VOL1 VOL1 VOL1 VOL1 VOL1 VOL1 VOL1 VOL1	-372.0HV -373.5HV -377.0HV -378.0HV -273.0HV -273.0HV -243.5HV 4.490 V 4.940 V	4.000 V 4.000 V 4.000 V 4.000 V 4.000 V 4.000 V 4.000 V	400.0MV 400.0MV 400.0MV 400.0MV 400.0MV 400.0MV 400.0MV 400.0MV 400.0MV
**** **** **** **** **** ** *** *** *** *** *** *** *** *** *** *** *** *** ** *** *** *** *** *** *** *** *** *** *** *** *** ** *** *** *** *** *** *** *** *** *** *** *** *** ** *** **	V0H2 V0H2 V0H2 V0H2 V0H2 V0H2 V0H2 V0L1 V0L1 V0L1 V0L1 V0L1 V0L1 V0L1 V0L1	-373.5MV -377.0MV -378.0MV -273.0MV -273.0MV -243.5MV 4.490 V 4.940 V	4.000 V 4.000 V 4.000 V 4.000 V 4.000 V 4.000 V 	400.0MU 400.0MU 400.0MU 400.0MU 400.0MU 400.0MU 400.0MU 400.0MU 400.0MU 400.0MU
注文章本 注文章本 注文章本 注文章本 注文章本 注文章本 注文章本 注文章本	V0H2 V0H2 V0H2 V0H2 V0H2 V0L1 V0L1 V0L1 V0L1 V0L1 V0L1 V0L1 V0L1	-377.0MV -378.0MV -273.0MV -273.0MV -243.5MV 4.490 V 4.940 V	4.000 V 4.000 V 4.000 V 4.000 V 4.000 V	400.0MU 400.0MU 400.0MU 400.0MU 400.0MU 400.0MU 400.0MU 400.0MU 400.0MU 400.0MU
	V0H2 V0H2 V0H2 V0H2 V0H2 V0L1 V0L1 V0L1 V0L1 V0L1 V0L1 V0L1 V0L1	-378.0MV -273.0MV -273.0MV -243.5MV 4.490 V 4.940 V 4.940 V 4.940 V 4.940 U 4.940 U 4.940 U 4.940 U 4.940 U 4.940 U 4.940 U	4.000 V 4.000 V 4.000 V 4.000 V 4.000 V	400.0MU 400.0MU 400.0MU 400.0MU 400.0MU 400.0MU 400.0MU 400.0MU 400.0MU 400.0MU
	V0H2 V0H2 V0H2 V0H2 V0L1 V0L1 V0L1 V0L1 V0L1 V0L1 V0L1 V0L1	-273.0MV -273.0MV -243.5MV 4.490 V 4.940 V	4.000 V 4.000 V 4.000 V 4.000 V	400.0MV 400.0MV 400.0MV 400.0MV 400.0MV 400.0MV 400.0MV 400.0MV 400.0MV
	V0H2 V0H2 V0H2 V0L1 V0L1 V0L1 V0L1 V0L1 V0L1 V0L1 V0L1	-273.0MV -243.5MV 4.490 V 4.940 V	4.000 V 4.000 V 4.000 V	400.0MU 400.0MU 400.0MU 400.0MU 400.0MU 400.0MU 400.0MU 400.0MU 400.0MU
	VOH2 VOH2 VOL1 VOL1 VOL1 VOL1 VOL1 VOL1 VOL1 VOL1	-243.5MV 4.490 V 4.940 V 4.940 V 4.940 V 4.940 V 4.940 V 4.940 V 4.940 V 4.940 V 4.940 V	4.000 V 4.000 V	400.0MV 400.0MV 400.0MV 400.0MV 400.0MV 400.0MV 400.0MV 400.0MV
**** **** **** **** **** ** *** *** *** *** *** *** *** *** *** *** *** *** ** *** *** *** *** *** *** *** **	VOH2 VOL1	4.490 V 4.940 V 4.940 V 4.940 V 4.940 V 4.940 V 4.940 V 4.940 V 4.940 V 4.940 V	4.000 V	400.0MV 400.0MV 400.0MV 400.0MV 400.0MV 400.0MV 400.0MV 400.0MV
	VOL1 VOL1 VOL1 VOL1 VOL1 VOL1 VOL1 VOL1	4.940 V 4.940 V 4.940 V 4.940 V 4.940 V 4.940 V 4.940 V 4.940 V 4.940 V	 	400.0ML 400.0ML 400.0ML 400.0ML 400.0ML 400.0ML 400.0ML 400.0ML
東京東 東京東 東京東 東京東 東京東 東京東 東京東 東京 東 東京 東 東 東 東 東 東 東 東	VOL1 VOL1 VOL1 VOL1 VOL1 VOL1 VOL1 VOL1	4.940 V 4.940 V 4.940 V 4.940 V 4.940 V 4.940 V 4.940 V 4.940 V 4.940 V	 	400.0MU 400.0MU 400.0MU 400.0MU 400.0MU 400.0MU 400.0MU 400.0MU
	VOL1 VOL1 VOL1 VOL1 VOL1 VOL1 VOL1 VOL1	4.940 V 4.940 V 4.940 V 4.940 V 4.940 V 4.940 V 4.940 V 4.940 V	=== === === === ===	400.0MU 400.0MU 400.0MU 400.0MU 400.0MU 400.0MU 400.0MU
	VOL1 VOL1 VOL1 VOL1 VOL1 VOL1 VOL1 VOL1	4.940 V 4.940 V 4.940 V 4.940 V 4.940 V 4.940 V 4.940 V	=== === === ===	400.0MU 400.0MU 400.0MU 400.0MU 400.0MU 400.0MU
	VOL1 VOL1 VOL1 VOL1 VOL1 VOL1	 4.940 V 4.940 V 4.940 V 4.940 V 4.940 V 4.940 V	 	400.0MV 400.0MV 400.0MV 400.0MV 400.0MV
	VOL1 VOL1 VOL1 VOL1 VOL1 VOL1	 4.940 U 4.940 V 4.940 V 4.940 V 4.940 V	 	400.0MU 400.0MU 400.0MU 400.0MU
	VOL1 VOL1 VOL1 VOL1 VOL1	 4.940 V 4.940 V 4.940 V 4.940 V	 	400.0MV 400.0MV 400.0MV
	VOL1 VOL1 VOL1 VOL1	 4.940 V 4.940 V 4.940 V		400.0MV 400.0MV
	VOL1 VOL1 VOL1	 4.940 V 4.940 V		400.0HU
**** *** *** *** *** *** *** *** *** *	VOL1	 4.940 V		400.0MU
**** *** *** *** *** *** *** *** *** *	VOL1	 		
		 4.940 V		
: * * * * * * * * * * * * * * * * * * *	เมาเ			400.0MU
(*************************************		 4.940 V		400.0MV
(**** (**** (**** (**** (*** (*** (***	VOL1	 4.940 V		400.0MU
***** **** **** **** **** **** ****	VOL1	 4.940 V		400.0MV
(*** (*** (*** (*** (***	VOL1	 4.940 V		400.0MV
(*** (*** (*** (*** (***	VOL1	 4.940 V		400.0MU
*** *** *** ***	VOL1	 4.940 V		400.0MU
*** *** ***	VOL1	 4.940 V		400.0MV
*** **** ****	VOL1	 4.940 V		400.0MV
*** ***	VOL1	 4.940 V		400.0MV
***	VOL1	 4.940 V		400.0MV
	VOL1	 4.940 V		400.0MU
LEEL	VOL1	 4.940 U		400.0MV
	VOL1	 4.940 V		400.0MV
	VOL1	 4.940 V		400.0MV
	VOL1	 4.940 U		400.0HV
	VOL1	 4.940 U 4.940 U		400.0MV
	VOL1	 		400.0HV
	VOL1	 4.940 U 4.940 U		400.0MV
	VOL1	 4.760 V		400.0MV 400.0MV
***		 4.940 V		400 000
	Unt 2	4.935 V		100.0MV
	VOL2	 94733 V		100.0MV
***	VOL2 VOL2 VOL2	 4.940 V		100.0MV

Figure V.A.12 - Post -1500 Volt Electrical Test (Cont.)

FILE UID :149 SERIAL NUMBER - 5
TESTED AT 25 DEG. C NO.13 ELECTRICALS
ON 27 SEP 83 AT 08:06 WITH THE 3260 TEST SYSTEM

	TEST	 MEASURED	LIMI	T C
CATI	TYPE	VALUE	MINIMUM	MAXIMUM
FAIL	1175	 VALUE	utatuon	UNYTHOU
***	VOL2	 4.940 V		100.0MV
***	VOL2	 4.940 V		100.0MV
***	VOL2	 4.940 V		100.0MV
****	VOL2	 4.940 V		100.0MV
****	VOL2	 4.940 V		100.0MV
***	VOL2	 4.940 V		100.0HU
****	VOL2	 4.940 V		100.0MV
***	VOL2	 4.945 V		100.0MV
***	VOL2	 4.950 V		100.0HV
***	VOL2	 4.950 V		100.0MV
***	VOL2	 4.945 V		100.0HV
***	VOL2	 4.945 V		100.0HV
***	VOL2	 4.950 V		100.0MV
***	VOL2	 4.940 V		100.0MV
***	VOL2	 4.945 V		100.0MV
***	VOL2	 4.940 V		100.0MV
***	VOL2	 4.945 V		100.0MV
***	VOL2	 4.945 V		100.0MV
***	VOL2	 4.950 V		100.0MU
****	VOL2	 4.945 V 4.950 V		100.0MV
****	V0L2	 4.950 V 4.950 V		100.0MV
***	VOL2 VOL2	 4.945 U		100.0MV 100.0MV
****	V0L2	 4.950 V		100.0HV
***	VOL2	 4.940 V		100.0HV
****	VOL2	 4.945 V		100.0HV
****	VOL2	 4.490 V		100.0HV
• • • •				
	IIL	 600.0PA	-1.000UA	1.000UA
	IIL	 150.0PA	-1.000UA	1.000UA
	IIL	 1.950NA	-1.000UA	1.000UA
	IIL	 0.000 A	-1.000UA	1.000UA
	IIL	 450.0PA	-1.000UA	1.000UA
	IIL	 200.0PA	-1.000UA	1.000UA
	IIL	 1.400NA	-1.000UA	1.000UA
	IIL	 -450.0PA	-1.000UA	1.000UA
	IIL	 350.0PA	-1.000UA	1.000UA
	IIL	 200.0PA	-1.000UA	1.000UA
	IIL	 1.300NA	-1.000UA	1.000UA
	IIL	 -600.0PA	-1.000UA	1.000UA
	IIL IIL	 400.0PA 300.0PA	-1.000UA -1.000UA	1.000UA 1.000UA
	İİL	 1.300NA	-1.000UA	1.000UA
	IIL	 -650.0PA	-1.000UA	1.000UA
	IIL	 -500.0PA	-1.000UA	1.000UA
	ΪΪ́	 250.0PA	-1.000UA	1.000UA
	IIL	 500.0PA	-1.000UA	1.000UA
	IIL	 0.000 A	-1.000UA	1.000UA
	IIL	 350.0PA	-1.000UA	1.000UA
	IIL	 650.0PA	-1.000UA	1.000UA
***	IIL	 2.100MA	-1.000UA	1.000UA

Figure V.A.12 - Post -1500 Volt Electrical Test (Cont.)

FILE UID :149 SERIAL NUMBER - 5
TESTED AT 25 DEG. C NO.13 ELECTRICALS
ON 27 SEP 83 AT 08:06 WITH THE 3260 TEST SYSTEM

	TEST		MEAGURED	. 7 4 1	· + c
FAIL	TYPE		MEASURED VALUE	LIMI MINIHUM	MAXIMUM
	,,,,		~	BINIDU	UBVIUU
****	IIL		2.100MA	-1.000UA	1.000UA
****	IIL		7.670MA	-1.000UA	1.000UA
***	IIL		7.670MA	-1.000UA	1.000UA
	IIL	- -	0.000 A	-1.000UA	1.000UA
	IIL		800.0PA	-1.000UA	1.000UA
	IIL		250.0PA	-1.000UA	1.000UA
	IIL		2.200NA	-1.000UA	1.000UA
	IIL		-400.0PA	-1.000UA	1.000UA
	IIL		2.000NA	-1.000UA	1.000UA
	IIL		-350.0PA	-1.000UA	1.000UA
	IIL		1.950NA	-1.000UA	1.000UA
	IIL		-500.0PA	-1.000UA	1.000UA
	IIL		1.800NA	-1.000UA	1.000UA
	IIL		-600.0PA	-1.000UA	1.000UA
	IIL		1.750NA	-1.000UA	1.000UA
	IIL		-650.0PA	-1.000UA	1.000UA
	IIL		1.700NA	-1.000UA	1.000UA
	IIL		-750.0PA	-1.000UA	1.000UA
	IIL		1.700NA	-1.000UA	1.000UA
	IIL IIL		-800.0PA 1.500NA	-1.000UA	1.000UA
	iil		-800.0PA	-1.000UA -1.000UA	1.000UA 1.000UA
	IIL		1.400NA	-1.000UA	1.000UA
	IIL		-1.000NA	-1.000UA	1.000UA
	IIL		1.400NA	-1.000UA	1.000UA
	IIL		-1.100NA	-1.000UA	1.000UA
	IIL		1.300NA	-1.000UA	1.000UA
	IIL		-1.200NA	-1.000UA	1.000UA
	IIL		1.300NA	-1.000UA	1.000UA
	IIL		-1.250NA	-1.000UA	1.000UA
	IIL		1.200NA	-1.000UA	1.000UA
	IIL		-1.200NA	-1.000UA	1.000UA
	IIL		1.250NA	-1.000UA	1.000UA
	IIL		-1.200NA	-1.000UA	1.000UA
	IIL		1.200NA	-1.000UA	1.000UA
	IIL		-1.200NA	-1.000UA	1.000UA
	IIL		1.200NA	-1.000UA	1.000UA
	IIL		-1.400NA	-1.000UA	1.000UA
	IIL		1.600NA	-1.000UA	1.000UA
	IIL		-1.450NA	-1.000UA	1.000UA
	IIL		1.100NA	-1.000UA	1.000UA
	IIL		-1.450NA	-1.000UA	1.000UA
	IIL		1.200NA	-1.000UA	1.000UA
	IIL		-1.750NA	-1.000UA	1.000UA
	IIL		1.150NA	-1.000UA	1.000UA
	IIL		-1.750NA	-1.000UA	1.000UA
	IIL IIL		1.150NA	-1.000UA	1.000UA
	IIL		-3.100NA 1.150NA	-1.000UA -1.000UA	1.000UA 1.000UA
****	IIL		-1.685MA	-1.000UA	1.000UA
****	IIL		1.105MA	-1.000UA	1.000UA
			212001111	**************************************	_ , , , , , , , ,

Figure V.A.12 - Post -1500 Volt Electrical Test (Cont.)

FILE UID :149 SERIAL NUMBER - 5
TESTED AT 25 DEG. C NO.13 ELECTRICALS
ON 27 SEP 83 AT 08:06 WITH THE 3260 TEST SYSTEM

FAIL	TEST Type		MEASURED VALUE	L I M I MINIMUM	T S MAXIMUM
	IOL		550.0PA	-1.000UA	1.000UA
	IOL		2.550NA	-1.000UA	1.000UA
	IOL		-200.0PA	-1.000UA	1.000UA
	IOL		2.250NA	-1.000UA	1.000UA
	IOL		-300.0PA	-1.000UA	1.000UA
	IOL	~	2.150NA	-1.000UA	1.000UA
	IOL		-400.0PA	-1.000UA	1.000UA
	IOL		2.000NA	-1.000UA	1.000UA
	IOL		-550.0PA	-1.000UA	1.000UA
	IOL		1.900NA	-1.000UA	1.000UA
	IOL		-700.0PA	-1.000UA	1.000UA
	IOL		1.750NA	-1.000UA	1.000UA
	IOL		-800.0PA	-1.000UA	1.000UA
	IOL		1.600NA	-1.000UA	1.000UA
	IOL		-1.000NA	-1.000UA	1.000UA
	IOL		1.400NA	-1.000UA	1.000UA
	IOL		-1.600NA	-1.000UA	1.000UA
	IOL		2.100NA	-1.000UA	1,000UA
	IOL		-1.300NA	-1.000UA	1.000UA
	IOL		1.900NA	-1.000UA	1.000UA
	IOL		-950.0PA	-1.000UA	1.000UA
	IOL		1.600NA	-1.000UA	1.000UA
	10L		-500.0PA	-1.000UA	1.000UA
	IOL		1.200NA	-1.000UA	1.000UA
	IOL		-400.0PA	-1.000UA	1.000UA
	IOL		1.250NA	-1.000UA	1.000UA
	IOL		-600.0PA	-1.000UA	1.000UA
	IOL		1.500NA	-1.000UA	1.000UA
	IOL		-950.0PA	-1.000UA	1.000UA
	IOL		1.950NA	-1.000UA	1.000UA
	IOL		-1.350NA	-1.000UA	1.000UA
	IOL		2.050NA	-1.000UA	1.000UA

Figure V.A.12 - Post -1500 Volt Electrical Test (Cont.)

Number	of	Failures	a٤	∂in	Locations
--------	----	----------	----	-----	-----------

						Custing est	12. 12. 13. 13. 13. 13. 13. 13. 13. 13. 13. 13
3	7	8	9	10			Voltages
			14				+250
15		2	14				-250
15		3	15	2			+500
15	2	3	15	3			-500
15	3	5	15	5		5	+750
 15	15	15	15	15		15	-75 0

Figure V.A.13 - CD Stress, Cumulative Leakage Current Failures

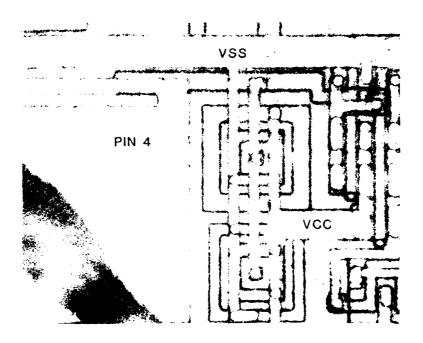


Figure V.A.14 - Pin 4 Input

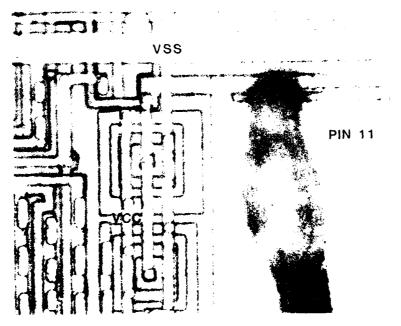


Figure V.A.15 - Pin 11 Input

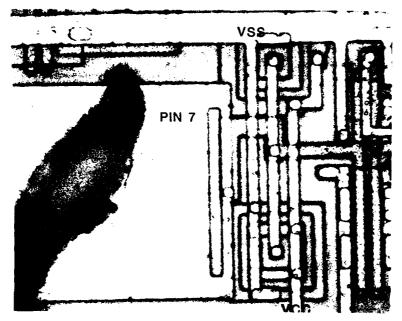


Figure V.A.16 - Pin 7 Input

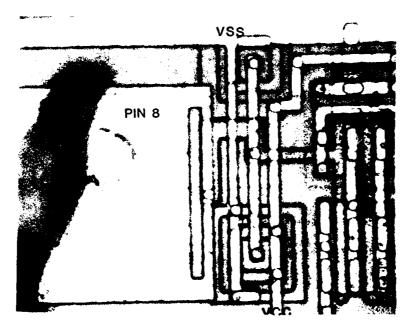


Figure V.A.17 - Pin 8 Input

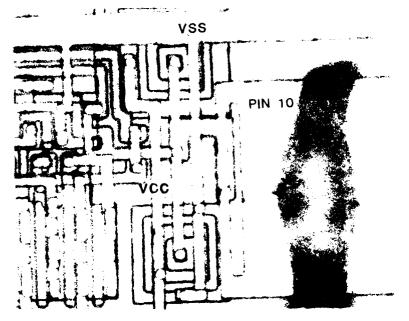


Figure V.A.18 - Pin 10 Input

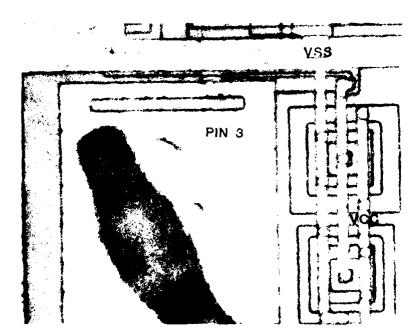


Figure V.A.19 - Pin 3 Input

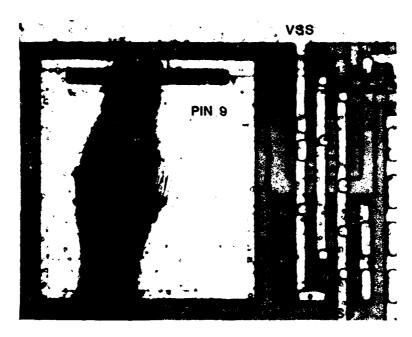


Figure V.A.20 - Pin 9 Input

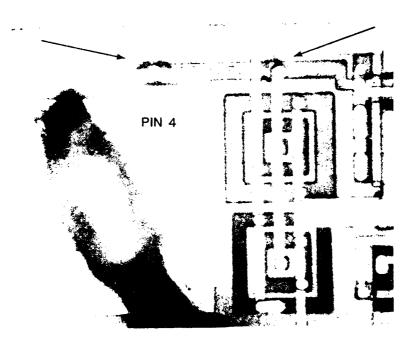


Figure V.A.21 - CD Stress, Pin 4 Input Polysilicon Damage

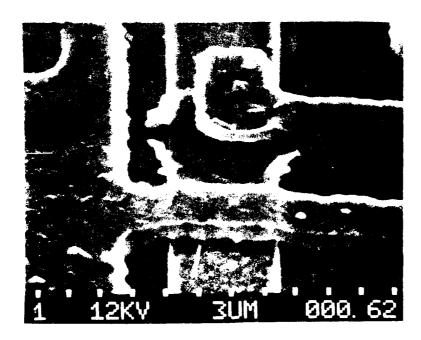


Figure V.A.22 - CD Stress, SEM Micrograph of Pin 4 Polysilicon at Diode Metalization Contact

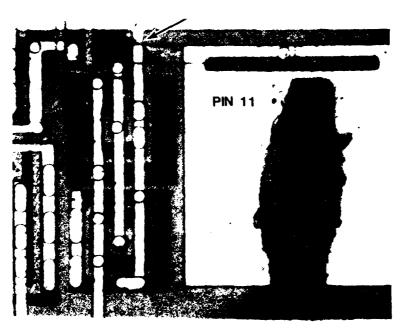


Figure V.A.23 - CD Stress, Pin 11 Input Polysilicon Damage



Figure V.A.24 - CD Stress, SEM Micrograph of Pin 11 Input Polysilicon.

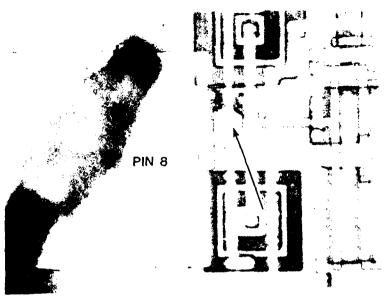


Figure V.A.25 - CD Stress, Pin 8 Input Polysilicon Damage

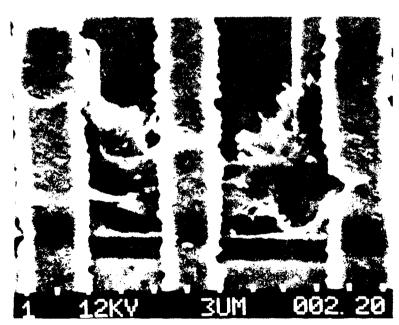


Figure V.A.26 - CD Stress, SEM Micrograph of Pin 8 Input Polysilicon Damage

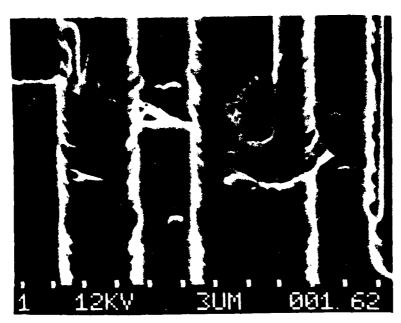


Figure V.A.27 - CD Stress, SEM Micrograph of Pin 7 Input Polysilicon Damage

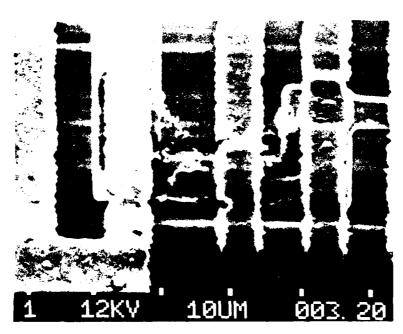


Figure V.A.28 - CD Stress, SEM Micrograph of Pin 9 Input Polysilicon Damage

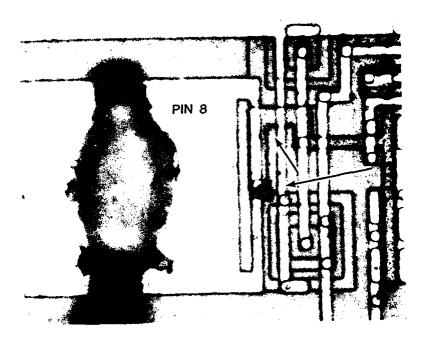


Figure V.A.29 - CD Stress, SEY Micrograph of Pin 8 Input Polysilicon Damage

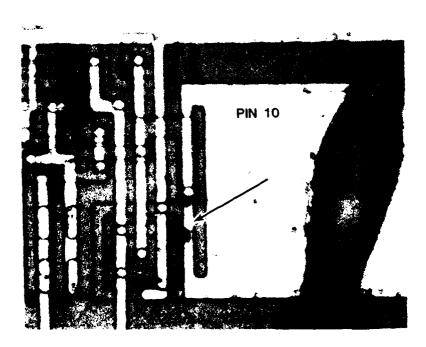


Figure V.A.30 - CD Stress, Pin 10 Breakdown Site from Metallization to Silicon

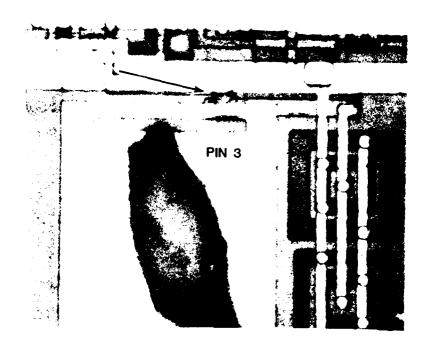


Figure V.A.31 - CD Stress, Pin 3 Input Polysilicon Damage



Figure V.A.32 - CD Stress, SEM Micrograph of Pin 3 Polysilicon Damage

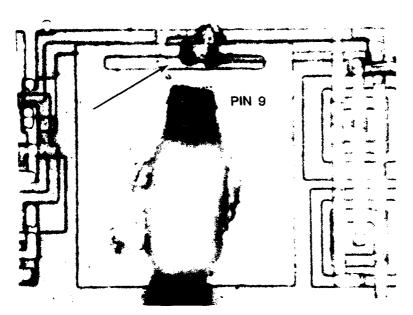


Figure V.A.33 - CD Stress, SEM Micrograph of Pin 9 Polysilicon Damage

Number of Failures at Pin Locations										
								\mathcal{I}^-		
									Cumulat	ga cal
									Jini Rel	
3	7	8	9	10	11	19	27	33	<u> </u>	Voltage
										+250
			1			l				-250
			1			1				+500
	1		1			1				-500
	i		11			1				+7°0
	:		12	i		1	1	1	1	-750
	<u> </u>	!	15	1		1	1	1		+1000
!	1		15	1		1	1	1	2	-1000
2			15	1		į	1	1	2	+1250
10		1	15	1		1	1	1	4	-1250
15	 	 	15	1		1	1	1	5	+1500
15	1	2	15	3	1	1	1	1	15	-1500

Figure V.A.34 - HBD Stress, Cumulative Leakage Failure

Serial Number											
								LEGEND: 0 = open X = short S = slight damage			
2	6	8	9	11	12	15	16	ND = nc visible damage			
S	Х	S	Х	S	S	S	S	pin 3			
S	0	S	S	S	ND	S	ND	pin 4			
S		0	0	S	S	S	/	pin 7			
S	0	0	0	S	S	S	0	pin 8			
ND	ND	ND	ND	ND	0	ND	ND	pin 9			
S	S	S	0	S	S	S	0	pin 10			
ND	0	0	0	ND	S	0	/	pin 11			
-750	-1500	-1500	-1500	+1250	+1250	+1500	-1500	Final Voltage Stress			

Figure V.A.35 - HBD Stress, Damage Summary

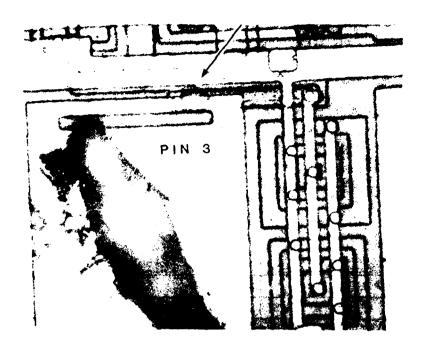


Figure V.A.36 - HBD Stress, Pin 3 Input Polysilicon Damage

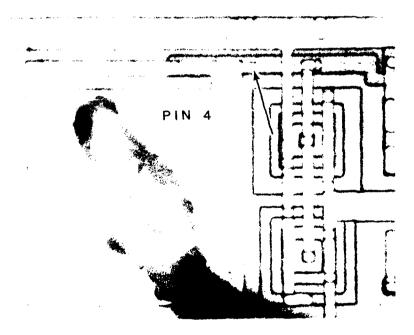


Figure V.A.37 - MBD Stress, Pin 4 Input with Minor Polysilicon Damage

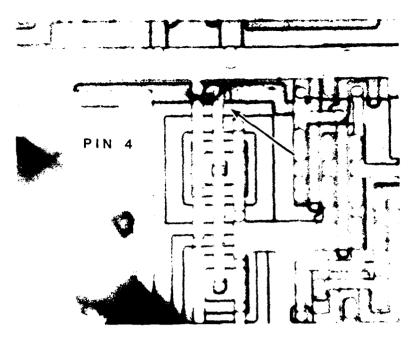


Figure V.A.38 - HBD Stress, Pin 4 Input Polysilicon Damage

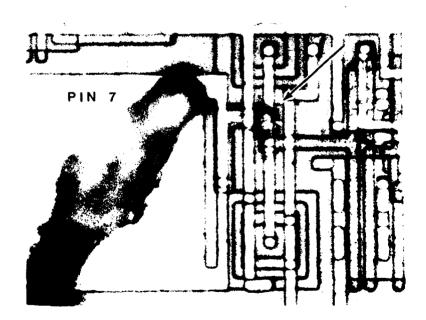


Figure V.A.39 - HBD Stress, Pin 7 Input Polysilicon Damage

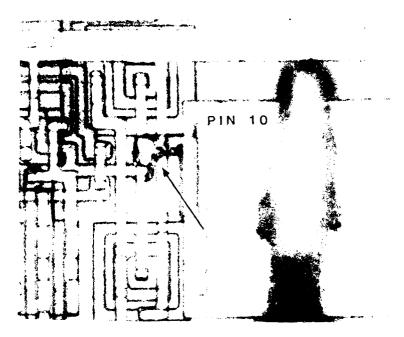


Figure V.A.40 - HBD Stress, Pin 10 Input Polysilicon Damage

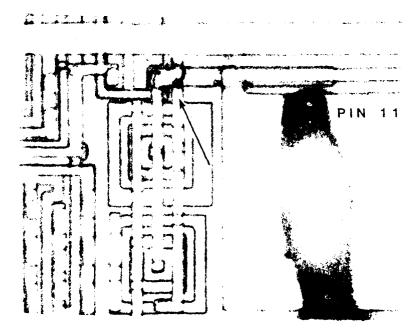


Figure V.A.41 - HPD Stress, Pin 11 Input Polysilicon Damage

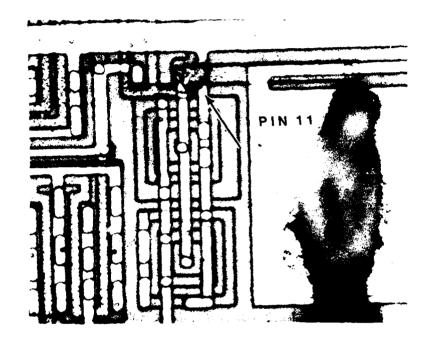


Figure V.A.42 - HBD Stress, Pin 11 Input Polysilicon Damage

B. Part B Analysis

This device is a 1K x 8-bit static RAM manufactured using an advanced NMOS process. The metallization and polysilicon linewidths are 3 microns. There is one polysilicon layer and one metallization layer. This was in a 24-pin dual-in-line ceramic package. An overall die photo is shown in Figure V.B.l. VCC is pin 24 at the top of Figure V.B.l and VSS is pin 12 at the bottom. VCC and VSS are distributed via aluminum metallization across the die. The distribution pattern was noted for future reference to use during geometric sensitivity analysis. The VCC bond pad is shown in Figure V.B.2. The metallization connects to numerous n+ source diffusions. No points were found where it connected to polysilicon gates. The VSS metallization pad is shown in Figure V.B.3. The multi-contact metallization directly below the pad is part of the input protection network for pin 13. The ground metallization connects to numerous n+ source diffusions. This metallization does not connect to polysilicon. Between pins 1 and 2 is a bond pad (substrate bias generator) which has a wire connected from it to the substrate (Figure V.B.4). This connection does not come to the outside. The bond pad is connected to polysilicon which runs along the outside edge of the die and is also connected to the silicon die substrate. An input circuit is shown in Figure V.B.5. The bond pad metallization makes contact to an n+ diffusion and then continues on as a thick oxide gate between that n+ diffusion and an n+ diffusion which is connected to VSS or VCC. Pins 1-4 and 21-23 go to VSS and pins 5-8 and 18-20 go to VCC. The resistor travels about halfway around the pad and connects to an n+ source diffusion. Above a portion of this resistor is a polysilicon stripe which is connected back to the substrate. A schematic representation is shown in Figure V.B.6. The resistor measured 650 ohms. The gate dielectric failed at 45 VDC. The input resistor to substrate breakdown voltage was 22 VDC. This is the same as the transistor junction breakdown.

A second input protection circuit is shown in Figure V.B.7. This is connected to pin 8 and is located along the edge of the die away from the bond pad. The components are labeled.

One of the combination input-output pins is shown in Figure V.B.8. The input section is identical to the inputs discussed previously and the output schematic is shown in Figure V.B.9. Pin 13 has its input protect transistor going to VSS and pins 9-11 and 14-17 go to VCC.

Microsections were performed to examine the construction of the protect network. Figure V.B.10 shows an input with an area marked where a cross-section was performed. The cross-section is below the photograph. The polysilicon was approximately 0.6 microns thick, the metallization was 1.0 microns thick, and the diffusion depth was about 0.5 microns. The thick oxide areas beneath the polysilicon were approximately 1.0 microns thick. The gate oxide thickness was not discernible in this microsection. Two photographs of a microsection are shown in Figure V.B.11.

Electrical Testing

A sample of the electrical data taken on each of the stressed parts and the control part at each iteration during the testing is shown in Figures V.B.12 and V.B.13. Figure V.B.12 shows the initial readings on serial number 9 and Figure V.B.13 shows the readings after the -2000 volt stress. The data in/data out pins were measured for $V_{OH},\,V_{OL},\,$ and $I_{OL}.\,$ The I_{OL} reading was taken with the outputs in the high impedance configuration. This reading was influenced by the condition of the inputs during the latter stages of the stress due to the outputs not being fully disabled. The V_{OH} and V_{OL} measurements indicated that the outputs could be forced to a given state. Note that the limits were not correct on the initial readings. They should be as shown in Figure V.B.13. This testing also provided a functional check of the following. The control lines (OE, WE, and CE) and the I/O bus were completely tested. In the memory cell matrix only address 000 was written and read as 1's and 0's.

The I_{IL} reading provided leakage measurements on each of the address lines. This was measured with the input at 5 volts and did provide data which indicated the gradual damage being done to the input circuits. These data were supplemented by curve tracer data taken after the stresses at 500 volts, 1000 volts, 1500 volts, and 2000 volts. The voltage level at a current reading of 25 microamps was recorded for each of the pins. The pins were taken positive with respect to VSS.

Charged Device Data Analysis

The fifteen devices, S/N 17-31, proceeded through the -500 volt stress level with no device functional failures. No evidence of output leakage occurred, however, there was low level leakage evident on input pins as will be discussed. The maximum leakage was 21.8 nanoamps after the -500 volt stress. After the +750 volt stress there were eight devices with functional failures. These were S/N 17, 18, 20, 21, 22, 27, 28, and 30. The failure mode was an inability of the part to force the outputs to $V_{\rm OH}$ or $V_{\rm OL}$ at the proper times. There was no increase in output leakage currents. The maximum input leakage current was 1.2 microamps.

Following the -750 volt stress there were no new failures except for 1 device which failed 1 $V_{\mbox{\scriptsize OH}}$ measurement.

Following the +1000 volt stress the remaining 7 devices failed functionally. Failures for $V_{\rm OH},~V_{\rm OL},$ and $I_{\rm OL}$ occurred. Leakage currents up to the maximum forced by the automatic test equipment (1.024 milliamps) occurred.

The data and the devices were analyzed to understand the failure modes and the sensitivity variations. The average of the input leakage currents were calculated for the stress levels up through +750 volts. These are shown in Figure V.B.14. The last column shows the maximum leakage current level measured at each voltage level. There is an increase in leakage current following each level of positive voltage stress and a slight decrease in leakage following the negative voltage stresses. The

Human Body Discharge Data Analysis

Device serial numbers 2 through 16 were stressed with the human body ESD simulation test method.

These parts went through -1250 volts of stress with no parametric or functional failures. Following the stress at +1500 volts there were 2 parts with input current leakage failures, this increased to 7 parts following the +1750 volt stress, and to 14 parts following the +2000 volt stress. As was seen for the charged device model, the negative stress did not have much of an effect on the leakage failures.

After the +2000 volt stress 6 devices had I_{OL} failures. The output transistors were not in the fully disabled state. There were still no functional failures. Serial number 7 was pulled for failure analysis. The -2000 volt stress did affect the parts. This indicates that the magnitude was more important than the polarity at this level. Functional failures occurred on 5 of the remaining 14 devices. All devices exhibited I_{IL} failures and 8 exhibited I_{OL} failures. The stress testing was stopped at this point.

A summary of the leakage current after 0 volts, +500 volts, +1000 volts, and +1500 volts is given in Figure V.B.26. The two inputs with the long metallization runs had a decreased sensitivity to stress. This was likely due to a reduction in the voltage level reaching the input resistor due to the parasitic capacitance and inductance of the metallization.

Pin 5 was the most sensitive to HBD stress. It was also the most sensitive to CD stress. The failures on it caused silicon damage in the necked down portion of the protect resistors. This is apparently a less tolerant system to stress than the other resistor layouts. The reason for the increased sensitivity of pin 4 is not evident, and it may not be significant since it has a very low leakage level at +1000 volts and was higher only after the + 1500 volt stress.

The increase in leakage current is shown in a different manner in Figure V.B.27. This shows the maximum leakage current at each voltage level and the serial number and pin association. This shows the leakage level increase after each positive stress and the high level of the leakage at the end of the stressing.

Failure analysis was performed on serial numbers 4, 7, 9 and 11. It was found that the location of the breakdown site could be determined by applying power to the part with liquid crystal (MBBA) on the device. The polysilicon on the resistor would appear to show movement within the liquid crystal when viewed under crossed polarizers depending upon the location of the failure. About half of the leaky pins were shorted to the polysilicon. Visually all of the first contact points between metallization and the input resistor showed some damage. The polysilicon shorts were not visible. The enable transistor gate oxides were not checked on these devices. The analysis only identified shorts that went to VCC, VSS, or Substrate.

The appearance seen is shown on serial number 4 in Figures V.B.28 - V.B.31. Figure V.B.28 shows pin 5 which was the most sensitive to leakage increase. Figure V.B.29 shows pin 22 which is layout style number 1. Figure V.B.30 shows pin 21 which is layout style number 2. Figure V.B.31 shows pin 20 and the adjacent input protect resistor which is not connected to any pin. The damage on pin 20 can be compared with the undamaged resistor.

Output pins did not exhibit any visible damage and electrical measurement found no increase in leakage current. The parametric failures on the output pins were due to the output transistors not being fully disabled because of other circuit problems.

The human body discharge stress found results similar to the charged device model stress. Inputs were susceptible to the stress and outputs were not. Pin 5 was the most sensitive to increases in low level leakage current with stress. The leve' at which parts exhibited functional failure was relatively high, -2000 volts. The major difference in sensitivity was the fact that the long metallization stripes prior to the protect circuits decreased sensitivity to the human body discharge stress and had no apparent effect upon the charged device stress.

This analysis indicates that one of the principle failure modes was shorting to the substrate polysilicon stripe. Removal of this polysilicon or an increase in the oxide thickness would likely produce a more tolerant system. The second failure mode, current leakage to an adjacent n+ diffusion, could be made less likely by increasing the spacing between the two n+ diffusions or by keeping corners farther apart.

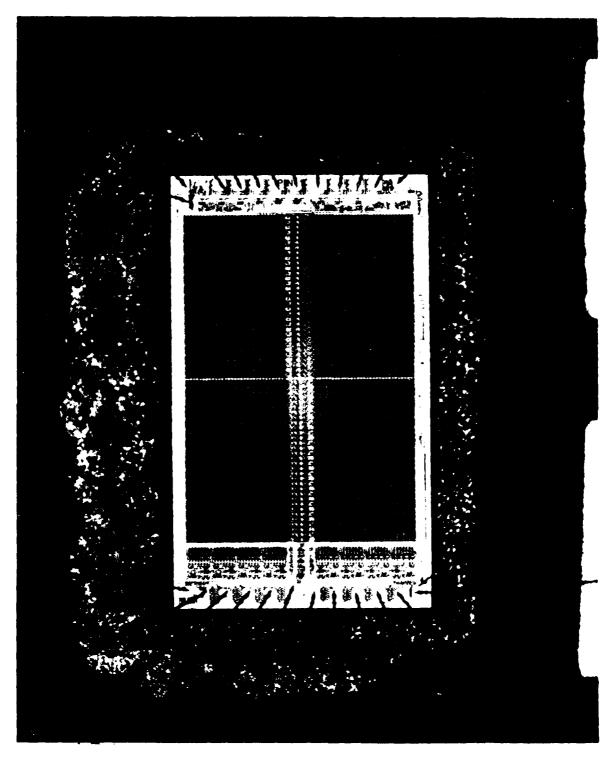


Figure V.B.1 - Overall Die Photograph

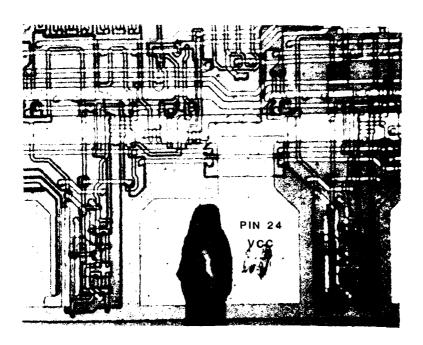


Figure V.B.2 - VCC Bond Pad and Connections

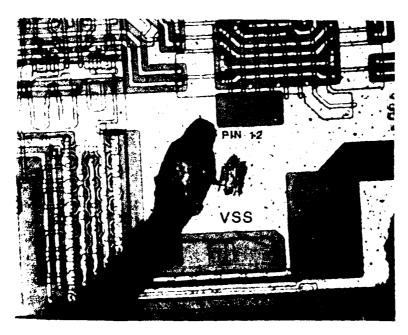


Figure V.B.3 - VSS Bond Pad and Connections

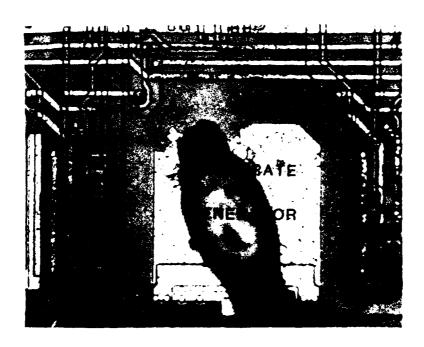


Figure V.B.4 - Substrate Bias Generator Pad

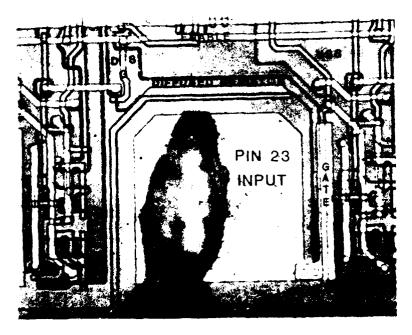


Figure V.B.5 - Pin 23 Input

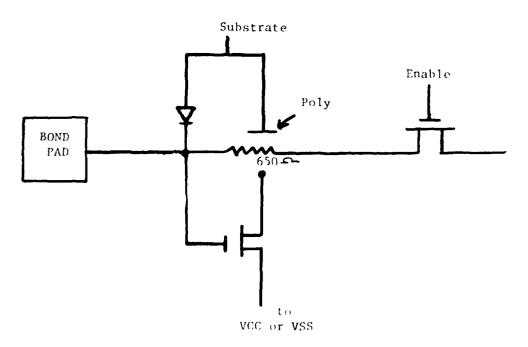


Figure V.B.6 - Input Schematic

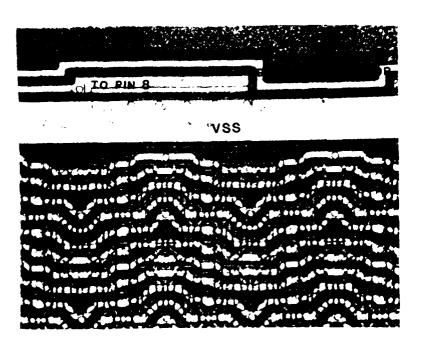


Figure V.B.7 - Pin 8 Input

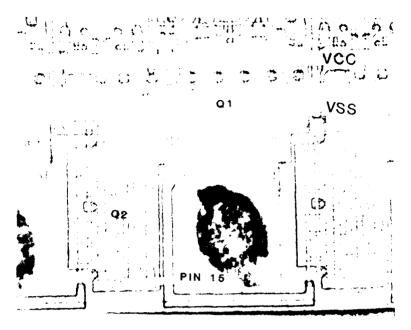


Figure V.B.8 - Pin 15 with Output Components Labeled.

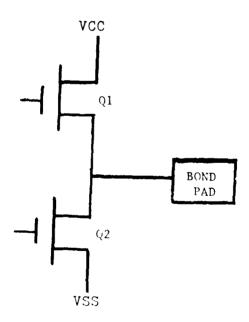
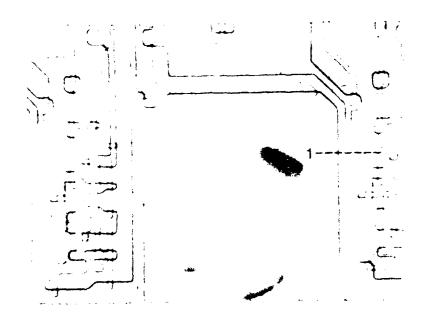


Figure V.B.9 - Output Schematic



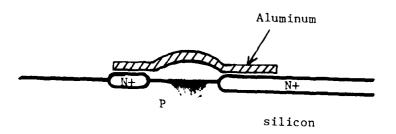


Figure V.B.10 - Input Pin with Location of Cross-Section and Drawing of Appearance of Cross-Section

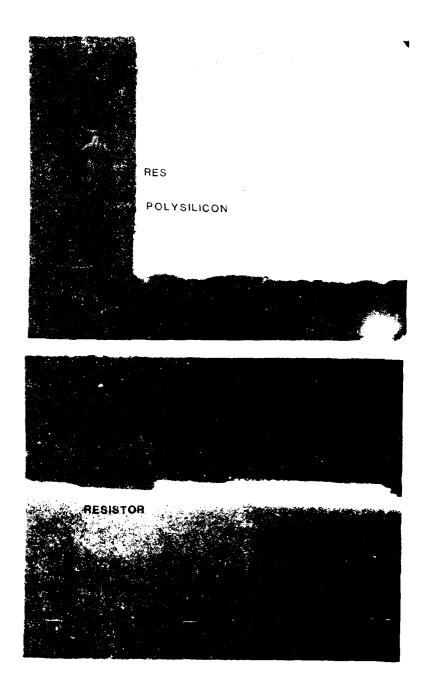


Figure V.E.11 - Input Resistor and Polysilicon Top and Side Views

MARTIN MARIETTA AEROSPACE -- DENVER DIVISION -- PARTS EVALUATION LAB

FILE UID :150 SERIAL NUMBER - 9
TESTED AT 25 DEG. C INITIAL ELECTRICAL TEST
UN 13 JUN 83 AT 12:17:17 WITH THE 3260 TEST SYSTEM

FAIL	TEST TYPE	MEASURED VALUE	L I M I MINIMUM	T S MAXIMUM
	VOH	 3.900 V	2.400 V	
	VOH	 3.910 V	2.400 V	
	VOH	 3.905 V	2.400 V	
	VOH	 3.900 V	2.400 U	
	VOH	 3.895 V	2.400 V	
	VOH	 3.900 V	2.400 ∪	
	VOH	 3.895 V	2.400 V	
	VOH	 3.890 V	2.400 V	
	VOL	 73.50MV	~	400.0MV
	VOL	 71.50MV		400.0MV
	VOL	 71.00MV		400.0MV
	VOL	 72.50MV		400.0MV
	VOL	 71.50MV	~~	400.0MV
	VOL	 72.00MU		400.0MV
	VOL	 72.50MV		400 - OMV
	VOL	 75.00MV		400.0MV
	ICC1	 48.00MA		125.0MA
	IIL	 1.200NA	-200.0UA	
	IIL	 850.0PA	-200.0UA	
	IIL	 1.000NA	-200.0UA	
	IIL	 550.0PA	-200.0UA	
	IIL	 500.0PA	-200.0UA	
	IIL	 550.0PA	-200.0UA	
	IIL	 400.0PA	-200.0UA	
	IIL	 450.0PA	-200.0UA	
	IIL	 500.0PA	-200.0UA	
	IIL	 500.0PA	-200.0UA	
	IOL	 1.000NA	-10.00UA	10.00UA
	IOL	 850.0PA	-10.00UA	10.00UA
	IOL	 500.0PA	-10.00UA	10.00UA
	IOL	 600.0PA	-10.00UA	10.00UA
	IOL	 650.0PA	-10.00UA	10.00UA
	IOL	 600.0PA	-10.00UA	10.00UA
	IOL	 500.0PA	-10.00UA	10.00UA
	IOL	 650.0PA	-10.00UA	10.00UA

TEST RUNTIME IS 8 SECONDS PRINT / DISPLAY TIME IS 26 SECONDS

Figure V.B.12 - Initial Electrical Readings

MARTIN MARIETTA AEROSPACE -- DENVER DIVISION -- PARTS EVALUATION LAB

FILE UID :150 SERIAL NUMBER - 9
TESTED AT 25 DEG. C RE-RUN WITH CHANGED LIMITS 180CT83
ON 18 OCT 83 AT 09:44:36 WITH THE 3260 TEST SYSTEM

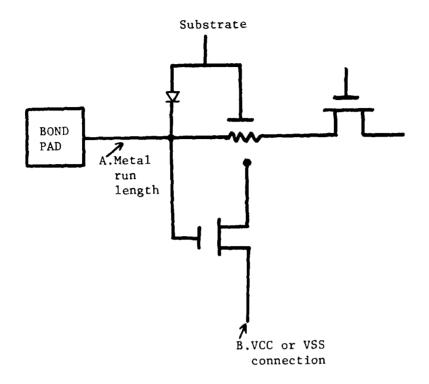
FAIL	TEST TYPE		MEASURED VALUE	L I M I MINIMUM	T S MAXIMUM
	VOH		3.865 V	2.400 V	
	VOH		3.345 V	2.400 V	
	VOH		3.865 V	2.400 V	
	VOH VOH		3.865 V 3.905 V	2.400 V 2.400 V	
	VOH		3.900 V	2.400 V	
	VOH		3.900 V	2.400 V	
	VOH		3.905 V	2.400 V	
	VUH		3.703 V	2.400 0	
	VOL		74.00MU		400.0MV
	VOL		207.0MV		400.0MU
	VOL		71.00MV		400.0MV
	VOL		84.50MV		400.0MV
	VOL		71.50MV		400.0MU
	VOL		72.50MV		400.0MV
	VOL		73.00MV		400.0MU
	VOL		74.50MV		400.0MU
	ICC1		54.50MA		120.0MA
	IIL		10.60NA	-10.00UA	10.00UA
	IIL		10.05NA	-10.00UA	10.00UA
	IIL		17.45NA	-10.00UA	10.00UA
***	IIL		22.50UA	-10.00UA	10.00UA
	IIL		7.350NA	-10.00UA	10.00UA
	IIL	-	4.000NA	-10.00UA	10.00UA
	IIL		4.530UA	-10,00UA	10.00UA
	IIL		1.865UA	-10.00UA	10.00UA
	IIL		200.5NA	-10,00UA	10.00UA
	IIL		36.85NA	-10.00UA	10.00UA
	IOL		5.730UA	-50,00UA	50.00UA
****	IOL		1.024MA	-50.00UA	50.00UA
	IOL		5.460UA	-50.00UA	50.00UA
	IOL		5.080UA	-50.00UA	50.00UA
	IOL		3.910UA	-50.00UA	50.00UA
	IOL		4.770UA	-50.00UA	50.00UA
	IOL		5.100UA	-50,00UA	50.00UA
	IOL		5.115UA	-50.00UA	50.00UA

TEST RUNTIME IS 8 SECONDS FRINT / DISPLAY TIME IS 26 SECONDS

Figure V.B.13 - Post -2000 Volt Electrical Readings

		Voltage	0	+250	-250	+500	-500	+750		Sensitivity Classif.	A. Metal Run Length	B. VCC or VSS Connect	C. Layout Style
	Max	Level	1.9	4.2	5.9	27.8	1.9 21.8	25.1					
(nA)	\	23	1,1	1,1	1.3	2.0 27.8	1.9	3.5 25.1		2	short short	VSS	2
Leakage Current by Pin Number (nA)		22	0.7	0.5	0.5	0.6	0.7	1.5		3	short	VSS	1
/ Pin		8	1.1	0.9	1.6 1.1	1.7	1.4	3.7		2	long	N _{CC}	4
ent by		7	1.6	1.5	1.6	2.5	2.3	7.3		2	long	DD _V	4
e Curr		9	0.9	0.9	0.8	9.4 1.1	7.7 1.0	1.6		3	short	ος Λ	
eakag		5	0.9	0.8	1.2		7.7	4.0 10.8		1	short	DD _A	3
		4	0.8	0.8	1.3	3.3	2.7	4.0		2	short short short long long	VSS	2
		3	1.2	1.0	1.0	1.2	1.1	2.6		3	short	VSS	1
		2	0.8	9.0	1.1	1.0 1.6	1.1 1.5	4.0		2	short shortshort	VSS	2
		.	0.7 0.8	0.6 0.6	0.6 1.1	1.0	1.1	3.0 4.0		3	short	V.SS	-

Figure V.B.14 - CD Stress, Leakage Current Summary (S/N 17-31)



Layout Style

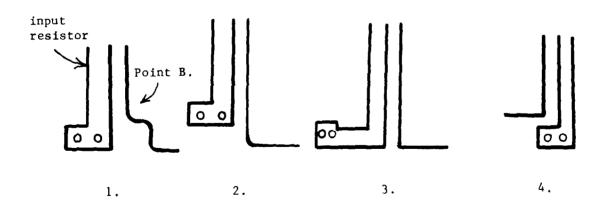


Figure V.B.14A - Layout Variations and Input Schematic

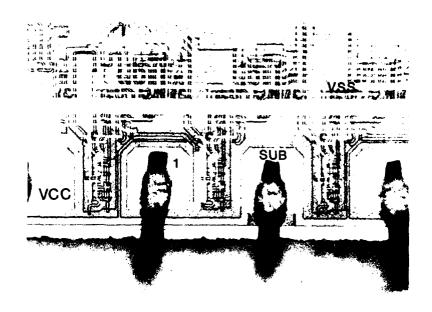


Figure V.B.15 - Pin 1 Input

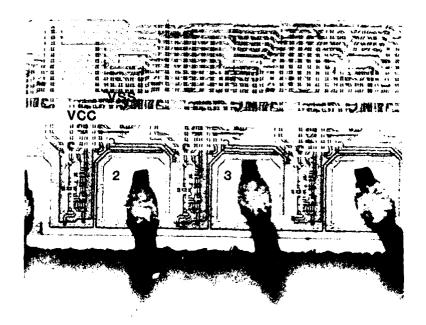


Figure V.B.16 - Input Pins 2 and 3

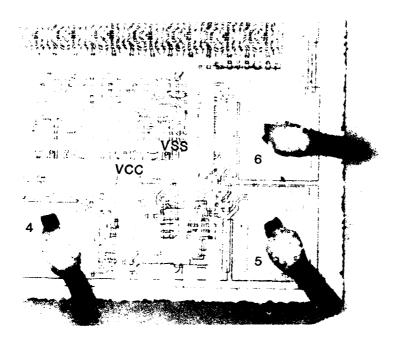


Figure V.B.17 - Input Pins 4, 5 and 6

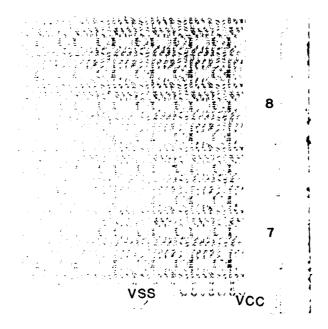


Figure V.B.18 - Input Resistors for Pins 7 and 8

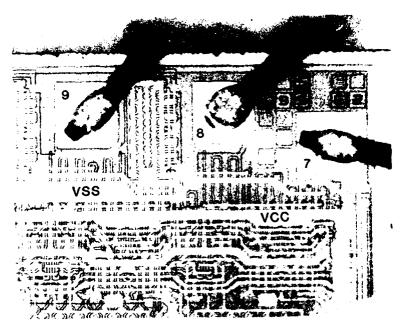


Figure V.B.19 - Input Pins 7, 8 and 9

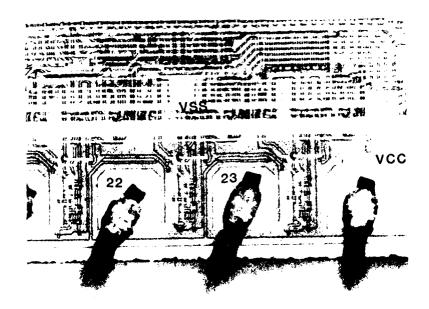


Figure V.B.20 - Input Pins 22 and 23

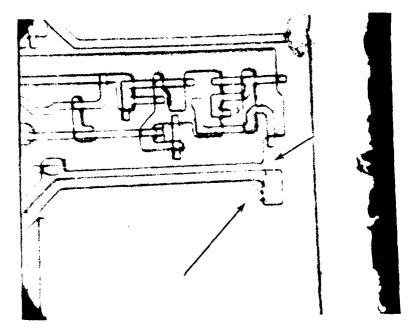


Figure V.B.21 - CD Stress, Pin 22 Input Damage

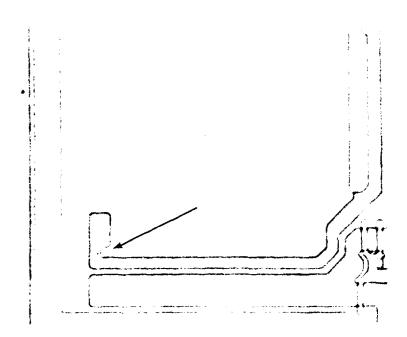


Figure V.B.22 - CD Stress, Pin 5 Input Damage

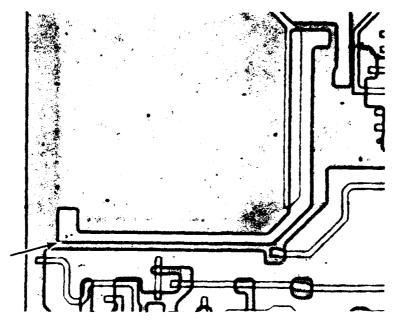


Figure V.B.23 - CD Stress, Pin 4 Input Damage

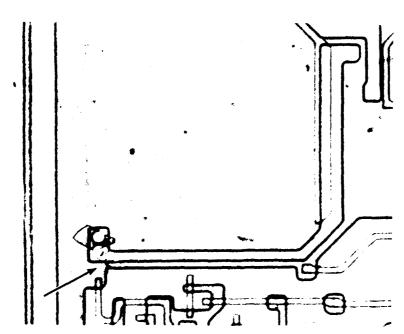


Figure V.B.24 - CD Stress, Pin 3 Input Damage

Figure V.B.25 - CD Stress, Pin 13 Input/Output Circuit with No Visible Damage

		Voltage	0	+500	+1000	+1500	Sensitivity Classif.	A. Metal Run Length	B. VCC or VSS Connect	C. Layout Style
(Ar		_								
er (r		23	1.0	3.1	22.0	29.0	2	short	VSS	2
n Num		22	0.8	1.5	41.0 22.0	28.3 29.0	2	short	$^{\rm V}_{\rm SS}$	1
by Pi		8	0.9	1.4	9.2	19.4	3	long long short short	Vcc	7
ırrent	\	7	1.5	2.3	11.5		3	long	vcc	7
Leakage Current by Pin Number (nA)	\	9	0.9	1.4	37.1 11.5	46.5 15.1	2	short	$^{\Lambda}$	1
Leak	\	5	0.9	0.9	50.9	33.1 25.3 108.6 132.7	1	short short shortshort short	ρος	3
		4	0.9	1.1	10.8	108.6	-	short	VSS	2
!		3	1.1	1.8	13.0 17.5	25.3	2	short	VSS	-
j		2	0.8	1.0	i i	33.1	2	short	VSS	2
'		-	0.8	2.0	35.2	36.3	2	short	VSS	-

Figure V.B.26 - HBD Stress, Leakage Current Summary

Chr. Car. 18	<u>\$</u>	-	
	setial humb	Ritt kindiget	
		*HIGHTS	
CA	set'	Rith	Voltage
1.9nA	5	7	0
3.5nA	15	23	+250
6.4nA	15	23	-250
8.2nA	15	23	+500
6.1nA	15	23	-500
73nA	5	1	+750
70nA	5	1	- 750
270nA	15	5	+1000
277nA	15	5	-1000
340nA	11	3	+1250
369nA	11	3	-1250
15uA	7	22	+1500
15uA	7	22	-1500
21uA	11	23	+1750
20uA	11	23	-1750
692uA	<u>i1</u>	2	+2000
756uA	11	2	-2000

Figure V.B.27 - HPD Stress, Maximum Leakage Current at each Stress Level

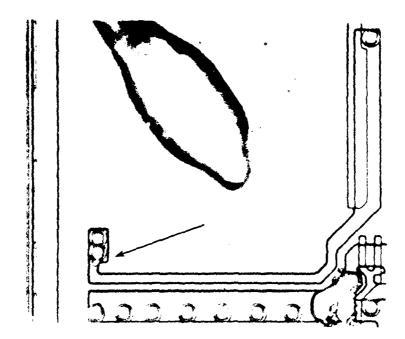


Figure V.B.28 - HBD Stress, Pin 5 Input Damage

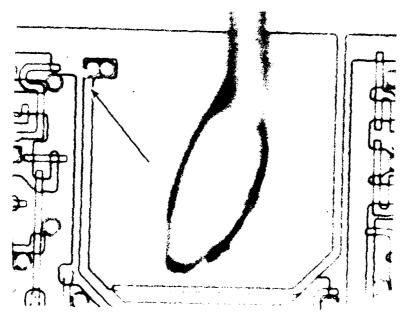


Figure V.B.29 - HBD Stress, Pin 22 Input Damage

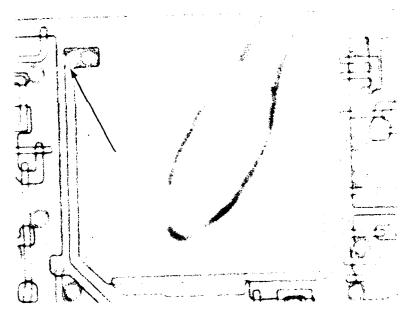


Figure V.B.30 - HBD Stress, Pin 21 Input Damage

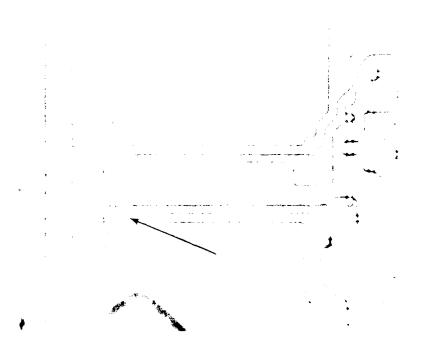


Figure V.R.31 - HFD Stress, Pin 20 Input Damage

EOS (ELECTRICAL OVERSTRESS) PROTECTION FOR VLSI (VERV LARGE SCALE INTEGRA. (U) MARTIN MARIETTA AEROSPACE DENVER CO D D MILSON ET AL. SEP 84 MCR-84-596 RADC-TR-84-183 F38682-82-C-9111 F/G 9/1 AD-A150 333 2/3 UNCLASSIFIED NL Ţ. 1 į, 11 U L. 10 1



MICROCOPY RESOLUTION TEST CHART NATIONAL BUREAU OF STANDARDS-1963-A

C. Part C Analysis

This device is an octal D-type transparent latch manufactured using Advanced Low-Power Schottky (ALS) processing. This utilizes an oxide-isolated, ion-implanted process.

There are two layers of metallization. The top layer is primarily the VCC and VSS interconnects. This part was in a 20-pin dual-in-line ceramic package. An overall die photo is shown in Figure V.C.l. VCC is pin 20 at the top of the figure and VSS is pin 10 at the bottom.

The VCC pin is shown in Figure V.C.2. It has two bond wires and the metallization exits from it and goes to numerous points, primarily pull-up resistors.

The ground pin is shown in Figure V.C.3 and it also has two bond wires. The metallization is connected to diodes and to the emitter of numerous transistors.

The 8 latch input pins are along the left side of the die. These are identical except for longer metallization runs on pins 2, 3, 8 and 9. A typical input is shown in Figure V.C.4. The components are labeled and correspond to the schematic in Figure V.C.5. The inputs on pins 1 and 11 are a different layout than the other eight. The schematics are essentially the same.

The reverse bias junction breakdowns of Dl and Ql base-emitter and Ql base-collector were all 28 volts. The NPN transistor was characterized and had a base-emitter breakdown of 7 volts and a base-collector breakdown of 30 volts. Other component configurations were electrically characterized to aid in the failure isolation. It was difficult to determine visually the different junction contacts, however, by characterizing the test structures the components could be more easily recognized.

The eight outputs are along the right hand side of Figure V.C.1 and one of these is shown in Figure V.C.6. This is a standard output stage as shown in Figure V.C.7.

The output layouts are identical except for longer metallization runs to pins 12, 13, 18 and 19.

Microsections were performed to examine the structures utilized. Figure V.C.8 shows a microsection through an input structure. The components are labeled the same way as in Figure V.C.4. A second microsection is shown in Figure V.C.9. This was etched for a shorter time and the diffusion depths are more readily measurable. The dimensions measured include: epitaxial thickness = 7 microns, p-diffusion = 4 microns, n-type layer = 1 micron, shallow p-diffusion = 0.5 microns, dielectric between metallization layers = 0.5 microns, dielectric between metallization = 0.5 to 1.5 microns.

Electrical Testing

A sample of the electrical data taken on each of the stressed parts and the control part at each iteration during the testing is shown in Figures V.C.10 and V.C.11. Figure V.C.10 shows the initial readings on serial number 3 and Figure V.C.11 shows the readings after the +1000 volt stress.

The input pins were measured for I_I , I_{IH} , I_{IL} and V_{IK} . The first three measurements are input current measurements taken at 7.0 volts, 2.7 volts, and 0.4 volts respectively. The V_{IK} measurement verifies the presence of a reverse bias protection diode at each input.

The output pins were measured for v_{OH} , v_{OL} , I_{O} , I_{OZH} and I_{OZL} . These measurements verified proper functional operation of the outputs in their normal operating mode and in their high impedance mode.

A functional verification of the output control pin was included, however, the enable pin was not placed in the low state (disabled condition).

Charged Device Data Analysis

Serial numbers 17-31 were stressed with the charged device simulation model. A summary of the pins which failed the $I_{\rm IH}$ or $I_{\rm I}$ measurements and the point at which they failed is shown in Figure V.C.12. These data indicate that the parts are more susceptible to a negative stress than a positive stress and that there is a significant difference in sensitivity between pins.

The leakage currents seen on a single device, serial number 17, are shown in Figure V.C.13. The leakage currents go from low nanoamp readings to microamp readings. This size of change is different than was seen on the bipolar input protect circuitry on the MOS devices, which degraded slowly through the nanoamp region.

No functional failures occurred during this testing. The inputs were removed from stress as soon as they exceeded the 20 microamp specification. This leakage current level was enough to provide sensitivity information without creating excessive damage to the part.

The input pin layouts are shown in Figures V.C.14 through 18. Figure V.C.14 shows pin 1 and Figure V.C.15 shows pin 11. These inputs have similar layouts. The junction which became leaky was the base/collector and this is labeled. This is the standard PNP input with the base connected to the input pin and the collector connected to ground.

Pins 2 through 9 have the same input schematic and layout with the only difference being the length of the metallization connecting the bond pad to the base.

The layout of pin 2 is the same as pin 9 and the layout of pin 3 is the same as pin 8. These are shown in Figures V.C.16 and V.C.17.

Pins 4 through 7 have identical layouts and are as shown in Figure V.C.18.

Visual inspection found no apparent damage on the inputs which had excessive leakage current. Various failure analysis techniques were used to locate the failures. Input to ground electrical measurements found that the damage on pins 1 and 11 created leakage at low voltage levels, i.e. 10 microamps at 0.2 volts. The damage on pins 2 through 9 created leakage at a higher voltage level, i.e. 10 microamps at 2.0 volts. Inputs 1 and 11 developed degraded base/collector junctions while inputs 2 through 9 developed degraded D1 diodes (reference Figure V.C.5).

One device was chemically stripped and examined. No damage was visible on the die surface. The part was stained with sirtl etch and examined. No damage was visible. Current was forced through the damaged junctions on a second device, serial number 18, with liquid crystal on the part. The locations of the failures were evident. The die surface was then washed to remove the liquid crystal and higher current (50 mA) was forced through the failure sites to make the damaged area visible for documentation. The damage produced was at the leakage current sites and made the damage much worse than was caused by the ESD stress.

Input pin 11 is shown in Figure V.C.19. This was typical of the location of the failures which occurred on pins 1 and 11. Input pin 7 is shown in Figure V.C.20. The location is typical of the location of the failures which occurred on pins 2 through 9.

With an understanding of the physical layout and the failure modes a better understanding of the variation in pin sensitivity is possible. The stress which created the major leakage on these parts was the negative voltage. This is due to the fact that this polarity produced a reverse bias stress on the input junction. The device is charged negative and then discharges out of the pin which is connected for stress. The pin is the cathode connection and the rest of the part which is charged negative is the anode connection, thus the reverse bias stress. Note that this is opposite of that which occurs for the human body discharge failure mode.

In Figure V.C.12 the -750 volt stress level appears to be the best point at which to analyze the data since all parts were still in stress and all but four of the pins were damaged.

Pins 1 and 11 are not very susceptible to damage. The base/collector junction is much more tolerant of ESD stress than the Schottky diode. Pins 2, 3, 8 and 9 are much less susceptibe to damage than pins 4, 5, 6 and 7. This is due to the longer metallization in series with the discharge path.

Two changes could decrease the input sensitivity; l. Place the Schottky diodes (D1) on the opposite side of the input structure from the base contact, 2. Increase the metallization length between the bond pad and the

base contact. The first change appears to be a practical method for reduced sensitivity. The second change may require excessive chip real estate and some loss in speed, however, it could also be incorporated with little change in the manufacturing of the device.

Human Body Discharge Data Analysis

Device serial numbers 2 through 16 were stressed with the human body ESD simulation test method. A summary of the pins which failed $I_{\rm IH}$ or $I_{\rm I}$ measurements and the point at which they failed is shown in Figure V.C.21. These data indicate that the parts are more susceptible to a positive stress than a negative stress.

The leakage currents seen on a single device, serial number 3, are shown in Figure V.C.22. These leakage currents go from low nanoamp readings to microamp readings. This is the same type of change as that experienced by the charged device parts.

No functional failures occurred during this testing. This is due to the inputs being removed from stress when they reached 20 microamps. The sensitivity of the devices to the positive stress is due to the input being an n-type diffusion. The reverse biased input junction is much more susceptible to stress than a forward biased junction.

Visual inspection was performed on each of the 15 parts. There was no visible damage. One device was sequentially stripped and examined and no damage was visible. Serial number 8 was then examined with liquid crystal and the failure locations were found to be the same as seen for the charged device group. Examples of two of these inputs are shown in Figures V.C.23 and V.C.24. The failure sites were accentuated by forcing current through them.

The major factor that affects the sensitivity of the various inputs is the type of diffusion that is adjacent to the input base contact. Pins 1 and 11 have the collector adjacent to the base and these were the least sensitive. This remains true up to the final stress with the exception of pin 9 which is very insensitive to damage. No physical reason was found for this.

The two groups of parts were found to fail with the same failure mode and with similar layout sensitivity. The HBD stress created earlier leakage current failures than the CD stress but the CD parts all had failed at a lower voltage.

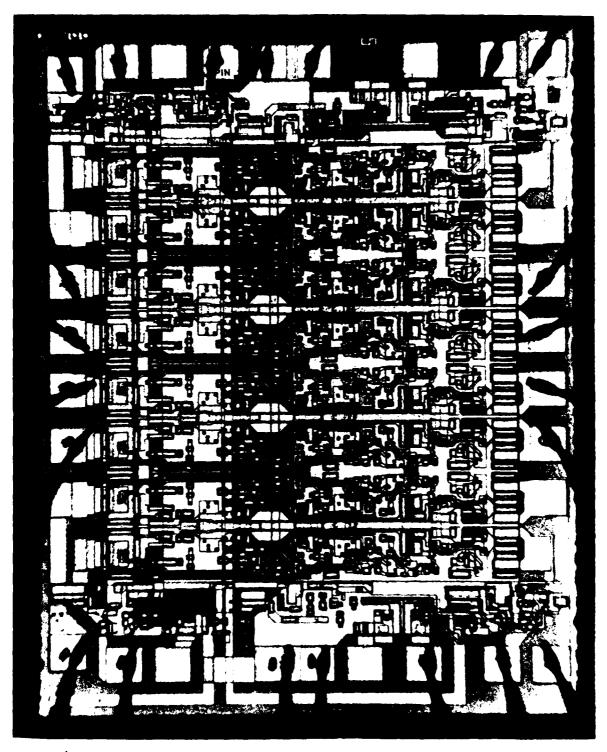


Figure V.C.1 - Overall Die Photograph

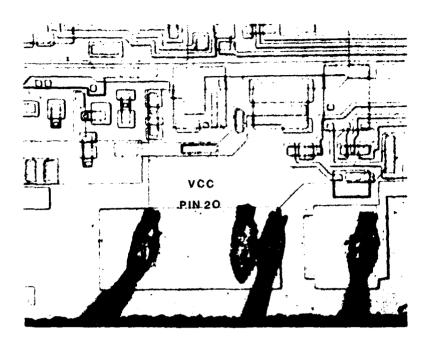


Figure V.C.2 - VCC Bond Pad

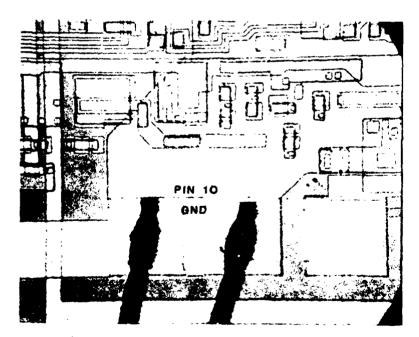
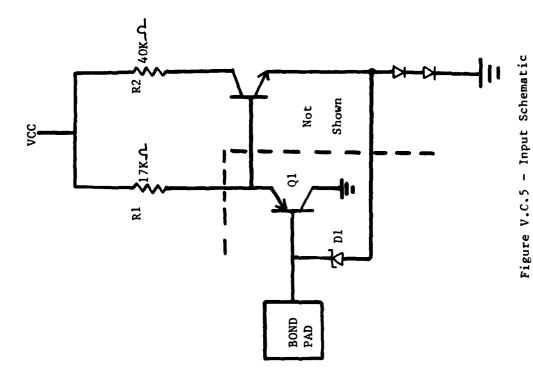


Figure V.C.3 - VSS Bond Pad



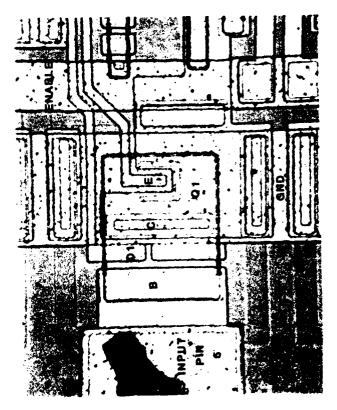
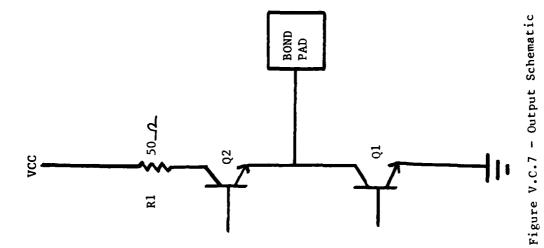


Figure V.C.4 - Pin 5 Input



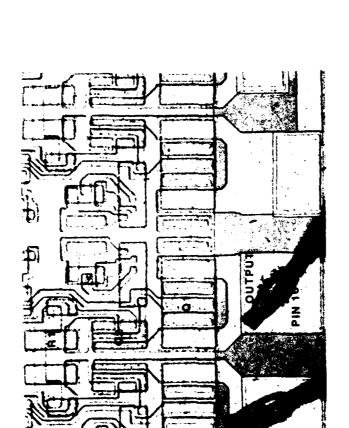


Figure V.C.6 - Pin 16 Output

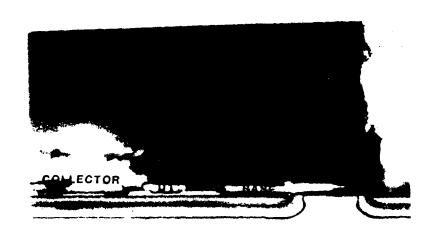


Figure V.C.8 - Input Transistor Cross-Section

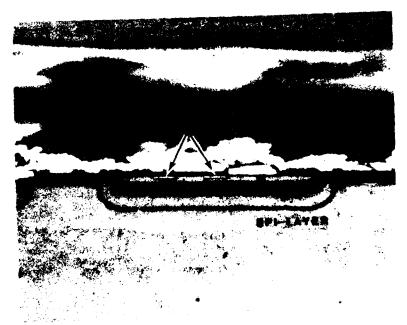


Figure V.C.9 - Internal Transistor Cross-Section

MARTIN MARIETTA AEROSPACE -- DENVER DIVISION -- PARTS EVALUATION LAB

FILE UID :147 SERIAL NUMBER - 3
-ESTED AT 25 DEG. C NO. 1 ELECTRICAL
ON 30 JUN 83 AT 08:16:51 WITH THE 3260 TEST SYSTEM

FAIL	TEST Type	MEASURED VALUE	L I M I MINIMUM	T S MAXIMUM
	VOH	 2.935 V	2.400 V	
	VOH	 2.935 V	2,400 V	
	VOH	 2.935 V	2.400 V	
	VOH	 2.930 V	2.400 V	
	VDH	 2.935 V	2.400 V	
	VOH	 2.930 V	2.400 V	
	VOH	 2.930 V	2.400 V	
	VOH	 2.930 V	2.400 V	
	VOL	 274.5MU		400.0MV
	VOL	 272.5MV		400.0MV
	VOL	268.0MV		400.0MU
	VOL	267.5MV		400.0MV
	AOF AOF	268.5MV		400.0MV
	VOL	294.0MV		400.0MV
	VOL	274.0MV		400.0MV
	VOL	274.0MV		400.0MV
	VUL	272+3110		400.000
	VIK	 -925.0MV	-1.500 V	- -
	VIK	 -925.0MV	-1.500 V	
	VIK	 -920.0MV	-1.500 V	
	VIK	 -920.0MV	-1.500 V	
	VIK	 -920.0HU	-1.500 V	
	VIK	 -920.0MV	-1.500 V	
	UIK	 -925.0MV	-1.500 V	
	VIK	 -925.0MV	-1.500 V	
	IIH	 2.650NA		20.00UA
	IIH	 1.650NA		20.0000
	IIH	 1.450NA		20.00UA
	IIH	 1.350NA		20.00UA
	IIH	 1.400NA		20.00UA
	IIH	 1.300NA		20.00UA
	IIH	 1.350NA		20.00UA
	IIH	 1.400NA		20.00UA
	IIL	 -40.50UA	-200:0UA	
	IIL	 -40.00UA	-200.00A	
	IIL	-41.00UA		
	IIL		-200.0UA	
	IIL	 -40.50UA	-200.0UA	
	IIL	 -42.00UA -41.50UA	-200.0UA	
	IIL	 -40.00UA	-200.0UA	
	IIL	 -40.00UA	-200.0UA -200.0UA	
	•	** *****		
	10	 -35.90MA	-120.0MA	-20.00MA
	10	 -36.30MA	-120.0MA	-20.00MA
	10	 -36.30MA	-120.0MA	-20.00MA
	10	 -36.50MA	-120.0MA	-20.00MA

Figure V.C.10 - Initial Electrical Measurements

FILE UID :147 SERIAL NUMBER - 3
1ESTED AT 25 DEG. C NO. 1 ELECTRICAL
ON 30 JUN 83 AT 08:17:20 WITH THE 3260 TEST SYSTEM

FAIL	TEST TYPE	MEASURED VALUE	L I M I MINIMUM	T S MAXIMUM
	10	 -36.25MA	-120.0MA	-20.00MA
	10	 -35.20MA	-120.0MA	-20.00MA
	10	 -36.05MA	-120.0MA	-20.00MA
	10	 -36.25MA	-120.0MA	-20.00MA
	ICCH	 11.15MA		14.00MA
	ICCL	 17.05MA		22.00MA
	ICCZ	 18.15MA		24.00MA
	IOZH	 4.350NA		20.00UA
	IOZH	 3.500NA		20.00UA
	IOZH	 3.750NA		20.00UA
	IOZH	 3.100NA		20.00UA
	IOZH	 3.050NA		20.00UA
	IOZH	 2.950NA		20.00UA
	IOZH	 3.200NA		20.00UA
	IOZH	 3.050NA		20.00UA
	IOZL	 1.750NA	-20.00UA	
	IOZL	 1.700NA	-20.00UA	
	IOZL	 1.900NA	-20.00UA	
	IOZL	 1.950NA	-20.00UA	
	IOZL.	 2.150NA	-20.00UA	
	IOZL	 1.950NA	-20.00UA	
	102L	 2.200NA	-20.00UA	
	IOZL	 2.150NA	-20.00UA	
	II	 7.100NA		100.0UA
	II	 4,650NA		100.0UA
	ΙΙ	 4.000NA		100.0L!A
	ΙΙ	 3.500NA		100.0UA
	11	 3.000NA		100.0UA
	ΙΙ	 3.000NA		100.0UA
	II	 3.000NA		100.0UA
	11	 2.900NA		100.0UA

TEST RUNTIME IS 11 SECONDS PRINT / DISPLAY TIME IS 53 SECONDS

Figure V.C.10 - Initial Electrical Measurements (Cont.)

MARTIR MARTETTA AFROSPACE -- DERVER DIVISION -- PARTS EVALUATION LCB

FILE UID (147 SERTAL RUMBER - 3 ON 02 SEP 83 AT 08:38 WITH THE 3260 TEST SYSTEM

FAUL	TEST TYPE	·	MEASURED VALUE	t. 1 m i Minimum	T S MAXIMUM
	V0H	-2:930 U	2,930 0	2,400 V	
	VOH	-2.925 V	2.925 V	2,400 0	
	VOH	-2.930 U	2.930 V	2.400 U	
	YUH	- 930 comu	2,930 (2,400 0	
	VOH	-2:923 U	2,930 U	2:400 0	
	HOV	-1:000F+33 U	2.920 0	2,400 0	
	VOH	-J.915 V	2,915 0	27400 0	
	VOH	-2.920 V	27925 0	2,400 U	
	VOL	-290.0KU	290.089	- -	100 , 01
	VOL	-282:SMV	2827,580		100:01
	VOL	222.4KV	277 (560		
	VOI.	1.718 Ú	2827040		400 i 00 400 i 00
	VOL.	~283.0KU	283.060		
	VUL	+321 con0	321 conv		400 aur
	VOL	29.66 U	338.040		400.00
	AOC	980, 185.	2817000		400.00 400.00
	VIK	930 . OnV	-930,06U	-1.500 V	
	Vik	925 contt	-925.06V	-1,500 V	
	VXK	935 a OñO	-935 conv	-1.500 V	
	VTK	925.660	-925.0MU	-1,500 V	
	VIK	940.0hV	-940.0MU	-1,500 V	
	AT9	925.0K0	-925.08Q		
	VIK	965.060	-96U. ONV	-1,500 0	
	UTK	935,040	-935.080	-1,500 V -1,500 V	
K 2 3	LTH	-31,0000	41:00UA		17. 20.11
	J. i H	-2 : 05 03(n)	1 - 10086		.10 , 000
* 4.4	IIH	an estable.	14 continue		thio, etc.
★定項	OH	-66.5Udin	60 a 5500		20 000
# 5 %	CIH	-36,8000	36.8000		, a coett
	1 TH	-2.6520NA	1.650000		29.000
	JJН	-20 COOPA	1.40000		20.000
***	ETH	-23.25UA	73.75UA		70,000
	CFH	950.0FA	400:0FA		20.000
***	ÜН	-81.25UA	81,20UA		1000 - 91. Here , 91.
	111	2,000 A	-42,00UA	-200,0UA	
	3.1.L	39750UA	-39,50UA	-200700W	- ·
	f.t.i.	43,5000	-43,50UA	-200 coun	
	111.	43.00UA	-43,00UA	-2007.000 -2007.000	
	111	1.000 A	-44.50UA	-200.00A	
	3.34	100,0ma	-41.00UA	-1'00 ; OHA	
	f fL.	-1:000F+33 A	-40,00UA	+.100+000	
	411	1,000 A	-42,50UA	-2007004s	
	TIL	25g 53nA	-26.00UA	-200 coun	
	111	53.00UA	-51,000A	-20070UA	
	10	357.75FA	-35 (25MA	+120.0mm	-70 a QQ16.

Figure V.C.11 - Electrical Measurements Following the +1000 Volt Stress

FILE UTD :147 SERIAL NUMBER - 3
TESTED AT 25 DEG. C NO. 7 ELECTRICALS
ON 02 SEP 83 AT 08:38 WITH THE 3260 TEST SYSTEM

FAU.	TEST TYPE		MEASURED VALUE	L I M I MINIMUM	L S NAXIKUK
	10	223.5E+0a A	-35,90MA	-120.08A	-20.00MA
	10	35 i 85nA	-35.8566	-120,0HA	~20.00mA
	ΤÜ	35.80KA	-35,80MA	-120 c0fee	-20.00MA
	70	35.65NA	-35.65MA	-120 a 0hA	-20.00MA
	10	34 a 0 0 ma	-34,0000	-120.0mA	-20.00MA
	70	33,2000	-33,20MA	-120.0MA	-20,00KA
	70	35.85KA	-35,85KA	-120.08A	-20,00MA
	TOCH	-11.1566	il (15ma		14.00m
	rect.	-14,85MA	16.85%A		22 - 00h
	ICCZ	-18.10%6	18.10mA		24.000
	TOZH	-5.150NA	5.150NA		20,0000
	10ZH	- 4.100RA	4.100NA		20,000
	£02H	-4.250NA	4.250RA		.'0 - 000
	X07H	-3.550RA	37550NA		20.000
	3 () ZH	-3,400RA	3,400RA		يان ۾ پري
	(0ZH	3.250RA	3.250RA		الارون وي
	3.01ZH	3+300RA	3.300NA		./0 . 000
	#V0.1	37000NA	AN00018		20 : GOU
	TOZL	906,8E409 A	27000NA	-20.0006	
	TUZL	10:51E+06 A	ANOCH I	-20:00UA	
	.(OZL	-1 :850NA	1,85006	-20.00UA	
	(07)	219.4KA	4,800MA	-20,000A	
	£0ZL	-1.750NA	1 c ZSONA	-20.00UA	
	TOZL	203.0KA	1 . ZOONA	-20 cootia	
	.0071	-1.200RA	1 a 2000A	-20.00UA	
	TUZL	1.65086	1,65000	-20.00UA	
C# 5.8	Ĺ	-526.50A	526,500	**	100.00
	11	3.315 0	37000046		100.00
(本常常	3.1	- 442 (SUA	4427,504		199,90
***	1.1	−203 c5UA	753 (5UA		109.00
* \$ #	U	-283, QUA	2837000		100.001
	1.1	~3×250NA	ANOUN S		100.00
	11	-3:000NA	31000NA		100.00
K 本 注 容	1)	-1:0246A	1.024MA		100,00
	11	-37200NA	3 (250NA		100,00
×	£ 7	-1:024ha	1.02486		100,000

Figure V.C.11 - Electrical Measurements Following the +1000 Volt Stress (Cont.)

	Nt	ımber (of Fai	lures	at Pir	n Loca	tions				
1 2 3 4 5 6 7 8 9 11 Voltage											
I	2	3	4	5	6	7	8	9	11	CD 40	Voltage
											+250
											-250
											+500
											-500
					3	1					+750
1		2	6	6	9	5	2	1			-750
1	1	3	7	8	9	6	2	2	1	3	+1000
2	6	8	11	12	11	7	9	3	11	15	-1000

Figure V.C.12 - CD Stress, Cumulative Leakage Failures

	Leakage Current by Pin Number (nA except as noted)												
	/		/ .	/ .	/ ,	/	/ .	/ .	/ ,	/ ,	/		
	1	2	3	4	5	6	7	8	9	11	Voltage		
ſ	-	2.1	1.3	0.8	0.7	0.6	0.6	0.4	0.5	-	0		
T		2.4	1.3	1.1	0.7	0.6	0.6	0.6	0.6	-	+250		
T	-	2.1	1.2	1.0	0.7	0.6	0.7	0.6	0.6	_	-250		
r	-	2.4	1.4	1.1	1.0	0.7	1.0	1.0	1.1		+500		
1	0.8	2.7	1.7	1.4	1.2	1.0	1.0	0.9	1.0	0.8	-500		
	4.2	2.8	2.5	2.5	1.0uA	4.1	1.4	l.luA	6.7	0.6	+750		
1	4.2	2.3	2.0	2.2	1.OuA	15 uA	0.6	28uA	7.2	1.0	-750		
1	4.0	2.6	2.4	2.5	1.0uA	19uA	0.5	11uA	6.6	1.0	+1000		
	4.0	35uA	19	6.0	1.9uA	61uA	10	35uA	1.OuA	167uA	-1000		

Figure V.C.13 - CD Stress, Serial Number 17 Leakage Current Summary

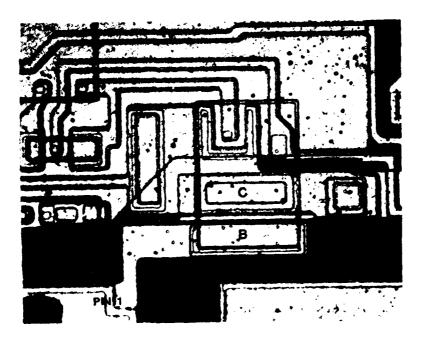


Figure V.C.14 - Pin 1 Input

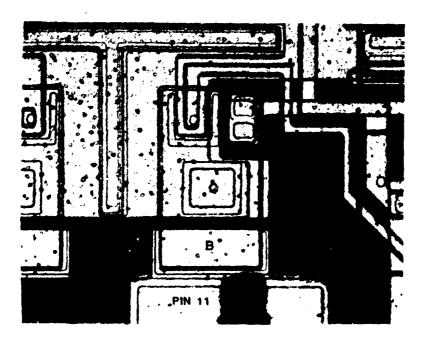


Figure V.C.15 - Pin 11 Input

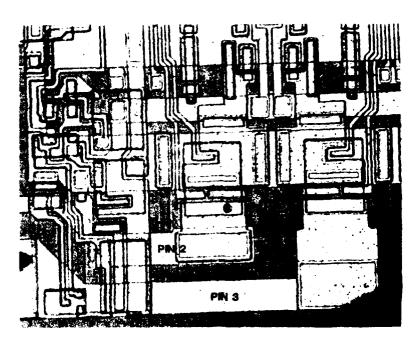


Figure V.C.16 - Input Pins 2 and 3

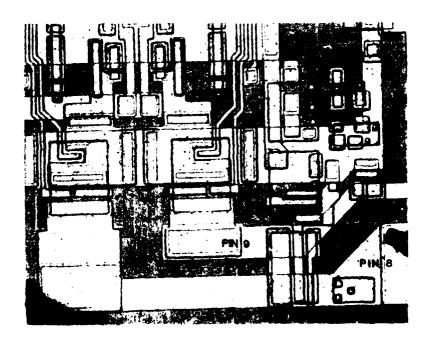


Figure V.C.17 - Input Pins 8 and 9

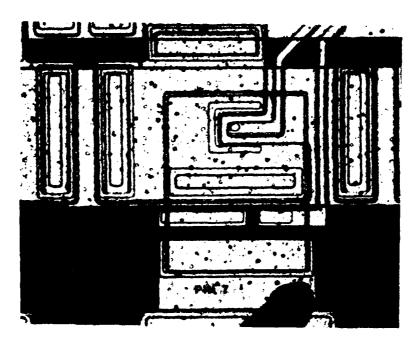


Figure V.C.18 - Pin 7 Input

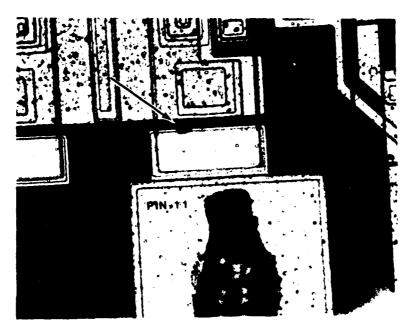


Figure V.C.19 - Pin 11 Input Failure Location.

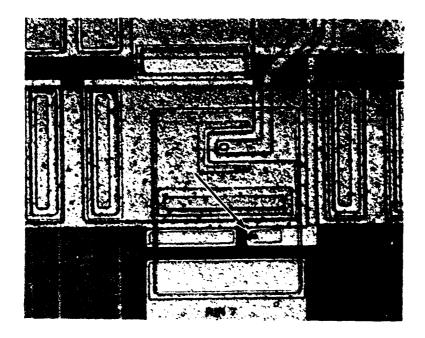


Figure V.C.20 - Pin 7 Input Failure Location.

Number of Failures at Pin Locations

	1 2 3 4 5 6 7 8 9 11 Catal de la constant de la con											
1	2	3	4	5	6	7	8	9	11	0 4	Voltage	
<u></u>							1				+250	
							1				-250	
	2	2	3	2	2	1	5		1		+500	
	2	2	3	2	2	1	5		1		-500	
	2	2	3	2	2	1	_ 5		1		+750	
	2	2	3	2	2	1	5		1		-750	
	4	4	4	3	4	2	5	2	2	3	+1000	
	4	4	4	3	5	2	6	2	2	_3	-1000	
	5	5	5	7	9	4	7	2	3	5	+1250	
	5	5	5	7	9	4	7	2	3		-1250	
4	10	13	9	10	11	5	8	3	11	15	+1500	

Figure V.C.21 - HBD Stress, Cumulative Leakage Failures

Leakage Current by Pin Number (nA except as noted)

1	2	3	4	5	6	7	8	9	11	Voltage
-	2.6	1.6	1.4	1.3	1:4	1.3	1.3	1.4	-	0
_	2.7	1.9	1.7	1.6	1.5	1.6	1.5	1.6	_	+250
_	2.6	1.8	1.5	1.4	1.4	1.4	1.4	1,4	-	-250
_	2.4	1.4	43uA	1.6	83uA	0.9	0.7	0.8		+500
1.3	3.0		36uA		80uA	1.7	1.5	1.4	1.4	-500
0.8					58uA	1_1_	0_9	0.9	0.8	+750
0.6	7 - 1		44uA		35uA	1.2	0.9	0.8	0.7	- 750
0.4			44uA		37uA	1.6	1.4	ſ	81uA	+1000

Figure V.C.22 - HBD Stress, Serial Numbr 17 Leakage Current Summary

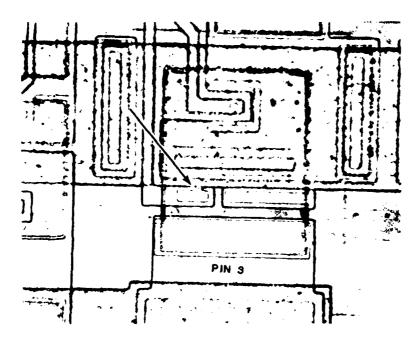


Figure V.C.23 - HBD Stress, Pin 3 Input Damage

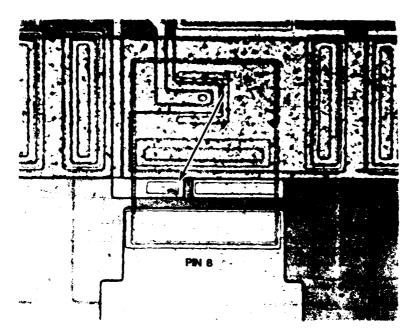


Figure V.C.24 - HBD Stress, Pin 8 Input Damage

D. Part D Analysis

This device is an Octal Transparent Latch with 3-state outputs manufactured with the Isoplanar II process. This is an oxide isolated technique which allows the oxide to come up to the edge of the emitter contact (walled emitter). This has a single level of metallization for the interconnects. These parts were in 20-pin dual-in-line ceramic packages.

An overall die photograph is shown in Figure V.D.1. VCC is pin 20 and is at the top of the figure and GND is pin 10 at the bottom of the figure. The ground metallization runs around the perimeter of the die and provides the contact to the anode for the diode on each input and output. The VCC metallization is in the center of the die. It is connected to pull-up resistors.

An input structure is shown in Figure V.D.2. The components are labeled corresponding to Figure V.D.3. The input transistor base-emitter and base-collector junctions and diode Dl all measured 20 VDC breakdown.

An output structure is shown in Figure V.D.4 and the schematic is shown in Figure V.D.5. The protect diode is not shown in Figure V.D.4 but is visible in the overall photograph.

Microsections were performed to examine the construction of the components. The input transistor is shown in Figure V.D.6. The top view is shown at 500% while the side view is shown at 1200%. The approximate thicknesses of the layers are: Metallization = 1.0 microns; p-Layer = 1.8 microns; n-Layer = 1.0 microns, dielectric between metallization and silicon = 1.0 microns.

The p-type emitter diffusion was not visible in the sections. The Schottky diode on each pin was also microsectioned and is shown in Figure V.D.7. The p-type Schottky diffusion is very shallow and is not visible in the section.

Electrical Testing

A sample of the electrical data which was taken on each of the stressed parts and the control part at each iteration during the testing is shown in Figure V.D.8 and V.D.9. Figure V.D.8 shows the initial readings on serial number 11 and Figure V.D.9 shows the readings on serial number 11 after the -2500 volt stress.

The VCD measurement verified the presence of the protect diode. Four devices failed this measurement at initial test, a resistive Schottky contact was found on these parts and they were not included in this test. These were serial numbers 2, 15, 16, and 18.

Device functionality was verified by the VOH and VOL tests. A functional verification of the output enable pin was included, however, the

latch enable pin was not placed in the low state (disabled condition). Leakage current at the inputs was measured with the I $_{\rm IH}$ (V $_{\rm IN}$ = 2.7 V) and I $_{\rm IL}$ (V $_{\rm IN}$ = 0.5 V) readings. Output circuit leakage was measured with the I $_{\rm OZH}$ (V $_{\rm OUT}$ = 2.4 V) and I $_{\rm OZL}$ (V $_{\rm OUT}$ = 0.5 V) readings.

The two readings which provide the most information on the gradual leakage increase are $I_{\,IH}$ and $I_{\,OZH}.$ $I_{\,IH}$ increased considerably while little change occurred in the outputs.

Charged Device Data Analysis

Fourteen devices, serial number 17 and 19 through 31, were subjected to the charged device ESD simulation model. The first leakage failure (greater than 20 microamps) occurred at -750 volts and all parts were removed from test after the +1500 volt stress. All inputs became leaky and no other pins became leaky. The pin number and the voltage level at which leakage failures occurred are shown in Figure V.D.10. It is apparent that pins 1 and 11 were more sensitive to stress. It is also evident that the negative stress causes more damage than the positive stress. The negative stress sensitivity is consistent with the results seen on part C. This stress reverse biases the junction connected to the input pins and results in junction breakdown degradation.

The leakage current changes with stress application are shown for pin l on serial number 26 in Figure V.D.ll. There is a jump from picoamps to microamps and damage is only worsened by the negative stress.

All inputs had identical layouts except for pins 1 and 11. The input shown in Figure V.D.2 and the inputs shown in Figure V.D.12 are the layout used on pins 3, 4, 7, 8, 13, 14, 17 and 18. The layout shown in Figure V.D.13 is the layout for pins 1 and 11.

Failure analysis found no evidence of physical damage; however, mechanical probing and isolation determined the component which degraded. This was the Schottky diode on the input. Slight degradation of the base-collector junction on the input transistor was noted for some pins. Current was forced through pin 18 and pin 11 on serial number 27. This accentuated the failure sites and these are shown in Figure V.D.14 and V.D.15.

The increased sensitivity of pins 1 and 11 is apparently due to the fact that the current is forced to flow out of the contact at the end of the Schottky diffusion rather than spread over the whole diode. Additional heating and damage results. The large ground metallization acts as a major portion of the capacitance which discharges out of the pin being stressed. This is the reason for the Schottky diode being damaged (as will be discussed, this is not the junction that is damaged by the human body discharge model).

Human Body Discharge Data Analysis

Twelve devices, serial numbers 3 through 14, are subjected to the human body ESD simulation model. The first leakage failure occurred at +500 volts and the last device was removed after the +2750 volt stress (Figure V.D.16). The failures at +500 V and +750 V occurred primarily on serial numbers 7 and 9. These were removed and there were no additional leakage failures until +1250 volts. The positive stress causes the major device damage due to the reverse biased junctions for this polarity. Typical leakage current changes are shown in Figure V.D.17 for pin 1 on serial number 3.

Failure analysis found no evidence of physical damage. Mechanical isolation and probing found that the junction which degraded was the base-collector junction on the input transistor. This was not expected since the Schottky diode had failed on the parts stressed with the charged device model. Current was forced through pins 7 and 11 on serial number 4 to accentuate the failure sites. These are shown in Figure V.D.18 and V.D.19.

This result indicates that the weakest junction is the base-collector. This junction was not damaged for the charged device model because it received a much lower stress level than the Schottky diode. The increased sensitivity of pins 1 and 11 to the HBD stress does not appear to be strictly related to physical layout. The layout does not appear to provide an explanation for the sensitivity difference. There is a difference in the current path to ground. The schematic is basically the same but the components are not identical. The junction marked D4 in Figure V.D.2 is different than the base-emitter junction on transistor Q1 in Figure V.D.20. The general layout and interconnects are also different.

These results indicate the significance of the different stress methods. The charged device model causes damage to junctions which are connected to large metallization areas while the human body model damages the most susceptible junction in the current path to ground.

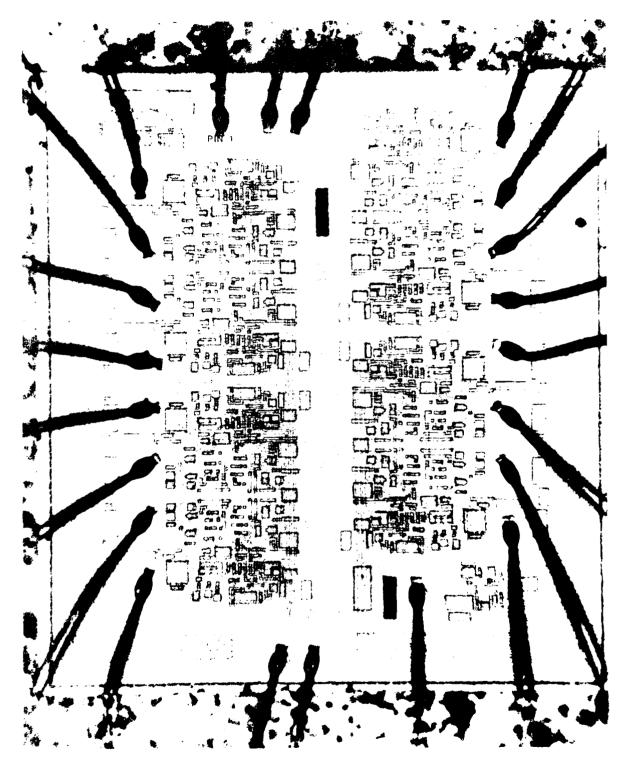
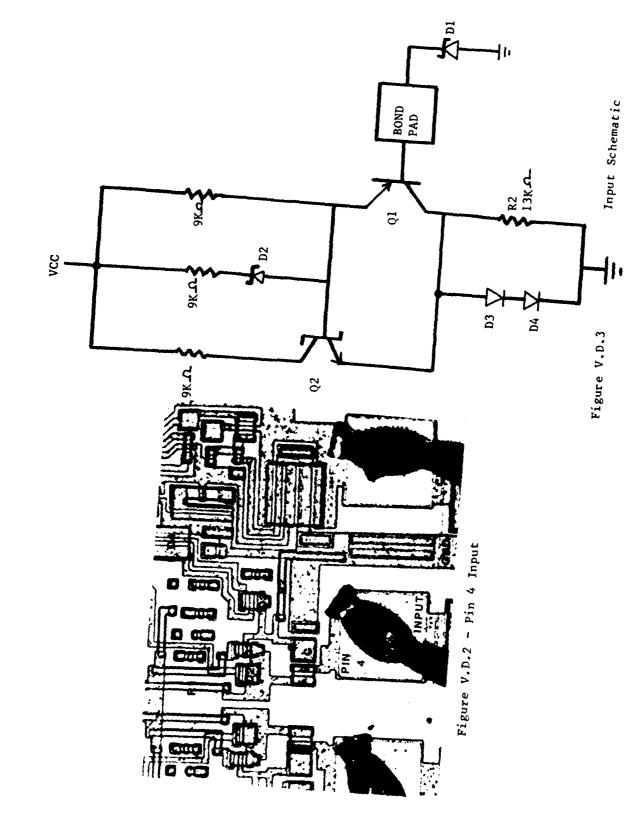


Figure V.P.1 - Overall Tie Brotograph



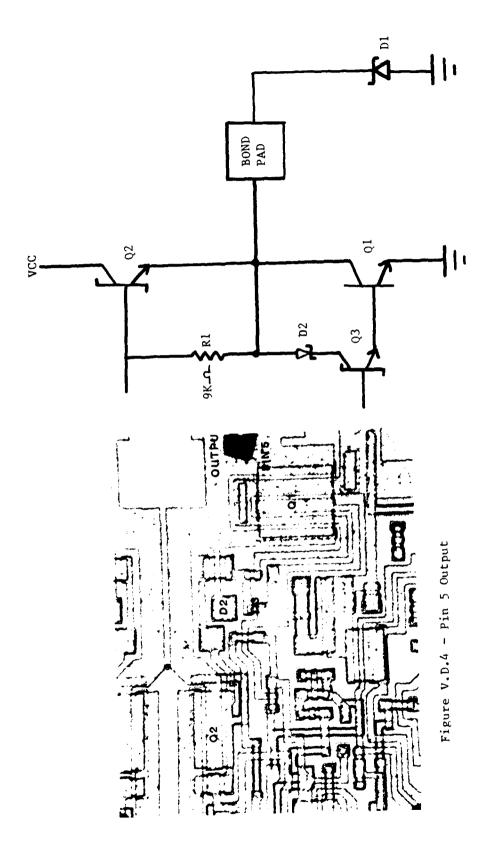
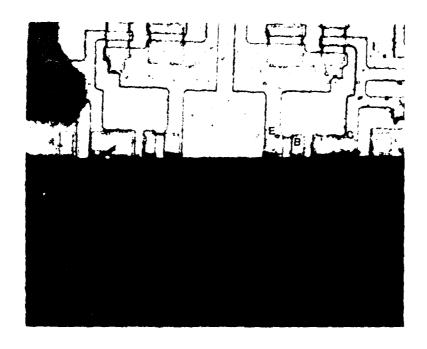


Figure V.D.5 - Output Schematic



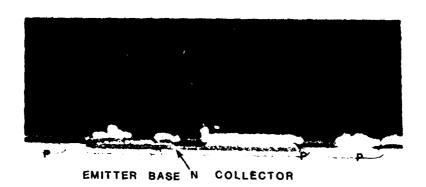
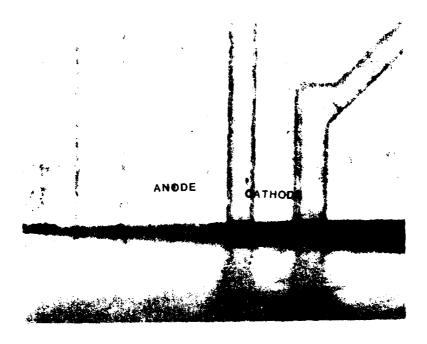


Figure V.D.6 - Input Transistor



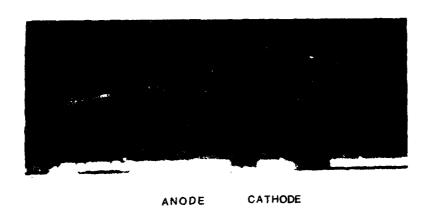


Figure V.D.7 - Input Diode Top View and Side View

MARTIN MARIETTA AEROSPACE -- DENVER DIVISION -- PARTS EVALUATION LAB

FILE UID :146 SERIAL NUMBER - 11
TESTED AT 25 DEG. C NO. 1 ELECTRICAL
ON 04 AUG 83 AT 15:36:27 WITH THE 3260 TEST SYSTEM

FAIL	TEST TYPE		MEASURED VALUE	L I M I MINIMUM	T S MAXIMUM
	ICC		30.10MA		55.00MA
	VCD		-705.0MV	-1.200 V	
	VCD		-705.0HV	-1.200 V	
	VCD		-705.0MV	-1.200 V	
	VCD		-705.0HV	-1.200 V	
	VCD		-705.0MV	-1.200 V	
	VCD		-700.0MV	-1.200 V	
	VCD		-700.0MV	-1.200 V	
	VCD		-700.0MV	-1.200 V	
	VCD		-720.0MV	-1.200 V	
	VCD		-710.0MV	-1.200 V	
	VOH		3.160 V	2.700 V	
	VOH		3.165 V	2.700 V	
	VOH		3.160 V	2.700 V	
	VOH		3.155 V	2.700 V	
	VOH		3.160 V	2.700 V	
	VOH		3.165 V	2.700 V	
	VOH		3.160 V	2.700 V	
	VOH		3.155 V	2.700 V	
	VOL		353.5MV		500.0MV
	VOL		349.0MV		500.0M
	VOL		349.0HU		500.0MU
	VOL	~	351.0MV		500.0M
	VOL		353.0MV		500.0M
	VOL		349.5MV		500.0M
	VOL		351.5MV		500.0H
	VOL		359.0MV		500.0M
	IIH		450.0PA		20.0004
	IIH		500.0PA		20.0004
	IIH		700.0PA		20.0004
	IIH		-200.0PA		20.0004
	IIH		950.0PA		20.0004
	IIH		700.0PA		20.0004
	IIH		500.0PA		20.0004
	IIH		250.0PA		20.000
	IIH		300.0PA		20.0004
	IIH		600.0PA		20.0004
	IIL		-356.5UA	-600.0UA	
	IIL		-351.5UA	-600.0UA	
	IIL		-353.0UA	-600.0UA	
	IIL		-351.0UA	-600.0UA	
	IIL		-357.5UA	-600.0UA	
	IIL		-360.5UA	-600.0UA	
	IIL		-358.0UA	-600.0UA	

Figure V.D.8 - Initial Electrical Data

FILE UID :146 SERIAL NUMBER - 11
1ESTED AT 25 DEG. C NO. 1 ELECTRICAL
ON 04 AUG 83 AT 15:36:57 WITH THE 3260 TEST SYSTEM

FAIL	TEST TYPE	 MEASURED VALUE	L I M MINIMUM	I T S MAXIMUM
	IIL	 -360.5UA	-600.0UA	
	IIL	 -352.5UA	-600.0UA	
	IIL	 -370.0UA	-600.0UA	~-
	IOZH	 4.700NA		50.00UA
	IOZH	 3.000NA		50.00UA
	IOZH	 3.200NA		50.00UA
	IOZH	 127.0NA		50.00UA
	IOZH	 4.600NA		50.00UA
	IOZH	 178.0NA		50.00UA
	IOZH	 312.0NA		50.00UA
	IOZH	 601.0NA		50.00UA
	IOZL	 1.300NA	-50.00UA	
	IOZL	 1.100NA	-50.00UA	
	IOZL	 700.0PA	-50.00UA	
	IOZL	 3.450NA	-50.00UA	
	IOZL	 2.600NA	-50.00UA	
	IOZL	 2.950NA	-50.00UA	
	IOZL	 3.000NA	-50.00UA	
	IOZL	 37.75NA	-50.00UA	
	108	 -68.00MA	-150.0MA	-60.00MA
	105	 -71.50MA	-150.0MA	-60.00MA
	IOS	 -71.50MA	-150.0MA	-60.00MA
	IOS	 -71.00MA	-150.0MA	-60.00MA
	105	 -71.00MA	-150.0MA	-60.00MA
	IOS	 -72.00MA	-150.0MA	-60.00MA
	IOS	 -71.50MA	-150.0MA	-60.00MA
	IOS	 -71.00MA	-150.0MA	-60.00MA

TEST RUNTIME IS 21 SECONDS PRINT / DISPLAY TIME IS 51 SECONDS

Figure V.D.8 - Initial Electrical Data (Cont.)

MARTIN MARIETTA AEROSPACE -- DENVER DIVISION -- PARTS EVALUATION LAB

FILE UID :146 SERIAL NUMBER - 11
IFSTED AT 25 DEG. C N2500V STRESS
ON 15 NOV 83 AT 12:31:09 WITH THE 3260 TEST SYSTEM

FAIL	TEST TYPE		MEASURFI VALUE	L I M 1 MINIMUM	T S MAXIMUM
	ICC		29.60MA		55.00MA
	VCD		-780.0MV	-1.200 V	
	VCD		-730.0MV	-1.200 V	
	VCD		-780.0MV	-1.200 V	
	VCI		-750.0MV	-1.200 V	
	VCD		-855.0MV	-1.200 V	
	VCD		-830.0MV	-1.200 V	
	VCD		-755.0MV	-1.200 V	
	VCD		-730.0MU	-1.200 V	
	VCD		-725.0MV	-1.200 V	
	VCD		-955.0MV	-1.200 V	
	VOH		3.110 V	2.700 V	
	VOH		3.105 V	2.700 V	
	VOH		3.105 V	2,700 V	
	VOH		3.105 V	2.700 V	
	VOH		3.105 V	2.700 V	
	VOH	-	3.105 V	2,700 V	
	VOH		3.105 V	2.700 V	
	VOH		3.110 V	2.700 V	
	VOL		386.5MV		500.0M
	VOL		381.5MV	- -	500.0M
	VOL		382.0MV		500.0M
	VOL		383.5MV		500.000
	VOL		380.0MV		500.0M
	VOL		376.5MV		500.0M
	VOL	-	3/7.0MU		500.0M
	VOL		400.0MV		500.0M
***	IІН	~	103.0UA		20.0004
	IIH		2.450NA		20.0004
	IIH		336.5NA		20.0004
	IIH		5.200NA		20.0004
	IIH		128.5NA		20.000
	IIH		300.0FA		20.0004
	IIH		27.35NA		20.0004
***	IIH		122.0UA		20.0006
***	IIH		77,95UA		20.0004
***	IIH		229.5UA	- -	20.0004
	IIL		-355.0UA	-600.0UA	
	IIL		-345.0UA	-600.0UA	
	IIL		-346.5UA	-600.0UA	
	IIL		-344.5UA	-600.0UA	
	IIL		-350.5UA	-600.0UA	
	IIL		-354.QUA	-600.0UA	
	IIL		-351.0UA	-600.QUA	

Figure V.D.9 - Post -2500 Volt Electrical Data

FILE UID :146 SERIAL NUMBER - 11

IESTED AT 25 DEG. C N2500V STRESS UN 15 NOV 83 AT 12:31:38 WITH THE 32-0 TEST SYSTEM

FAIL	TEST TYPE	MEASURED VALUE	MINIMUM	T S MAXIMUM
	IIL	 ~359.0UA	-600.0UA	
	IIL	 -353.0UA	-600.0UA	
	IIL	 -375.5UA	-600.0UA	
	IOZH	 3.400NA		50.00UA
	IOZH	 2.200NA		50.00UA
	IOZH	 1.800NA		50.0 A
	IOZH	 108.5NA		50.00UA
	IOZH	 2.600NA		50.00UA
	IOZH	 154.5NA		50.00UA
	IOZH	 263.0NA		50.00UA
	IOZH	 528.5NA		50.000A
	IOZL	 350.0FA	-50.00UA	
	IOZL	 800.0FA	-50.00UA	
	IOZL	 1.200NA	-50.00UA	
	IOZL	 2.400NA	-50.00UA	
	IOZL	 1.200NA	-50.00UA	
	IOZL	 1.700NA	-50.00UA	
	IOZL	 2.500NA	-50.00UA	
	IOZL	 30.80%	-50.0000	
	IOS	 -60.00MA	-150.0mA	-60.00mn
	IOS	 -63.50MA	-150.0MA	-60.00MA
	IOS	 -64.00MA	-150.0MA	AH00.00HA
	IOS	 -63.00MA	-150.0MA	-50.00MA
	108	 -65.00MA	-150.0MA	-40.00mA
	105	 ~65.00MA	-150.0ma	-60.00MA
	108	 -65.50MA	-150.0MA	-60.00MA
	108	 -63.50MA	-150.0MA	-60.00MA

TEST RUNTIME IS 20 SECONDS FRINT / DISPLAY TIME IS 51 SECONDS

Figure V.D.9 - Post -2500 Volt Electrical Data (Cont.)

Number of Failures at Pin Locations											
1 3 4 7 8 11 13 14 17 18 Cuffique Voltage											
1	3	4	7	8	11	13	14	17	18	C. 4.	Voltage
					1						- 750
	 				1						+1000
10	2		1	1	10	2	1	1	3	2	-1000
12	2		1	ī	13	2	1	1	4	2	+1250
14	9	9	9	10	14	8	9	6	9	10	-1250
14	10	10	9	10	14	9	11	8	10	14	+1500

Figure V.D.10 - CD Stress, Cumulative Leakage Failures (14 parts total)

Figure V.D.11 - CD Stress, Serial Number 26 Pin 1 Leakage Current

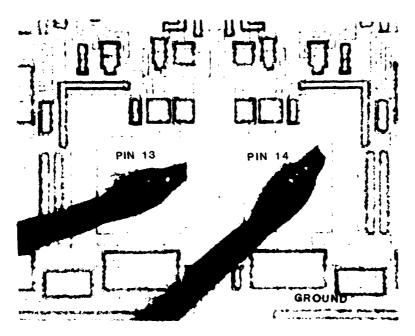


Figure V.D.12 - Input Pins 13 and 14

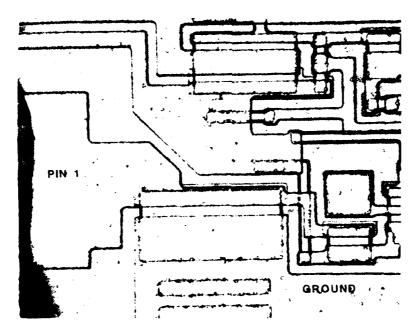


Figure V.D.13 - Input Pin 1

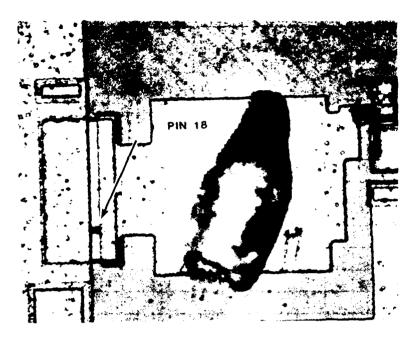


Figure V.D.14 - CD Stress, Input Pin 18 Damage Site

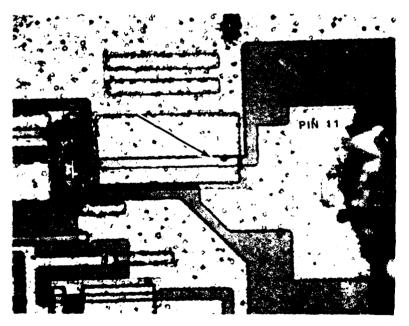


Figure V.D.15 - CD Stress, Input Pin 11 Damage Site

		Numb	er of	Failu	res at	Pin I	ocatio	ons			
	/ /										[j ² ,2 ⁶]
										CHILL P.	
1	3	4	7	8	11	13	14	17	18	(G.)	ine d Spools Voltage
1	1	2	1		1	1		1	2		+500
											-500
3				1	2		2	3		2	+750
											-750
	1	 		 							+1000
					ļ						-1000
	 	 !		1		2					+1250
	1				1						-1250
9		 			3		-		!		+1500
	 	<u> </u>									-1500
12	2	3	2		5			4			+1750
					6						-1750
	3			2	10		3		4		+2000
		4									-2000
12	5	5	2	3	11	2	4		8	4	+2250
											-2250
	9	7	4				7	5	11	8	+2500
											-2500
1.2	10	8	5	5	11	3	8	6	11	12	+2750

Figure V.D.16 - HBD Stress, Cumulative Leakage Failures (12 parts total)

Initial	<u>-1250 volts</u>	+1500 volts
600 pA	300 pA	63.2 u A

Figure V.D.17 - HBD Stress, Serial Number 3 Pin 1 Leakage Current

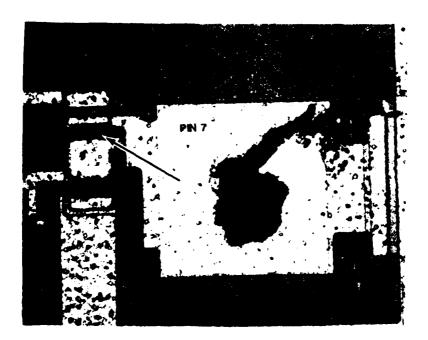


Figure V.D.18 - HBD Stress, Input Pin 7 Damage Site

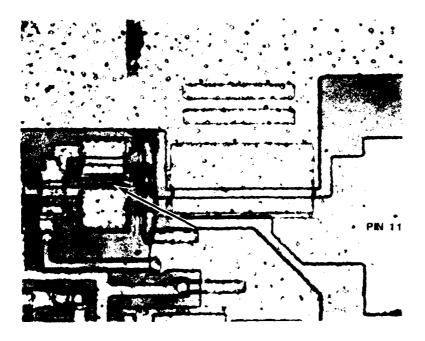


Figure V.D.19 - HBD Stress, Input Pin 11 Damage Site

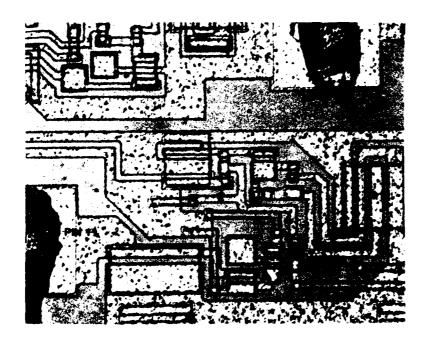


Figure V.D.20 - Pin 11 Layout

E. Part E Analysis

This device is a RAM-I/O-Timer manufactured using an n-channel, depletion load, silicon gate (HMOS) technology. There is a 2048-bit static RAM, 2 programmable 8-bit I/O ports, 1 programmable 6 bit I/O port, and a 14-bit timer. There is one metallization layer and one polysilicon layer. Both conductors are approximately 3.5 microns in width.

An overall die photograph is shown in Figure V.E.1. VCC, pin 40, is at the top of the figure. On its left is a bond pad that is only connected to the substrate. VSS, pin 20, is at the bottom of the figure. The distribution pattern is basically an interdigitated structure. The VSS metallization has two parallel stripes that are approximately 8 microns apart near the outer edge. The reason for the separation may be that the wider outside stripe carries the majority of the current flow and the inside stripe is a solid ground reference for the internal circuitry.

The VCC metallization is shown in Figure V.E.2. This contacts n+ source diffusions. The VSS metallization is shown in Figure V.E.3. The two parallel metallization stripes are visible. This metallization also contacts n+ source diffusions.

The substrate connection is shown in Figure V.E.4.

A typical input is shown in Figure V.E.5 with the corresponding schematic in Figure V.E.6. The input layouts were identical on the different pins. The input metallization overlays the input resistor and acts as a gated diode. Dielectric breakdown on the gates was 100 VDC. The input resistor is a diffused resistor. The breakdown voltage from it to the substrate was 28 VDC. This is the same as the transistor junction breakdown.

An output is shown in Figure V.E.7 and the corresponding schematic is shown in Figure V.E.8. This is pin 6 which is the only output on this device that is not an input/output combination.

An input/output combination is shown in Figure V.E.9 and the corresponding schematic is shown in Figure V.E.10. The input section is identical to the other inputs and the output layout is the same as the outputs on the other I/O pins.

Microsections were performed to examine the construction of this device. Very shallow diffusions were used. An input resistor diffusion is shown in Figure V.E.ll. The edge of the bond pad is on the right hand side of the photograph and the metallization which interconnects the bond pad and the resistor is above the diffusion. This diffusion is 0.4 microns deep and the metallization is 1.2 microns thick. A transistor structure is shown in Figure V.E.l2. The polysilicon gate is 0.4 microns thick. The edge of the die is shown in Figure V.E.l3. There is an n diffusion which is about 2 microns deep which travels around the perimeter of the die and

is contacted by metallization on its inside edge. The oxide thickness between the polysilicon and the metallization is 1.2 microns and the thickness between the polysilicon and the silicon is 0.9 microns.

Electrical Testing

A sample of the electrical data taken on each of the stressed parts and the control part at each iteration during the testing is shown in Figures V.E.14 and V.E.15. V_{OH} and V_{OL} were measured on the output pin and on each of the 30 input/output pins. Current leakage was measured at +5 volts and 0 volts on all pins except the timer output, VCC and VSS. This measurement provided interface circuit damage information. This testing also provided a functional check of the following. The control logic (IO/M, CE, ALE, RD, WR, and RESET), the three ports and associated data direction registers, the timer, and the address/data buffers and latches were tested for operation in their various modes. One 8 bit wide section of the 256 section RAM was accessed.

Charged Device Data Analysis

Fourteen devices, serial numbers 15 through 28 were stressed with the charged device ESD stress simulation. The principle failure mode experienced was input circuit leakage. A summary of the inputs and the point at which they developed leakage current is shown in Figure V.E.16. The inputs are seen to degrade with positive stress. The order of sensistivity is: 4, 7, 9, and 10 most sensitive 3 and 11 less sensitive, and pin 8 least sensitive.

Numerous V_{OH} and V_{OL} failures occurred, however, this was due to the input damage. In addition to the input becoming inoperative because of the junction damage the substrate bias generator would not be able to keep the part properly biased with the additional current load put on it through the inputs.

Three devices exhibited leakage on pins other than the inputs. Serial numbers 17 and 25 had leakage on output pin 6 and serial number 21 had leakage on output pin 6 and I/O pin 2.

The layouts are as shown in Figure V.E.17 through V.E.23. Pin 2 in Figure V.E.17 is an input/output and pin 3 is an input only. Input pins 3 and 4 are shown in Figure V.E.18. Figure V.E.19 shows input/output pin 5 and output pin 6. Figures V.E.20 through V.E.22 show input pins and Figure V.E.23 shows input pin 11 and input/output pin 12.

Curve tracer measurements were performed on all devices. Input leakages were noted on pins 3, 4, 7, 8, 9, 10, and 11 on most devices. Pin 6 was leaky on serial numbers 17, 21, and 25. Pin 2 was leaky on serial number 21.

Internal visual examination was performed on all of the devices. No damage was visible on the input/output pins which did not exhibit leakage. Damage was seen on numerous pins and this is documented on two parts, serial numbers 20 and 21. Serial number 21 had leakage on pins 2 and 6 in addition to the inputs.

Failure appearance on serial number 20 is documented in Figures V.E.24 and V.E.25. This is pins 7, 8, and 9. The current path is from the n-type resistor to the n-type diffusion around the perimeter of the die. This latter diffusion is not connected to any other point so the current flows from it back to a grounded pin.

The failures on pins 7 and 8 on serial number 21 are shown in Figure V.E.26. The failure on pin 2 (input/output) is different than the failures on the inputs (Figure V.E.27). The breakdown sites which indicate the direction of the current are on the edge of the resistor contact closest to pin 3. The distance from the edge of the pin 2 resistor diffusion to the edge of the pin 3 resistor diffusion is 26 microns. This is shorter than the distance to the edge of the die (32 microns). The damage created indicates that a stress occurred between pins 2 and 3. Numerous pairs of input/output pins had this same spacing between resistors (26 microns) but they were not damaged. This indicates that the damage on pin 2 was not the result of a stress originating at pin 2 but rather was the result of an opposite polarity pulse originating at pin 3. The close spacing to the adjacent pin resulted in the stress occurring between these points rather than to the edge of the die.

The failure on pin 6 produced a visible breakdown site (Figure V.E.28). This site was verified by mechanically isolating the other two contact points and probing each. The only one that was leaky was the one shown. This was drain to body leakage.

With an understanding of the physical layouts and an understanding of the failure modes, the sensitivity variations can be analyzed.

Pin 8 is less sensitive to stress than the other inputs because it is connected to an additional diffusion. This makes its sensitivity less than the other inputs but more than the outputs which have more than one diffusion contact.

Pins 3 and 11 were the next most sensitive and they have in common the fact that they are paired with an input/output pin (Figures V.E.17 and V.E.23) and they are the last input pin either direction around the die. Since current flow occurs out to the edge of the die and then back through a grounded circuit, the pins on the end would tend to receive less stress. The ones in the middle would be stressed when pins on either side of them receive a stress.

For the same reason as stated above the four internal input pins 4, 7, 9, and 10 were the most sensitive during this test. For a single stress event it is likely that the inputs would exhibit a more uniform stress sensitivity.

Due to the lack of a low resistance current path back to the substrate these parts were very resistant to ESD stress.

Human Body Discharge Data Analysis

Thirteen devices, serial numbers 2 through 14 were subjected to the human body discharge ESD simulation. A summary of the input circuit leakage failures with voltage stress is shown in Figure V.E.29. The first leakage failure which occurred was pin 4 on serial number 5 at +2000 volts. Two devices proceeded all of the way through the -5000 volt stress level. One of these was functional and had only slight current leakage.

In addition to the input leakages listed, pins were leaky as shown here: serial number 2 pin 1, and pin 37, serial number 4 pin 13, serial number 5, pin 12 and pin 37, serial number 7, pin 2 and pin 6, serial number 8, pin 12, serial number 9 pin 2 and serial number 14 pin 12. The HBD stress caused failures on more different pins than the CD stress. With the exception of pin 37 these were all physically close to the input pins.

All 13 parts were opened and visually examined. The damage was much less severe than on the CD stressed parts. Very slight damage was visible on a few inputs but stripping was required to enhance the failure sites.

Serial number 2 was analyzed since it had leakage on pins 1 and 37 as well as inputs. The leakage on pins 1 and 37 was low, measuring 10 microamps at 6.5 volts on pin 1 and 10 microamps at 9.5 volts on pin 37. There was no visible damage on these two pins. Pins which did exhibit damage are shown in Figures V.E.30 through V.E.33. Figure V.E.30 shows input/output pin 2 and input pin 3. Figure V.E.31 shows input pin 4. Figure V.E.32 shows input pin 11 and input/output pin 12.

Input/output pins 2 and 12 were the only two I/O pins which exhibited visible damage. They both had leakage currents of 1 microamp at 10 volts. The input pins generally had damage on the side of the resistor closest to the edge of the die. There is also visible damage along the edge of the n-diffusion on the perimeter of the die.

There was very little difference in sensitivity between pins like was seen on the CD stressed parts. The susceptibility to damage was low on these parts with the inputs being more sensitive to stress than outputs or I/O combinations. This part is designed very well for ESD tolerance due to the absence of a current path from the inputs through the substrate back to an external ground.

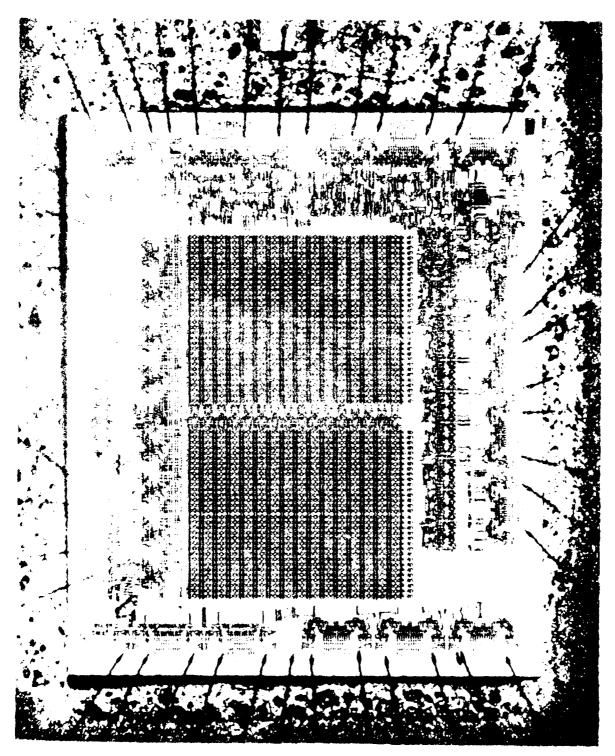


Figure V.F.1 - (veral) to Smotograph

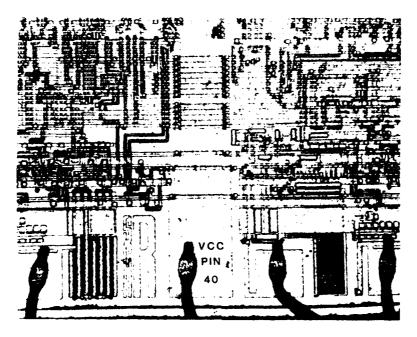


Figure V.E.2 - VCC Bond Pad

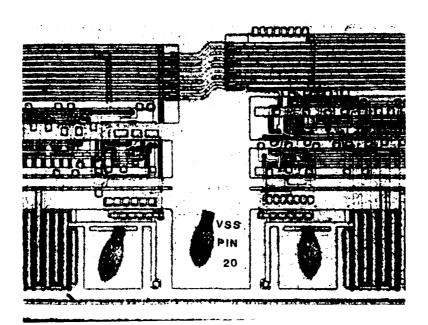


Figure V.E.3 - VSS Bond Pad

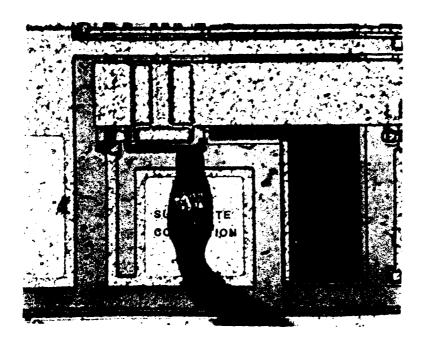


Figure V.E.4 - Substrate Connection

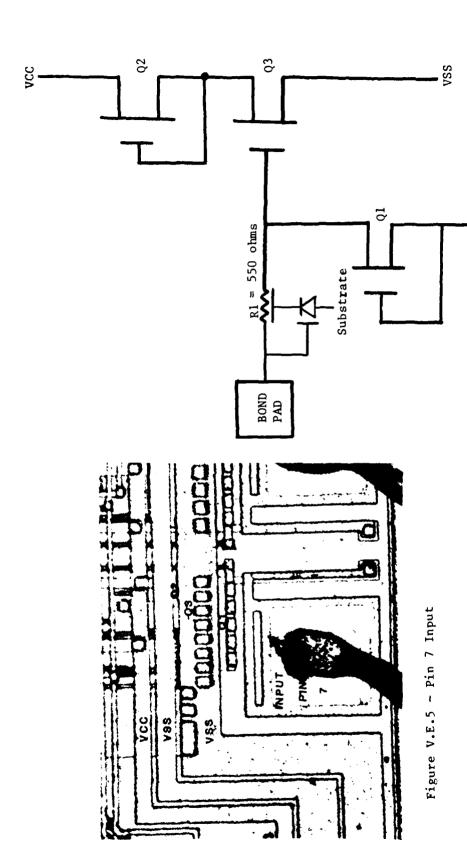
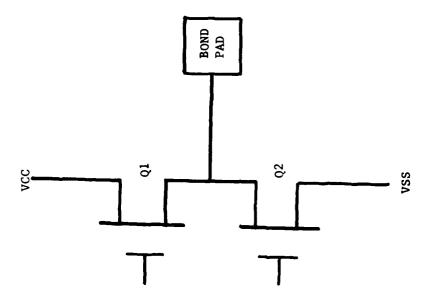


Figure V.E.6 - Input Schematic

VSS



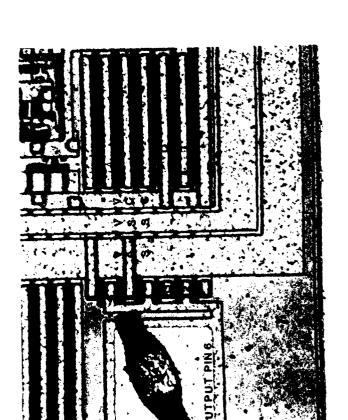


Figure V.E.7 - Pin 6 Output

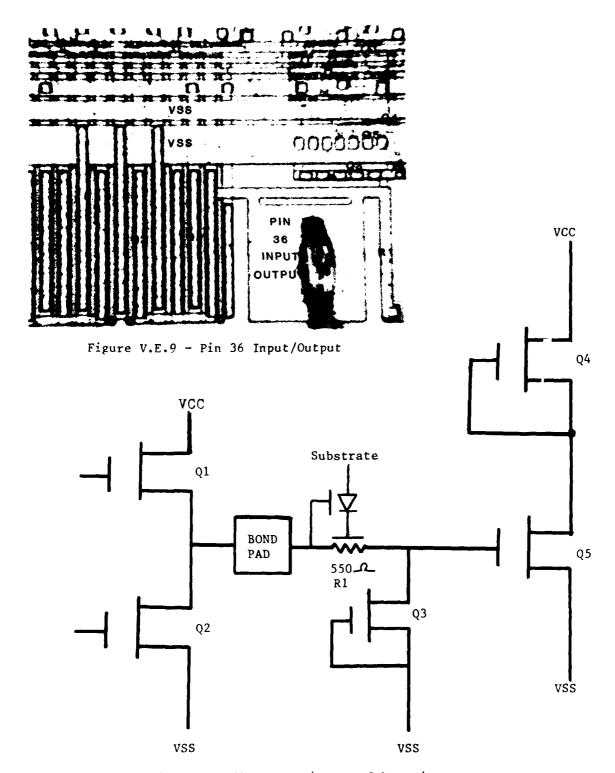


Figure V.E.10 - Input/Output Schematic



Figure V.E.11 - Input Resistor Diffusion Side View

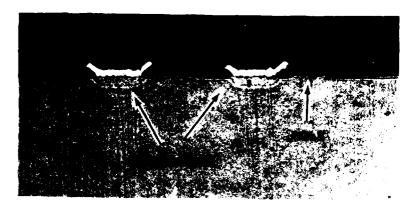


Figure V.E.12 - Transistor Cross-Section

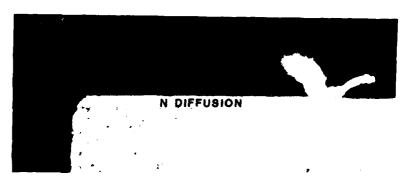


Figure V.E.13 - Side View of Edge of Die

MARTIN MARIETTA AEROSPACE -- DENVER DIVISION -- PARTS EVALUATION LAB

PART NUMBER -TESTED AT 25 DEG. C

FILE UID : SERIAL NUMBER -

UN 03 AUG 83 AT 14:10 WITH THE 3250 TEST SYSTEM

FAIL	TEST TYPE		MEASURED VALUE	L I M I MINIMUM	MUNIXAM
	V9H		2.910 V	2.400 V	
	VOH		2.89 0 V	3.400 V	
	VCH		2.895 V	2.400 V	
	VOH		2.905 V	2 400 V	
	VOH		2.700 V	2 400 V	
	YOH		2.7Ø5 V	2.400 V	
	AOH		a.875 V	2 400 V	
	VQH	- -	2.89Ø V	a 400 V	
	MOA		골. 쿠골 의 V	2.400 V	
	YOH		2.99 0 V	3 40만 V	~-
	VOH.		2.92 0 V	2 400 ୯	
	₩ DH		2.915 V	3 400 V	
	VOH		2.935 V	2.400 V	~-
	VOH.		2.92 0 V	2 400 V	~-
	HOY		2.900 V	2.400 V	
	VOH		2.910 V	2.435 V	~-
	VOH		2.905 ∀	2 400 V	~~
	70H		2 905 V	2 430 V	
	VØH.		8.895 V	5 400 V	
	V©H		E. 900 V	2. 400 V	~
	∨oH	·	2.395 V	3 488 V	
	YOH	- -	2.900 Y	2.400 V	
	VØH.		2.950 V	2.400 V	
	YOH		2.955 V	2.400 V	
	VOH		2.950 V	2.400 V	
	VOH		2.945 V	2 400 V	
	VOH		2.955 V	3 400 Y	~-
	VOH		2.960 V	2.400 V	~-
	V∂H		2.955 √	2 00 √	
	VOH		ā. 97ā V	2 400 V	***
	YOH		2 425 V	2 400 V	
	VOL		156.5MV		450,28
	YOL		167 ØMV		450 0M
	YOL		175.5MV		450 0H
	VOL		159.8MV		450.0M
	YOL		151.5MV		450.0M
	VOL		160.0MV		45 @ . @M\
	VOL		164.5MV		450.0M
	VOL		168.0MV		450.0M
	VOL		160.0MV		450.0M
	VOL		168.0MV		450.0M\
	VOL		159.5MV		450.0MV
	VOL		160.0MV		450.0M
	VOL		157.5MV		450.0MV
	VOL		157.5MV		450.0MV
	YOL		167.5MV		450.0M
	VOL		167.0MV		450.0MV
	YOL		167.5MV		450.0MV

Figure V.E.14 - Initial Electrical Measurements

PART NUMBER - FILE UID : SERIAL NUMBER - 9
TESTED AT 25 DEG. C

ON 03 AUG 83 AT 14:10 WITH THE 3250 TEST SYSTEM

FAIL	TEST TYPE		MEASURED VALUE		T S MAXIMUM
	VOL				450.0MV
	VOL		169.5MV		450.0MV
	VOL		169.5MV		450.0MV
	VOL		171.0MV		450.0MV
	VOL		170.0MV		450.0MY
	ADE		161.5MV		450.0MV
	VOL		161.0MV		450 0MV
	VOL		179.5MV		450.0MV
	AOF		182.5MV		450 0MV
	VOL		180.5MV		450.0MV
	VOL		187.0MV		450 0MV
	VOL		193.5MV		450 0MV
	VOL		171.0MV		450.0MV
	VOL		270.0MV		450 0MV
	IIL		2 900NA	-10 00UA	10 00UA
	IIL		-1.350NA	-10.00UA	10.00UA
	IIL		2.950NA	-12.00UA	10 00UA
	IIL		-700 0FA	-10 00UA	10 00UA
	IIL		8.800NA	-10 00UA	10 ଉପ୍ତନ
	IIL		-1 400NA	-10 00UA	10 00UA
	IIL		3 500NA	-10 00UA	10 0004
	IIL		-1.15@NA	-10.00UA	10 ବିଷ୍ଠନ
	IIL		2 550NA	-10.00UA	18 98UA
	IIL		-1 100NA	-10 00UA	10 00UA
	IIL		3.35 0 NA	-10 00UA	10 30UA
	IIL		-1.45@NA	-10.00UA	10 00UA
	IIL		2.800NA	-10.00UA	10 00UA
	IIL IIL		-900.0PA	-10.00UA	10 000A
	IIL		3.250NA -1.550NA	-10.00UA	10 ୧୯୮
	IIL		3 200NA	-10.00UA	10 0004
	IIL		-750.0PA	-10.00UA	10 00UA
	IIL		2.500NA	-10,00UA -10,00UA	10 00UA
	IIL		-1.55@NA	-10.00UA	10 00UA 10 00UA
	IIL		3.200NA	-10.00UA	10 000A
	IIL	- - -	-1.000NA	-10.00UA	10 00UA
	IIL		2. LOONA	-10 00UA	10 ଜନ୍ମ
	IIL		-1.300NA	-10 0004	10 000A
	IIL		3.506NA	-10.00UA	10 000A
	IIL		-1.300NA	-10 00UA	10 02UA
	IIL		8.550NA	-10 00UA	10 00LA
	IIL		-1.600NA	-10 00UA	10 00UA
	IIL		2 45 0NA	-10 00UA	10 00UA
	IIL	 -	-1 600%	-10 00UA	10 000A
	IIL		2 700NA	-10 00UA	10 00LA
	IIL		-1 600NA	-10 0004	10 0004
	IIL		2 65 QNA	-10 ଉପ୍ତାଧ	10 00UA
	IIL		-1.600NA	-10 00UA	10 20UA
	IIL		a soona	-10 000A	
			C ONDIAM	-10 00UA	10 0004

Figure V.E.14 - Initial Electrical Measurements (Cont.)

FART NUMBER - FILE OIL SERIAL NUMBER - 4 TESTED AT 28 BEG C

ON 03 403 93 AT 14 10 WITH THE 3250 TEST SYSTEM

	7E5T		MEASURED	<u> </u>	I T 5
FAIL	TYPE		VALUE	MINIMUM	
	II.		2 700NA	2 3364	10 0004
	IIL		-1 500tiA	-18 900A	10 0004
	IIL		3 500NA	-13 33_A	13 0004
	IIL		-1 400NA	-10 00UA	13 330A
	IIL		AMODO . S	-10 00UA	10 00UA
	IIL		-1 400NA	-10 0004	10 00UA
	IIL		2 7501A	-10 00UA	10 00UA
	II∟		-1 400NA	-10 00UA	AUDG GI
	IIL		2 BOONA	-10 00UA	10 00UA
	IIL		-1.25@NA	-10.00UA	10 00UA
	IIL		2 35 0NA	-10 00UA	AUGG Gt
	IIL		-1.200NA	-10 0004	10 ರಚ್ಚಸ
	ΙIĻ	+	2.600NA	−10 0004	13 3004
	IIL		-1.200NA	-10 00UA	10 000A
	IIL		2 350NA	-10 @@UA	10 000±
	IIL		-1 150NA	-10 0004	1చే చేత∵న
	IIL		2.75@NA	-13.03UA	10 00UA
	IIL		-1 BERNA	-10 Jaya	10 000
	II.		3.000NA	∼1తె చెడ్డువ	:3 3094
	IIL	~	-1 200NA	-10 3304	10 0004
	ΙΙL		3.95 <i>3</i> NA	-ti できりA	:3 23UA
	IIL		-1.150KA	-10.23UA	18.30%4
	IIL		3 700NA	-10.00UA	10.00UA
	IIL		-1.35@NA	-10.00UA	10.00UA
	IIL		3.200NA	-13.00UA	10.00UA
	IIL		-1 050NA	-10.00UA	10.00UA
	IIL		3. 35 ONA	-10.00UA	10 00UA
	IIL		-1 100NA	-10.0004	10 00UA
	IIL		3 200ha	- 63 0004	13 3304
	IIL		-1 000NA	-10 00UA	10 0004
	IIL		3 29 3 NA	-13 3304	18 88.4
	IIL		-300 DPA	-12 B0UA	10 3004
	IIL		3.400NA	-10.30UA	10 0004
	IIL		-1.000MA	-13.3304	10 000A
	IIL		3 200NA	-13 33UA	13 39UA
	IIL		-8 00 .0PA	-10 00UA	19.90UA
	IOL	~	-600 0PA	-10 00UA	10 00UA
	IOL	~	3 550NA	-10 00UA	10.00UA
	IOL		-1.200NA	-10 00UA	10.00UA
	IOL		3.400NA	-10.00UA	12 30UA
	IOL		-1.45 ØNA	-10 00UA	10 0004
	IOL		3.35@NA	-10.0004	10 00UA
	IOL		-1 35 0NA	-10 00UA	10.00UA
	IOL		3.200NA	-10.00UA	10 0004
	IOL		-1.25 @NA	-10.00UA	10 0004
	IOL		2.900NA	-10 00UA	10 0004
	IOL		-1.050NA	-10 00U4 -10 00U4	10.00JA
	IOL		-1.000NA	-10.00UA	10 000A
	IOL		-750.0FA	-10 000A -13 000A	10 0004
	100		2 500NA	+10 000A	T# #0500#

Figure V.E.14 - Initial Electrical Measurements (Cont.)

PART NUMBER - FILE UID SEFIAL NUMBER - C

ON 03 AUG 83 AT 14 10 WITH THE 3850 TEST SYSTEM

FAIL	TEST TYPE	 MEASURED VALUE	E I M MINIMUM	I T 3 Malimum	
	IOL IOL	 -750 0PA 2 600NA	-10 00UA -10 00UA	13 მდეგ 13 მტეგ	
	ICC	 AMଭିକ ଭିଳ		120 কুদান	
	IILCE IILCE	 26 2004 -723.5NA	-100 JUA -100 JUA	100 00A 100 00A	

Figure V.E.14 - Initial Electrical Measurements (Cont.)

MARTIN MARIETTA AEROSPACE -- DENVER DIVISION -- PARTS EVALUATION LAB

FILE UID: :151 SERIAL NUMBER - 9
TESTED AT 25 DEG. C 95000V STRESS
ON 17 NOV 83 AT 09:06:53 WITH THE 3260 TEST SYSTEM

FAIL	TEST TYPE		MEASURETI VALUE	I M I	T 5 MAXIMUM
****	VOH		23.85MV	2.400 V	
****	VOH		21.50MV	2,400 U	
***	VOH		19.70MU	2.400 V	
****	VOH		22.10MV	2.400 V	
***	VOH		20.80mV	2.400 V	
***	VOH		18.30MV	2.400 V	
***	VOH		20.20MV	2,400 V	
* * * *	VOH	- -	22.75MV	2.400 V	
	VOH		2,925 V	2.400 V	-
	VOH		2.910 V	2.400 V	
	AOH		2.950 V	2,400 9	
	YOH		2.935 V	2.400 U	
	VOH		2.955 V	2.400 V	
	YOH		2.955 V	2.400 V	
	VOH		2.930 V	2.400 V	
	YOH		2.930 V	2.400 V	
	VOH		2.915 V	2.400 V	
	VOH		2.930 V	2.400 V	
	199)) (2.930 V	2.400 V	
	90H		2.950 V	2,400 9	
	무이번		2.945 V	2.400 V	
	90H		2.970 V	2.400 V	
	ADH		3.000 V	2.400 V	
	VOH		3.005 V	2.400 V	
	VOH		3.035 V	2.400 V	
	VOH		3.020 V	2.400 V	
	VOH		3.050 V	2.400 V	
	VOH		3.030 V	2,400 V	
	HON		3.030 V	2.400 V	
	VOH		3.040 V	2.400 V	
	YOH		2.985 V	2.400 V	
	VOL		166.5MV	~-	450.0MU
	VOL		165.0MV		450.0mV
	VOL		169.0MU		450.0MV
	AOF.		158.0MV	~~	450.0MV
	VOL		159.0MV	~-	451.0MV
	VOL		158.0MV		450.0MV
	VOL		161.0MV		450.0MU
	VOL		159.0MV		450.0MV
	VOL		172.5MV		450.0mV
	VOL		173.5MV		450.0MV
****	VOL		174.5MU		450.0MU
****	VOL		4.905 V		450.0MU
	VOL		4.905 V		450.0MU
****	VOL		4.905 V		450.0MV
****	VOL		4.905 U		450.0MU
ተ ች ች ች	VOL		4.905 V		450.0MV
	VOL		192.0MV		450.0MV

Figure V.E.15 - -5000 Volt Electrical Measuremen*

FILE UID: :151 SERIAL NUMBER - 9
TESTED AT 25 DEG. C P5000V STRESS
ON 17 NOV 83 AT 09:07:25 WITH THE 3260 TEST SYSTEM

***				MAXIMUM
	VOL	 191.5MV		450.0MU
	VOL	 4.905 V		450.0MV
***	VOL	 4.905 V		450.0MV
***	VOL	 4.905 V		450.0MV
***	VOL	 4.910 V	~-	450.0MV
***	VOL	 4.905 V		450.0MV
* * * *	VOL	 4.905 V		450.0MV
	VOL	 200.0MV		450.0MV
***	YOL	 4.905 V		450.0MU
	VOL	 201.0MV		450.0MU
****	VOL	 4.905 V	~-	450.0MU
***	VOL	 4.905 V	~-	450.0MU
***	VOL	 4.905 V	~-	450.0MV
***	VOL	 4.905 V	~	450.0MV
****	IIL	 217.5UA	-10.00UA	10.00UA
****	IIL	 ~992.0UA	-10,00UA	10.00UA
****	ΙΙL	 220.0UA	-10.00UA	10.00UA
***	IIL	 -938.0UA	-10,00UA	10.00UA
***	II∟	 186.0UA	-10,00UA	10.00UA
***	IIL	 -918.5UA	-10.00UA	10.00UA
* * * *	ŢĪĹ	 196.5UA	-10.00UA	10.00UA
* * * *	IIL.	 ~915.0UA	-10.00UA	10.00UA
****	IIL	 185.0UA	-10.00UA	10.00UA
***	IIL	 -886.5UA	-10,00UA	10.00UA
***	IIL.	 187.0UA	-10.00UA	10.00UA
***	IIL	 ~882.0UA	-10.00UA	10.00UA
***	I I L	 165.0UA	-10,00UA	10.00UA
***	IIL	 -816.0UA	-10.00UA	10.00UA
****	IIL	 168.5UA	-10.00UA	10.00UA
****	IIL	 -840.0UA	~10,00UA	10.00UA
	IIL	 27,20UA	-10.00UA	10.00UA
****	IIL IIL	 -17.40UA 107.0UA	-10.00UA -10.00UA	10.00UA 10.00UA
***	IIL	 -6.570UA	-10.00UA	10.00UA
***	IIL	 83.40UA	-10.00UA	10.00UA
****	III.	 8.620UA	-10.00UA	10.000A
****	IIL	 48.00UA	-10.00UA	10.0004
тттт	IIL	 3.790UA	~10.00UA	10.00UA
****	ÎÎL	 13.55UA	~10.00UA	10.00UA
	I I L	 154.5NA	-10.00UA	10.00UA
	IIL	 16.35NA	~10.00UA	10.00UA
	ĪĪL	 -1.790UA	-10.00UA	10.00UA
	IIL	 14.00NA	-10.00UA	10.00UA
	III	 -1.435UA	-10,00UA	10.00UA
	IIL	 10.05NA	-10.00UA	10.00UA
	IIL	 -2.075UA	-10,00UA	10.00UA
	IIL	 916.5NA	-10.00UA	10.00UA
	III.	 -2.030UA	-10.00UA	10.0004
	IIL	 12.20NA	-10.00UA	10.00UA
	IIL	 -2.425UA	-10.00UA	10.00UA

Figure V.E.15 - Post -5000 Volt Electrical Measurements (Cont.)

FILE UID :151 SERIAL NUMBER - Y
TESTED AT 25 DEG. C P5000V STRESS
GN 17 NOV 83 AT 09:07:59 WITH THE 3260 TEST SYSTEM

FAIL	TEST TYPE	MEASURED VALUE	L I M	I T S MAXIMUM
	IIL	 13.90NA	-10.00UA	10.00UA
	IIL	 -2.425UA	-10.00UA	10.00UA
	IIL.	 43.85NA	-10.00UA	10.00UA
	IIL	 -5.035UA	-10.00UA	10.00UA
	IIL	 334.5NA	-10.00UA	10.00UA
	IIL.	 -7.810UA	-10.00UA	10.00UA
	IIL	 73.45NA	-10.00UA	10.00UA
	IIL.	 -9.270UA	-10,00UA	10.0004
	IIL	 56.15NA	-10.00UA	16.9004
	IIL	 -9.765UA	-10.00UA	10.00UA
	IIL	 54.80NA	-10.00UA	10.00UA
	IIL.	 -6.585UA	-10.00UA	10.00UA
	111	 235.0NA	-10.00UA	10.00UA
	IIL	 -6.550UA	-10.00UA	10.00UA
	IIL.	 48.95NA	-10.00UA	10.00UA
	III.	 -4.425UA	-10.00UA	10.00UA
	IIL	 29.90NA	-10.00UA	10.00UA
	II∟	 -4.090UA	-10.00UA	10.00UA
	IIL	 46.20NA	-10.00UA	10.00UA
	IIL.	 -7.915UA	-10.00UA	10.00UA
	IIL	 50.15NA	-10.00UA	10.00UA
	IIL	 -9.145UA	-10.00UA	10.00UA
	IIL	 49.45NA	-10.00UA	10.00UA
	IIL.	 -9.230UA	-10.00UA	10.00UA
	IIL	 125.5NA	-10.00UA	10.00UA
	IIL	 -7,985UA	-10.00UA	10.00UA
	IIL	 61.60NA	-10.00UA	10.00UA
	IIL	 -9.185UA	-10.00UA	10.00UA
	IIL	 915.5NA	-10.00UA	10.00UA
***	ΙIL	 -10.25UA	-10.00UA	10.00UA
****	IIL	 14.50UA	-10.00UA	10.00UA
	IIL.	 -9.755UA	-10.00UA	10.00UA
	IIL	 39.60NA	-10.00UA	10.00UA
	IIL	 -8.520UA	-10.00UA	10.00UA
***	IIL	 25.25UA	-10.00UA	10.00UA
	IIL	 512.0NA	-10.00UA	10.00UA
****	I O L.	 -479.0UA	-10.90UA	10.00UA
***	IOL	 58.90UA	-10.00UA	10.0004
***	IOL	 -434.0UA	-10.00UA	10.00UA
***	IOL	 59.85UA	-10.00UA	10.00UA
***	IOL	 -391.5UA	-10.00UA	10.00UA
****	IOL	 45.85UA	-10.00UA	10.00UA
***	IOL	 -371.5UA	-10.00UA	10.00UA
***	IOL	 43.40UA	-10.00UA	10.00UA
***	IOL	 -359.0UA	-10.00UA	10.0004
***	IOL	 40.05UA	-10,00UA	10.00UA
***	IOL	 -359.SUA	-10.00UA	10.00UA
***	IOL	 41.60UA	-10.00UA	10.00UA
* * * *	IOL	 -310.5UA	-10.00UA	10.00UA
****	IOL	 35.65UA	-10.00UA	10.0006

Figure V.E.15 - Post -5000 Volt Electrical Measurements (Cont.)

FILE UID :151 SERIAL NUMBER - 9
TESTED AT 25 DEG. C P5000V STRESS
ON 17 NOV 83 AT 09:08:33 WITH THE 3260 TEST SYSTEM

FAIL	TEST TYPE		MEASURED VALUE	L I M MINIMUM	I T S MAXIMUM
****	IOL		-317.5UA 36.45UA	-10.00UA -10.00UA	10.00UA 10.00UA
	ICC		102.3MA		180.0MA
	IILCE		98.30UA -25.75UA	-100.0UA -100.0UA	100.0UA 100.0UA

TEST RUNTIME IS 19 SECONDS FRINT / DISPLAY TIME IS 109 SECONDS

Figure V.E.15 - Post -5000 Volt Electrical Measurements (Cont.)

	Number of Failures at Pin Locations							
			/	/				
							Cumul 20	74 ED
							Cumulae	\$ <u>`</u>
3	4	7	8	9	10	11	6 .	Voltage
		1		1	2			+1250
	1	1		2	2			-1250
	6	4	1	6	5	3		+1500
	7	4	1	6	5	3		-1500
8	10	7	1	7	9_	8	1	+1750
8	11	11	11	7	10	8	4	-1750
13	14	14	8	13	13	13	14	+2000

Figure V.E.16 - CD Stress, Cumulative Leakage Current Failures

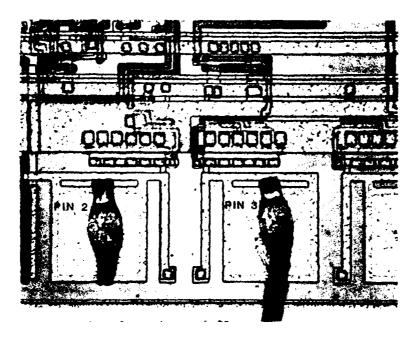


Figure V.E.17 - Input Pin 3 and Input/Output Pin 2.

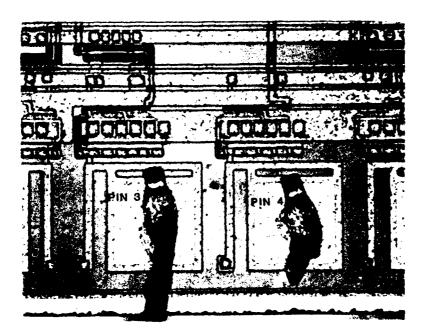


Figure V.E.18 - Input Pins 3 and 4.

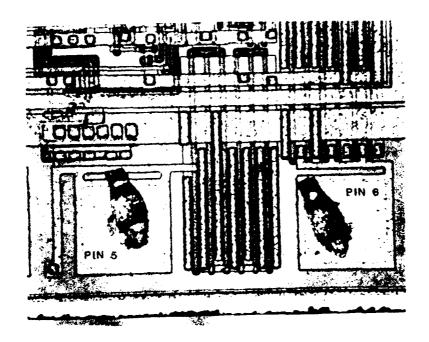


Figure V.E.19 - I/O Pin 5 and Output Pin 6

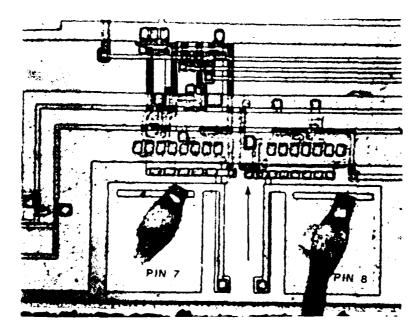


Figure V.E.20 - Input Pins 7 and 8, Arrow Indicates Extra Diffusion Contact

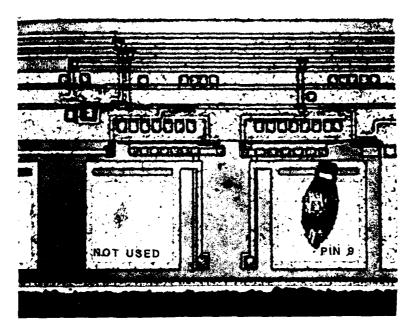


Figure V.E.21 - Pin 9 Input

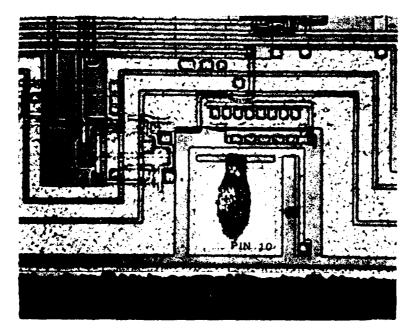


Figure V.E.22 - Pin 10 Input

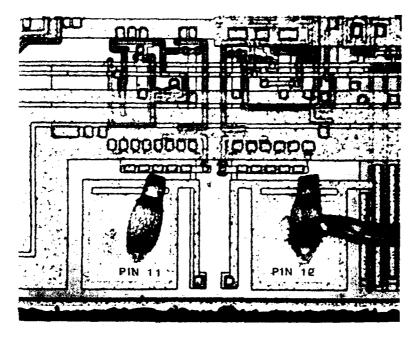


Figure V.E.23 - Pin 11 Input and Pin 12 Input/Output

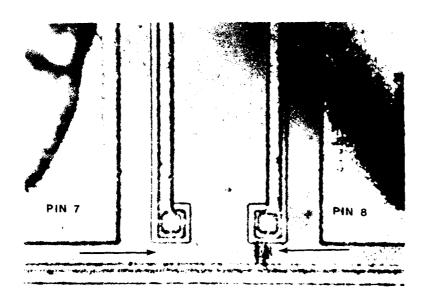


Figure V.E.24 - CD Stress, Damage on Pins 7 and 8

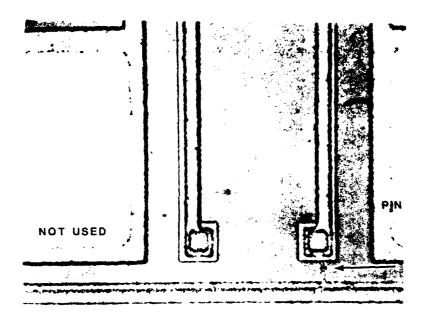


Figure V.E.25 - CD Stress, Damage on Pin 9

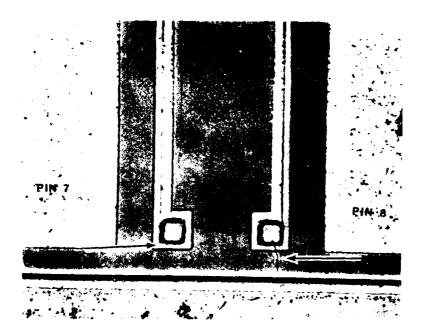


Figure V.E.26 - CD Stress, Damage on Pins 7 and 8

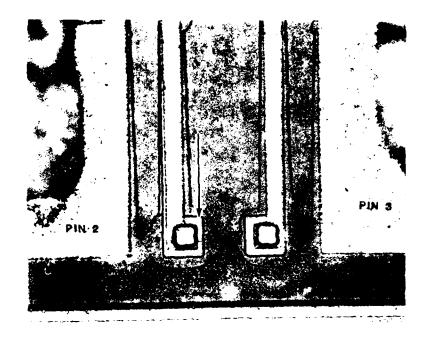


Figure V.F.27 - CD Stress, Damage on Pins 2 and 3

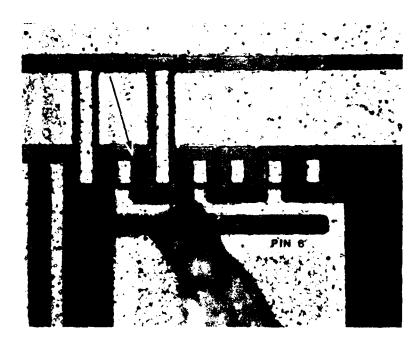


Figure V.F.28 - CD Stress, Pin 6 Output Damage

	Number of Failures at Pin Locations							
/	/ /	/ ,	/ ,	/ ,	/ ,	/ ,	/ ,	Voltage
							imi 2	2 enod
3	4	7	8	9	10	11		Voltage
ī	1	1	1				2	less than +3500
		2	2		2	1	2	+3500
		4	3	2			3	+3750
2					3		5	-3750
4	2	6				2		+4000
	3			3		3	7	-4000
	4	7				4		+4250
				4			8	-4250
5		8						+4500
		9	4				9	-4500
6	4	9	4	5	4	4	11	-4750

Figure V.E.29 - HBD Stress, Cumulative Leakage Current Failures (13 devices total)

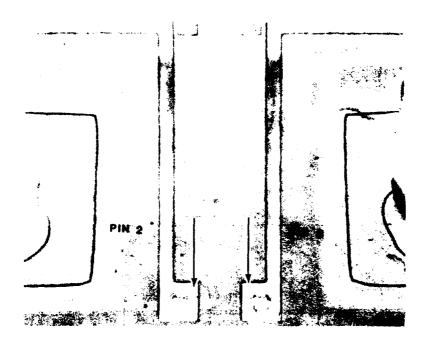


Figure V.E.30 - HBD Stress, Damage on Pins 2 and 3

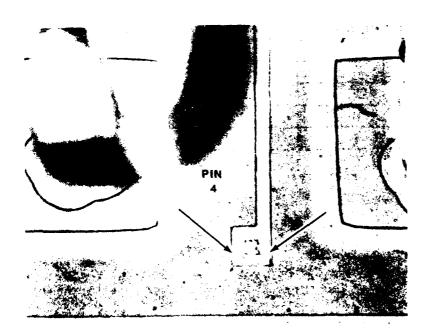


Figure V.E.31 - HBD Stress, Damage on Pin 4

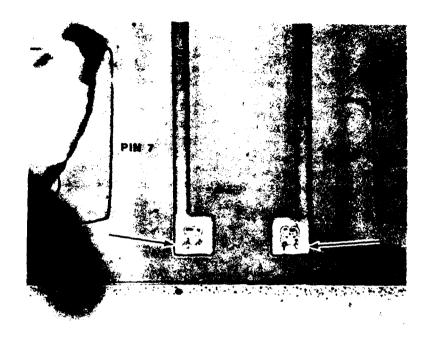


Figure V.E.32 - HBD Stress, Damage on Pins 7 and 8

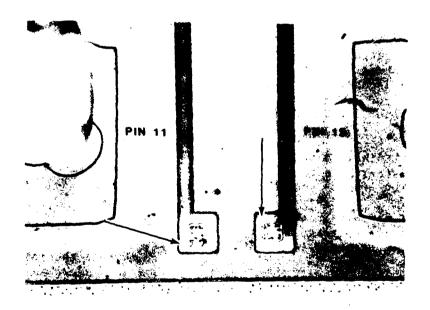


Figure V.E.33 - HBD Stress, Damage on Pins 11 and 12

F. Part F Analysis

This device is a 4096 x 1-bit static RAM manufactured using a CMOS polysilicon self aligned process. The metallization linewidth was about 4.5 microns and the two polysilicon layer linewidths were about 3.0 microns. This was in an 18-pin dual-in-line ceramic package.

An overall die photograph is shown in Figure V.F.l. VCC is pin 18 at the top of Figure V.F.l and GND is pin 9 at the bottom. VCC is shown in Figure V.F.2. A bond wire from pin 18 also is connected to a chip on the package substrate. The VCC metallization makes contact to the substrate at various points around the perimeter of the die, it contacts the protect diodes, and the source diffusions on the P-channel MOS transistors.

Groun is shown in Figure V.F.3. Its metallization makes contact to the protect diodes and to the source diffusion on the N-channel MOS transistors.

An input circuit is shown in Figure V.F.4 and the corresponding schematic is shown in Figure V.F.5. The connection to the body of the transistors were not evident in the input section.

The layouts of the inputs varied considerably. A second type of input structure is shown in Figure V.F.6 (input A5) and in the schematic in Figure V.F.7. The polysilicon gate for the P-Channel transistor is in series with the N-Channel transistor and there is a shift in the order of the resistors and diodes.

There are 5 separate input layouts. These include the two shown above and the following combinations: 1) resistor, VCC diode, resistor, GND diode, series gates; 2) resistor, diodes, resistor, series gates; 3) resistor, diodes, resistor, series gates and also another resistor to parallel gate inputs. The resistors vary from about 280 ohms to 900 ohms. The gate dielectric breakdown was about 45 volts. D1 breakdown was 28 VDC, D2 breakdown was 25 VDC, Q1 junction breakdown was 25 VDC, and Q2 junction breakdown was 20 VDC.

There is a single output on this device. It is connected to the two output transistors by a long metallization run. The transistors are shown in Figure V.F.8 and the schematic is shown in Figure V.F.9.

Microsections were performed to look at the transistor diffusions and the metallization coverage over the polysilicon. Figure V.F.10 shows the metallization and polysilicon. The metallization is about 1.0 microns thick, the polysilicon is about 0.35 microns thick, and the insulating oxide is about 0.5 microns on either side of the polysilicon. The polysilicon was approximately 55 ohms per square.

Cross-sections through the output transistors are shown in Figures V.F.11 - V.F.13. Figure V.F.11 is a top view showing the location of the high magnification cross-section photographs. Figure V.F.12 shows the edge

of the N-Channel transistor. Figure V.F.13 shows the other edge of the N-Channel transistor and the edge of the P-Channel transistor. The diffusion depths are approximately, n+ diffusion = 0.5 microns, p body diffusion = 3.0 microns, and p+ diffusions = 1.2 microns.

Electrical Testing

A sample of the electrical data which was taken on each of the stressed parts and the control part at each iteration during the testing is shown in Figures V.F.14 and V.F.15. Figure V.F.14 shows the initial readings on serial number 9 and Figure V.F.15 shows the readings after the -1000 volt stress. Supply current, input leakage at 0 volts and 5.5 volts, leakage current with output disabled, and the output high and low voltage levels were measured. This testing provided a functional verification of the control lines (W,E) and of the data input pin. Additional testing was performed at the same points as the parametric testing. This was done with a benchtop test setup and included writing and reading all highs and all lows and verifying the functions of write enable and chip enable.

In Figure V.F.15 the supply current readings are very high and one of the inputs is shorted. Testing with the part having this type of parametric readings found them to be nonfunctional.

Charged Device Data Analysis

Fifteen devices, serial numbers 17-31 were stressed with the charged device model. There was no gradual change in the device characteristics. The parts would work properly following one stress level and would then fail with high supply current and input leakage after the next stress. The input pins which showed leakage and the point at which they showed the leakage are shown in Figure V.F.16. This is a summary for only 10 of the devices. Five parts were pulled and analyzed after they failed functionally.

The wide variations in physical layout did cause variations in the sensitivity. Unfortunately the failures encountered on these parts were not due to limitations in the design used for the input protect circuits. The failures occurred due to the layouts of the polysilicon and metallization coming from the device pins and weaknesses in the oxide beneath these two layers. Comparison of the results on this part to the results on the other devices indicates the importance of input layout to sensitivity. The protect network on pins 1-3 and 15-17 worked well while the remainder of the pins had numerous problems. The layout for these 6 acceptable pins is similar to that shown in Figure V.F.4 while the extended layout problems were due to layouts similar to that shown in Figure V.F.6.

Failure analysis found shorts between metallization and polysilicon, and between polysilicon and silicon. Several of these are shown in Figures V.F.17 - V.F.22. Figures V.F.17 and V.F.18 show a short between pins 7 and 14. This is at a point where metallization goes over a polysilicon crossunder. Figures V.F.19 and V.F.20 show shorts which occurred between

pins 6 and 7 and between pin 6 and the substrate. Figure V.F.21 shows a short between the metallization going to pin 7 and the polysiticon connected to pin 12. A more subtle failure is shown in Figure V.F.22. This is damage to the polysilicon line connected to pin 13.

The failure threshold of these parts to charged device ESD stress was very low. This was due to poor layout and possibly inadequate oxide thickness or processing.

Human Body Discharge Data Analysis

Device serial numbers 2 through 16 were stressed with the human body discharge test method.

A summary of the input pins and the point at which they failed leakage testing are shown in Figure V.F.23. The inputs went rapidly from no leakage to high leakage conditions.

The failure analysis on these parts found the same basic failure modes as the charged device model with some differences in location. Pins 1-3 and 15-17 were somewhat more sensitive to this stress than to the CD stress.

Samples of several of these failures are shown in Figures V.F.24 - V.F.27, Figure V.F.24 shows a breakdown between pins 6 and 7. This is similar to the HBD stress failures. Figure V.F.25 shows a failure between pins 12 and 7 and also between GND and pin 13. Figure V.F.26 shows damage which occurred on the polysilicon input resistor on pin 1. This was shorted to VCC (substrate). Figure V.F.27 shows damage on pin 17 input. This point had shorted to the substrate.

The polysilicon resistors do become damaged with stress as evidenced in Figure V.F.26. This limits their usefulness for input protection circuits. On this device the major limitation was the physical layout which allowed overlying metallization and input polysilicon to cross. There is little useful sensitivity variation information available from this device.

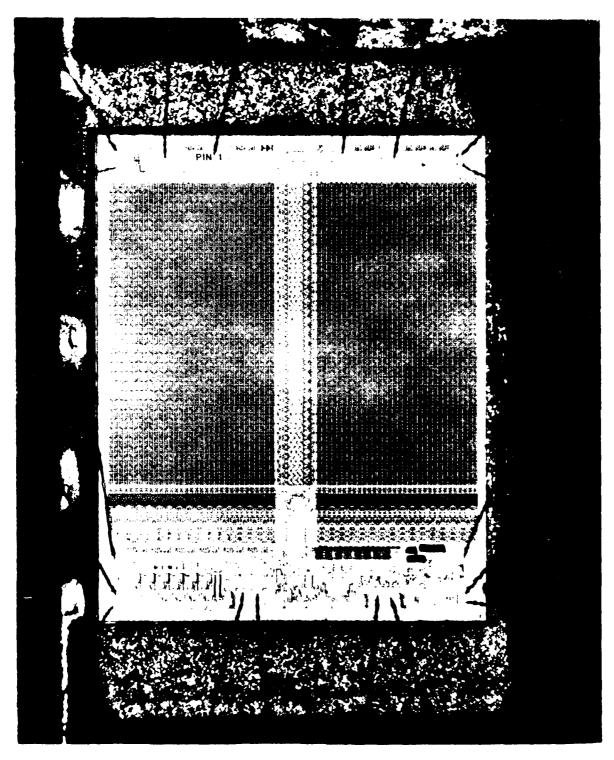


Figure V.F.1 - Overall Die Photograph

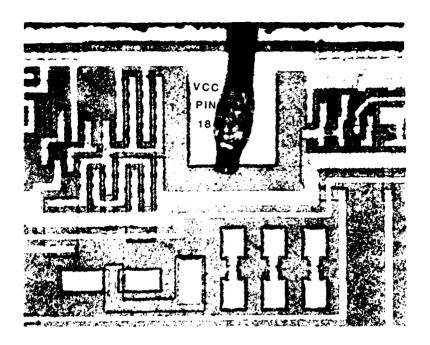


Figure V.F.2 - VCC Bond Pad

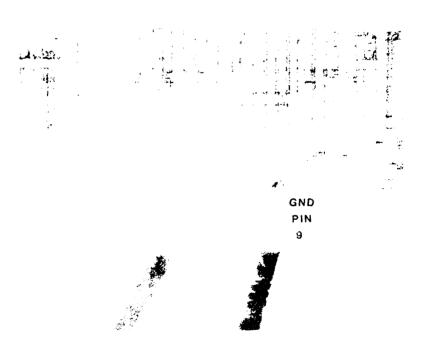


Figure V.F.3 - GND Bond Pad

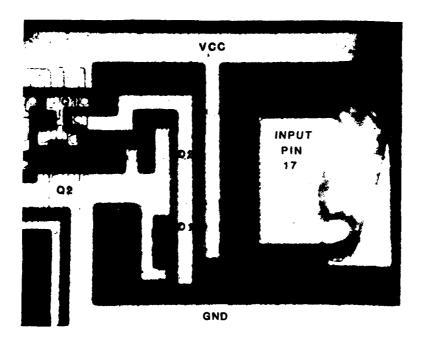


Figure V.F.4 - Pin 17 Input

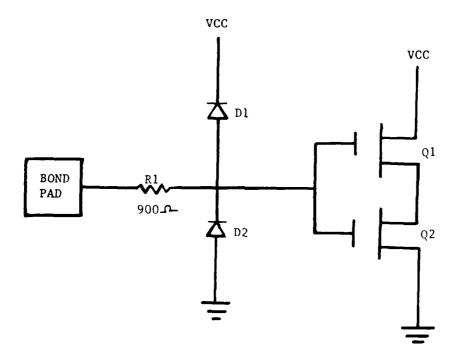


Figure V.F.5 - Pin 17 Input Schematic

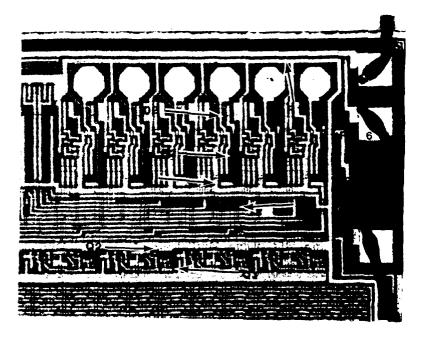


Figure V.F.6 - Pin 6 Input

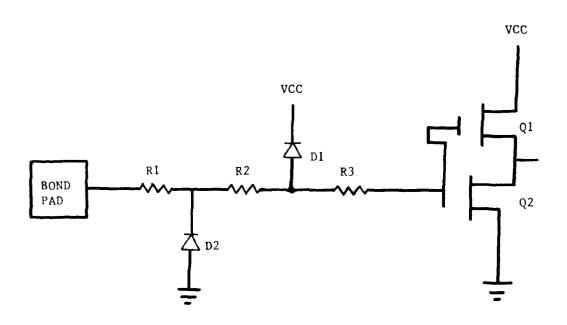


Figure V.F.7 - Pin 6 Input Schematic

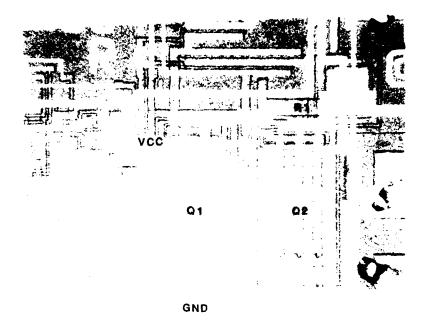


Figure V.F.8 - Pin 7 Output

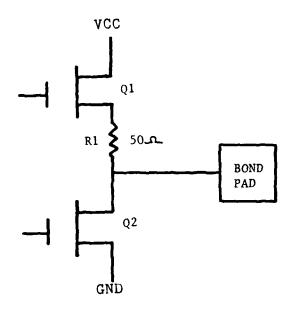


Figure V.F.9 - Pin 7 Output Schematic

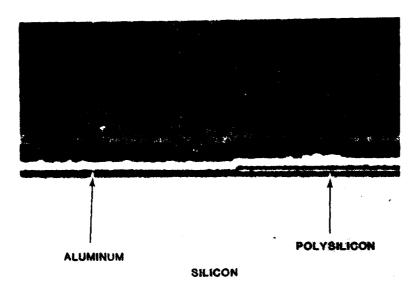


Figure V.F.10 - Cross-Section of Metallization and Polysilicon

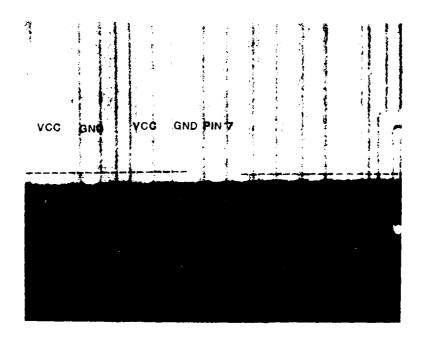


Figure V.F.11 - Top View of Output Transistors

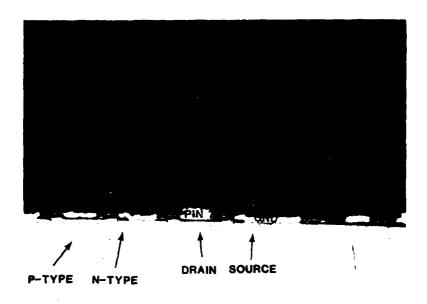


Figure V.F.12 - Cross-Section of N-Channel Transistor

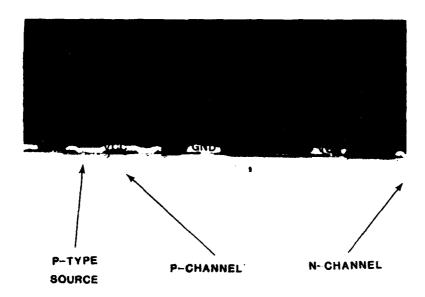


Figure V.F.13 - Cross-Section of edge of P-Channel and edge of N-Channel Transistors

MARTIN MARIETTA AEROSPACE -- DENVER DIVISION -- PARTS EVALUATION LAB

FILE UID 114H SERIAL NUMBER + 4
(FSTED AT 25 DEG. C NO. 1 ELECTRICAL
ON 13 JUL 83 AT 14:45:09 WITH THE 3260 TEST SYSTEM

FAIL	TEST TYPE		MEASURFII VALUE	J I M I hininum	T S MAXIMUM
	ICCSB		2.400NA		50.0004
	ICCSB		2:200NA		50.00UA
	ICCOF		3.751MA		7.000HA
	ICCDR		500,0FA		25.0004
	ICCDR		1.000NA		25.00UA
	II		-290 OFA	-1.000UA	1.000UA
	ΙΙ	 -	1.220NA	~1.000UA	1.000UA
	II		-500.0FA	~1.000UA	1 (000UA
	II		1,150NA	-1.000UA	1.000UA
	ΙΙ		~530.0FA	~1.000UA	1.000UA
	ΙΙ		1,150NA	-1.000UA	1,00000
	11		~520+0FA	~1.000UA	1,00000
	ΙΙ		1,090NA	-1.000UA	1.0000UA
	II		-515.0PA	~1 (000UA	1.00000
	TT		1.085NA	-1.000UA	1.000UA
	ΙΙ		-540.0FA	-1,000UA	1.000UA
	1.1	- -	1.08586	-1.00000	1.00000
	ΙΙ		-565.0PA	-1.000UA	1.000004
	11		1 - 150NA	-1.000UA	1 - 00000A
	ΪΪ		~540.0FA	-1.000UA	1.00000
	11		1,100MA	-1.000UA	1.00000
	II		-560.0FA	-1.000UA	1.00000
	11				1.000UA
			1.180NA	-1.000UA	
	1:		~540.0FA	-1.000UA	1 / 000UA
	11		1.090NA	-1.000UA	1.00004
	I i		-560.0PA	-1.000UA	1,000UA
	II		1.090NA	-1.000UA	1.000UA
	I:		~575.0PA	-1.000UA	1 - 000UA
	11		1,115NA	-1.000UA	1.000UA
	7.1		-585.0PA	~1.000UA	1.000UA
	ΙΙ		1 - 130NA	-1.000UA	1.000UA
	ΙΙ		-590.0FA	-1.000UA	1.00000
	11		1.100NA	-1.000UA	1 - 000000
	ΙΙ		-650.0FA	-1:000UA	1 000006
	1.1		1 - 1 40NA	-1.000UA	1.00004
	IOZ		3.400NA	-1.000UA	1.00004
	IUZ		-1.800NA	-1.000UA	1.00004
	VOL		74.50MV		400 a 0 n U
	чон		4.355 0	2:400 V	

FEST RUNTIME IS 21 SECONDS FRINT / DISPLAY TIME IS 29 SECONDS

Figure V.F.14 - Initial Electrical Measurement

WE WERE ATTO SENDENCE -- DERIVER BESTELL -- PARTS ENGLISTED - L

FILE UID (148 SERIAL AGARGA -)
F-TED AT 25 DEG. C NO. 9
ON 10 SEP 83 AT 15:20:49 WITH THE 3260 TEST SYSTEM

er no	TEST TYPE		MEASURED VALUE	MINTONIA.	2.27 (1)
	10058		-8 - 4000dA		
* # K #	10055		9.500000	er	
	ICCOF		13,1466		-
* * * *	ICCLR		162.006		20.0
* * * *	ICCOR		3 : 430min		
	I 1		-155,0PA	-1.00000	2 02 20
	ĪĪ	_ ~	300.0FA	-1.00000	1 00 600
	11		-339.JEA	-1.05000	
	ĪŢ	_ ~	715.0PA	-1.000ba	
	ĪĪ		-345.060	-1.000007	
	I i		705,08A	-1.00000	
	= 1		-340,0PA	-1.00000	
	ĪĪ		585.0FA		
	i f		-325.08A	-1.00000	1 5
				- <u>;</u>	<u>.</u>
	: 1		495.0FA	$= \{ (1, 1), (0, 1) \}$	
7 K & 8			=10.24mb	- * , 1600 pgg.*	
	ŗ I		-985.10A	-1	:
	J. L		-380.060	#1 (PC)/(00)	. • 1 1 1 2 €
	ΞI		550.0F6	±1.40⊕ Nu∗	1000
	I 1		-385.068	-1,000000	1.35 1.00
	1.1		575.ARA	-1 (h)000	; · · · ·
	11		-380.0FA	$-1 + \omega \partial \Theta t G$.	the second special
	Ϊl		735.084	-1 0000	
	ΙI	_ ~	-20°, A⊬A		
	ĪΪ	_ ~	4 , 75 (20)		
	ĪĪ		475	-1 11313	
	7.7		5 1	4	
	÷ ,		marine marine		
	11		್ ಪ್ರಾಥಾಗಳಲ್ಲಿ ಹೃತ್ತಿಕ್ಕಳಲ್ಲಿ		
	: L		- \$±6.0e0 - \$±6.0e0		
				= 1	•
	ĪĪ		<u>a</u> ži. 081	~ 1 (44)	:
	II		-390.0H7	= 1 Jerker*	
	7.1		705. AMA	-1 C	•
	• •		= 3 → · · · · · · · · · · · · · · · · · ·	- *	•
	7.1		590 OFA	-1	•
	102		2 226 12	<u></u>	
	₽₽₽		*** = 5 5 m * 5	And the second	•
	65		The state		•
	~ _		, general	2 100 0	

the section of the se

Figure V.F.15 - Post -1000 Volt Electrical Measurement

The Contract of the Contract o

	Voltage	+250	-250	+500	-500	+750	-750
	17						
	16						
;	15					1	2
	14			5		9	
	13	3	7	6	10		10
Number of Fallures at Fin Locations	12			1	7	5	9
п госа	=			1	6	10	10
at Pi	10			1	3	7	10
Jules	8			2	6		6
or ral	9			2	5	9	7
i acimir	5					6	6
•	47			7		C.1	10
	3						-
(2			- · ·			•
	-		-				

Figure V.F.16 - (D) Stress, Cumulative Leakage Failures (Summary of 10 parts)

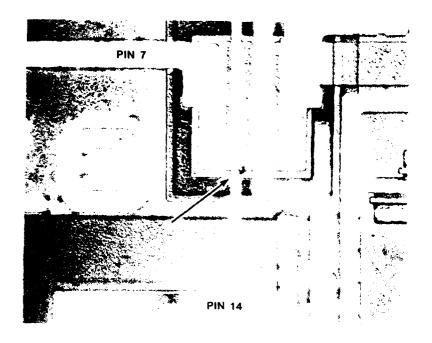


Figure V.F.17 - CD Stress, Pin 7 to Pin 14 Short

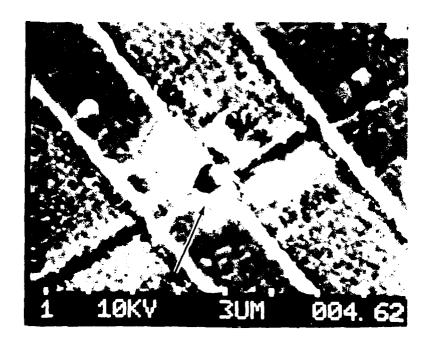


Figure V.F.18 - CD Stress, SEM Micrograph of Pin 7 to Pin 14 Damage

PIN 6

PIN 7



Figure V.F.19 + CD Stress, SEM Micrograph of Pin 6 to Pin 7 Damage

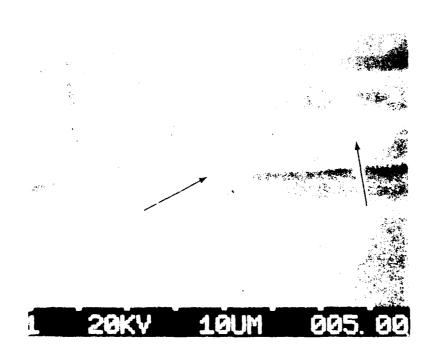


Figure V.F.20 - CD Stress, SFM Micrograph of Same Area as Previous Photo

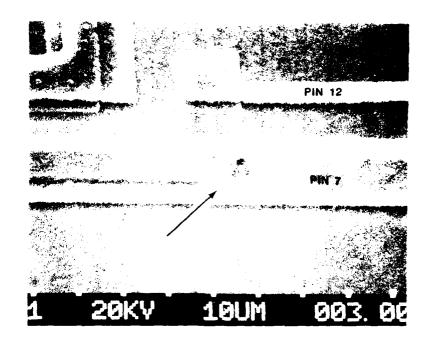


Figure V.F.21 - CD Stress, Short Between Pins 7 and 12

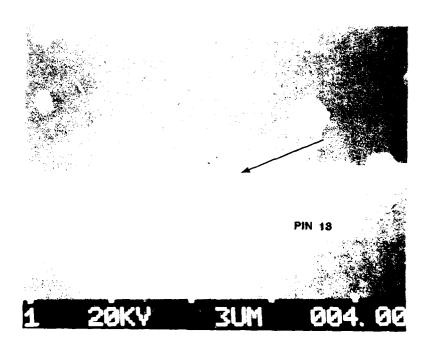


Figure V.F.22 - CD Stress, Short to Pin 13 tolysalac c

	Voltage	-500	+750	-750	+1000	-1000	+1250	-1250	+1500
	17			-			2	3	3
	16			-			2	3	3
	15			-			2	3	3
ions	14	1	2	3	7		7	6	6
Number of Failures at Pin Locations	13	2		5		9	8	6	6
t Pin	12			1		2	7	5	2
ures a	11			1			2	3	3
Fail	10		1	2			7	5	5
iber of	∞			1			2	3	7
Nun	9			1	3	7	8	6	6
	2			1			4	2	7
	4			-			2	3	3
	3			-			2	3	8
	2			-			2	~	2
				C1					2

Figure V.F.23 - HBD Stress, Cumulative Leakage Failures (Summary of 10 Parts)

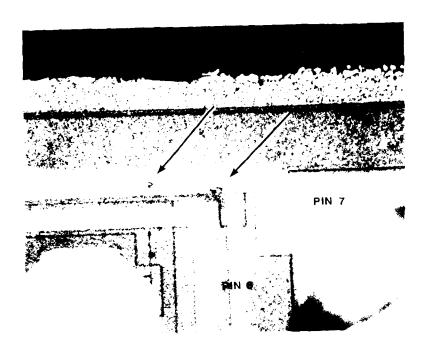


Figure V.F.24 - HBD Stress, Pin 6 to Pin 7 Damage

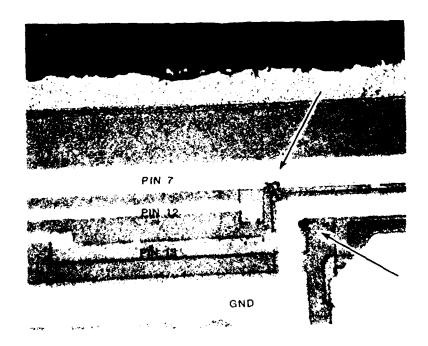


Figure V.F.25 - HBD Stress, Damage Sites Between Pins 7 and 12 and Between Pin 13 and CND



Figure V.F.26 - HBD Stress, Polysilicon Damage and Possible Short Site at Corner

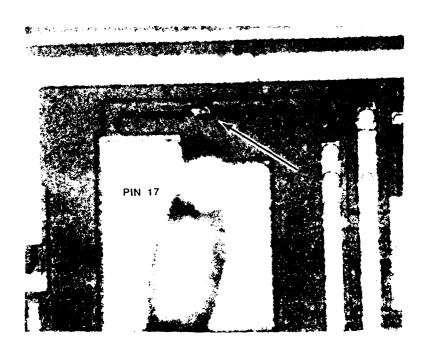


Figure V.F.27 - HBD Stress, Pin 17 Polysilicon Damage

G. Part G Analysis

This device is a 16-Bit Microprocessor manufactured using a high-density, N-channel silicon-gate depletion load process (HMOS). There is one layer of metallization and one layer of polysilicon. The metallization stripes are approximately 3.5 microns wide and the polysilicon is 2.5 microns wide. This was in a 64-pin dual-in-line ceramic package with a metal lid.

An overall die photo is shown in Figure V.G.1. VCC is connected to pins 14 and 49 and GND is connected to pins 16 and 53. These are shown in Figures V.G.2 and V.G.3. The metallization distribution pattern is visible in the photograph. There is a pad (substrate bias generator) which is connected to a metal chip on the substrate between pads 16 and 17. This does not go to the external pins. A photograph of this pin is shown in Figure V.G.4.

An input is shown in Figure V.G.5 and the corresponding schematic is shown in Figure V.G.5a. The contact between the diffused resistor and the bond pad is a polysilicon pad. The ground metallization is over the edge of the resistor making a gated diode to substrate. The dielectric breakdown measured on Q3 was 38 volts. The diode to substrate is the n-type resistor to p-type substrate. The clock input has a resistor which measured 425 ohms. The resistors on the other inputs are 2 to 3 times this value as indicated by their physical dimensions. The breakdown voltage for the input transistor junctions and the input resistor to the substrate is 22 volts.

An output circuit is shown in Figure V.G.6 and in the schematic in Figure V.G.7. This is the standard NMOS output circuit. There is no separate protection circuitry.

An input/output circuit is shown in Figure V.G.8 and in the schematic in Figure V.G.9. The circuitry is the same as shown previously however the layout is different.

Microsections were performed to examine the device construction and dimensions. A section through an input polysilicon to resistor connection is shown in Figures V.G.10 and V.G.11. Figure V.G.10 shows the top view and Figure V.G.11 shows the side view. The metallization is approximately 1.0 microns thick, the polysilicon is 0.25 microns thick, and the oxide on either side of the polysilicon is 0.5 microns thick. The microsection was chemically stained and the diffusions were examined. A top view is shown in Figure V.G.12 and a side view is shown in Figure V.G.13. The diffusions are about 0.4 microns deep.

Electrical Testing

Electrical data was taken on each of the stressed parts and the control part at each iteration during the testing. If the parts did not have a leakage failure, the data was not printed except at the initial, +500, +1000, +1500, +2000, +2500, and +3000 volt levels. In addition to the

leakage current information by serial number the average leakage current at each voltage level for each pin was calculated. These data are shown in Figures V.G.14 and V.G.15. Figure V.G.14 is the initial averages and Figure V.G.15 is the averages following the +2250 volt stress.

The readings taken on the Tektronix 3260 ATE were the input current leakage of each pin with respect to VCC and GND which were connected together. The readings were taken at +3 volts (NDV) and +10 volts (NDVR). This provides information on interface circuit damage. One additional measurement should have been made to ensure continuity. The failure mode which developed on the inputs was often opens rather than shorts and this was not easily identifiable in this test.

Functional testing was performed on a Part Type G Educational Computer Board. This was done after each testing sequence. The operations which each chip was asked to perform included; Abort, Help, Memory Set, Memory Display, and Block of Memory Search. This is not a complete functional test but does exercise a good portion of the device.

Charged Device Data Analysis

Fifteen devices, S/N 17-31, were stressed with the charged device ESD simulation model. Serial number 31 was taken through the test and stress sequence until it failed, in order to provide an early indication of the voltage level which would be required. It failed functionally after the -750 volt stress. The remainder of the devices were taken through the testing sequence and failed functionally as follows: -250V S/N 29, +500V S/N 20, 25, 26, 27, 30, -500V S/N 21, 22, 23, 24, 28, +750V S/N 18, -750V S/N 17, 19. Serial number 29 was pulled for failure analysis and the remainder of the parts were left in test to gain further information on input circuit degradation.

The testing was stopped after the +2250 volt stress. Leakage current failures are summarized in Figure V.G.16. This includes the input pins and pins 17 and 18. A few of the other pins failed at voltage levels of 1750 and greater. The output pins were more susceptible than the I/O pins. A printout of the average value of leakage current for each pin is shown in Figure V.G.16a. The leakage current failures do not provide all of the information required to understand the variation in pin sensitivity. The leakage current on pin 10 of serial number 30 is shown in Figure V.G.17. The current is erratic and measures 4 nA after the +2250 volt stress. This pin was electrically open when measured at this time.

Ten devices were electrically measured and the condition of the inputs and of pins 17 and 18 are shown in Figure V.G.17a. The primary failure mode of the inputs is an electrical open condition. The two I/O pins developed excess leakage current.

The variations in circuit layout are shown in Figures V.G.18 through V.G.22. Figure V.G.18 shows the standard input circuit. Figure V.G.19 shows the input configuration used for the clock, pin 15. Figure V.G.20

shows the standard output configuration. Figure V.G.21 shows the standard input/output configuration. Figure V.G.22 shows the configuration used for pins 17 and 18. These outputs have sink transistors but no source transistor. The input is the standard configuration.

All devices were visualy examined and further documentation was performed on serial numbers 20 and 22. Inputs are shown in Figures V.G.23 through V.G.26. Figure V.G.23 shows five inputs on serial number 22 that are all electrically open. Figure V.G.24 shows an open on pin 10 of serial number 22. Figure V.G.25 shows damage on pins 12 and 13. Pin 12 is open and pin 13 is shorted to ground. Figure V.G.26 shows a short on pin 15. Typical output damage is shown for pin 7 on S/N 20 in Figure V.G.27. Damage on pins 17 and 18 occurred on the current sink transistors (Figures V.G.28 and V.G.29). This was junction damage drain to body or drain to source (ground).

These parts were found to have inputs that were sensitive to stress due to damage created in the polysilicon interface between the bond pad and the input resistor. Pin 15 was the most sensitive to stress. This pin had a polysilicon stripe parallel to the protect resistor. This polysilicon was connected to ground and it also went beneath the bond pad metallization. The ground metallization represents a large capacitance and causes this pin to be readily damaged by the charged device model stress.

Two of the I/O pins, 17 and 18, were sensitive to stress. These had fewer contacts than the other I/O pins and the output pins. The more contact area the less sensitive a pin was to stress. This made the output pins the next most sensitive and the remainder of the I/O pins the least sensitive.

Human Body Discharge Data Anaylysis

Fifteen devices, S/N 2 through 16, were stressed with the human body ESD simulation test method. Serial number 2 was taken through the test and stress sequence until it failed. It failed functionally at -1250 volts. The remainder of the devices were taken through the testing sequence and failed functionally as follows: -1250V S/N 13, -2250 S/N 11, 15 and 16, -2500V S/N 14, +2750 S/N 3, 4, 5, 8 and 9, -2750V S/N 7, 10 and 12, +3000V S/N 6. The parts were removed from further stress as they failed. Leakage increases followed a pattern similar to that seen on the charged device models except that pin 15 was not damaged on any of the devices. The configuration with the ground metallization away from the interface polysilicon is not as susceptible as the other inputs to the human body ESD simulation.

Figure V.G.30 shows the leakage currents with the corresponding pin numbers and functions after the -2250 volt stress. Several inputs are leaky and pin 17 is leaky. This was found to be true on other parts as shown in Figure V.G.31. Input pins 10, 12, 13, 21, 23, 24 and 25 showed opens and/or leakage. Input pin 22 which is the same layout as the other 7 inputs did not have apparent damage. It appears that the inputs that are

the closest to output or I/O pins are more susceptible to damage. This makes 10 and 12 the most susceptible, 21 and 25 the next most susceptible and 22, 23 and 24 the least susceptible. This conclusion agrees with the electrical data. Pin 15 was not susceptible to stress. Pin 17 developed leakage current due to the fact that there was only one connection on the sink transistor. Pin 18 had multiple connections to the sink transistor and it was not damaged. The output and other I/O pins also were not damaged.

Photos of the type of damage that occurred is shown in Figures V.G.32 and V.G.33. Figure V.G.32 shows opens on pins 10 and 12. Figure V.G.33 shows slight visible damage on pins 22 and 23.

These devices had above average tolerance to ESD stress. The input configuration used allowed leakage to develop to the ground metallization and opens developed in the polysilicon.

The difference between the two test methods was evident on this device. The reason is that the package capacitance is a large factor for the charged device model and is not a factor for the human body simulation.

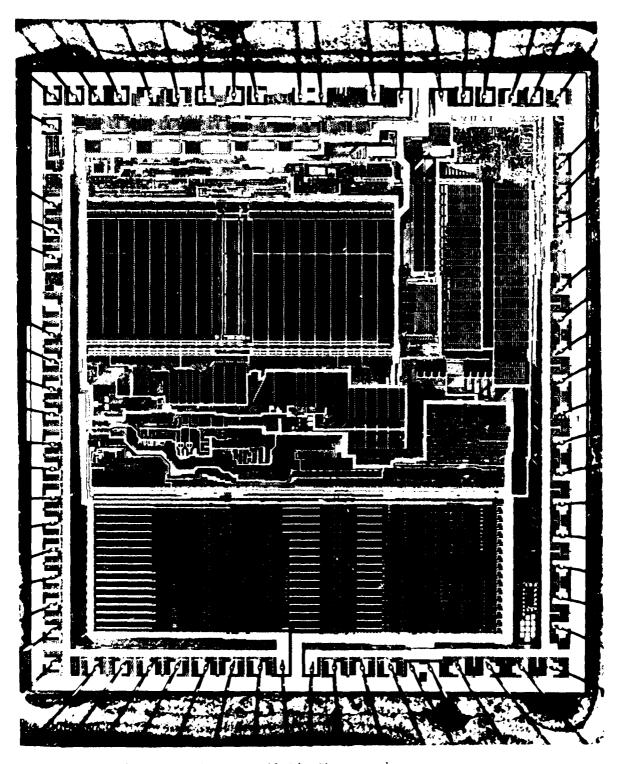


Figure V.G.1 - Overall Die Photograph

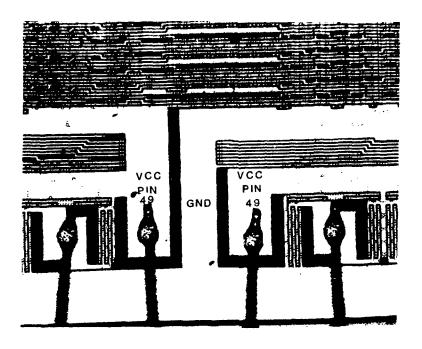


Figure V.G.2 - VCC Bond Pad and GND Metallization

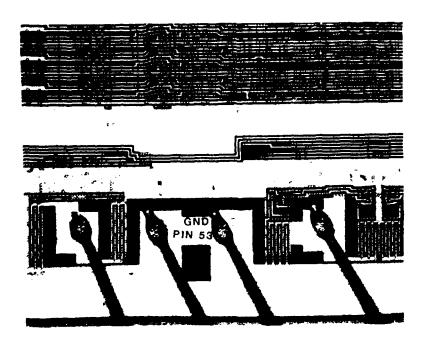


Figure V.G.3 - GND Bond Pad

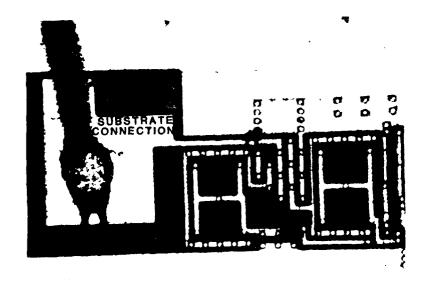


Figure V.G.4 - Substrate Connection

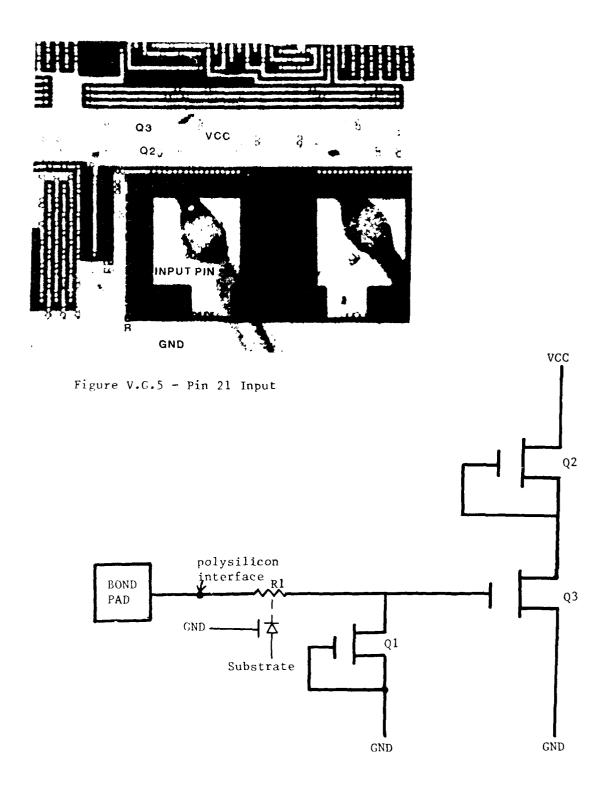
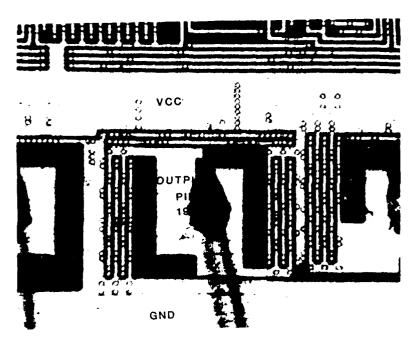


Figure V.G.5a - Input Schematic



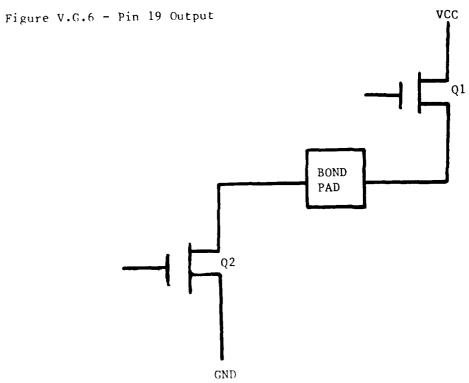


Figure V.G.7 - Output Schematic

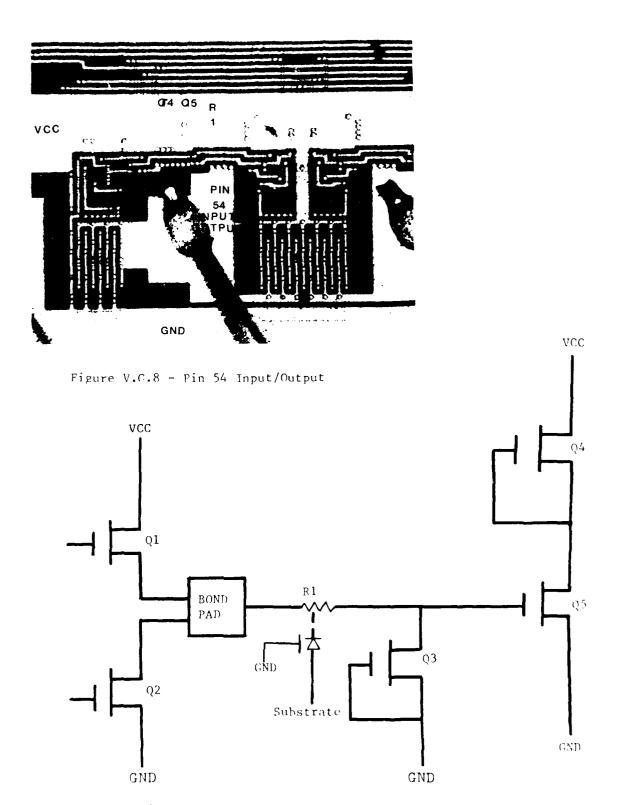


Figure V.G.9 - Input/Output Schematic

AD-R150 333

EOS (ELECTRICAL OVERSTRESS) PROTECTION FOR VLSI (VERY LARGE SCALE INTEGRA. (U) MARTIN HARIETTA AEROSPACE DENVER CO D D MILSON ET AL. SEP 84 NCR-84-596

UNCLASSIFIED RADC-TR-84-183 F39602-82-C-0111

F/G 9/1

NL

10/1

10/2

10/4

10/4

10/4

10/4

10/4

10/4

10/4

10/4

10/4

10/4

10/4

10/4

10/4

10/4

10/4

10/4

10/4

10/4

10/4

10/4

10/4

10/4

10/4

10/4

10/4

10/4

10/4

10/4

10/4

10/4

10/4

10/4

10/4

10/4

10/4

10/4

10/4

10/4

10/4

10/4

10/4

10/4

10/4

10/4

10/4

10/4

10/4

10/4

10/4

10/4

10/4

10/4

10/4

10/4

10/4

10/4

10/4

10/4

10/4

10/4

10/4

10/4

10/4

10/4

10/4

10/4

10/4

10/4

10/4

10/4

10/4

10/4

10/4

10/4

10/4

10/4

10/4

10/4

10/4

10/4

10/4

10/4

10/4

10/4

10/4

10/4

10/4

10/4

10/4

10/4

10/4

10/4

10/4

10/4

10/4

10/4

10/4

10/4

10/4

10/4

10/4

10/4

10/4

10/4

10/4

10/4

10/4

10/4

10/4

10/4

10/4

10/4

10/4

10/4

10/4

10/4

10/4

10/4

10/4

10/4

10/4

10/4

10/4

10/4

10/4

10/4

10/4

10/4

10/4

10/4

10/4

10/4

10/4

10/4

10/4

10/4

10/4

10/4

10/4

10/4

10/4

10/4

10/4

10/4

10/4

10/4

10/4

10/4

10/4

10/4

10/4

10/4

10/4

10/4

10/4

10/4

10/4

10/4

10/4

10/4

10/4

10/4

10/4

10/4

10/4

10/4

10/4

10/4

10/4

10/4

10/4

10/4

10/4

10/4

10/4

10/4

10/4

10/4

10/4

10/4

10/4

10/4

10/4

10/4

10/4

10/4

10/4

10/4

10/4

10/4

10/4

10/4

10/4

10/4

10/4

10/4

10/4

10/4

10/4

10/4

10/4

10/4

10/4

10/4

10/4

10/4

10/4

10/4

10/4

10/4

10/4

10/4

10/4

10/4

10/4

10/4

10/4

10/4

10/4

10/4

10/4

10/4

10/4

10/4

10/4

10/4

10/4

10/4

10/4

10/4

10/4

10/4

10/4

10/4

10/4

10/4

10/4

10/4

10/4

10/4

10/4

10/4

10/4

10/4

10/4

10/4

10/4

10/4

10/4

10/4

10/4

10/4

10/4

10/4

10/4

10/4

10/4

10/4

10/4

10/4

10/4

10/4

10/4

10/4

10/4

10/4

10/4

10/4

10/4

10/4

10/4

10/4

10/4

10/4

10/4

10/4

10/4

10/4

10/4

10/4

10/4

10/4

10/4

10/4

10/4

10/4

10/4

10/4

10/4

10/4

10/4

10/4

10/4

10/4

10/4

10/4

10/4

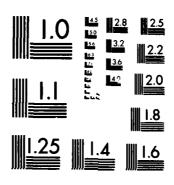
10/4

10/4

10/4

10/4

10/4



MICROCOPY RESOLUTION TEST CHART NATIONAL BUREAU OF STANDARDS-1963-A

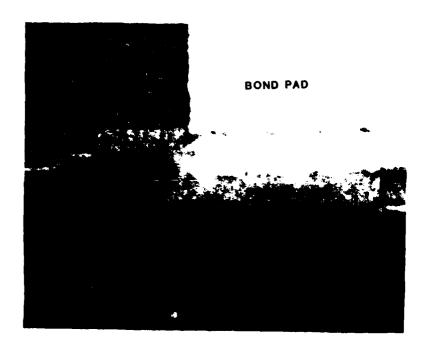


Figure V.G.10 - Top View of Section Through Input

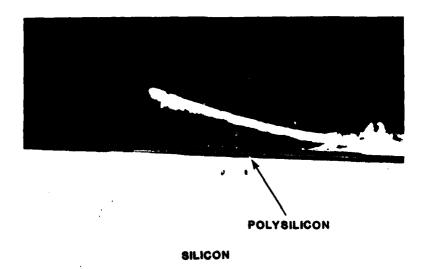


Figure V.G.11 - Side View of Section Through Input



Figure V.G.12 - Top View of Section Through Input

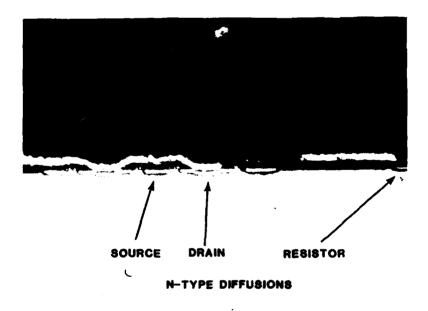


Figure V.G.13 - Side View of Section Through Input

MARTIN MARIETTA AEROSPACE -- DENVER DIVISION -- PARTS EVALUATION LAB

TESTED AT 25 DEG. (ON 31 OCT 83 AT 14:		IAL NUMBER - VARIOUS
TEST FAIL TYPE	MEASURED VALUE	L I M I T S MINIMUM MAXIMUM
PIN AVERAGE OF S	SERIAL NUMBERS:	

3,4,5,6,7	,8,9,10,1	1,12,13,	14,15,16

NIIV		903.6FA	 1.000MA
NEW		567.9FA	 1.000MA
NEW		610.7FA	 1.000MA
NDU		503.6FA	 1.000MA
NDV		396.4FA	 1.000MA
NEW		500.0FA	 1.000MA
NIO		432.1FA	 1.000MA
NDO		382.1FA	 1.000MA
NDU		510.7FA	 1.000MA
NDU		2.550NA	 1.000MA
NIO		2.854NA	 1.000MA
NDU		2.675NA	 1.000MA
NDV		4.675NA	 1.000MA
NIIV		3.607NA	 1.000MA
NIIU		1.800NA	 1.000MA
NIIU		3.832NA	 1.000MA
NEIU		1.825NA	 1.000MA
NDV		2.021NA	 1.000MA
NDU		3.404NA	 1.000MA
NDV		2.793NA	 1.000MA
NDV		2.896NA	 1.000MA
NDV		2.779NA	 1.000MA
NEW		2.907NA	 1.000MA
NIO		2.675NA	 1.000MA
NDO		2.864NA	 1.000MA
NEW		2.754NA	 1.000MA
NIIV		2.696NA	 1.000MA
NDV		2.796NA	 1.000MA
NIIU		2.711NA	 1.000MA
NDU		2.911NA	 1.000MA
NDV		2.961NA	 1.000MA
NEW		2.761NA	 1.000MA
NIO		3.661NA	 1.000MA
NDU	-	3.564NA	 1.000MA
VŪV		3.621NA	 1.000MA
NIO		3.007NA	 1.000MA
NIIU		3.000NA	 1.000MA
NIIV		2.511NA	 1.000MA
NIIU		2.646NA	 1.000MA
NDV		2.689NA	 1.000MA
NDU		3.257NA	 1.000MA
NEW		3.486NA	 1.000MA
NIIU		639.3FA	 1.000MA
NEW		628.6PA	 1.000MA

Figure V.G.14 - Average Leakage Current at Initial Electrical Test

FILE UID :153 SERIAL NUMBER - VARIOUS

FAIL	TEST TYPE		MEASURED VALUE	L I M MINIMUM	I T S MAXIMUM
f I P	N AVERAGE	OF SERIAL NUM	BERS:		
3,4	4,5,6,7,8	,9,10,11,12,13	,14,15,16		
	NDV		1.239NA		1,000M
	NIIV		1.471NA		1.000MA
	NDV		1.500NA		1.000MA
	NIO		1.461NA		1.000MA
	NDU		1.554NA		1.000MA
	NEW		1.389NA		1.000MA
	NDV		1.575NA		1.000MA
	NIIV		1.357NA		1.000MA
	NDV		1.421NA		1.000MA
	NDV		1.354NA		1.000MA
	NDV		1.346NA		1.000MA
	NDV		1.318NA		1.000MA
	NIIV		1.207NA		1.000ma
	NIIV	-	1.393NA		1.000ma
	NIIV		1.193NA		1.000MA
	NDV		1.321NA		1.000ma
	NIVR		2.879NA		1.000MA
	NEIVR		2.175NA		1.00004
	NIVR		2.057NA		1.000006
	NIVE		1.804NA		1.000mA
	NIVR		1.775NA		1.000MA
	NDVR		1.729NA		1.000MA
	NDVR		2.039NA		1.000MA
	NDUR		1.900NA		1.000MA
	NIVR		1.832NA		1.000#
	NIVE		1.335UA		1.000MA
	NIVR		1.844UA		1.000MA
	NIVE		1.584UA		1.000MA
	NEVR		14.57UA	-	1.000MA
	NDVR		10.99UA		1.000MA
	NOVE		2.330UA		1.000MA
	NEUR		16.10UA		1.000MA
	NEUR		2.198UA		1.000MA
	NIVE		2.353UA		1.000MA
	NOUR		10.62UA		1.000MA
	NIVE		1.952UA	-	1.000MA
	NIVE		1.865UA		1.000MA
	NDUR		1.534UA		1.00 MA
	NIVE		1.503UA		1.000MA
	NDVR		1.548UA	~-	1.000MA
	NEUR		1.381UA		1.000MA
	NIVE		1.129UA		1.000MA
	NIOR		1.273UA		1.000MA
	NEUR		1.418UA		1.000MA
	NDVR		1,788UA		1.000MA

Figure V.G.14 - Average Leakage Current at Initial Electrical Test (Cont.)

FILE UID :153 SERIAL NUMBER - VARIOUS TESTED AT 25 Deg. C INITIAL TEST ON 31 OCT 83 AT 14:22 WITH THE 3260 TEST SYSTEM

FAIL	TEST TYPE			MEASURED VALUE	L I M I MINIMUM	T S MAXIMUM
PI	N AVERAGE	OF SEF	RIAL NUMBER	s:		
3,	4 • 5 • 6 • 7 • 8	,9,10,1	11,12,13,14	,15,16		
	NDVR			2.040UA		1.000MA
	NEWR			2.199UA		1.000MA
	NEUR			1.583UA		1.000mA
	NIIVR			14.33UA		1.000MA
	NITUR			14.42UA		1.000MA
	NDUR			17.28UA		1.000MA
	NEUR			5.111UA		1.000mA
	NIVE			5.378UA		1.000MA
	NDUR			3,169UA		1.000MA
	NDVR			2.726UA		1.000MA
	NEUR			2.535UA		1.000MA
	NEIVR			9.574UA		1.000MA
	NIVR			15.24UA		1.000MA
	NDUR			7.146NA		1.000MA
	NEUR			3.064NA		1.000MA
	NEUR			11,56NA		1.000MA
	NIIUR			11.59NA		1.000mA
	NDVR			11.75NA		1.000mA
	NIVE			11.60NA		1.000MA
	NDVR			12.50NA		1.000mA
	NIUR			12.10NA		1.000MA
	NEUR			11,50NA		1.000MA
	NIOR			11.23NA		1.000ma
	NDVR			10.81NA		1.000mm
	NEUR			11.32NA		1.000MA
	NDUR			11.68NA		1.00066
	NDVR			11.41NA		1.000mA
	NDVR			14.93NA		1.000MA
	NDVR			14.02NA		1.000MA
	NEOR			15.72NA		1.000MA
	NEUR			14.61NA		1.000ma

Figure V.G.14 - Average Leakage Current at Initial Electrical Test (Cont.)

MARTIN MARIETTA AEROSPACE -- DENVER DIVISION -- PARTS EVALUATION LAB

AIL	TEST TYPE							MEASURED VALUE	L I M I MINIMUM	T S MAXIMUM
6.13	l AVERAGE				 t		MILLER	F00+		
								,26,27,28,29,3	0	
	NEW	-		-	-	-	-	832.1FA		1.000M
	NEW	-	-	_	_	-	-	678.6PA		1.0⊍0୍ଲ
	NIIV	-		-	_	-	-	500.0FA	-+	1.000m
	NDV	-		-	-	-	-	482.1PA		1.000M
	NEW	-	-	_	-	-	-	517.9PA		1.000M
	NEW	-	-	-	-	-	-	382.1FA		1.000m
	NIO	-	-	_	-	-	-	489.3PA		1.000M
	NEW	-	-	-	-	-	-	475.0FA		1.000M
	NDV	-		-	-	-	-	375.0FA		1.000m
	NEW	-		_	-	-	-	3.379NA		1.000M
	NEW	-	-	-	-	-	-	3.111NA		1.000M
	NEW	-	-	-	-	-	-	3.011NA		1.000M
	NDV	-	_	-	_	-	-	4.386NA		1.000M
	NDV	-	-	-	-	_	-	2.971NA		1.000m
	NDV	-	-	-	-	-	-	1.946NA		1.000M
	NIV	-	-	-	-	_	-	4.143NA		1.000M
	NEW	-	-	-	-	-	-	1.954NA		1.000M
	NEW	-	-	_	-	_	-	1.839NA		1.000M
	NIIU	-	-	-	-	-	-	3.768NA		1.000M
	NDU	-	_	-	-	-	-	3.896NA		1.000M
	NEO	-	-	-	-	-		4.371NA		1.000m
	MEIU	-	-	-	-	-	-	4.854NA		1.000M
	พถูบ	-	-	-	-	-	-	4.836NA		1.000m
	NDV	-	-	-	-	_	-	4.807NA		1.000M
	NEW	_	_	-	-		-	4.900NA		1.000M
	NIO	-	-	-	-	-		5.507NA		1.000m
	NEW	-	-	-	_	-	-	5.436NA		1.000m
	NIO	_	_	_	_	-	-	4.711NA		1.000M
	NIO	_	_	_	_	_	-	5.179NA		1.000M
	NIN	-	-	-	-	-	-	5.921NA		1.000M
	NIIV	_	-	_	-	-	-	6.768NA		1.000M
	NIIU	-	-	-	-	-	-	5.443NA		1.000M
	NIV	_	-	_	-		-	6.132NA		1.000M
	NIO	-	-	-	_	_	-	4 • 446NA		1.000M
	NIO	-	-	-	-	-	-	3.979NA		1.000M
	NDV	-	-	-	-	_	-	3.507NA		1.000M
	NIV	-	-	-	_	_	_	2.839NA		1.000M
	NDV	_	-	-	-	-	-	2.386NA		1.000M
	NDV	-	. <u>-</u>	_	_	_	_	2.186NA		1.000%
	NDV	-		-	_	-	-	2.725NA		1.000M
	NIV	_	-	-	-			3.911NA		1.000M
	NIV	_	-	-	_	-	-	3.768NA		1.000M
	ИDV	-	-	_		_	-	1.189NA	- -	1.000M

Figure V.G.14 - Average Leakage Current at Initial Electrical Test (Cont.)

3.768NA 1.189NA 407.1FA

1.000MA

FILE UID :153 SERIAL NUMBER - VARIOUS

TESTED AT 25 DEG, C INITIAL TEST
ON 31 OCT 83 AT 14:31 WITH THE 3240 TEST SYSTEM

AIL	TEST TYPE		MEASURED VALUE	L I M MINIMUM	I T S MAXIMUM
F·11	N AVERAGE	OF SERIAL NUM	BERS:		
17	18,19,20	,21,22,23,24,2	15,26,27,28,29,30)	
) Tali		1 700110		1 000#
	NEW		1.300NA		1.000MA
	NDU NDU		1.236NA 18.79NA		1.000MA 1.000MA
	NDV		8.393NA		1.000MA
	NIIV		1.311NA		
	NIIV		1.311NA 1.461NA		1.000MA
	MDV		1.461NA 1.207NA		1.000MA 1.000MA
	NEIU		1.439NA		1.000MF
	NEU		1.189NA		1.000MA
	NĪIU		1.311NA		1.000MA
	NIIV		1.332NA		1.000#4
	NEW		1.054NA		1.000MA
	NEW		1.339NA		1.000mA
	NTIU		1.064NA		1.000ma
	NEIU		1.325NA		1.00000
	NIIV		1.111NA		1.000046
	NIVE		2,957NA		1.000MA
	NEVR		2.121NA		1.000MA
	NDUR		1.768NA		1.000ma
	NEUR		1.764NA		1.000MA
	NOUR		1.611NA		1.000MA
	NEUR		1.450NA		1.000MA
	NDVR		1.614NA		1.000me
	NIVE		1.446NA		1.000MA
	NEUR		1.418NA		1.000me
	NIVE		47.42UA		1.000MA
	NOVE		39.81UA		1.00000
	NIJUR		31.70UA		1.000MA
	NDUR		28.98UA		1.000MA
	NIVE		11.51UA		1.000#4
	NEWR		2.710UA		1.000MA
	NIVE		16.84UA		1.000MA
	NDUR		2.035UA		1.000MA
	NDUR		1.775UA		1.000MA
	NEUR		10.14UA		1.000MA
	NEUR		64.59UA		1.000MA
	NEUR		76.56UA		1.000MA
	NDVR		77.73UA		1.000MA
	NEUR		78.36UA		1.000MA
	NDVR		78.32UA		1.000MA
	NEUR		79.00UA		1.000MA
	NEWR		79.12UA		1.000MA
	NDVR		79.79UA		1.000MA
	NDUR		80.65UA		1.000ma
	NDVR		82.15UA		1.000MA

Figure V.G.14 - Average Leakage Current at Initial Electrical Test (Cont.)

FILE UID :153 SERIAL NUMBER - VARIOUS

TESTED AT 25 DEG. C INITIAL TEST ON 31 OCT 83 AT 14:31 WITH THE 3260 TEST SYSTEM

NEWR

NIVR

NEVE

NIVE

NEUR

NEIVR

のでは、Marie できるでは、「Marie Marie
FAIL	TEST TYPE		MEASURED VALUE	L I M MINIMUM	I T S MAXIMUM
		OF SERIAL			
17:	,18,19,20	,21,22,23,24	1,25,26,27,28,29,3	0	
	NDUR		- 85.53UA		1.000MA
	NDVR		- 97.66UA		1.000MA
	NDVR		- 110.6UA		1.000MA
	NDVR		- 105.4UA		1.000MA
	NIVE		- 68.00UA		1.000MA
	NEVR		- 52.20UA		1.000MA
	NEVR		- 28.10UA		1.000MA
	NEUR		- 19.61UA		1.000MA
	NDVR		- 4.500UA		1.000MA
	NIVE		- 2.895UA		1.000MA
	NDVR		- 5.966UA		1.000MA
	NDVR		- 32.39UA		1.000MA
	NEUR		- 30.86UA		1.000MA
	NDVR		- 24.82NA		1,000MA
	NDVR		- 2.082NA		1.000MA
	NDVR		- 11.85NA		1.000MA
	NDUR		- 11.40NA		1.000MA
	NEIVR		- 55.04NA		1.000MA
	NDVR		- 32.25NA		1.000MA
	NDVR		- 12.95NA		1.000MA
	NEUR		- 11.80NA		1.000MA
	NEVE		- 11.79NA		1.000MA
	NEWR		- 12.55NA		1.000MA
	NDVR		- 12.52NA		1.000MA
	NIVE		- 14.04NA		1.000MA

13.80NA

13.89NA

22.86NA

22.99NA 21.66NA

19.01NA

1.000MA

1.000MA

1.000MA

1.000MA

1.000MA

1.000MA

Figure V.G.14 - Average Leakage Current at Initial Electrical Test (Cont.)

MARTIN MARIETTA AEROSPACE -- DENUER DIVISION -- PARTS EVALUATION LAB

FILE UID :153 SERIAL NUMBER - VARIOUS
TESTED AT 25 DEG. C P2250U STRESS
ON 10 DEC 83 AT 12:51 HITH THE 3260 TEST SYSTEM

FAIL	TEST TYPE	MEASURED VALUE	LIMITS MINIMUM MAXIMUM	•
				-

PIN AVERAGE OF SERIAL NUMBERS: 3,4,5,6,7,8,9,10,11,12,14,15,16

NDU	NDU 8.478UA 1.888MA NDU 12.81NA 1.888MA NDU 12.81NA 1.888MA NDU 12.79UA 1.888MA NDU 12.79UA 1.888MA NDU 86.36UA 1.888MA NDU 19.64NA 1.888MA NDU 19.64NA 1.888MA NDU 3.531NA 1.888MA NDU 3.531NA 1.888MA NDU 3.958NA 1.888MA NDU 3.958NA 1.888MA NDU 3.585NA 1.888MA NDU 4.658NA 1.888MA NDU 2.661NA 1.888MA NDU 2.731NA 1.888MA NDU 2.731NA 1.888MA NDU 2.731NA 1.888MA NDU 2.819NA 1.888MA NDU 2.819NA 1.888MA NDU 3.650NA 1.888MA NDU 3.650NA 1.888MA NDU 3.650NA 1.888MA NDU 3.650NA 1.888MA NDU 3.652NA 1.888MA NDU 3.658NA 1.888MA NDU			
NDU	NDU 12.91NA 1.000MA NDU 43.68UA 1.000MA NDU 12.79UA 1.000MA NDU 26.36UA 1.000MA NDU 23.47NA 1.000MA NDU 19.04NA 1.000MA NDU 8.231NA 1.000MA NDU 3.538NA 1.000MA NDU 3.538NA 1.000MA NDU 3.585NA 1.000MA NDU 3.585NA 1.000MA NDU 3.585NA 1.000MA NDU 2.681NA 1.000MA NDU 2.681NA 1.000MA NDU 2.691NA 1.000MA NDU 2.691NA 1.000MA NDU 2.819NA 1.000MA NDU 2.819NA 1.000MA NDU 2.819NA 1.000MA NDU 3.650NA 1.000MA NDU 3.650NA 1.000MA NDU 3.650NA 1.000MA NDU 3.662NA 1.000MA NDU 3.662NA 1.000MA NDU 3.650NA 1.000MA NDU 3.660NA 1.000MA NDU 3.650NA 1.000MA NDU	NDU	 2.588NA	 1.888MA
NDU	NDU 43.68UA 1.888MA NDU 12.79UA 1.888MA NDU 18.68UA 1.888MA NDU 18.69UA 1.888MA NDU 19.64NA 1.888MA NDU 19.231NA 1.888MA NDU 3.538NA 1.888MA NDU 3.535NA 1.888MA NDU 3.585NA 1.888MA NDU 3.585NA 1.888MA NDU 3.585NA 1.888MA NDU 2.681NA 1.888MA NDU 2.681NA 1.888MA NDU 2.691NA 1.888MA NDU 2.819NA 1.888MA NDU 2.819NA 1.888MA NDU 2.819NA 1.888MA NDU 2.819NA 1.888MA NDU 3.650NA 1.888MA NDU 3.650NA 1.888MA NDU 3.758NA 1.888MA NDU 3.758NA 1.888MA NDU 3.538NA 1.888MA NDU 3.538NA 1.888MA NDU 3.538NA 1.888MA NDU 3.538NA 1.888MA NDU 3.588NA 1.888MA NDU 3.688NA 1.888MA NDU 3.688NA 1.888MA NDU	NDU	 8.478UA	 1.000MA
NDU	NDU	NDU	 12.81NA	 1.000MA
NDU	NDU	NDU	 43.68UA	 1.000MA
NDU 23.47NA 1.080 NDU 19.84NA 1.080 NDU 8.231NA 1.080 NDU 3.538NA 1.080 NDU 3.538NA 1.080 NDU 3.538NA 1.080 NDU 3.585NA 1.080 NDU 4.658NA 1.080 NDU 4.658NA 1.080 NDU 2.681NA 1.080 NDU 2.731NA 1.080 NDU 2.731NA 1.080 NDU 2.819NA 1.080 NDU 2.819NA 1.080 NDU 3.650NA 1.080 NDU 3.750NA 1.080 NDU 3.650NA 1.080 NDU 3.652NA 1.080 NDU 3.662NA 1.080 NDU 3.662NA 1.080 NDU 3.650NA 1.080 NDU 3.581NA 1.080 NDU 3.585NA 1.080 NDU 3.585NA 1.080 NDU 3.585NA 1.080 NDU 3.585NA 1.080 NDU 3.385NA 1.080 NDU 3.585NA 1.080	NDU	NDU	 12.79UA	 1.000MA
NDU	NDU	NDU	 86.36UA	 1.000MA
NDU 8.231NA 1.888 NDU 3.538NA 1.888 NDU 3.538NA 1.888 NDU 3.585NA 1.888 NDU 3.585NA 1.888 NDU 4.658NA 1.888 NDU 5.823NA 1.888 NDU 5.7.38NA 1.888 NDU 5.7.38NA 1.888 NDU 2.819NA 1.888 NDU 2.819NA 1.888 NDU 3.658NA 1.888 NDU 3.658NA 1.888 NDU 3.658NA 1.888 NDU 3.652NA 1.888 NDU 3.652NA 1.888 NDU 3.652NA 1.888 NDU 3.658NA 1.888 NDU 3.538NA 1.888 NDU 3.658NA 1.888 NDU 3.658NA 1.888 NDU 3.658NA 1.888 NDU 3.658NA 1.888 NDU 3.542NA 1.888 NDU 3.788NA 1.888 NDU 3.885NA 1.888 NDU 3.885NA 1.888 NDU 3.354NA 1.888	NDU	NDU	 23.47NA	 1.080MA
NDU	NDU	NDU	 19.04NA	 1.000MA
NDU	NDU	NDU	 8.231NA	 1.000MA
NDU	NDU	NDU	 3.538NA	 1.000MA
NDU	NDU	NDU	 3.958NA	 1.000MA
NDU	NDU 4.658NA 1.000MA NDU 2.681NA 1.000MA NDU 57.38NA 1.000MA NDU 2.731NA 1.000MA NDU 20.13NA 1.000MA NDU 3.650NA 1.000MA NDU 3.652NA 1.000MA NDU 3.642NA 1.000MA NDU 3.652NA 1.000MA NDU 3.581NA 1.000MA NDU 3.588NA 1.000MA NDU 3.988NA 1.000MA NDU 3.980NA 1.000MA NDU 3.900NA 1.000MA NDU	NDU	 3.585NA	 1.000MA
NDU 2.681NA 1.000 NDU 57.38NA 1.000 NDU 2.731NA 1.000 NDU 2.819NA 1.000 NDU 2.819NA 1.000 NDU 3.650NA 1.000 NDU 3.650NA 1.000 NDU 3.662NA 1.000 NDU 3.662NA 1.000 NDU 3.538NA 1.000 NDU 3.658NA 1.000 NDU 3.658NA 1.000 NDU 3.658NA 1.000 NDU 3.658NA 1.000 NDU 3.551NA 1.000 NDU 3.551NA 1.000 NDU 3.558NA 1.000 NDU 3.558NA 1.000 NDU 3.588NA 1.000 NDU 3.788NA 1.000 NDU 3.788NA 1.000 NDU 3.788NA 1.000 NDU 3.788NA 1.000 NDU 3.885NA 1.000 NDU 3.988NA 1.000	NDU 2.681NA 1.000MA NDU 2.731NA 1.000MA NDU 2.819NA 1.000MA NDU 20.13NA 1.000MA NDU 20.13NA 1.000MA NDU 3.650NA 1.000MA NDU 3.652NA 1.000MA NDU 3.662NA 1.000MA NDU 3.662NA 1.000MA NDU 3.538NA 1.000MA NDU 3.652NA 1.000MA NDU 3.658NA 1.000MA NDU 3.658NA 1.000MA NDU 3.658NA 1.000MA NDU 3.658NA 1.000MA NDU 3.581NA 1.000MA NDU 3.581NA 1.000MA NDU 3.581NA 1.000MA NDU 3.581NA 1.000MA NDU 3.588NA 1.000MA NDU 3.598NA 1.000MA NDU 3.900NA 1.000MA NDU 1.000MA NDU 1.000MA NDU 1.000MA NDU 1.000MA NDU 1.000MA NDU 1.000MA NDU	NDU	 5.823NA	 1.000MA
NDU 57.38NA 1.000 NDU 2.731NA 1.000 NDU 2.819NA 1.000 NDU 20.13NA 1.000 NDU 3.650NA 1.000 NDU 3.750NA 1.000 NDU 3.642NA 1.000 NDU 3.652NA 1.000 NDU 3.652NA 1.000 NDU 3.652NA 1.000 NDU 3.658NA 1.000 NDU 3.581NA 1.000 NDU 3.581NA 1.000 NDU 3.582NA 1.000 NDU 3.583NA 1.000 NDU 3.583NA 1.000 NDU 3.788NA 1.000 NDU 3.788NA 1.000 NDU 3.885NA 1.000 NDU 3.988NA 1.000	NDU		 4.658NA	 1.800MA
NDU 2.731NA 1.000 NDU 20.13NA 1.000 NDU 3.650NA 1.000 NDU 3.750NA 1.000 NDU 3.642NA 1.000 NDU 3.662NA 1.000 NDU 3.538NA 1.000 NDU 3.668NA 1.000 NDU 3.668NA 1.000 NDU 3.568NA 1.000 NDU 3.581NA 1.000 NDU 3.581NA 1.000 NDU 3.588NA 1.000 NDU 3.788NA 1.000 NDU 3.788NA 1.000 NDU 4.358NA 1.000 NDU 3.885NA 1.000 NDU 3.885NA 1.000 NDU 3.885NA 1.000 NDU 3.885NA 1.000	NDU	_	 2.681NA	 1.000MA
NDU 2.819NA 1.000 NDU 20.13NA 1.000 NDU 3.650NA 1.000 NDU 3.652NA 1.000 NDU 3.662NA 1.000 NDU 3.662NA 1.000 NDU 3.653NA 1.000 NDU 3.650NA 1.000 NDU 3.650NA 1.000 NDU 3.650NA 1.000 NDU 3.538NA 1.000 NDU 3.571NA 1.000 NDU 3.571NA 1.000 NDU 3.572NA 1.000 NDU 3.5630NA 1.000 NDU 3.588NA 1.000 NDU 3.588NA 1.000 NDU 3.588NA 1.000 NDU 3.588NA 1.000 NDU 3.885NA 1.000 NDU 3.785NA 1.000 NDU 3.900NA 1.000 NDU 3.900NA 1.000 NDU 3.900NA 1.000 NDU 4.227NA 1.000	NDU 2.819NA 1.000MA NDU 20.13NA 1.000MA NDU 3.650NA 1.000MA NDU 3.650NA 1.000MA NDU 3.642NA 1.000MA NDU 3.652NA 1.000MA NDU 3.652NA 1.000MA NDU 3.538NA 1.000MA NDU 3.668NA 1.000MA NDU 3.669NA 1.000MA NDU 3.550NA 1.000MA NDU 3.578NA 1.000MA NDU 3.591NA 1.000MA NDU 3.591NA 1.000MA NDU 3.5630NA 1.000MA NDU 3.581NA 1.000MA NDU 3.581NA 1.000MA NDU 3.588NA 1.000MA NDU 3.598NA 1.000MA NDU 3.598NA 1.000MA NDU 3.598NA 1.000MA NDU 3.598NA 1.000MA NDU 3.988SNA 1.000MA NDU 3.988SNA 1.000MA NDU 3.378SNA 1.000MA NDU 3.378SNA 1.000MA NDU 3.378SNA 1.000MA NDU 3.378SNA 1.000MA NDU 3.388SNA 1.000MA NDU 3.398NA 1.000MA NDU 3.980NA 1.000MA NDU 3.980NA 1.000MA NDU 3.980NA 1.000MA NDU	NDU	 57.38NA	 1.000MA
NDU	NDU		 2.731NA	 1.000MA
NDU	NDU 3.650NA 1.000MA NDU 3.750NA 1.000MA NDU 3.642NA 1.000MA NDU 3.652NA 1.000MA NDU 3.538NA 1.000MA NDU 3.550NA 1.000MA NDU 3.650NA 1.000MA NDU 3.650NA 1.000MA NDU 3.550NA 1.000MA NDU 3.551NA 1.000MA NDU 3.552NA 1.000MA NDU 3.552NA 1.000MA NDU 3.788NA 1.000MA NDU 3.788NA 1.000MA NDU 3.550NA 1.000MA NDU 3.558NA 1.000MA NDU 3.598NA 1.000MA NDU 4.498NA 1.000MA NDU 4.498NA 1.000MA NDU 3.354NA 1.000MA NDU 3.355NA 1.000MA NDU 3.355NA 1.000MA NDU 3.355NA 1.000MA NDU 3.595NA 1.000MA NDU 3.900NA 1.000MA NDU 3.900NA 1.000MA		 2.819NA	 1.000MA
NDU	NDU	_	 20.13NA	 1.000MA
NDU	NDU 3.642NA 1.800MA NDU 3.652NA 1.000MA NDU 3.538NA 1.000MA NDU 3.658NA 1.000MA NDU 3.658NA 1.000MA NDU 3.477NA 1.000MA NDU 3.581NA 1.000MA NDU 3.542NA 1.000MA NDU 3.658NA 1.000MA NDU 3.658NA 1.000MA NDU 3.788NA 1.000MA NDU 3.788NA 1.000MA NDU 4.558NA 1.000MA NDU 4.404NA 1.000MA NDU 3.885NA 1.000MA NDU 3.885NA 1.000MA NDU 3.785NA 1.000MA NDU 3.900NA 1.000MA NDU 3.900NA 1.000MA NDU 3.900NA 1.000MA NDU 3.900NA 1.000MA NDU 1.000MA		 	 1.900MA
NDU	NDU 3.662NA 1.000MA NDU 3.652NA 1.000MA NDU 3.652NA 1.000MA NDU 3.658NA 1.000MA NDU 3.477NA 1.000MA NDU 3.581NA 1.000MA NDU 3.542NA 1.000MA NDU 3.658NA 1.000MA NDU 3.788NA 1.000MA NDU 3.788NA 1.000MA NDU 4.558NA 1.000MA NDU 4.484NA 1.000MA NDU 4.484NA 1.000MA NDU 3.005NA 1.000MA NDU 3.000MA 1.000MA NDU 1.000MA NDU		 3.75 0 NA	 1.800MA
NDU 3.53BNA 1.000 NDU 3.658NA 1.000 NDU 3.68BNA 1.000 NDU 3.477NA 1.000 NDU 3.581NA 1.000 NDU 3.542NA 1.000 NDU 3.542NA 1.000 NDU 3.788NA 1.000 NDU 3.588NA 1.000 NDU 4.558NA 1.000 NDU 4.488NA 1.000 NDU 3.005NA 1.000 NDU 3.000NA 1.000	NDU 3.538NA 1.000MA NDU 3.658NA 1.000MA NDU 3.668NA 1.000MA NDU 3.581NA 1.000MA NDU 3.581NA 1.000MA NDU 3.542NA 1.000MA NDU 3.658NA 1.000MA NDU 3.789NA 1.000MA NDU 3.789NA 1.000MA NDU 3.568NA 1.000MA NDU 4.558NA 1.000MA NDU 4.488NA 1.000MA NDU 4.488NA 1.000MA NDU 3.885NA 1.000MA NDU 3.785NA 1.000MA NDU 3.535NA 1.000MA NDU 3.535NA 1.000MA NDU 3.535NA 1.000MA NDU 3.595NA 1.000MA		 3.642NA	 1.800MA
NDU	NDU 3.650NA 1.000MA NDU 3.600NA 1.000MA NDU 3.477NA 1.000MA NDU 3.542NA 1.000MA NDU 3.542NA 1.000MA NDU 3.780NA 1.000MA NDU 3.780NA 1.000MA NDU 3.500NA 1.000MA NDU 4.550NA 1.000MA NDU 4.404NA 1.000MA NDU 4.480NA 1.000MA NDU 3.805NA 1.000MA NDU 3.300NA 1.000MA NDU 3.300NA 1.000MA NDU 3.354NA 1.000MA NDU 3.423NA 1.000MA NDU 3.535NA 1.000MA NDU 3.598NA 1.000MA NDU 3.598NA 1.000MA NDU 3.598NA 1.000MA		 	 1.000MA
NDU 3.608NA 1.000 NDU 3.477NA 1.800 NDU 3.581NA 1.000 NDU 3.542NA 1.000 NDU 3.658NA 1.000 NDU 3.788NA 1.000 NDU 4.558NA 1.000 NDU 4.404NA 1.000 NDU 3.885NA 1.000 NDU 3.988NA 1.000 NDU 3.958NA 1.000 NDU 3.958NA 1.000 NDU 3.958NA 1.000 NDU 3.535NA 1.000 NDU 3.535NA 1.000 NDU 3.535NA 1.000	NDU 3.609NA 1.000MA NDU 3.581NA 1.000MA NDU 3.581NA 1.000MA NDU 3.558NA 1.000MA NDU 3.658NA 1.000MA NDU 3.788NA 1.000MA NDU 3.509NA 1.000MA NDU 4.558NA 1.000MA NDU 4.404NA 1.000MA NDU 4.499NA 1.000MA NDU 3.885NA 1.000MA NDU 3.354NA 1.000MA NDU 3.535NA 1.000MA NDU 3.900NA 1.000MA NDU 3.900NA 1.000MA NDU 1.000MA		 –	 1.000MA
NDU 3.477NA 1.000 NDU 3.581NA 1.000 NDU 3.582NA 1.000 NDU 3.650NA 1.000 NDU 3.788NA 1.000 NDU 4.558NA 1.000 NDU 4.404NA 1.000 NDU 4.404NA 1.000 NDU 3.885NA 1.000 NDU 3.885NA 1.000 NDU 3.384NA 1.000 NDU 3.384NA 1.000 NDU 3.354NA 1.000 NDU 3.354NA 1.000 NDU 3.354NA 1.000 NDU 3.3535NA 1.000 NDU 3.535NA 1.000	NDU 3.477NA 1.800MA NDU 3.581NA 1.800MA NDU 3.542NA 1.000MA NDU 3.658NA 1.000MA NDU 3.788NA 1.000MA NDU 4.558NA 1.000MA NDU 4.404NA 1.000MA NDU 4.404NA 1.000MA NDU 3.885NA 1.000MA NDU 3.885NA 1.000MA NDU 3.785NA 1.000MA NDU 3.535NA 1.000MA NDU 3.535NA 1.000MA NDU 3.596NA 1.000MA NDU 3.596NA 1.000MA NDU 3.960NA 1.000MA NDU 3.900NA 1.000MA NDU 1.000MA		 	 1.000MA
NDU	NDU 3.581NA 1.000MA NDU 3.542NA 1.000MA NDU 3.658NA 1.000MA NDU 3.788NA 1.000MA NDU 3.598NA 1.000MA NDU 4.558NA 1.000MA NDU 4.488NA 1.000MA NDU 4.488NA 1.000MA NDU 3.885NA 1.000MA NDU 3.785NA 1.000MA NDU 3.785NA 1.000MA NDU 3.354NA 1.000MA NDU 3.355NA 1.000MA NDU 3.535NA 1.000MA NDU 3.535NA 1.000MA NDU 3.535NA 1.000MA NDU 3.900NA 1.000MA NDU 3.900NA 1.000MA NDU 3.900NA 1.000MA NDU 3.900NA 1.000MA NDU 1.000MA		 	
NDU	NDU 3.542NA 1.000MA NDU 3.658NA 1.000MA NDU 3.788NA 1.000MA NDU 4.558NA 1.000MA NDU 4.558NA 1.000MA NDU 4.488NA 1.000MA NDU 3.985NA 1.000MA NDU 3.985NA 1.000MA NDU 3.785NA 1.000MA NDU 3.785NA 1.000MA NDU 3.354NA 1.000MA NDU 3.355NA 1.000MA NDU 3.535NA 1.000MA NDU 3.535NA 1.000MA NDU 3.535NA 1.000MA NDU 3.990NA 1.000MA NDU 3.990NA 1.000MA NDU 4.227NA 1.000MA NDU 4.227NA 1.000MA		 	
NDU	NDU 3.650NA 1.000MA NDU 3.789NA 1.000MA NDU 3.508NA 1.000MA NDU 4.558NA 1.000MA NDU 4.404NA 1.000MA NDU 3.885NA 1.000MA NDU 3.885NA 1.000MA NDU 3.885NA 1.000MA NDU 3.785NA 1.000MA NDU 3.785NA 1.000MA NDU 3.423NA 1.000MA NDU 3.535NA 1.000MA NDU 3.535NA 1.000MA NDU 3.535NA 1.000MA NDU 3.535NA 1.000MA NDU 3.595NA 1.000MA NDU 4.227NA 1.000MA NDU 4.227NA 1.000MA		 • •	
NDU 3.788NA 1.809 NDU 4.558NA 1.009 NDU 4.404NA 1.009 NDU 4.488NA 1.009 NDU 3.885NA 1.009 NDU 3.785NA 1.009 NDU 3.354NA 1.009 NDU 3.423NA 1.009 NDU 3.998NA 1.009 NDU 4.227NA 1.009 NDU 4.227NA 1.009 NDU 4.227NA 1.009 NDU 1.009 1.009 NDU 1.009 1.009 NDU 1.009 1.009 NDU	NDU 3.788NA 1.000MA NDU 3.509NA 1.000MA NDU 4.558NA 1.000MA NDU 4.404NA 1.000MA NDU 4.489NA 1.000MA NDU 3.885NA 1.000MA NDU 3.785NA 1.000MA NDU 3.785NA 1.000MA NDU 3.354NA 1.000MA NDU 3.423NA 1.000MA NDU 3.535NA 1.000MA NDU 3.595NA 1.000MA NDU 3.595NA 1.000MA NDU 3.900NA 1.000MA NDU 1.000MA		 	
NDU	NDU 3.509NA 1.000MA NDU 4.558NA 1.000MA NDU 4.404NA 1.000MA NDU 4.498NA 1.000MA NDU 3.885NA 1.000MA NDU 3.785NA 1.000MA NDU 3.354NA 1.000MA NDU 3.354NA 1.000MA NDU 3.535NA 1.000MA NDU 3.535NA 1.000MA NDU 3.595NA 1.000MA NDU 3.900NA 1.000MA NDU 3.900NA 1.000MA NDU 4.227NA 1.000MA NDU 1.000MA			
NDU	NDU 4.558NA 1.000MA NDU 4.404NA 1.000MA NDU 4.489NA 1.000MA NDU 3.885NA 1.000MA NDU 3.785NA 1.000MA NDU 3.354NA 1.000MA NDU 3.423NA 1.000MA NDU 3.535NA 1.000MA NDU 3.535NA 1.000MA NDU 3.900NA 1.000MA NDU 4.227NA 1.000MA NDU 4.227NA 1.000MA NDU 1.442NA 1.000MA		 	
NDU	NDU 4.404NA 1.000MA NDU 4.498NA 1.000MA NDU 3.885NA 1.000MA NDU 3.785NA 1.000MA NDU 3.354NA 1.000MA NDU 3.423NA 1.000MA NDU 3.535NA 1.000MA NDU 3.535NA 1.000MA NDU 3.900NA 1.000MA NDU 4.227NA 1.000MA NDU 4.227NA 1.000MA		 	
NDU 4.488NA 1.000 NDU 3.885NA 1.000 NDU 3.785NA 1.000 NDU 3.354NA 1.000 NDU 3.423NA 1.000 NDU 3.535NA 1.000 NDU 3.535NA 1.000 NDU 4.227NA 1.000 NDU 1.442NA 1.000	NDU 4.488NA 1.000MA NDU 3.885NA 1.000MA NDU 3.785NA 1.000MA NDU 3.354NA 1.000MA NDU 3.423NA 1.000MA NDU 3.535NA 1.000MA NDU 3.535NA 1.000MA NDU 3.900NA 1.000MA NDU 4.227NA 1.000MA NDU 4.227NA 1.000MA NDU 1.442NA 1.000MA		 	
NDV	NDV 3.885NA 1.888MA NDV 3.785NA 1.888MA NDV 3.354NA 1.888MA NDV 3.423NA 1.888MA NDV 3.535NA 1.888MA NDV 3.988NA 1.888MA NDV 4.227NA 1.888MA NDV 1.888MA NDV 1.888MA	_	 	
NDU 3.785NA 1.800 NDU 3.954NA 1.800 NDU 3.423NA 1.800 NDU 3.535NA 1.800 NDU 3.988NA 1.800 NDU 4.227NA 1.800 NDU 1.442NA 1.800	NDU 3.785NA 1.880MA NDU 3.354NA 1.880MA NDU 3.423NA 1.880MA NDU 3.535NA 1.880MA NDU 3.980NA 1.880MA NDU 4.227NA 1.880MA NDU 1.442NA 1.880MA		 	
NDU	NDU 3.354NA 1.000MA NDU 3.423NA 1.000MA NDU 3.535NA 1.000MA NDU 3.900NA 1.000MA NDU 4.227NA 1.000MA NDU 1.442NA 1.000MA		 	
NDU	NDU 3.423NA 1.000MA NDU 3.535NA 1.000MA NDU 3.900NA 1.000MA NDU 4.227NA 1.000MA NDU 1.442NA 1.000MA		 	
NDU 3.535NA 1.000 NDU 3.900NA 1.000 NDU 4.227NA 1.000 NDU 1.442NA 1.000	NDU 3.535NA 1.000MA NDU 3.900NA 1.000MA NDU 4.227NA 1.000MA NDU 1.442NA 1.000MA		 	
NDU 3.988NA 1.888 NDU 4.227NA 1.888 NDU 1.442NA 1.888	NDU 3.988NA 1.888MA NDU 4.227NA 1.888MA NDU 1.442NA 1.888MA		 	
NDU 4.227NA 1.888 NDU 1.442NA 1.888	NDV 4.227NA 1.888MA NDV 1.442NA 1.888MA		 	
NDU 1.442NA 1.888	NDU 1.442NA 1.888MA		 	
	מאס 29.84UA 1.880MA		 	
700 29.84UA 1.890		NDU	 29.84UA	 1.000MA

Figure V.G.15 - Average Leakage Current after +2250 Volt Stress

FILE UID :153 SERIAL NUMBER - VARIOUS TESTED AT 25 DEG. C P2250V STRESS ON 10 DEC 83 AT 12:51 WITH THE 3260 TEST SYSTEM

	TEST						MEASURED		HIT	
AIL	TYPE						VALUE	MINIMUM	M	AXIMUM
	VERAGE 0					_				
3,4,5	,6,7,8,9	. 10	5. 11	. 1	2,	14,15	, 16			
	NDU		-	-	-	-	2.100NA			1.000MA
	NDV			-	-	-	2.815NA			1.000MA
	NDU		-	-	-	-	2.415NA			1.000MA
	NDU		-	-	-	-	2.696NA			1.000MA
	NDU		-	-	-	-	2.392NA			1.000MA
	NDU			-	-	-	2.088NA			1.900MA
	NDU		-	-	-	-	2.219NA			1.000MA
	NDU				-	-	2.219NA			1.000MA
	NDU			-	-	_	2.900NA			1.000MA
	NDU			-	-	-	2.281NA			1.000MA
	NDU			-	-	-	1.946NA			1.000MA
	NDU			-	-	-	2.181NA			1.000MA
	NDU			-	-	-	2.000NA			1.000MA
	NDU		-	-	_	-	2.100NA			1.000MA
	NDU			-	-	-	2.085NA			1.000MA
	NDU			-	-	-	1.946NA			1.000MA
	NDUR		-	-	-	-	14.00NA			1.000MA
	NDUR			-	-	-	12.9BUA			1.000MA
	NDUR			-	-	-	42.75NA			1.000MA
	NDUR			-	-	-	98.68UA			1.800MA
	NDUR			-		_	28.88UA			1.000MA
	NDUR			-	-	-	173.9UA			1.000MA
	NDUR			-	-	_	80.75NA			1.000MA
	NDUR			-	-	-	65.75NA			1.000MA
	NDUR			-	-	-	30.21NA			1.000MA
	NDUR			-	-	-	967.9NA			1.000MA
	NDUR			-	_	-	1.298UA			1.000MA
	NDUR	- •		-	-	-	1.133UA			1.000MA
	NDUR			-	-	-	8.275UA			1.000MA
	NDUR			-	_	_	6.442UA			1.000MA
	NDUR			-	-	-	1.377UA			1.000MA
	NDUR			-	-	-	15.7 0 UA			1.890MA
	NDUR			-	_	_	1.306UA			1.800MA
	NDUR			-	_	_	1.482UA			1.000MA
	NDUR			-	_	-	6.201UA			1.000MA
	NDUR			-	_	_	1.35BUA			1.000MA
	NDUR			-	-	-	1.302UA			1.000MA
	NDUR			_	_	_	1.086UA			1.800MA
	NDUR			_	-	_	1.055UA			1.000MA
	NDUR			_	_	_	1.096UA			1.000MA
	NDUR			-	_	_	998.1NA			1.000MA
	NDUR			_	-	_	820.5NA			1.000MA
	NDUR			_	_	_	913. BNA			1.000MA
	NDUR			-	_	-	1.016UA			1.000MA
	NDUR			_	-	_	1.249UA			1.000MA

Figure V.G.15 - Average Leakage Current after +2250 Volt Stress (Cont.)

FILE UID :153 SERIAL NUMBER - VARIOUS TESTED AT 25 DEG. C P2250V STRESS ON 10 DEC 83 AT 12:51 WITH THE 3260 TEST SYSTEM

AIL	TEST Type							MEASURED VALUE	L I M Minimum	I T S MAXIMUM
	1176								UTMINON	
D T	N AVERAGE	. 05	e s	- P 1	<u>ا</u> م ا		JI IMBI	FDC:		
_	4,5,6,7,8	-					_			
	NDUR	_	_	_	_	_	_	1.404UA		1.000M
	NDUR	-	-	-	-	_	-	1.513UA		1.000M
	NDUR	-	-	-	-	-	-	1.1 09 UA		1.800M
	NDUR	-	-	-	-	-	-	8.070UA		1.000M
	NDUR	_	-	-	-	-	-	7.99 8 UA		1.006M
	NDUR	-	-	-	-	-	-	9.553UA		1.000M
	NDUR	-	-	-	-	-	-	3.166UA		1.000M
	NDUR	-	-	-	-	-	-	3.270UA		1.800M
	NDUR	-	-	-	-	-	-	1.994UA		1.000M
	NDUR	_	-	-	-	-	-	1.76 0 UA		1.000M
	NDUR	-	-	-	-	-	-	1.665UA		1.000M
	NDUR	-	-	-	-	-	-	5.417UA		1.000M
	NDUR	_	-	-	-	-	-	8.791UA		1.000M
	NDUR	_	-	-	-	-	-	9.377NA		1.000M
	NDUR	-	-	-	-	-	-	160.3UA		1.000M
	NDUR	-	-	-	_	-	_	12.23NA		1.000M
	NDUR	-	-	-	-	-	-	12.89NA		1.000M
	NDUR	_	-	-	-	-	-	12.15NA		1.000M
	NDUR	_	-	-	-	-	_	14.03NA		1.000M
	NDUR	_	-	-	-	-	-	12.48NA		1.000M
	NDUR	-	-	-	-	-	-	11.97NA		1.000M
	NDUR	-	-	-	-	_	-	12.38NA		1.000M
	NDUR	-	-	-	-	-	-	11.99NA		1.000M
	NDUR	-	-	-	-	-	-	11.88NA		1.888M
	NDUR	-	-	-	-	-	-	11.92NA		1.000M
	NDUR	-	-	-	-	-	-	12.18NA		1.000M
	NDUR	-	-	-	-	-	-	11.98NA		1.000M
	NDUR	-	-	-	-	-	-	14.91NA		1.000M
	NDUR	-	-	-	-	-	-	14.89NA		1.000M
	NDUR	-	-	-	-	-	-	15.83NA		1.000M
	NDUR	_	_	_	_	_	_	14.45NA		1.000M

Figure V.G.15 - Average Leakage Current after +2250 Volt Stress (Cont.)

MARTIN MARIETTA AEROSPACE -- DENUER DIVISION -- PARTS EVALUATION LAB

FILE UID :153 SERIAL NUMBER - VARIOUS TESTED AT 25 DEG. C P22500 STRESS ON 10 DEC 83 AT 12:58 WITH THE 3260 TEST SYSTEM

FAIL	TEST	MEASURED	L I M 1	T S
	TYPE	VALUE	Minimum	MAXIMUM

PIN AUERAGE OF SERIAL NUMBERS: 17,18,19,20,21,22,23,24,25,26,27,28,30

NDU	 629,8UA	 1.000MA
NDU	 248.2UA	 1.000MA
NDU	 26.20UA	 1.000MA
NDU	 234.ZUA	 1.000MA
NDU	 106.0UA	 1.000MA
NDU	 236.2UA	 1.000MA
NDU	 226.6UA	 1.000MA
NDU	 349.0UA	 1.000MA
NDU	 113.6UA	 1.000MA
NDU	 5.277NA	 1.000MA
NDU	 4.181NA	 1.000MA
NDU	 78.73UA	 1.000MA
NDU	 4.592NA	 1.000MA
NDU	 238.9UA	 1.000MA
NDU	 167.7UA	 1.000MA
שמא	 479.1UA	 1.000MA
NDU	 472.4UA	 1.000MA
NDV	 157.5UA	 1.000MA
NDU	 159.5UA	 1.000MA
שמא	 4.138NA	 1.000MA
NDU	 78.74UA	 1.000MA
NDU	 5.404NA	 1.000MA
NDU	 78.74UA	 1.000MA
NDU	 6.435NA	 1.800MA
NDU	 78.74UA	 1.000MA
NDU	 6.165NA	 1.000MA
NDU	 78.74UA	 1.000MA
NDU	 5.484NA	 1.000MA
NDU	 5.454NA	 1.000MA
NDU	 6.769NA	 1.000MA
NDU	 78.74UA	 1.000MA
NDU	 6.523HA	 1.000MA
NDU	 6.677NA	 1.000MA
NDU	 78.74UA	 1. 000 ma
NDU	 4.815NA	 1.000MA
שמא	 5.812NA	 1.000MA
NDU	 78.74UA	 1.000MA
NDU	 157.5UA	 1.000MA
NDU	 128.4NA	 1.000MA
NDU	 2.992NA	 1.000MA
NDU	 157.5UA	 1.000MA
NDU	 4.627NA	 1.800MA
NDU	 934.5UA	 1.000MA
NDU	 689.9UA	 1.000MA

Figure V.G.15 - Average Leakage Current after +2250 Volt Stress (Cont.)

FILE UID :153 SERIAL NUMBER - VARIOUS TESTED AT 25 DEG. C P2250V STRESS ON 10 DEC 83 AT 12:58 WITH THE 3260 TEST SYSTEM

AIL	TEST TYPE		MEASURED VALUE	L I M MINIMUM	I T S MAXIMUM
		OF SERIAL NUME			
17	18,19,26	3,21,22,23,24,25	, 26, 27, 28, 38		
	NDU		78.73UA		4 20044
	NDU		66.61NA		1.000MA
	NDU		78.75UA		1.000MA 1.000MA
	NDU		9.919NA		1.000MA
	NDU		9.335NA		1.000MA
	NDU		4.569NA		1.000MA
	NDU		78.73UA		
	NDU		6.100NA		1.000MA 1.000MA
	NDU		1.942NA		1.000MA
	NDU		1.846NA		1.000MA
	NDU		1.973NA		1.000MA
	NDU		1.669NA		1.000MA
	NDU		3.031NA		1.000MA
	NDU		1.819NA		
	NDU		5.681NA		1.000MA
	NDU		3.204NA		1.800MA
			0.2041111		1.000MA
	NDUR		629.8UA		4 000
	NDUR		315.8UA		1.800MA
	NDUR		78.76UA		1.000MA
	NDUR		314.9UA		1.000MA
	NDUR		157.5UA		1.000MA
	NDUR		236.2UA		1.000MA
	NDUR		314.9UA		1.000MA
	NDUR		393.7UA		1.000MA
	NDUR		157.5UA		1.000MA
	NDUR		25.95UA		1.000MA
	NDUR		20.57UA		1.000MA
	NDUR		95.63UA		1.000MA
	NDUR		13.93UA		1.000MA
	NDUR				1.000MA
	NDUR		317.4UA		1.000MA
	NDUR		318.2UA 567.3UA		1.000MA
	NDUR				1.000MA
	NDUR		473.3UA		1.000MA
	NDUR		158.2UA		1.000MA
	NDUR		240.8UA		1.000MA
	NDUR		37.23UA		1.000MA
	NDUR		130.3UA		1.000MA
	NDUR		57.99UA		1. 800 MA
	NDUR		142.8UA		1.000MA
			61.85UA		1.000MA
	NDUR		144.6UA		1. 000 MA
	NDUR		76.03UA		1.000MA
	NDUR	,	159.4UA		1.000MA
	NDUR		60.96UA		1.000MA
	NDUR		66.45UA		1.000MA

Figure V.G.15 - Average Leakage Current after +2250 Volt Stress (Cont.)

SERIAL NUMBER - VARIOUS ON 18 DEC 83 AT 12:58 WITH THE 3268 TEST SYSTEM

aIL.	TEST Type		MEASURED VALUE	L I M Minimum	ITS MAXIMUM
PI	N AVERAGE	OF SERIAL NUM	1BERS:		
17	.18.19.20	, 21, 22, 23, 24, 2	25,26,27,28,30		
	NDUR		84.91UA		1.000
	NDUR		170.5UA		1.000
	NDUR		94.95UA		1.000
	NDUR		84.49UA		1.000
	NDUR		115.5UA		1.000
	NDUR		27.36UA		1.0001
	NDVR		14.18UA		1.000
	NDUR		88.41UA		1.0001
	NDUR		159.5UA		1.000
	NDUR		158.7UA		1.0001
	NDUR		3.1 0 2UA		1.8001
	NDUR		174.8UA		1.000
	NDUR		16.56UA		1.0001
	NDUR		944. BUA		1.0001
	NDUR		866. 0 UA		1.000
	NDUR		78.76UA		1.0001
	NDUR		78.75UA		1.000
	NDUR		78.77UA		1.000
	NDUR		53.63NA		1.800
	NDUR		182.4NA		1.0001
	NDUR		83.13NA		1.000
	NDUR		78.79UA		1.000
	NDUR		291.8NA		1.000
	NDUR		17.82NA		1.000
	NDUR		25.51NA		1.000
	NDUR		17.59NA		1.000
	NDUR		16.93NA		1.000M
	NDUR		55.55NA		1.000
	NDUR		26.62NA		1.000
	NDUR		86.17NA		1.000
	NDUR		35.28NA		1.000

Figure V.G.15 - Average Leakage Current after +2250 Volt Stress (Cont.)

				Nu	umber	of Fai	lures	at Pi	n Loca	tions	
10	12	13	15_	17	18	21	22	23	24	25	Voltage
			13			1					+750
1				5							-750
	1			12						1	+1000
							1				-1000
		1		13		3			1		+1250
				!	1	5	3				-1250
	1				3						+1500
2					8	6					-1500
					10						+1750
					12						-1750
		2		! !			5	1	3		+2000
	2	3									-2000
	<u> </u>										

Figure V.G.16 - CD Stress, Cumulative Leakage Failures
(Total of 13 parts)

MARTIN MARIETTA AEROSPACE -- DENVER DIVISION -- PARTS EVALUATION LAB

FILE UID: 153 SERIAL NUMBER - VARIOUS
TESTED AT 25 DEG. C N750V STRESS
UN 17 NOV 83 AT 08:27 WITH THE 3260 TEST SYSTEM

TEST MEASURED L I M I T S
FAIL TYPE VALUE MINIMUM MAXIDUM

PIN AVERAGE OF SERIAL NUMBERS: 17.18,19,20,21.22.23,24,25.26,27.28,30

			PIÑ	FUNCTION	
***	NIIV		15 1.024mA	INPUT -	1.000mA
	NEW		22 1.735NA	1	1.000mA
	NEW		25 9.507UA	1 -	1.000ma
	NIV		24 1.319UA	-	I.000ma
	NIN		23 19.10NA		- 1.000mA
	NDU		13 3.123NA	- 1 -	1.000MA
	NEW		12 44.29NA	-	1,000ma
	NIIV		21 609.3UA		1.000ma
	NEW		10 73.74UA	1 -	1.000ma
	NEW		28 3.219NA	INPUT -	1.000mA
	NDV		27 3.058NA	OUTPUT -	1. Midela
	NEW		26 2.727NA	↑ -	1.335m.
	NEW	~	20 4.012NA	-	1, 13 j. m.y.
	NEW		19 2.746NA	- }	المنظم الأراثي المناطب
	NIV		6 1.738NA	-	1.000ma
	NEW		9 3.219NA	-	1.000ma
	NEW		7 1.715NA	-	1.000mA
	NEW		8 1.773NA		- 1.000MA
	NEW		11 3.104NA	-	1.000MA
	NEW		29 3.738NA	- 1	- 1.000MA
	NEU		30 4.231NA	-	1.000MA
	NIIV		31 4.569NA	-	- 1 ტიგოგ
	NIIV		32 4.750NA	-	1.000mA
	NEW	~	33 4.281NA	-	- 1.390ma
	NIIU		34 4.500NA	-	- 1.000 MH
	NEW		35 5.015NA	-	1.636ma
	NIO		36 5.046NA	-	1.000ma
	NEW		37 4.323NA	-	1.000mA
	NIO		38 4.612NA	j -	- 1.000MA
	NUV		39 5.600NA	i -	1.000MA
	NEW		40 5.265NA	-	- 1.000MA
	NEW	-	41 5.246NA	-	1.000MA
	NEW	~	42 5.715NA	-	1.000 MA
	NIIV		43 4.000NA	-	1.000MA
	NIIV		44 3.512NA	-	1.000MA
	NIIV		45 3.173NA	-	∵= 1.ିମ୍ଚଳA
	NIIU		46 2.545NA	-	- 1.000MA
	NDU		47 1.985NA	- 1	- 1.000mA
	NEW		48 2.015NA	-	- 1.000MA
	NIIV		50 2.277NA	-	1.000ma
	NEW		51 3.362NA	↓ -	1.000MA
	NIIV		52 3.331NA	OUTPUT -	1.000MA
	NIO		18 2.012NA	I,0 -	·= 1.0000MA
	NIIN		17 414.0UA	1.70	- 4MO(400 + 1 -

Figure V.G.16a - CD Stress, Average Leakage Current Values

FILE UID :153 SERIAL NUMBER - VARIOUS TESTED AT 25 DEG. C N750V STRESS ON 17 NOV 83 AT 08:27 WITH THE 3260 TEST SYSTEM

	TEST	MEASURED	LINITS
FAIL	TYPE	VALUE	MUMIYAM MUMINIM

FIN AVERAGE OF SERIAL NUMBERS: 17,18,19,20,21,22,23,24,25,26,27,28,30

		PIN	<u>FUNCTION</u>	
NEW		5 1.112NA	1/0	1.000MA
NEW		4 1.381NA	↑	1.000MA
NIIV	- -	3 14.25NA		1.000MA
NIV		2 7.462NA	- -	1.000MA
NIV		1 1.296NA	[1.000MA
NEW		64 1.108NA		1.000MA
NIIV		63 1.250NA		1.000MA
NEW		62 1.062NA	- -	1.000MA
NEW	 -	61 1.277NA		1.000MA
NIIV		60 1.054NA		1.000mA
NIIV		59 1.150NA		1.000MA
NEV		58 1.069NA		1.000ma
NEW		57 1.054NA		1.000ma
MEIV		56 1.177NA		1.000004
NEW		55 1.015NA	\	1.000##
NEW	-	54 1.223NA	1/0	1.000MA

Figure V.G.16a - CD Stress, Average Leakage Current Values (Cont.)

NDVR reading	Voltage
1	0
20	-500
7	+750
40	-750
45	-1000
31	+1250
88	-1250
88	-1500
145	+1750
4	-1750
278	-2000
4	+2250

Figure V.G.17 - CD Leakage Current on S/N 30, Pin 10 (Nanoamps)

	Pin Number												
10	12	13	15	17	18	21	22	23	24	25	Electrical Condition		
7	8	6	4			6	4	5	7	7	Open		
2	1	2	6	9	9	3	4	2	2	1	Leaky		
1	1	2		1	1	1	2	3	1	2	Normal		

Figure V.G.17a- CD Stress, Failure Summary

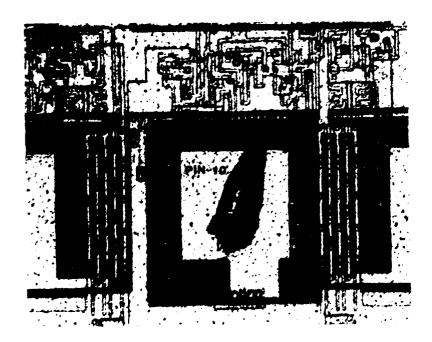


Figure V.G.18 - Pin 10 Input

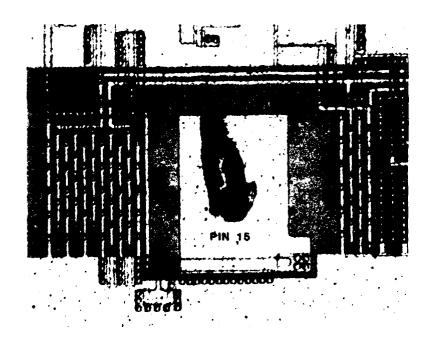


Figure V.G.19 - Pin 15 Clock Input

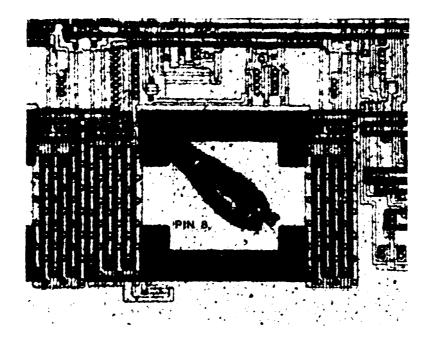


Figure V.G.20 - Pin 8 Output

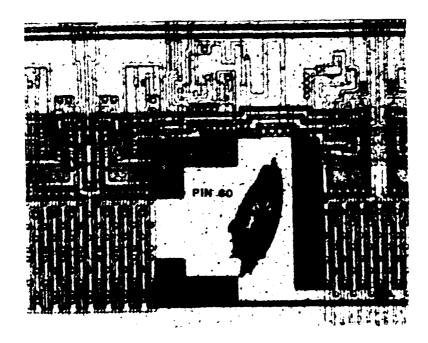


Figure V.G.21 - Pin 60 Input/Output

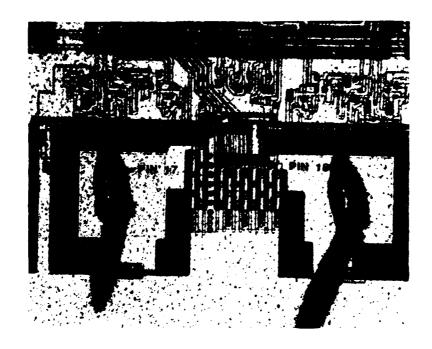


Figure V.G.22 - Pin 17 and 18 Input/Output

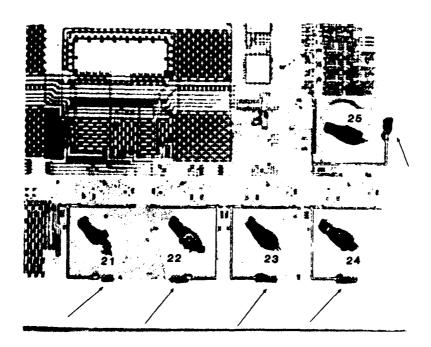


Figure V.G.23 - CD Stress, Damage at the Inputs

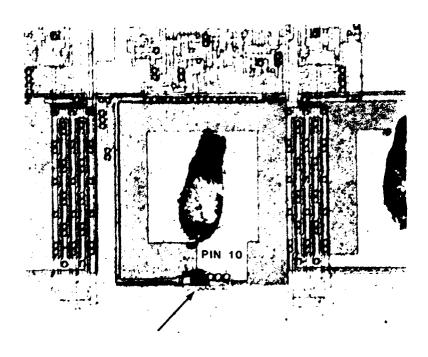


Figure V.C.24 - CD Stress, Damage at Pin 10 Inputs

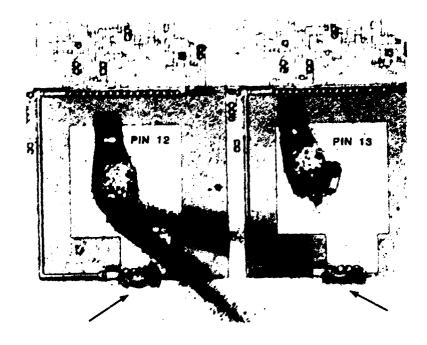


Figure V.G.25 - CD Stress, Damage at Pin 12 and 13

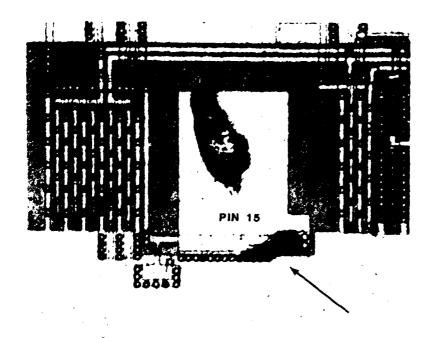


Figure V.G.26 - CD Stress, Damage on Pin 15

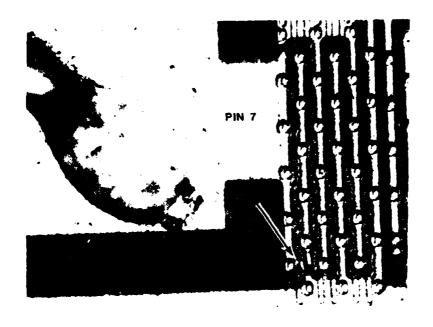


Figure V.G.27 - CD Stress, Short on Pin 7 Output

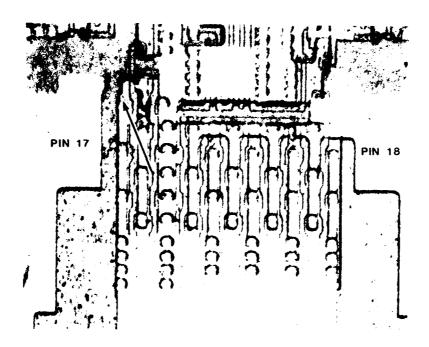


Figure V.G.28 - CD Stress, Pin 17 is Open to the Output Section and Pin 18 has Leakage Current

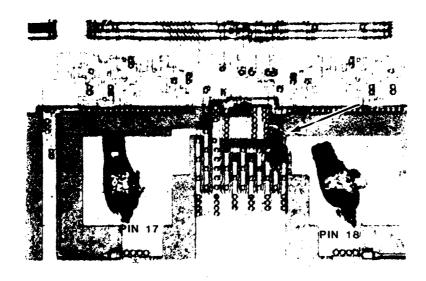


Figure V.G.29 - CD Stress Pin, 17 Has Leakage Current and Pin 18 is Open to the Output Section

MARTIN MARIETTA AEROSPACE -- DENVER DIVISION -- PARTS EVALUATION LAB

FILE UID :153 SERIAL NUMBER - VARIOUS TESTED AT 25 DEG. C N2250V STRESS ON 13 DEC 83 AT 06:45 WITH THE 3260 TEST SYSTEM

	TEST	MEASURED	LIMI						
FAIL	TYPE	VALUE	MINIMUM	MAXIMUM					

PIN AVERAGE OF SERIAL NUMBERS: 3,4,5,6,7,8,9,10,11,12,14,15,16

	PIN	FUNCTION		
NBU	 15 2.115NA	INPUT		1.000MA
VON	 22 7.976UA	1		1.000MA
NDV	 25 10.83NA	İ		1.000MA
NDU	 24 40.48UA	1		1.000MA
NDV	 23 12.21UA	i		1.000MA
NDV	 13 30.63UA			1.000MA
NDV	 12 20.73NA			1.000MA
NDV	 21 12.99NA	!		1.000MA
NDV	 10 7.473NA	1		1.000MA
NDV	 28 3.412NA	INPUT		1.000MA
NDV	 27 3.450NA	OUTPUT		1.000MA
NDV	 26 3.442NA	T		1.000MA
NDV	 20 5.288NA			1.000MA
NDV	 19 4.346NA	1		1.000MA
NDV	 6 2.442NA	[1.000MA
NDV	 9 72.70NA	i		1.000MA
NDV	 7 2.388NA	1		1.000MA
NDV	 8 2.477NA			1.000HA
NDV	 11 26.04NA			1.000MA
NDV	 29 3.388NA	1		1.000MA
NDV	 30 3.469NA			1.000MA
NDV	 31 3.392NA			1.000MA
NDV	 32 3.369NA	1		1.000MA
NDV	 33 3.296NA	1		1.000MA
NDV	 34 3.369NA	1		1.000MA
NDV	 35 3.358NA			1.000MA
NDV	 36 3.246NA			1.000MA
NDU	 37 3.304NA	1		1.000MA
NDV	 38 3.327NA			1.000MA
NDV	 39 3.392NA			1.000MA
NDV	 40 3.596NA			1.000MA
VDV VDN	 41 3.231NA	l l		1.000MA
	 42 4.342NA	į.		1.000MA
NDV	 43 4.204NA	j		1.000MA
VDV VDV	 44 4.254NA	ł		1.000MA
NDV	 45 3.665NA	ľ		1.000MA
אםט עמא	 46 3.512NA 47 3.154NA			1.000MA
NDV VDN	 47 3.154NA 48 3.154NA	J		1.000MA
NDV	 50 3.288NA	Į.		1.000MA 1.000MA
עמא	 51 3.742NA	ł		
NDV	 52 4.000NA	• 1.12m		1.000MA
NDV	 	OUTPUT		1.000MA 1.000MA
אםט עמא	 18 1.173NA 17 109.8UA	I/O		1.000MA
	 1/ 107.00H	1/0	*	* + OOOHH

Figure V.G.30 - HBD Stress, Average Leakage Currents with Pin Numbers and Functions

FILE UID :153 SERIAL NUMBER - VARIOUS TESTED AT 25 DEG. C N2250V STRESS ON 13 DEC 83 AT 06:45 WITH THE 3260 TEST SYSTEM MEASURED LIMITS FAIL TYPE VALUE MUMINIM MAXIMUM PIN AVERAGE OF SERIAL NUMBERS: 3,4,5,6,7,8,9,10,11,12,14,15,16 FUNCTION NDV 1.688NA 1/0 1.000MA 1.927NA NDV 1.000MA 3 1.808NA NDV 1.000MA NDV 2.665NA 1.000MA NDV 1.815NA 1.000MA 64 NDV 1.000MA 1.927NA 1.892NA 63 NTIU 1.000HA 62 NDU 1.846NA 1.000MA 61 1.942NA NDU 1.000MA 1.715NA 1.946NA NDV 60 1.000MA NDV 59 1.000MA NDV 58 1.654NA 1.000MA 57 NDV 1.869NA 1.000MA 1.781NA NDV 1.000MA 55 1.712NA 54 1.885NA 1.000MA NITU NDV 1/0 1.000MA

Figure V.G.30 - HBD Stress, Average Leakage Currents with Pin Numbers and Functions (Cont.)

	ELECTRICAL CONDITION	OPEN	LEAKY	NORMAL
	25	2	2	9
1	24		2	8
	23		1	6
SERS	22			10
PIN NUMBERS	21	3	1	9
PI	18			10
	17		2	5
	15			10
	13		2	8
	12	9		4
	$\frac{7}{10}$	2		5

Figure V.G.31 - HBD Stress, Failure Summary

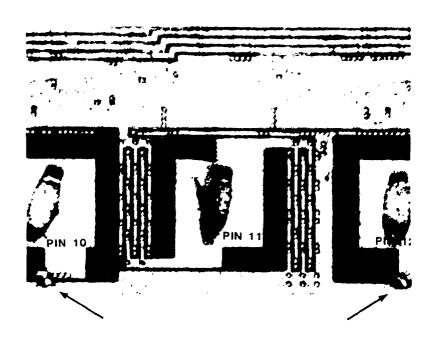


Figure V.G.32 - HBD Stress, Damage on Pins 10 and 12

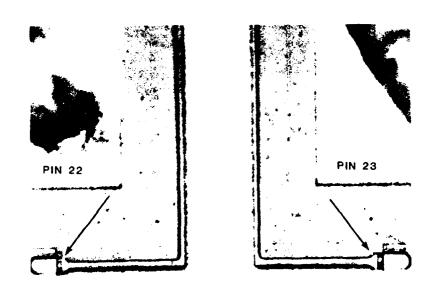


Figure V.G.33 - HBD Stress, Damage on Pins 22 and 23

H. Part H Analysis

This device is a 16-bit Microprocessor manufactured using HMOS. This is an N-channel, depletion load, silicon gate process. There are two polysilicon layers and one metallization layer. The minimum polysilicon width was about 2.5 microns and the minimum metallization width was about 3.5 microns. This was in a 40 pin dual-in-line ceramic package.

An overall die photograph is shown in Figure V.H.1. VCC is pin 40 and is on the left side of the figure. There are two ground connections, pins 1 and 20. Between VCC, pin 40, and pin 1 there is a bond pad and a wire which goes to substrate. A similar connection is made between pins 20 and 21.

The VCC bond pad is shown in Figure V.H.2. This metallization traverses the perimeter of the die to make contact with each of the inputs and outputs. It also connects to the central sections of the die. It connects to numerous n+ source diffusions.

The ground pads are shown in Figures V.H.3 and V.H.4. This metallization traverses the perimeter of the die just inside of the VCC metallization.

An input circuit is shown in Figure V.H.5 and the corresponding schematic is shown in Figure V.H.6. The input resistance measures 700 ohms. At the connection between the metallization and the diffused resistor is a polysilicon square. This is likely for ESD protection to reduce the chance of metal fusing into the silicon. The VCC metallization lays over the edge of the input resistor and produces a gated diode to substrate. The gate dielectric breakdown was about 33 volts. The input resistor to substrate and the transistor junction breakdowns were 18 volts.

An output structure is shown in Figure V.H.7 and the corresponding schematic is shown in Figure V.H.8.

The same type of output configuration is used on combination I/O pins, however a different input is used. An I/O pin is shown in Figure V.H.9 and the schematic is shown in Figure V.H.10.

In this case the input section is connected directly to a polysilicon gate. All of the outputs are the same electrically however there are three separate layouts.

Microsections were performed and the construction of the devices examined. Figure V.H.ll shows a transistor cross-section. The n-type diffusion was about 0.45 microns, the polysilicon was about 0.5 microns thick, and the metallization was about 1.0 micron thick. The oxide between the polysilicon and the silicon was 0.9 microns thick and the oxide between the polysilicon and the metallization was 1.1 microns thick.

Electrical Testing

Electrical data was taken on each of the stressed parts and the control part at each iteration during the testing. If the parts did not have a leakage failure, the data was not printed except at the initial, +500, +1000, +1500, +2000, etc., voltage levels. In addition to the leakage current information by serial number the average leakage current at each voltage level for each pin was calculated. These data are shown in Figures V.H.12 and V.H.13. Figure V.H.12 is the initial averages and Figure V.H.13 is the averages following the -2250 volt stress.

The readings taken on the Tektronix 3260 ATE were the input current leakage of each pin with respect to VCC and GND which were connected together. The readings were taken at +3 volts (NDV) and +10 volts (NDVR). This provided information on interface circuit damage. One additional measurement should have been made to ensure continuity. The failure mode which developed on several of the inputs was opens rather than shorts and this was not easily identifiable in this test.

Functional testing was performed on an SDK-86 System Design kit. This was done after each testing sequence. The operations which each chip was asked to perform included; system reset, addition, and subtraction. This is not a complete functional test but does exercise a good portion of the device. A more complete functional test was used initially and at the end of the test. This included transferring control to a terminal, modifying and reading memory and transferring control back to the keyboard. It was found that if devices passed the first functional they would pass the latter functional and if they failed the first they would fail the latter.

Charged Device Data Analysis

Fifteen devices, S/N 17 - 31, were stressed with the charged device ESD simulation model. Serial number 31 was taken through the test and stress sequence until it failed in order to provide an early indication of the voltage level which would be required. It failed functionally after the +2000 volt stress. The remainder of the devices were taken through the testing sequence and failed functionally as shown in Figure V.H.14. Serial number 25 was pulled for failure analysis and the remainder of the parts were left in test to gain further information on input circuit degradation.

The testing was stopped after the +2500 volt stress. Leakage current failures are summarized in Figure V.H.15. This includes input pins 17, 18, 19, 21, 22, 23, and 33, output pins 25, 26, and 32 and I/O pins 5, 14, 16, and 39. The measurement used to compile this table was a curve tracer reading at 10 volts after the final stress. This is in agreement with the pin averages for leakage current which was taken on the Tektronix 3260. Figure V.H.16 shows the average values after the +2500 volt stress. These can be compared to the initial averages shown in Figure 12.

To understand the variation in sensitivities the failure modes and the layouts need to be understood. Figures V.H.17 - V.H.25 show the layouts.

Figure V.H.17 - V.H.19 show input/output layouts. The I/O in Figure V.H.19 is pin 5 which was very susceptible to the charged device stress but not to the human body simulation. Two output pins are shown in Figures V.H.20 and V.H.21. Pins 25 and 26 in Figure V.H.21 failed open during the charged device testing. These pins did not develop leakage current. Figure V.H.22 shows output pin 32 and input pin 33. Figures V.H.23 - V.H.25 show input pin layouts. Pin 21 in Figure V.H.25 was one of the most susceptible pins to stress.

Failure analysis found the cause for the increased sensitivity of certain pins to be the physical layout. The damage on several inputs is shown in Figures V.H.26 through V.H.30. The distance between adjacent n+diffusions determined the sensitivity. Pins 18 and 19 were the least sensitive, followed by pins 22 and 23, and pin 21 was the most sensitive.

Additional damage which occurred on the inputs is shown in Figures V.H.31 and V.H.32. Figure V.H.31 shows a breakdown which occurred between pin 22 and VCC. Two opens occurred on this pin. The close spacing between the polysilicon and the VCC metallization caused breakdowns to occur as shown in Figure V.H.32. This pin was not shorted or leaky when measured.

Pins 25 and 26 were found to fail open as shown in Figure V.H.33. Mechanical probing found these transistors to have normal junction characteristics. The opens are likely due to these outputs being forced to interface with shorted inputs during the functional test.

Pins 32 and 33 developed leakage current due to their physical layout. This was the only output which failed due to leakage current. These pins are shown in Figures V.H.34 and V.H.35.

The other pin that failed consistently was I/O pin 5. This pin had gate oxide failures as shown in Figures V.H.36 and V.H.37. The large ground contact beside the input gate caused this part to be susceptible to the CD stress but not the HBD stress. The ground metallization capacitance would discharge through this pin and rupture the gate oxide.

These parts were very tolerant to ESD stress. Slight variations in the layout could improve this further.

Human Body Discharge Data Analysis

Fifteen devices, S/N 2 through 16, were stressed with the human body ESD simulation test method. Serial number 2 was taken through the test and stress sequence first. It was taken through the -2250 volt level with no functional or leakage problems. The remainder of the devices were taken through the testing sequence and failed functionally as follows: +2750V S/N 11, +4500V S/N 10, and -5000V S/N 14. These were the only three parts that failed the functional test. The parts were removed from further stress as they failed. Leakage increases followed a pattern similar to that seen on the charged device models except that pin 5 was not damaged on

any of the devices. The configuration with the ground metallization beside the input gate does not create an input that is more sensitive to the human body ESD simulation.

Figure V.H.38 shows the leakage current averages after the +5000 volt stress for the 3 volt reverse bias situation. Pins 17, 18, 19, 21, 22, 23, 32 and 33 exhibited leakage increase. These are all inputs except for pin 32.

The electrical condition of 13 parts as measured on a curve tracer are shown in Figure V.H.39. The leakage in this case was measured at 1 volt reverse bias. There were no opens measured for these parts.

The leakage current increases were created by similar situations on these parts as compared to the charged device group parts. Figures V.H.40 through V.H.42 show examples. The physical layout variations cause the same pins and pin combinations to be susceptible to damage. Pin 21 was the most susceptible followed by pins 32 and 33.

These devices were found to be the most tolerant to ESD stress of any group tested. The combination of no current path available to the outside from the substrate and possibly the polysilicon interface material created this condition. A minor change on pin 21 and 33 could further decrease this sensitivity.

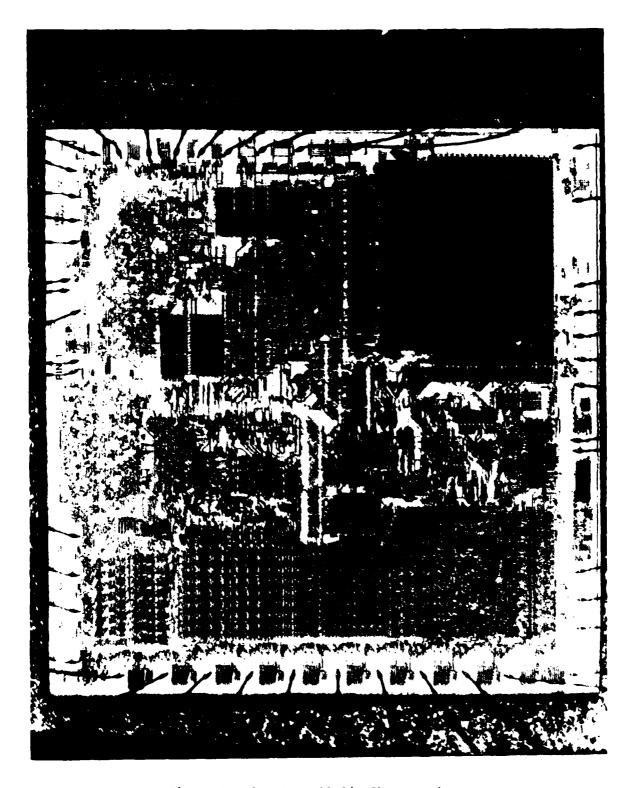


Figure V.H.1 - Overall Die Photograph

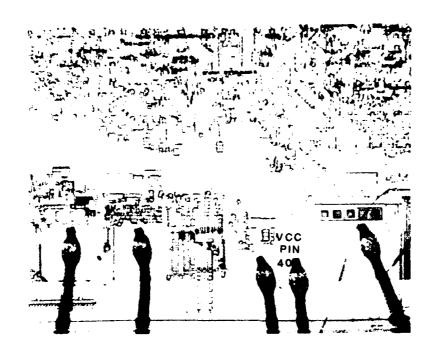


Figure V.H.2 - VCC Bond Pad

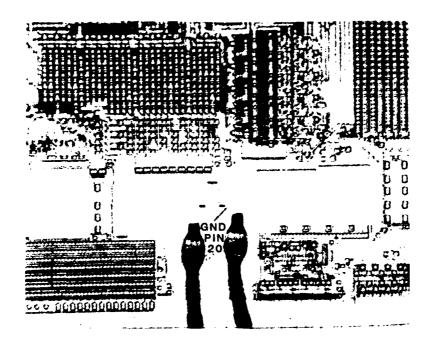


Figure V.H.3 - GND Bond Pad, Pin 20

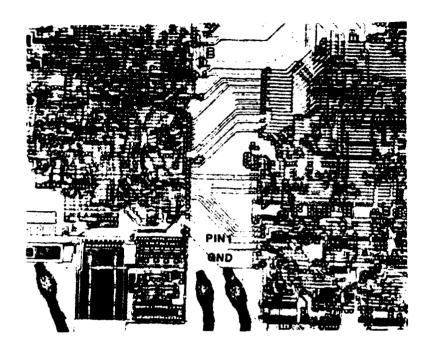


Figure V.H.4 - GND Bond Pad, Pin 1

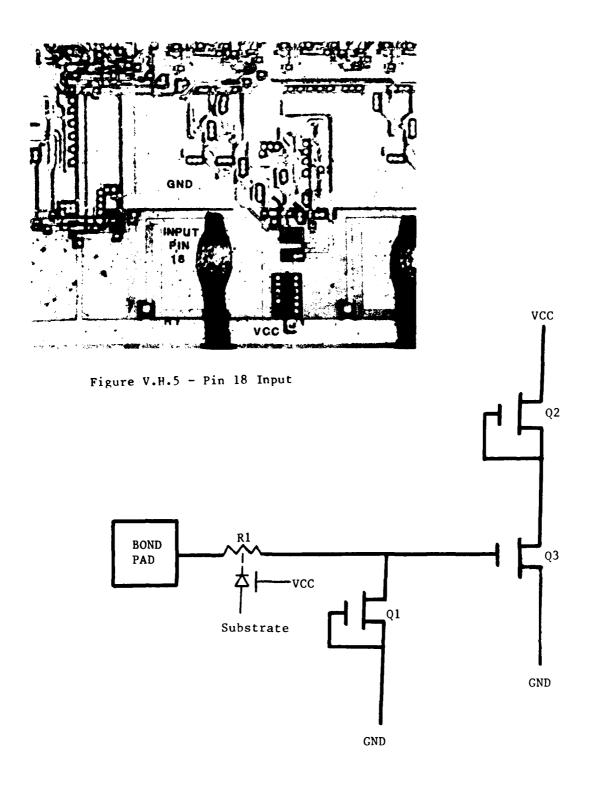


Figure V.H.6 - Input Schematic

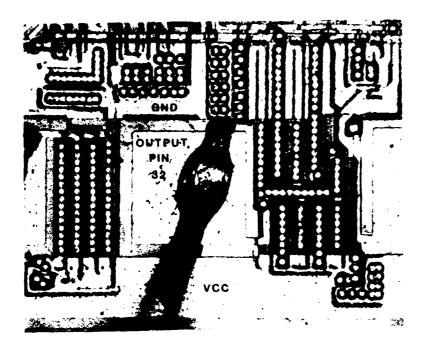


Figure V.H.7 - Pin 32 Output

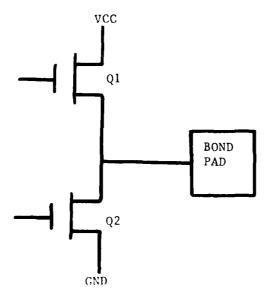
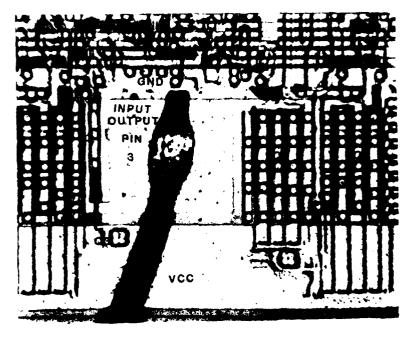


Figure V.H.8 - Output Schematic



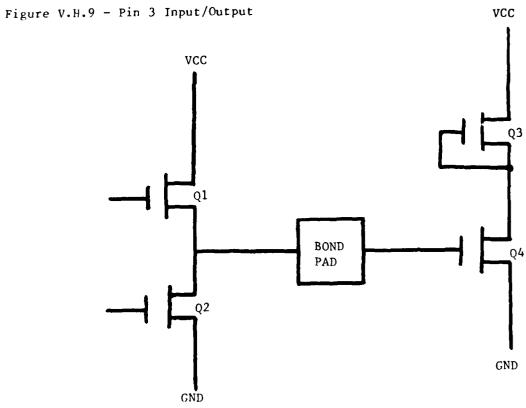


Figure V.H.10 - Input/Output Schematic



Figure V.H.11 - Transistor Cross-Section

```
- Mais Elimination におい
MARTIN MARTETTA APRICAPATE -- DENUTS II.II.
                           FILE UID :151
INITIAL TEST
                                               FROTED AT 25 DEG. C
UN 31 OCT NO AT 17:50 WITH THE 3260 TEST A
ig († Mol) 1000
Sjylmym – Saksjojam
                                    MEASUREI
         * 1 F E
                                    VALUE
    FIN AVERAGE OF SERIAL NUMBERS:
    1.1.2.3.5.5.7.0.9.10.11.12.13.14.15.10
                                              FUNCTION
                                                                    1.0006##
                  - - - - - 21
                                    1.319NA
          N\{i \, V
                                              INPUT
                                    503.1FA
                                             INPUT
                                                        -- --
                                                                    1.000#A
                   - - - - - 18
                                                                    1.000004
                                    540.8FA
                                              INPUT
          NEW
                     - - - - 19
                                   650.0FA
468.7FA
                                                                    1.000-4
                                              INPUT
                                                        - ~
          NEW
                  - - - - 22
- - - - - 23
                                                                    : . : > : > :
                                              INPUT
                                                        --
          NUU
          NEW
                                    871.9FA
                                              INPUT
                  - - - - - - - 31
                                                                    1.0000
                                    52a.5UC
                                                        --
          Nį[IŲ
                                              1/0
                                                        ---
          NEW
                                    1.056NA
                                              INPUT
                                                                    1.000000
                  - - - - - 24
- - - - - - 30
- - - - - 25
          N\Pi \vee
                                    1.050NF
                                              OUTPUT
                                                                    1.000664
                                                                    1.0000MA
1.000MA
          NIIU
                                    550.0UA
                                              1/0
                                    925.1FA
          NEW
                                              OUTPUT
                  - - - - - 26
                                                                    1.0 004
                                   803.1FA
                                              OUTPUT
                                                        - ~
          NTIU
                  - - - - - 28
- - - - - - 29
                                                                    1.09088
1.00988
          MEST
                                   815.8FA
                                              OUTPUT
          NTIL
                                    584,4FA
                                              TURTUO
                                                        ~ ~
                   - - - - - 32
          NEW
                                    791.3FA
                                              UUTPUT
                                                                    I. Alexand
                  - - - - - 27
                                    621.9FA
                                              OUTPUT
                                                        --
                                                                    1.00086
          NEW
                  - - - - - 34
                                                                    1.000
                                   803.1FA
                                              DUTPUT
                                                        --
          NEW
                  - - - - - 16
- - - - - - 15
                                                                    1.316#A
                                                        _ _
                                              1/0
          NEW
                                    200.084
                                              0\1
          NTI.
                                    759.48A
                                                        ---
                                                                    1.7
                                    834.4FA
                                              1/0
                                                        - -
          NIIV
                                                                    1.055.45
                  - - - - - 13
                                              1/0
          NIC
                                   659.4FA
                  - - - - - 12
- - - - - - 11
                                              1/0
                                    38.25NA
                                                        - --
          NIF
                                    637.CF4
                                              1/0
          NED
                   - - - - - 10
          NI
NI
                                    793.8FA
                                              1/0
                                                        -- --
                     -----
                                              I/0
                                                        ---
                                    618.8FA
                  - - - - - - 6
                                                                    1.300 55
                                              1/0
                                                        - -
          NIC
                                    753.1F4
          UBM
                                    800.0FA
                                              1/0
                                                                    1.00 -2
                                    643.884
                                              I/O
                                                                    : .
          41.0
                                    871.9FA
                                              1/0
                                                                    1000
                                    523.9F
521.8FA
                                              1/0
                                                                    ٠, ٠
                                                                    I/0
                                                        - -
          ٠. ٠
                                              1/0
          ~↓
                                    084.4F3
          ...
                                               1/0
                                                                        · ...
                         - - - -
- - -
                                               OUTPUT
                                                                        M.$.
                                38
                                    741.46
                                              DUTPUT
                                37
36
                         36 ...
                                              OUTPUT
                                              OUTPUT
          .
                                    1.0558
          . . .
                                    1. :000
                                                        - -
                                    7. - 7. Pro.
                                                                    : .
                                    3/
          . .
```

Figure V.H.12 - Average Leakage Currents at Initial Test

FILE UID :152 SERIAL NUMBER - VARIOUS TESTED AT 25 DEG. C INITIAL TEST UN 31 OCT 83 AT 13:50 WITH THE 3260 TEST SYSTEM MEASURED LIMITS TEST TYPE VALUE miwinum maximum FAIL PIN AVERAGE OF SERIAL NUMBERS: 1,1,2,3,5,6,7,8,9,10,11,12,13,14,15,16 1.097MA 1.000MA **** NTIUR NEIVE: 3.68804 1.000m NEWR 11.58UA 1.104MA NEWR 1.000mA 10.23NA 1.0000ma NEWR 5.925NA 1.000000 NTIVE NITUR 3.706NA 1.0000 NUVR 3.447NA 1.0000## 1.0000%4 NOVE 14.46NA 1.0000 mg NEWE 3.275MA NIVE 2.505NA NEWE 1.000rma 286.6NA 1.000 4.055NA NOUR 1. 19964 NEWE 3.034NA 1.00 NIFUR 2.813NA 1... Oma NITUR 58.61NA 1.0 000 MEVE 2.637NA 2.484NA 2.331NE 1.0000000 NEIVE NUVE 1.000MA 1.000mm NUVE 3.391NA NEWR 2.337NA 1.000086 2.655NA NEWE 1.0000## NTIVE 3.003NA 3.89"NA 1.000000 NEIVE 3.66°NA NEUE 1.55 ** หมีบลิ 3.441MA 1.70 304 NUUR 4.088NA

3.284NA

3.897KA 2.720NA

1.819NA

1.0 2354

1.0000000

1.50 00

Figure V.H.12 - Average Leakage Currents at Initial Test (Cont.)

NOVE

MOUR

NIFUR

NEWA

```
DARTIN MARIETTA ALEGSPACE -- DENDER (ID)SIDA -- CART E. . . . . . . .
                            FILE OID :: 15.1
LOITION TENT
                                                RESIDE WOMEN
ON 31 DEC 83 AT 14:08 WITH THE 3250 1887 PASTEM
          1651
                                    MEASURE !
         1.00
                                      12. m
TAIL
PIN
                                              FUNCTION
                                 21
                                               INPUT
          Set 10.
                                 17 846. F. V
                                                                           ٠.٠
                                               INPUT
          WE'S
                                 18 53.75 INPUL
                                 19 - 10 . 6 ...
          12[11]
                                              LNPUT
                                 22 INPUT 23 INPUT
          MING
          tile.
                                               INPUT
                                 31 214.13 I/O
33 T2000 INPUT
24 00 TPU
                   - - - - -
                                                                           سر.
          NEW
          *# ( . C
                                              INPUT
                                                                           ×.
          14100
                                               OUTPUT
                                 30 545. - ... 1/0
                                 25
                                 OUTPUI
          mi.
                                                                            ٠.
                                               OUTPUT
          ingles
Option
                                 28
                                               OUTPUT
                                                         - -
                                               CUTPUT
                                 32 725.76%
          (i_1,i_2,...)
                                               OUTPUT
                                 27 4.027 no
34 716.666
16 057.366
          \delta \in \mathcal{Q}
                                               OUTPUT
          MIN
                                                         . ..
                                                                           ~..
                                               OUTPUT
          315,00
                                               1/1)
                                 15 T29.9F 1
14 856.7FA
          arigo.
                                                                      I/D
                                                                      Ning
                                               1/0
                                                                           ~ .;,
          061
                     1/0
          1500
                      - - - -
                                 12 704,006
                                               1/0
                                11 100.0FM
10 703.88
          of V
                                               1/0
          diffu
                                               1/0
                                     14000
                                                                          1.5
                                               1/0
                                 8
7
                   _ . . . . _ _
          N for I
                                     700,00
                                               1/0
                                                                     _ _ _ _ _ _
                                     910.564
755.666
          -. GO
                                               1/0
          MED
                                               1/0
                                    836. TPA
          NUU
                                 5
                                               1/0
                                   853.3FA
          si(ii)
                                                                           ۹.4
                                               1/0
          43500
                                 3
                                    . हे १४. ४१०
                                                                           ٠.
                                               1/0
          بين] نج
                                    STO OFF
                                               1/0
                                 39 75A.7F.
          1100
                                               1/0
                                                                           100
                                 38 750.444
          #IDO
                                               OUTPUT
                                                                           •,4
                   _ _ _ _ _ _ _ _
          24700
                                 37 -413.3FA
                                               OUTPUT
          NUU
                                 36 Tan. THA
                                               DUTPUT
                                                                      1000
                                                                      35 555. PA
          NOV
                                              OUTPUT
          MINSE
                                     3.06766
                                                                     4 - 6 - 5
                   _ - - - - -
          \mathcal{H}[\mathcal{O}] \in
                                     2.140MA
          PDUR
                                     1.81.00
                                                                      1.03000
                                     1.00700
                                                                      1.0000
          \partial (\Gamma \partial_{z} (F)
                                     1.01 204
                                                                      Acres 100 May
```

Figure V.H.12 - Average Leakage Currents at Initial Test (Cont.)

 $\Omega[[0] \Omega]$

FILE UID :152 SERIAL NUMBER - VARIOUS

TESTED AT 25 DEG. C INITIAL TEST ON 31 DOT 83 AT 14:08 WITH THE 3260 TEST SYSTEM

	TEST	MEASURED	LIMI	T S
FAIL	TYFE	VALUE	MINIMUM	MAXIMUM

Fin Average of Serial Numbers: 17,18,19,20,21,22,23,24,25,26,27,28,29,30,31

****	NEWE		1.024MA		1.000ma
	NEWE		1.810NA		1.000MA
	NEUR		141.0UA		1.000MA
****	NLUR		1.024MA		1.000MA
	NEWS		7.766UA		1.000mA
	NOUP		2.9280A		1.000MA
	NOUR		1.063UA		1,000mA
	NEWR		875.2NA		1.000MA
	MOVE		24.70NA		1.000MA
	NEWE		1,213UA		1.000MA
	410,5		255.9NA		1.000MA
	NEWF		2.383UA		1.000mA
	24 [15 €		671.2NA		1.000mm
	455 F		484.4HA		1.000mA
	1,71,36		371,4NA		AMCOOLI
	A TOTAL		1.511UA		1.000ma
	NOUR		150.3NA		1.000MA
	NOVE		128.7NA		1.000MA
	MOUN		143.7NA		1.000MA
	NUMB		114.5NA		1.000ma
	NEILE		95.47NA	~-	1.000MA
	MOVE		105.6NA		1.000MA
	res s		198.4NA		1.000MA
	42		251.3NA	~-	1.000MA
	*1100 B		173.1NA	~ -	1.000MA
	2.11C as		125.4NA		1.000ma
	44.50		323.8NA		1.000%
	માં,લ, હ	<u>.</u>	140.8NA		1. ODOMA
	• 1		319.3NA		1.000mm
	NIO.15		351.0NA		Lightina
	NDUR	- -	3.633NA		1.000MA

Figure V.H.12 - Average Leakage Currents at Initial Test (Cont.)

MARTIN MARIETTA AEROSPACE -- DENVER DIVISION -- PARTS EVALUATION LAB

FILE UID :152 SERIAL NUMBER - VARIOUS TESTED AT 25 DEG. C N2250V STRESS ON 13 DEC 83 AT 06:28 WITH THE 3260 TEST SYSTEM

	TEST	MEASURED	LI	M I	TS	
FAIL	TYPE	VALUE	MUMINIM		MAXIMUM	

FIN AVERAGE OF SERIAL NUMBERS: 3,4,5,6,7,8,9,10,11,12,13,14,15,16

		PIN	FUNCTION		
NDU		21 29.95NA	INPUT		1.000MA
NEU		21 29.95NA 17 19.48NA	INPUT		1.000MA
NDV		18 13.94NA	INPUT		1.000MA
NIIV		19 14.90NA	INPUT		1.000MA
VIIV		22 11.18NA	INPUT		1.000MA
NDV		23 6.446NA	INPUT		1.000MA
NDV		31 526.1UA	1/0		1.000MA
NDV		33 7.332NA	INPUT		1.000MA
NDV		24 2.114NA	OUTPUT		1.000MA
NDU		30 548.6UA	1/0		1.000MA
NDV		25 2.011NA	OUTPUT		1.000MA
NDV		26 2.057NA	OUTPUT	- -	1.000MA
NDU		28 1.839NA	UUTPUT		1.000MA
NDV		29 1.989NA	OUTPUT		1.000MA
VON		32 16.55NA	OUTPUT		1.000MA
NDV		27 1.914NA	OUTPUT		1.000MA
VQN		34 1.843NA	OUTPUT		1.000MA
NDV		16 3.171NA	1/0		1.000MA
NDV		15 2.171NA	1/0		1.000MA
שמא		14 1.807NA	1/0		1.000MA
NDV		13 1.968NA	1/0		1.000MA
NDV		12 2.429NA	I/O		1.000MA
NDV		11 1.950NA	1/0		1.000MA
NDV		10 1.879NA	I/O		1.000MA
NDV		9 1.786NA	1/0		1.000MA
NDV		8 1.914NA	1/0		1.000MA
NDV		7 1.739NA	1/0		1.000MA
NDV		6 1.954NA	1/0		1.000MA
NIIV		5 1.804NA	I/O		1.000MA
NDV		4 1.907NA	1/0		1.000MA
NDV		3 1.907NA	1/0		1.000MA
NDV		2 1.839NA	1/0		1.000MA
VOV		39 1.964NA	1/0		1.000MA
NDU		38 1.714NA	OUTPUT		1.000MA
NDV		37 2.046NA	OUTPUT		1.000MA
NDV		36 1.743NA	OUTPUT		1.000MA
NDV		35 1.725NA	OUTPUT		1.000MA
NDUR		127.2NA			1.000MA
NDVR		128.1NA			1.000MA
NDVR		50.62NA			1.000MA
NDVR	-	51.59NA			1.000MA
NDUR		54.05NA			1.000MA
NDVR		23.60NA			1.000MA

Figure V.H.13 - Average Leakage Currents after -2250 volts

FILE UID :152 SERIAL NUMBER - VARIOUS
1ESTED AT 25 DEG. C N2250V STRESS
ON 17 DEC 87 AT 04:38 HITH THE 7240 TEST SYSTEM

FA1L	TEST TYPE	 						MEASURED VALUE	L I M I MINIHUM	T S MAXIMUM
	N AVERAGE 4,5,6,7,8									
***	NDUR	_	_	_		_	_	1.024MA		1.000M
~ ~ ~ ~	NDVR	_	_	_	_	_	_	30.95NA		1.000M
	NDVR	_	_	_	_	_	-	10.77UA		1.000M
***	NUVR	_	_	_	_	_	_	1.024MA		1.000M
	NDVR	_	_	_	_	_	_	10.72NA		1.000M
	NDVR	_	-	-	_	_	-	8.771NA		1.000M
	NDVR	-	_	_	_	-	-	7.846NA		1.000M
	NDVR	_	-	_	_	_	-	7.621NA		1.000M
	NDVR	_	-	-	_	-	-	150.6NA		1.000M
	NDVR	-	-	-	_	_	-	7.707NA		1.000M
	NDVR	-	-	-	_	-	-	7.107NA		1.000M
	NDUR	_	_	-	_	_	-	15.76NA		1.000M
	NDVR	-	-	-	_	-	-	9.971NA		1.000M
	NDVR	-	-	-	-	-	-	7.707NA		1.000M
	NDUR	-	-	-	-	_	-	7.307NA		1.000M
	NDVR	-	_	_	-	-	-	9.196NA		1.000M
	NDUR	-	-	-	-	-	-	7.454NA		1.000M
	NDVR	-	-	_	-	-	-	7.039NA		1.000M
	NDVR	-	-	-	-	-	-	7.211NA		1.000M
	NDVR	_	-	-	-	-	-	7.643NA		1.000H
	NDUR	-	-	_	-	-	-	7.164NA		1.000M
	NDVR	-	-	-	-	-	-	7.168NA		1.000M
	NDVR	-	-	-	-	-	-	7.386NA		1.000M
	NDVR	-	-	-	-	-	-	7.886NA		1.000M
	NDVR	-	-	-	-	-	-	7.689NA		1.000M
	NDUR		-	-	-	-	-	7.771NA		1.000M
	NDVR	-	-	-	-	-	-	7.904NA		1.000M
	NDVR	-	-	-	-	-	-	7.664NA		1.000M
	NDVR	-	-	-	-	-	-	8.014NA		1.000M
	NDUR	-	-	-	-	-	-	7.268NA		1.000M
	NDVR	_	_	_	_	_	_	6.843NA		1.000M

Figure V.H.13 - Average Leakage Currents after -2250 volts (cont.)

MARTIN MARIETTA AEROSPACE -- DENVER DIVISION -- PARTS EVALUATION LAB

FILE UID :152 SERIAL NUMBER - VARIOUS TESTED AT 25 DEG. C N2250V STRESS ON 13 DEC 83 AT 06:33 WITH THE 3260 TEST SYSTEM

	TEST	MEASURED	LIMI	T S
FAIL	TYPE	VALUE	MUMINIM	MAXIMUM
			· · · · · · · · · · · · · · · · · · ·	_

PIN AVERAGE OF SERIAL NUMBERS: 17,18,19,20,21,22,23,24,26,27,28,29,30

			PIN	FUNCTION	
	NBV		21 847.1UA	INPUT	 1.000MA
	NDV		17 420.4NA	INPUT	 1.000MA
	UDU		18 150.4NA	INPUT	 1.000MA
	NDV		19 74.77NA	INPUT	 1.000MA
	NDV		22 315.4UA	INPUT	 1.000MA
	NDV		23 389.2NA	INPUT	 1.000MA
	NDV		31 525.2UA	1/0	 1.000MA
	NDU		33 381.5UA	INPUT	 1.000MA
	NDV		24 1.938NA	OUTPUT	 1.000MA
	NDV		30 550.3UA	1/0	 1.000MA
	NDV		25 1.512NA	OLITPUT	 1.000MA
	NDV		26 1.519NA	CUTPUT	 1.000MA
	VDV		28 1.596NA	UUTPUT	 1.000MA
	NDV		29 1.492NA	OUTPUT	 1.000MA
***	NDV		32 1.024MA	OUTPU	 1.000MA
	NDV		27 5.612NA	OUTPUT	 1.000MA
	NDU		34 1.496NA	OUTPUT	 1.000MA
	NDV		16 195.3NA	I/O,	 1.000MA
	NDV		15 1.581NA	1/0	 1.000MA
	NDV		14 78,73UA	1/0	 1.000MA
	NDV		13 1.592NA	1/0	 1.000MA
	NDU		12 250.9NA	1/0	 1.000MA
	NDV		11 1.542NA	I/O	 1.000MA
	NDU		10 1.53BNA	1/0	 1.000MA
	NIIV		9 1.496NA	1/0	 1.000MA
	NDV		8 1.496NA	1/0	 1.000MA
	NDV		7 1.542NA	1/0	 1.000MA
	NDV		6 1.519NA	1/0	 1.000MA
***	NDV		5 1.024MA	1/0	 1.000MA
	NDV		4 1.665NA	1/0	 1.000MA
	NDV		3 1.635NA	1/0	 1.000MA
	NDV		2 1.550NA	1/0	 1.000MA
	NDV		39 1.581NA	1/0	 1.000MA
	NDV		38 1.438NA	OUTPUT	 1.000MA
	NDV		37 1.662NA	OLITPUT	 1.000MA
	NDU		36 1.400NA	CUTPUT	 1.000MA
	NDV		35 1.331NA	OUTPUT	 1.000MA
****	NDVR		1.024MA		 1.000MA
***	NDUR		2.309UA		 1.000MA
	NDVR		685.2NA		 1.000MA
	NDVR		267.7NA		 1.000MA
	NDUR		319.4UA		 1.000MA
	NDVR		3.567UA		 1.000MA
			3.30,04		_ T V V V I I I

Figure V.H.13 - Average Leakage Currents after -2250 volts (cont.)

FILE UID :152 SERIAL NUMBER - VARIOUS TESTED AT 25 DEG. C N2250V STRESS ON 13 DEC 83 AT 06:33 WITH THE 3260 TEST SYSTEM MEASURED LIMITS TEST MUNIMUM MAXIMUM VALUE FAIL TYPE PIN AVERAGE OF SERIAL NUMBERS: 17,18,19,20,21,22,23,24,26,27,28,29,30 1.000MA *** NDUR 1.024MA NUVR 1.000HA 552.0UA 143.0UA 1.000MA NDUR *** NDVR 1.024MA 1.000MA NDVR 29.47NA 1.000MA 1.000HA NDUR 1.777UA 1.000MA NDUR 531.0NA NDVR 435.5NA 1.000MA 1.000MA NDUR 1.024MA **** 1.000MA NDUR 775.6NA 1.000MA NDUR 142.5NA NDVR 838.1NA 1.000MA NDVR 311.1NA 1.000MA NDVR 78.97UA 1.000MA NDVR 183.2NA 1.000MA NDVR 439.2NA 1.000MA NDVR 70.73NA 1.000MA NDVR 61.20NA 1.000MA NDUR 68.30NA 1.000MA NDVR 54.71NA 1.000MA NDVR 1.000MA 45.88NA 1.000MA NDUR 51.34NA 1.000MA NDVR *** 1.024MA NDVR 125.7NA 1.000MA NDVR 83.56NA 1.000MA NDUR 62.52NA 1.000HA NDVR 163.8NA 1.000MA NDVR 1.000HA 73.62NA -----1.000MA 172.8NA NDUR

NDVR

NDVR

Figure V.H.13 - Average Leakage Currents after -2250 volts (cont.)

186.0NA

6.427NA

1.000MA

1.000MA

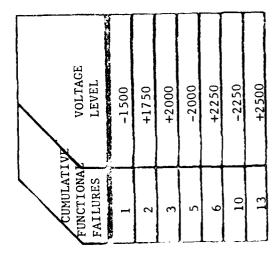


Figure V.H.14 - CD Stress, Functional Failure Summary

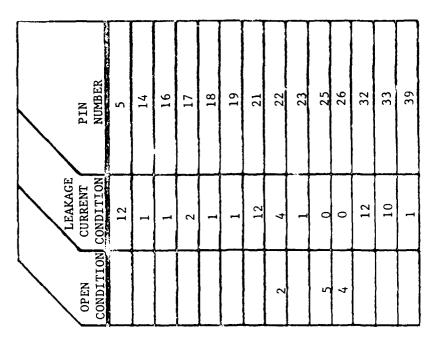


Figure V.H.15 - CD Stress, Failure Summary, Post + 2500 Volt Stress

MARTIN MARIETTA AEROSPACE -- DENUER DIVISION -- PARTS EVALUATION LAB

FAIL	TEST TYPE								MEASURE!	0	L I M MINIMUM	
911	N AVERAGE											
17,	, 18, 19, 20	. Or 1, 21	, 2	2,	23 M	L . 2	4.2	755K	5: 7,28,29,3			
						-	~,		.,,,.	•		
								PIN		FUNCTION	ī	
	NDU	-	-	-	-	-	-	11	859.5UA	INPUT		1.000MA
	NDU	-	-	-	-	-	-		71.81UA	trent		1.000M
	NDU	-	-	-	-	-	-	18	19.09UA	INPUT		1.000MA
	NDU	-	-	-	~	-	-		9.083UA	INPUT		1.000M
	NDU	-	-	-	-	-	-	22	315.6UA	INPUT		1.000MA
	NDU	_	-	-	-	-	_	23	4.611UA	INPUT		1.000MA
	NDU	-	-	-	-	-	-	31	527.3UA	1/0		1.800MA
	NDU	-	-	-	-	-	_	33	647.5UA	INPUT		1.000MA
	NDU	-	-	-	-	-	-	24	2.012NA	OUTPUT		1.000MA
	NDV	-	-	-	-	-	-	30	552.5UA	1/0		1.000MA
	NDU	-	-	-	~	-	-	25	1.592NA	OUTPUT		1.800MA
	NDU	-	-	-	-	-	-	26	1.400NA	OUTPUT		1.800MA
	NDU	-	-	-	-	-	-	28	1.600NA	DUTPUT		1.800MA
	NDU	-	-	-	-	-	_	29	1.492NA	OUTPUT		1.800MA
***	NDU	-	-	-	-	-	_	32	1.024MA	OUTPUT		1.880MA
	NDU	-	-	-	~	-	-	27	5.446NA	OUTPUT		1.800MA
	NDU	-	-	-	-	-	_	34	1.519NA	OUTPUT		1.800MA
	NDU	-	-	-	-	-	_	16	188.4NA	1/0		1.800MA
	NDU	-	-	-	-	-	_	15	1.44ZNA	1/0		1.000MA
	NDU	_	_	-	~	-	_	14	68.92UA	1/0		
	NDU	-	-	-	~	_	_	13	1.492NA	1/0		1.880MA
	NDU	_	-	-	~	_	-	12	249.8NA	1/0		1.998MA
	NDU	_	_	_	-	_	_	11	1.565NA	1/0		1.000MA
	NDU	_	_	_	-	_	_	-	1.481NA	1/0		1.000MA
	NDU	_	_	_	_	_	_	ĝ	1.469NA	1/0		1.900MA
	NDU	_	_	_	~	_	_	_	1.519NA	1/0		1.000MA
	NDU	_	_	_	_	_	_		1.519NA	1/0		1.000MA
	NDU		_	_	-				1 560NA	1/0		1.000MA

	NDU	 _	_						
		 _	_	-	-	13	1.492NA	1/0	 1.888MA
	NDU	 -	-	-	-	12	249.0NA	1/0	 1.000MA
	NDU	 -	-	-	_	11	1.565NA	1/0	 1.000MA
	NDU	 _	-	_	_	10	1.481NA	1/0	
	NDU	 _	_	_	_	Ģ	1.469NA	1/0	 1.800MA
	NDU	 _	_	_	_	g			 1. 00 0MA
	NDU	 _	_	_	_		1.519NA	1/0	 1.800MA
		 -	-	-	_	7	1.508NA	1/0	 1.000MA
	NDU	 -	~	_	-	6	1.369NA	I/O	 1.800MA
本本本本	NDU	 -	~	-	-	5	1.024MA	1/0	 1.888MA
	NDU	 -	-	-	-	4	1.681NA	1/0	 1.600MA
	NDU	 _	~	_	_	3	1.558NA	1/0	
	NDU	 _		_	_	2	1.581NA	1/0	1.800MA
	NDU	 _	_	Ξ	Ξ	-			 1.000MA
	NDU		_	_	_	39	78.73UA	I/O	 1.600MA
	-	 -	~	-	-	38	1.535NA	OUTPUT	 1.000MA
	NDU	 -	~	-	-	37	1.577NA	OUTPUT	 1.888MA
	NDU	 -	-	-	-	36	1.450NA	OUTPUT	 1.800MA
	NDU	 -	-	-	_	35	1.377NA	OUTPUT	
								001101	 1. 800 MA
***	NDUR	 _	_	_	_		1 03444		
	NDUR	 _	_		_		1.824MA		 1.800MA
	MOUR	 -	-	-	_		89.58UA		 1.000MA

Figure V.H.16 - CD Stress, Leakage Current Averages After the +2500 Volt Stress

79.32UA 25.38UA

319.3UA

12.61UA

NDUR

NDUR

NDUR

NDUR

1.888MA

1.888MA

1.000MA

1.000MA

1.000MA

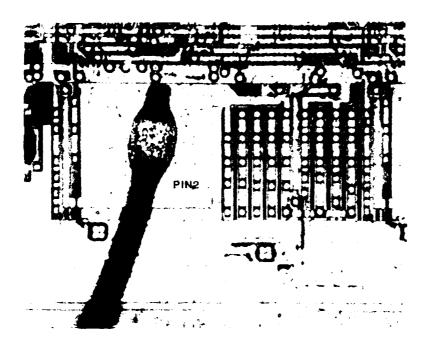


Figure V.H.17 - Pin 2 Input/Output

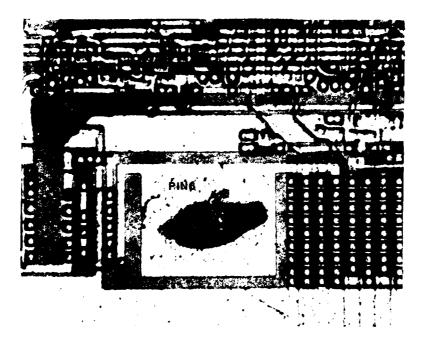


Figure V.H.18 - Pin 6 Input/Output

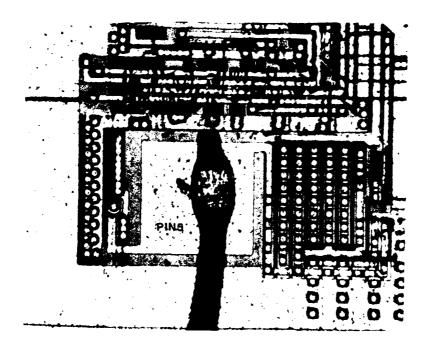


Figure V.H.19 - Pin 5 Input/Output

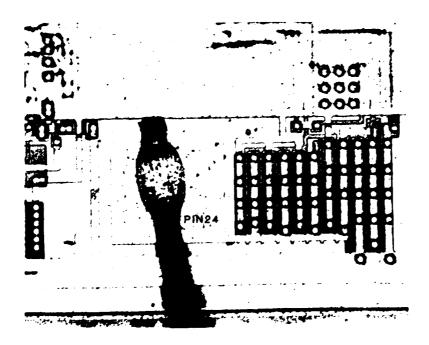


Figure V.H.20 - Pin 24 Output

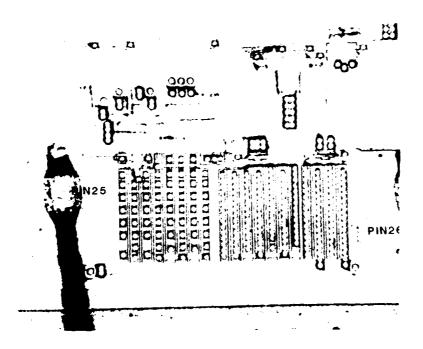


Figure V.F 21 - Output Pin 25 and 26

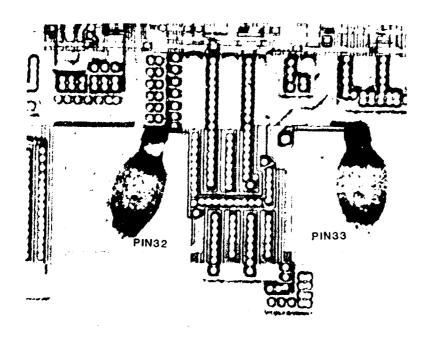


Figure V.H.22 - Output Pin 32 and Input Pin 33

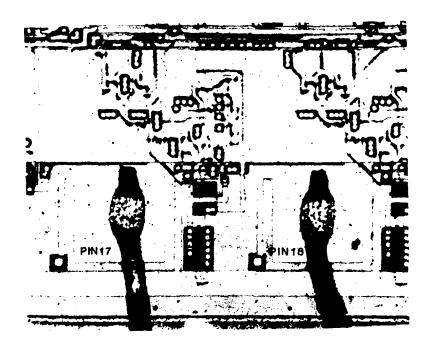


Figure V.H.23 - Input Pins 17 and 18

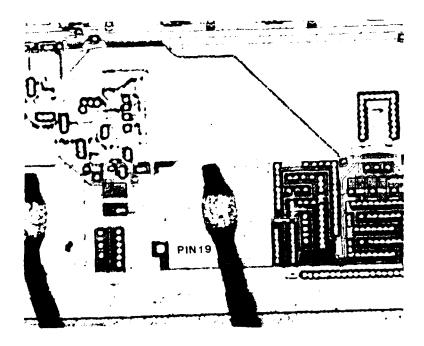


Figure V.H.24 - Pin 19 Input

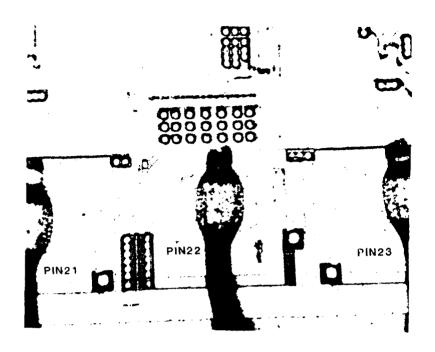


Figure V.H.25 - Pin 21, 22 and 23 Inputs

1.1

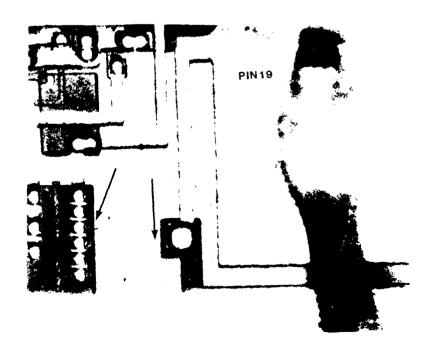


Figure V.H.26 - CD Stress, Electrical Damage from Pin 19 to Ground

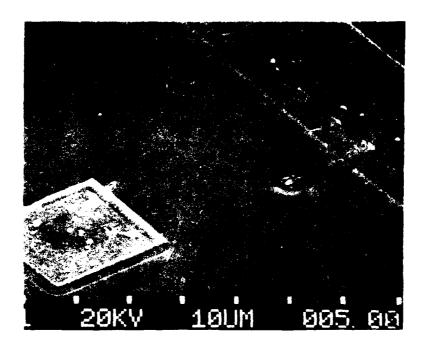


Figure V.H.27 - CD Stress, SEM Micrograph of Pin 19 Damage

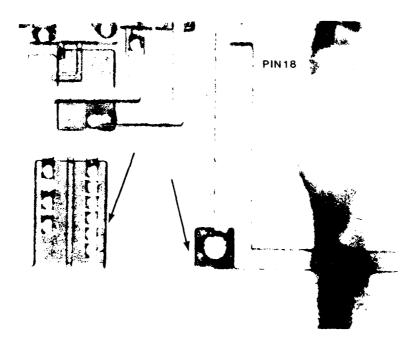


Figure V.H.28 - CD Stress, Pin 18 Degradation

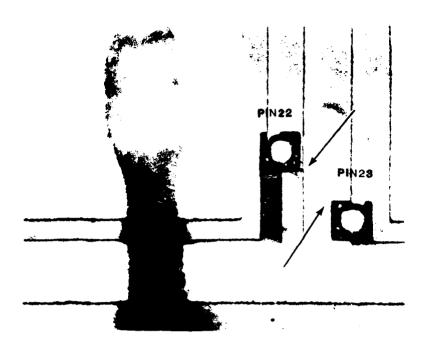


Figure V.P.29 - CD Stress, Pin 22 and Pin 23 Degradation

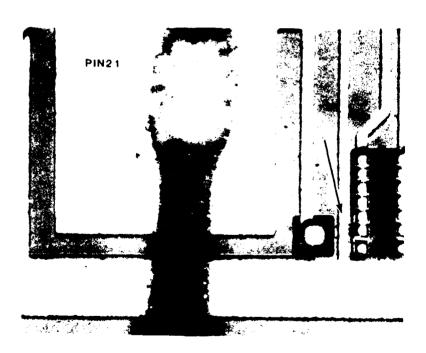


Figure V.H.30 - CD Stress, Pin 21 Damage

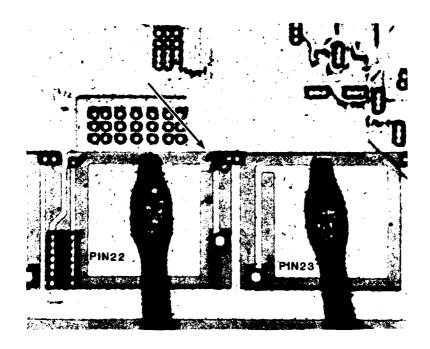


Figure V.H.31 - CD Stress, Open Metallization on Pin 22

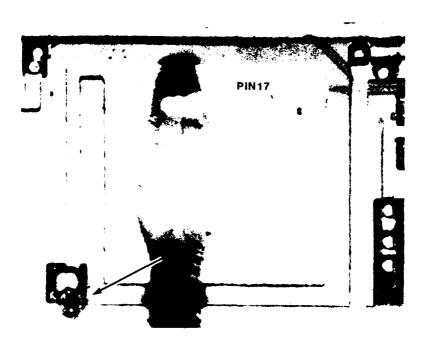


Figure V.H.32 - CD Stress, Pin 17 Shorted to Ground

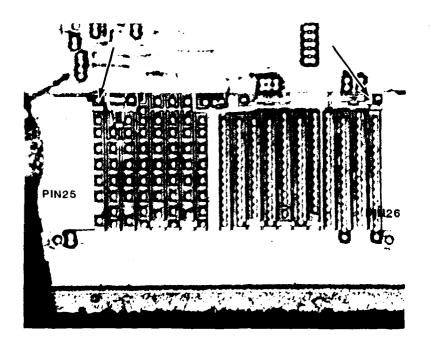


Figure V.H.33 - CD Stress, Opens on Pins 25 and 26

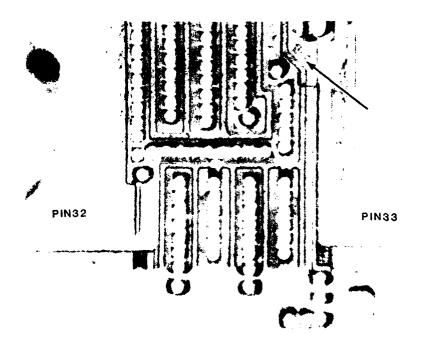


Figure V.H.34 - CD Stress, Damage Between Pins 32 and 33

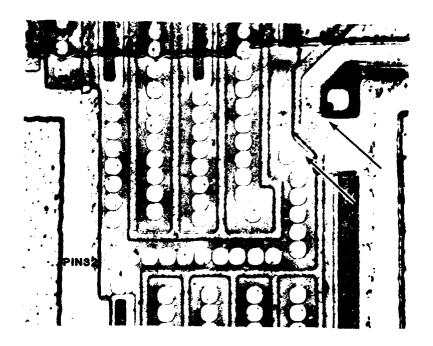


Figure V.H.35 - CD Stress, Same View as Previous Photo with Aluminum Stripped

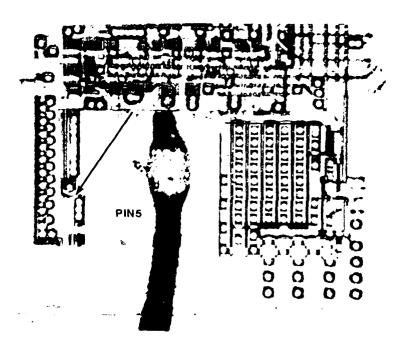


Figure V.H.36 - CD Stress, Pin 5 with Arrow Indicating

Location of Damage Site

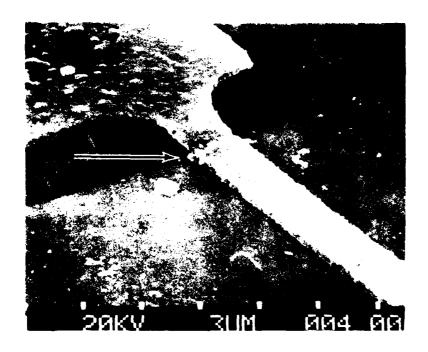


Figure V.H.37 - CD Stress, Pin 5 Polysilicon Breakdown Site

MARTIN MARIETTA AEROSPACE -- DENVER DIVISION -- PARTS EVALUATION LAB

TEST	MEASURED	LIMITS
FAIL TYPE	VALUE	MINIMUM MAXIMUM

PIN AVERAGE OF SERIAL NUMBERS: 3,4,5,6,7,8,9,12,13,14,15,16

		PIN		FUNCTION	
NUV		- 24	908.7UA		 1.000MA
NDV		- 21 - 17	113.7NA	INPUT	 1.000MA
NDV		- 18	186.7NA	INPUT	 1.000MA
NDU		- 19	52.45NA	INPUT	 1.000MA
NDV		- 22	3.697UA	INPUT	 1.000MA
NDV		- 23	3.067UA	INPUT	 1.000MA
NDV		- 31	525.6UA	1/0	 1.000MA
NDV		- 33	1.152UA	INPUT	 1.000MA
NDU		- 24	1.554NA	OUTPUT	 1.000MA
NDV		- 30	547.7UA	1/0	 1.000MA
NDV		- 25	1.404NA	OUTPUT	 1.000MA
NDU		- 26	1.192NA	OUTPUT	 1.000MA
NDU		- 28	1.367NA	OUTPUT	 1.000MA
NDV		- 29	1.108NA	OUTPUT	 1.000MA
NDV		- 32	92.51UA	OUTPUT	 1.000MA
NBV		- 27	1.258NA	OUTPUT	 1.000MA
NDV		- 34	6.387NA	UUTPUT	 1.000MA
NDV		- 16	18.50NA	1/0	 1.000MA
NDU	_`	- 15	25.20NA	1/0	 1.000MA
NDV		- 14	1.263NA	1/0	 1.000MA
NDV		- 13	1.225NA	I/Ó	 1.000MA
NDV		- 12	1.800NA	1/0	 1.000MA
NDV		- 11	1.288NA	1/0	 1.000MA
NBV		- 10	1.188NA	1/0	 1.000MA
NDU		- 9	1.225NA	1/0	 1.000MA
NDU		- 8	1.154NA	1/0	 1.000MA
NDV		- 7	1.208NA	1/0	 1.000MA
NDV		- 6	1.233NA	1/0	 1.000MA
NDV		- 5	1.229NA	1/8	 1.000MA
NDV		- 4	1.263NA	1/0	 1.000MA
NDV	~	- 3	1.254NA	1/0	 1.000MA
NDV		- 3	1.279NA	1/0	 1.000MA
NDV		- 39	1.421NA	1/0	 1.000MA
NDV		- 38	1.292NA	OUTPUT	 1.000MA
NDV		- 37	1.350NA	OUTPUT	 1.000MA
NDU		- 36	1.154NA	DUTPUT	 1.000MA
NDV		- 35	1.108NA	ÖÜTPÜT	 1.000MA
NDUR		_	999.9UA		 1.000MA
NDVR		_	457.5NA		 1.000MA
NDVR		-	1.324UA		 1.000MA
NDVR		_	234.7NA		 1.000MA
NDUR		-	53.52UA		 1.000MA
NDVR		-	48.97UA		 1.000MA

Figure V.H.38 - HBD Stress, Leakage Current Averages After the +5000 Volt Stress

LEAKAGE CURRENT	PIN NUMBER
13	21
6	22
5	23
5	32
2	33

Figure V.H.39 - HBD Stress, Leakage Current Failure Summary

(13 Parts Total)

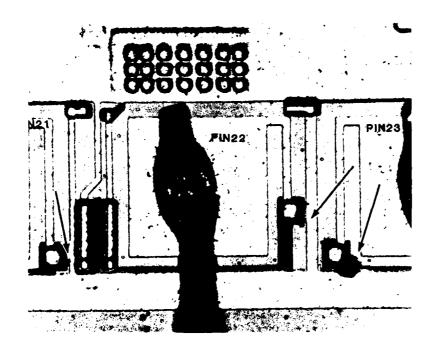


Figure V.H.40 - HBD Stress, Damage on Pins 21, 22, and 23

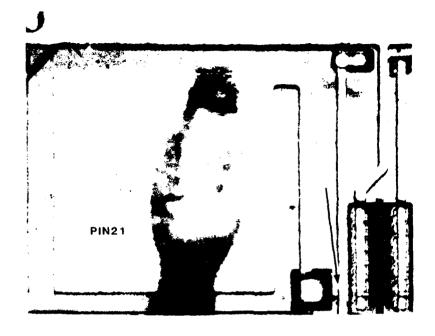


Figure V.H.41 - HBD Stress, Damage on Pin 21

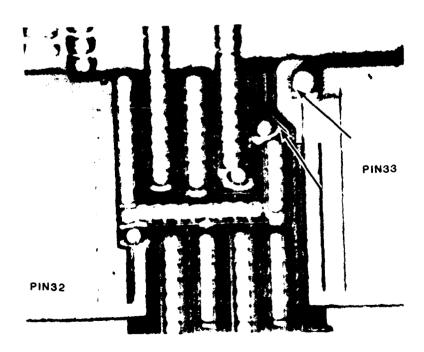


Figure V.H.42 - HBD Stress, Damage on Pins 32 and 33

A wide variation in the effectivenesss of protection schemes was experienced during this study. Analysis of the variations within each group of devices was included in the previous section. This section will discuss the variations between groups, the effect of reduction in dimensions, and recommendations for modifications or improvements.

Figure VI-1 shows the voltage range at which parts were removed from test for all eight groups of devices and for both types of stress. Examination of this figure reveals a number of conditions. With the exception of Part D, parts always failed at a lower level for the charged device model. There was not always the same relationship between the level of the charged device failures and the human body failures. The two groups which had the best tolerance to the HBD stress did have the best tolerance to the CD stress, however, the other parts did not follow this pattern. Part G was very sensitive to the CD stress but was relatively high in tolerance to the human body stress. This is due to the significant effect of the package size on the CD stress. The Part G devices were in the largest package and had the highest capacitance to ground. This created a much higher stress for the same voltage level.

A more quantitative display of the data in the above figure is provided in Figures VI-2 through VI-8. These figures show comparisons of the cumulative failures by manufacturer, by technology, and by functional type.

One manufacturer had two device types in this study. These were Part E and Part H and are shown in Figure VI-2. Similar trends are shown for both devices with the Part H being the more tolerant. These were the two best protection networks found in this study. The major difference was a polysilicon pad between the bond pad metallization and the diffused resistor on Part H. This reduced the development of leakage current. The basic layout was a diffused n-type resistor connected to a thin oxide transistor which had its gate and source connected to ground. The low sensitivity was due to the lack of a return current path due to the resistor being in a diffusion connected to substrate (internal connection only). Note that all devices did not fail during the human body model testing.

Figure VI-3 shows the summary for the four NMOS devices. This includes the devices shown in Figure VI-2 and also Part G and Part B. The four NMOS devices have substrate bias generators and diffused input protect resistors. These resistors measure 650 ohms for Part B, 550 ohms for Part E, 900 ohms for Part G, and 700 ohms for Part H. Part B has the most elaborate input protect network and includes a thick oxide metal gate transistor to VCC or VSS, and a field plate diode to the substrate. Part G failed at a lower level for the charged device model than Part B but Part B is still the weakest NMOS protection system as shown by the human body model. Part B received a lower stress for the charged device model than Part G for the physical reasons discussed previously.

Part E has a thin oxide polysilicon transistor to VSS and Part G and H have thin oxide polysilicon transistors to ground (VSS and ground are essentially the same). Part G and Part H have polysilicon interfaces between the bond pad metallization and the diffused resistor. There is a major difference in this polysilicon interface that makes Part H less susceptible to damage. The polysilicon on Part G is like a resistor between the diffusion and the metallization and tends to fail open. The polysilicon on Part H is sandwiched between the metallization and the diffused resistor contact and does not fail open. This figure shows a wide range of sensitivity and it indicates the type of protection which should be used. The thin oxide field plate on Part B should be removed and the distance between the source and drain on the thick oxide transistor should be increased. This increase would create a situation similar to that seen on the less sensitive inputs on Part H. The gate appears to provide no benefit since if it were removed the input would be more similar to the less sensitive Part H or Part E.

Figure VI-4 shows the cumulative failures for the two microprocessors. These were discussed in the last section.

Figure VI-5 shows the cumulative failures for the two CMOS devices. It is evident that these parts did prorly in the sensitivity testing. Both devices utilized polysilicon input resistors which created a weak system. In addition Part F had numerous different layouts and aluminum/polysilicon crossovers. Polysilicon resistors are not recommended for complex circuit input networks.

Figure VI-6 shows the cumulative failures for the two low power Schottky devices. Part D is more tolerant to stress and it appears that this is size related. The Schottky diode was much larger on Part D and consequently it was not as sensitive to stress. For the human body model the base-collector junction failed on Part D before the Schottky junction. This produced the higher voltage levels seen in Figure VI-6 for the human body stress. The charged device stress produced failure in the Schottky junction on both devices but Part D failed at a higher level. The recommendations for Schottky technology devices include increasing the size of the Schottky contact and/or placing the input base-collector junction between the input contact and the Schottky reverse bias protection diode.

Figure VI-7 shows the cumulative failures for the two RAM, I/O, Timers. Part A is CMOS and Part E is NMOS. The CMOS had the polysilicon input resistors and was sensitive to stress.

Figure VI-8 shows the cumulative failures for the two RAMs. Part F had the polysilicon input resistors and Part B had the close spaced thick oxide transistor and the field plate diode. The sensitivity variations are due to reasons previously discussed.

A number of the conventional schemes that are available have been seen on the devices in this study. The literature search found a number of other possibilities which are summarized below: 1. "Multiple I/O Protection with Single Protective Device" S. Chen, S. Park, R. Wong, IBM Tech. Disclosure Bulletin; September 1980.

Rather than conventional protection devices on each input, this article discusses using a depletion or enhancement transfer device on each input with their gates tied back to a common protective device.

 "Voltage Programmable Protect Circuit" C. Hoffman and F. Wiedman, IBM Tech. Disclosure Bulletin, March 1980.

A protect circuit is described for an electrically programmable read-only memory which allows a high voltage to be placed on a pin for programming, but limits the voltage level at that pin during normal usage by a protect diode with a gate over it to allow reverse bias breakdown voltage control.

3. "Floating Plate Protective Device" Y. S. Huang, IBM Tech. Disclosure Bulletin, April 1977.

This article discusses a floating capacitor design which has a large capacitor above a diffusion which is connected to the input metallization. Via a second diffusion this capacitor is normally isolated but if an excessive voltage is present on an input then the capacitor is connected into the circuit and absorbs the extra charge.

4. "Voltage Breakdown Characteristics of Close Spaced Aluminum Arc Gap Structures on Oxidized Silicon" F. Hickernell and J. Crawford, Reliability Physics Symposium 1977.

Arc gap structures were investigated as possible input protection networks. They have the advantage of being a nondestructive voltage limiting structure that can limit the voltage to 300 to 400 volts.

These ideas are a few that are being or have been considered for device protection against transients.

Additional ideas that could improve protection networks and be compatible with VLSI processing have been thought of during this work. Two of these are tungsten contact to the silicon and a deep insulator grown around the input protect resistor.

The tungsten contact would alleviate the aluminum silicon interdiffusion problem by acting as a barrier similar to the polysilicon interface. It should have less of a tendency to open with stress. It can also be useful in the remainder of the circuit by being the barrier contact to shallow source and drain diffusions and it can be selectively deposited on the polysilicon to reduce the effective resistance. This idea seems practical and could provide improved circuit performance as well as decreased sensitivity to stress.

A deep insulator grown on either side of the input resistor would force the current to flow through the diffused resistor or break down the junction in the bulk. This should provide an input that protects the sensitive gates as well as not degrading itself due to this stress.

The sections for each of the eight devices discussed the ESD sensitivity variations for the various pins on a given part. The preceding section discussed the sensitivity variations between the different groups. The following will discuss the variations by physical characteristics. These physical characteristics include, conductor cross-sectional area, junction area, dielectric thickness, conductor spacing, junction electrical breakdown characteristics, overall device layout, physical construction and packaging.

These physical characteristics are discussed here and are related to the failures which occurred.

Conductor cross-sectional area was seen to be a problem on devices with polysilicon input resistors. These were devices A, F, and G. This was a significant failure mode on Part Types A and G. Part Type A has a polysilicon cross-sectional area of 1.6 microns squared and Part Type G has a polysilicon cross-sectional area of 2.2 microns squared. The average voltage failure level for the human body simulation stress was about twice as high on Part Type G as on Part Type A. There were oth failure modes involved on both parts but the relationship between the voltage failure level and the cross-sectional area of the polysilicon does appear to be significant. For the charged device testing other factors override this one, eg. package size.

Junction area was significant on the two Schottky devices. It is not considered to be the significant factor in the other device failures, however, the spacing and shape of the diffusions were shown to be significant as discussed in-depth previously. The significance is again evident for the human body simulation but is not the controlling factor for the charged device test.

The base-collector junction failed on Part Type D. The width of the contact to the base was 13 microns. The Schottky diode failed on Part Type C. The width of the contact was 9 microns. Part Type D with a contact width of 13 microns failed at about twice the voltage level of Part Type C. The Schottky diode did not fail due to this stress on Part Type D because of its large, 39 micron, width.

Dielectric thickness was a significant factor in the failures on Part Types A, B, and F. These failures were, on Part A, polysilicon to polysilicon breakdown between closely spaced stripes on the same level, and polysilicon layer to layer shorts. On Part B, this was a thin oxide dielectric breakdown. On Part F there were polysilicon to overlying metallization and polysilicon to underlying silicon shorts. The thicknesses involved were: Part A poly to poly = 0.1 microns, Part B thin

oxide estimated to be 500 Angstroms, Part F poly to metal and poly to silicon both 0.5 microns. The lowest failure levels occurred on Part F. This is believed to be due to oxide defects rather than to the nominal dielectric thickness. The thin dielectric on Part A was a major cause for the relatively low failure levels. As discussed, routing changes could alleviate this. The dielectric failures on Part B were due to the thin oxide structure utilized. Quantitative comparison of the oxide thicknesses to failure level provides little information.

Conductor spacing was a significant factor on Part A due to close polysilicon spacing as mentioned above. A routing change could correct this.

Junction electrical breakdown characteristics were measured on each of the eight devices. A listing of the breakdown voltage looking into the input for each device is given here. Part A = 30VDC, Part B = 22 VDC, Part C = 28 VDC, Part D = 20 VDC, Part E = 28 VDC, Part F = 25 VDC, Part G = 22 VDC, Part H = 18 VDC. Other factors override these in controlling ESD sensitivity.

Overall device layout was seen to be an important factor which determined device sensitivity. The layouts which were analyzed included: metallization pattern, diffusion spacing and shape, and polysilicon patterns. Two effects were evident related to the metallization. Points which were connected to large metallization areas showed sensitivity to the CD stress. This created failure mode and stress level sensitivity differences in Parts D, G and H. On Part D the failure mode was a different junction for the human body stress than for the charged device stress due to a large ground metallization connected to one junction. This junction failed for the CD stress because it received a larger stress. Parts G and H had specific pins which were much more sensitive to the CD stress due to metallization layout. The second effect was longer metallization runs decreased sensitivity. This was seen on Parts B and C. This is due to a distributed capacitance and/or inductance effect.

Diffusion spacing and shape was an important factor on Parts B, E, and H. It was found that the pin or pins that failed had closer spacing and corners between adjacent n+ diffusions. Quantitatively this spacing was: Part B=2 microns, Part E=26 microns, and Part H=5 microns. The failure levels for E and H were much higher than for B, however Part H was higher than Part E. This indicates that spacing is important but more important for Part H was likely the polysilicon interface pad between the metallization and the silicon.

The effect of the physical construction and packaging on the device sensitivities is the last area to be discussed. All devices analyzed were in CERDIPs. There are two effects that likely occurred, however, they are not the controlling factor for sensitivity. These two effects are a decrease in sensitivity due to the longer lead trame lengths on the large packages and an increase in capacitance to ground for the charged device stress due to the additional area on these larger devices.

Recommendations

This study has shown how device sensitivities vary with the type of stress applied and with pin to pin physical differences.

An important result is the demonstration of the similarities and differences in device damage and sensitivity between the charged device simulation and the human body simulation. The charged device simulation produces damage at a lower level to pins that are connected to large expanses of metallization. An understanding of this effect could result in a reduced sensitivity to ESD at IC design by appropriate metallization layout.

The charged device test method has been shown to produce results which are consistent with ESD stress failures and it is recommended for the simulation of ESD on integrated circuits.

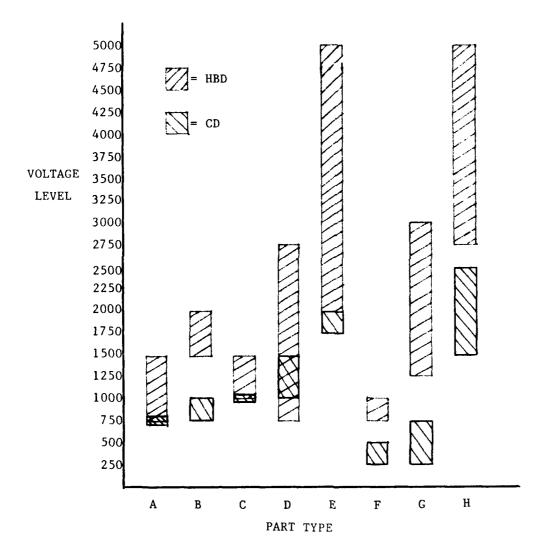


Figure VI-1 - Failures by Voltage Level For Each Part And For Both The Charged Device And Human Body ESD Models.

-5000				-5000		3
+5000				+5000		
-4750				-4750	11	
+4750				+4750		
-4500				-4500	9	
+4500				+4500		2
-4250				-4250	8	
+4250				+4250		
-4000				-4000	7	
+4000				+4000		
-3750				-3750	5	
+3750				+3750	3	
-3500				-3500		
+3500				+3500		
-3250				-3250		
+3250			•	+3250	2	
-3000				-3000		
+3000				+3000		
-2750				-2750		
+2750				+2750		1
-2500				-2500		
+2500		14		+2500		
-2250		11		-2250		
+2250		7		+2250		
-2000		6		-2000		
+2000	14	4		+2000	1	
-1750	4			-1750		
+1750	1	2		+1750		
-1500	_	1		-1500		
+1500				+1500		
-1250				-1250		
+1250				+1250		
-1000				-1000		
+1000				+1000		
750				-750		
+750				+750		
-500				-500		
+500				+500		
-250				-250		
+250				+250		
VOLTAGE	PART E	PART H		VOLTAGE	PART E	PART H
CHARGED DEVICE MODEL			HUMAN BODY MODEL			

Figure VI-2 - Cumulative Failures for the Parts from Manufacturer A

-5000					~ 5000				3
+5000					+5000				•
-4750					- 4750		11		
+4750					+4750				
-4500					-4500		9		
+4500					+4500				2
-4250					-4250		8		_
+4250					+4250		Ū		
-4000					-4000		7		
+4000					+4000		·		
-3750					-3750		5		
+3750					+3750		3		
-3500					-3500		•		
+3500					+3500				
-3250					-3250				
+3250					+3250		2		
-3000					-3000		•••		
+3000					+3000			15	
-2750					-2750			14	
+2750					+2750			11	1
-2500					-2500			6	-
+2500				14	+2500				
-2250				11	-2250			5	
+2250				7	+2250				
-2000				6	-2000	15			
+2000		14		4	+2000	14	1		
-1750		4			-1750	- '			
+1750		1		2	+1750	7			
-1500		-		1	-1500				
+1500				_	+1500	2			
-1250					-1250	-		2	
+1250					+1250				
-1000					-1000				
+1000	15				+1000				
-750			15		-750				
+750	8		12		+750				
-500	-		11		-500				
+500			6		+500				
-250			1		-250				
+250			_		+250				
VOLTAGE	В	E	G	Н	VOLTAGE	В	E	G	Н
		PART					PART		
CHAE	CED	DEVICE M	ODEI		uth	ANT DA	DDY MODE		
CHAP	KGED	DEATCE E	ODEL		num	ום וואו	זעטות זענ	باد	

Figure VI-3 - Cumulative Failures for the NMOS Devices

VOLTAGE	PART G	PART H	VOLTAGE	PART G	PART H
	D4DM 0	D4.D# **		DADE C	D 4 D 00 **
-250 +250	1		-250 +250		
+500	6		+500		
-500	11		-500		
+750	12		+750		
-750	15		-750 -750		
+1000			+1000		
-1000			-1000		
+1250			+1250		
~1250			-1250	2	
+1500			+1500	_	
~1500		1	-1500		
+1750		2	+1750		
-1750		•	-1750		
+2000		4	+2000		
-2000		6	-2000		
+2250		7	+2250		
-2250		11	-2250 -2250	5	
+2500		14	+2500	_	
-2500			-2500	6	
+2750			+2750	11	1
-2750			-2750	14	
+3000			+3000	15	
-3000			-3000	_	
+3250			+3250		
-3250			-3250		
+3500			+3500		
-3500			-3500		
+3750			+3750		
-3750			-3750		
+4000			+4000		
-4000			-4000		
+4250			+4250		
-4250			-4250		
+4500			+4500		2
-4500			-4500		
+4750			+4750		
-4750			-4750		
+5000			+5000		
-5000			-5000		3
5020			5000		•

Figure VI-4 - Cumulative Failures for the Two Microprocessors

CHARGED DEVICE MODEL

HUMAN BODY MODEL

-2000 +2000		-2000 +2000	
+2250		+2250	
-2750 +2750 -2500 +2500 -2250		-2750 +2750 -2500 +2500 -2250	
-3250 +3250 -3000 +3000		-3250 +3250 -3000 +3000	
+4000 -3750 +3750 -3500 +3500		+4000 -3750 +3750 -3500 +3500	
+4750 -4500 +4500 -4250 +4250 -4000		+4750 -4500 +4500 -4250 +4250 -4000	
-5000 +5000 -4750		-5000 +5000 -4750	

Figure VI-5 - Cumulative Failures for the Two CMOS Devices

-5000			-5000		
+5000			+5000		
-4750			-4750		
+4750			+4750		
-4500			-4500		
+4500			+4500		
-4250			-4250		
+4250			+4250		
-4000			-4000		
+4000			+4000		
-3750			-3750		
+3750			+3750		
-3500			-3500		
+3500			+3500		
-3250			~3250		
+3250			+3250		
-3000			~3000		
+3000			+3000		
-2750			~2750		
+2750			+2750		12
-2500			-2500		
+2500			+2500		8
-2250			-2250		
+2250			+2250		4
-2000			-2000		
+2000			+2000		
-1750			~1750		
+1750			+1750		
-1500			-1500		
+1500		14	+1500	15	
-1250		10	-1250		
+1250			+1250	5	
-1000	15	2	-1000		
+1000	3		+1000	3	
-750			-750		
+750			+750		2
-500			~500		
+500			+500		
-250			-250		
+250			+250		
VOLTAGE	PART C	PART D	VOLTAGE	PART (PART D
CHAR	GED DEVIC	E MODEL	HUMAN	BODY MO	DDEL

Figure VI-6 - Cumulative Failures for the Two Schottky Devices

-5000			-5000		
+5000			+5000		
-4750			-4750		11
+4750			+4750		•
-4500			-4500		9
+4500			+4500		
-425 0			-4250		8
+4250			+4250		_
-4000			-4000		7
+4000			+4000		_
~ 3750			-3750		5 3
+3750			+3750		3
-3500			-3500		
+3500			+3500		
-3250			-3250		
+3250			+3250		2
~3000			-3000		
+3000			+3000		
~2750			-2750		
+2750			+2750		
-2500			-2500		
+2500			+2500		
-2250			-2250		
+2250			+2250		
-2000			-2000		
+2000		14	+2000		1
-1750		4	-1750		
+1750		1	+1750	1 -	
-1500			-1500	15	
+1500			+1500	5	
-1250			-1250	4	
+1250			+1250		
-1000			-1000	•	
+1000			+1000	2	
-750	15		-750	1	
+750	5		+750		
-500			-500		
+500			+500		
-250			-250		
+250			+250		
VOLTAGE	PART A	PART E	VOLTAGE	PART A	PART E
CHAR	GED DEVIC	E MODEL	HUMAI	N BODY MOD	EL

Figure VI-7 - Cumulative Failures for the Two RAM, I/0, Timers.

CHAR	GED DEVI	CE MOI	DEL	HUMAN BODY MODEL				DEL		
VOLTAGE	PART B	PART	F		,	VOLTAGE	PART :	В	PART]
+250		4				+250				
-250		8				-250				
+500		15				+500				
-500	-					-500			-	
+750	8					+750			5	
-750						- 750			9	
+1000	15					+1000			1.5	
-1000						-1000			15	
+1250						+1250				
-1250						-1250	2			
+1500						+1500	2			
-1500						-1500	,			
+1750						+1750	7			
-1750						-1750	14			
+2000						-2000 +2000	14			
+2250 -2000						+2250	15			
-2250						-2250				
+2500						+2500				
-2500						-2500				
+2750						+2750				
-2750						-2750				
+3000						+3000				
-3000						-3000				
+3250						+3250				
-3250						-3250				
+3500						+3500				
-3500						-3500				
+3750						+3750				
-3750						-3750				
+4000						+4000				
-4000						-4000				
+4250						+4250				
-4250						-4250				
+4500						+4500				
-4500						-4500				
+4750						+4750				
-4750						-4750				
-5000 +5000						+5000				
-5000						-5000				

Figure VI-8 - Cumulative Failures for the Two RAMs

|

MISSION

of

Rome Air Development Center

RADC plans and executes research, development, test and selected acquisition programs in support of Command, Control Communications and Intelligence (C^3I) activities. Technical and engineering support within areas of technical competence is provided to ESP Program Offices (POs) and other ESD elements. The principal technical mission areas are communications, electromagnetic guidance and control, surveillance of ground and aerospace objects, intelligence data collection and handling, information system technology, ionospheric propagation, solid state sciences, microwave physics and electronic reliability, maintainability and compatibility.

END

FILMED

3-85

DTIC